

Cartilage Tissue Engineering

Strategies to maintain the chondrogenic differentiation potential of culture-expanded mesenchymal progenitor cells



Chantal Voskamp-Visser

Cartilage Tissue Engineering

Strategies to maintain the chondrogenic differentiation potential of culture-expanded mesenchymal progenitor cells

Chantal Voskamp-Visser

Colofon

Copyright © Chantal Voskamp-Visser, The Netherlands, 2023

ISBN: 978-94-6458-993-1

All rights reserved. No parts of this thesis may be reproduced, distributed, stored in a retrieval system, or transmitted in any form or by any means, without written permission of the author or, when appropriate, the publisher of the publication

The work presented in this thesis was conducted at the Department of Orthopaedics & Sports Medicine, University Medical Center Rotterdam, the Netherlands.

The research leading to these results was supported by the Dutch Arthritis Foundation (ReumaNederland; 16-1-201) and the TTW Perspectief grant from NWO (William Hunter Revisited; P15-23).

Cover design: Chantal Voskamp-Visser and Corinde Warmerdam

Layout: Chantal Voskamp-Visser

Printing: Ridderprint

Printing of this thesis was financially supported by:

Department of Orthopaedics & Sports Medicine, Erasmus MC, University Medical Center Rotterdam.

Anna Foundation|NOREF

Cartilage Tissue Engineering

Strategies to maintain the chondrogenic differentiation potential of culture-expanded mesenchymal progenitor cells

Regeneratie van kraakbeenweefsel

Strategieën om nieuw kraakbeen te kweken met mesenchymale stamcellen

Proefschrift

ter verkrijging van de graad van doctor aan de
Erasmus Universiteit Rotterdam
op gezag van de
rector magnificus

Prof.dr. A.L. Bredenoord

en volgens besluit van het College voor Promoties.
De openbare verdediging zal plaatsvinden op

donderdag 13 april 2023 om 13.00 uur

door

Chantal Voskamp-Visser
geboren te Zwijndrecht.

Promotiecommissie

Promotor	Prof. dr. G.J.V.M. van Osch
Overige leden	Dr. D. ten Berge Prof. dr. R.S.K. Schneider-Kramann Prof. dr. M. Stoddart
Copromotoren	Dr. R. Narcisi

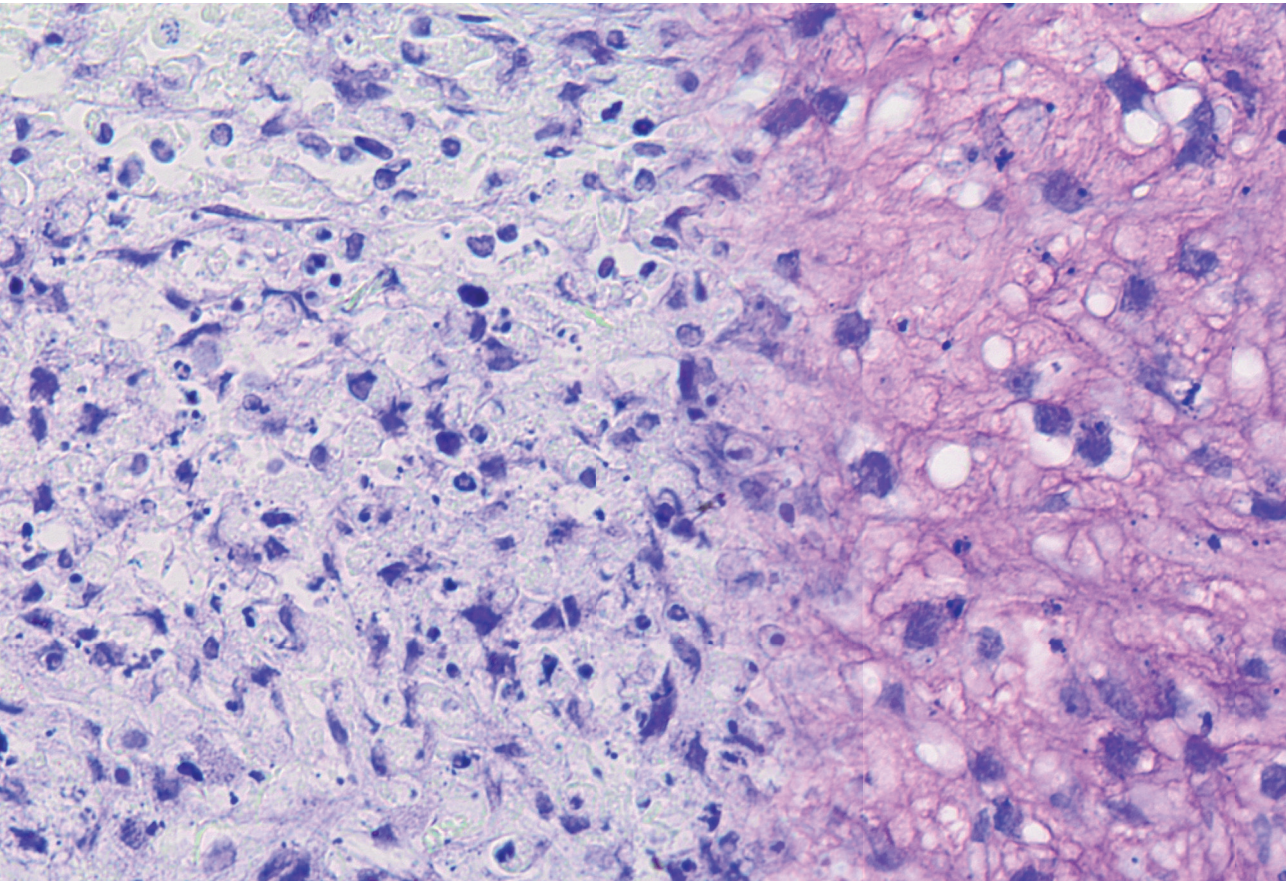
"Soms is het goed om eropuit te gaan
zonder te weten waarheen"

- JAMES NORBURY, *Grote Panda & Kleine Draak*

Table of contents

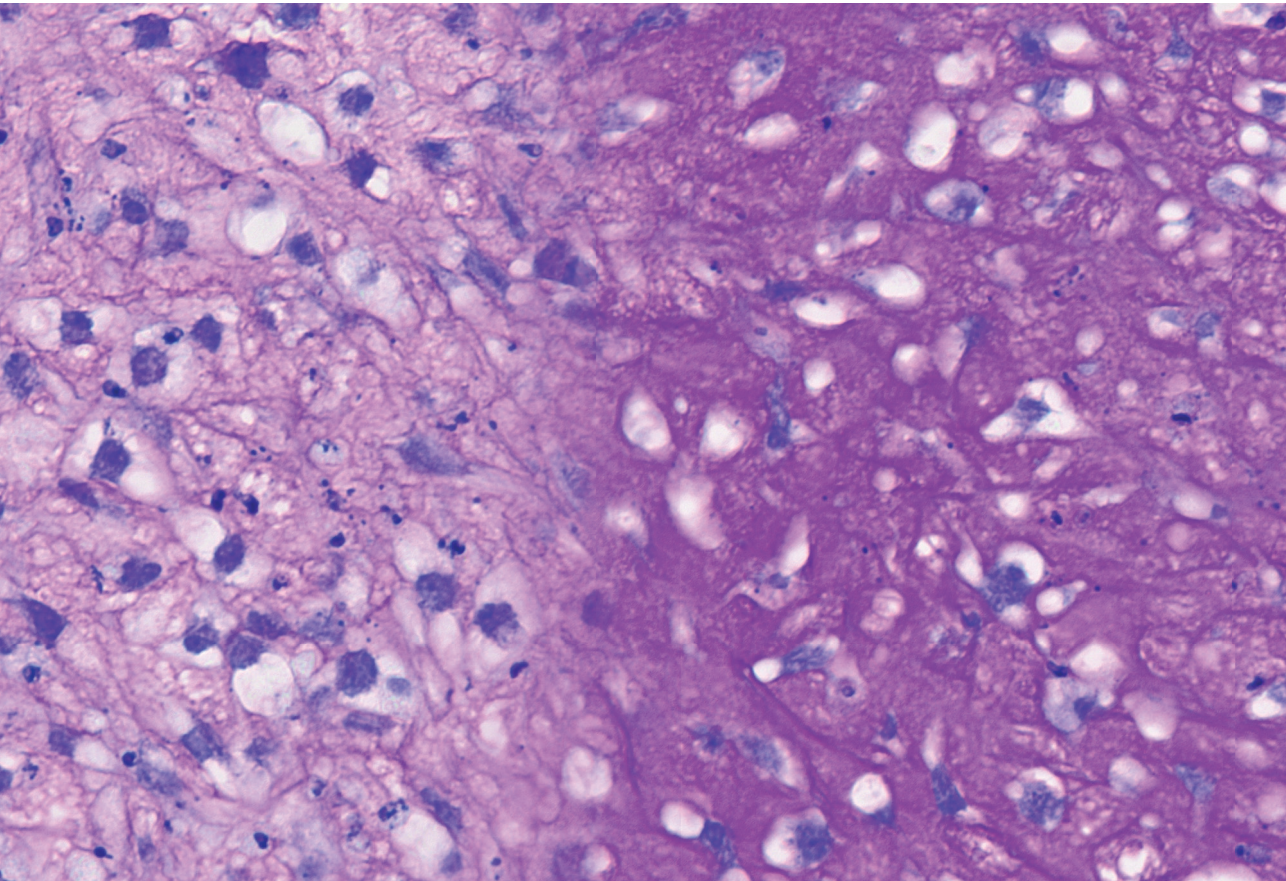
Chapter 1	General introduction, thesis aim and outline	8
Chapter 2	Inducing senescence during early differentiation reduced chondrogenic differentiation capacity of mesenchymal stem cells	26
Chapter 3	<i>TWIST1</i> controls cellular senescence and energy metabolism in mesenchymal stem cells	58
Chapter 4	Sorting living mesenchymal stem cells using a <i>TWIST1</i> RNA-based probe depend on incubation time and uptake capacity	82
Chapter 5	Enhanced chondrogenic capacity of mesenchymal stem cells after TNF α pre-treatment	100
Chapter 6	General discussion	130
Chapter 7	Summary	148
Chapter 8	References	154
Appendices		190
	Nederlandse samenvatting	193
	List of publications	197
	Acknowledgements	199
	PhD portfolio	203
	Curriculum vitae	207

1



Chapter 1

General introduction and aims and outline



1.1 Cartilage injury and treatment approaches

Articular cartilage is a connective tissue present on the articular surfaces of diarthrodial joints. Articular cartilage facilitates bone movements by providing a smooth surface for the joints and acting as a shock absorber. The unique properties of articular cartilage, such as carrying mechanical load without permanent distortion, are facilitated by the large amount of extracellular matrix (ECM), characterized by the presence of collagen and proteoglycan (Buckwalter and Mankin 1998). Type II collagen is the major collagen type present in articular cartilage, and forms a network of collagen fibrils (Strawich and Nimni 1971, Rhodes and Miller 1978, Myllyharju and Kivirikko 2004). Associated with these fibrils are proteoglycans with negatively charged sulphated glycosaminoglycan (GAG) side chains, which attracts cations and therefore retain water (Hardingham and Bayliss 1990). The ECM is maintained by chondrocytes which are located in matrix cavities (Stockwell 1978). Cartilage is avascular, therefore chondrocytes are nourished by the diffusion of nutrients and oxygen from synovial fluid in the joint cavity and the underlying bone (Maroudas, Bullough *et al.* 1968, Wang, Wei *et al.* 2013). Acute or repetitive trauma can cause cartilage damage, but cartilage has a low repair capacity. Damaged cartilage tissue loses its functional properties leading to degeneration and eventually this can lead to the degenerative joint disease osteoarthritis (OA) (Mankin 1982, Hunter 1995, Goldring and Goldring 2007). OA is a complex disease that affects the entire joint, including cartilage, subchondral bone and synovium, leading to pain, stiffness and disability. OA is the most common joint disease and affected around 7% of the population worldwide in 2019 (Hunter, March *et al.* 2020). Conventional treatment for OA include pain relief and physiotherapy and at the end stage, joint replacement, while no cure is yet available. Therefore, interventions to repair traumatic cartilage defects are necessary to prevent the development of OA.

1.1.1 Cartilage regeneration strategies

Surgical approaches commonly used to treat traumatic cartilage defects include, microfracture, osteochondral autograft, osteochondral allograft and autologous chondrocyte implantation (Kwon, Brown *et al.* 2019). Each of these treatments has its advantages and the preferred treatment depends on the size of the cartilage defect and on patient-specific factors. As far

as we are aware, no data exist showing that these surgical approaches prevent long-term cartilage degeneration and the development of OA. In addition, these treatments have a limited capacity to regenerate the articular cartilage surface (Kwon, Brown *et al.* 2019). As a consequence, alternative treatments to repair cartilage defects are emerging.

A promising alternative strategy to repair articular cartilage is the use of mesenchymal progenitor cells. Mesenchymal progenitor cells can be isolated from different tissues, such as bone marrow, adipose tissue and umbilical cord. After isolation, the mesenchymal progenitor cells can be cultured *in vitro* and have the potential to differentiate towards chondrocytes, osteoblasts, adipocytes, and other mesodermal cell types (Prockop 1997, Dennis, Merriam *et al.* 1999, Pittenger, Mackay *et al.* 1999). Besides their multilineage differentiation capacity, mesenchymal progenitor cells have immunomodulatory properties (Uccelli, Moretta *et al.* 2008). Mesenchymal progenitor cells are often referred to as mesenchymal stem or stromal cells (MSCs).

Cultured MSCs are a heterogeneous population of cells and are characterized by adherence to plastic, expression for CD105, CD73 and CD90 and negative expression for CD45, CD34, CD11b or CD14, CD79a or CD19 and HLA class II (Dominici, Le Blanc *et al.* 2006). However, these surface markers are not stably expressed in MSCs and the expression doesn't consistently correlate with the chondrogenic differentiation capacity of MSCs (Cleary, Narcisi *et al.* 2016). The use of autologous bone-marrow derived MSCs to repair articular cartilage defects in patients was first reported by Wakitani *et al.* in 2007 (Wakitani, Nawata *et al.* 2007). Since then, MSCs are used in multiple clinical trials to repair cartilage defects (Lee and Wang 2017). An important requirement for the clinical use of MSCs to repair cartilage defects, is a reproducible good chondrogenic differentiation potential. Unfortunately, the chondrogenic differentiation potential of MSCs is gradually lost during *in vitro* expansion, a required step to obtain enough cells to repair damaged cartilage (Banfi, Muraglia 2000). Another limitation is that there is inter- and intra-donor variation in the expansion and chondrogenic differentiation capacity. Therefore, there is a need to define methods to reduce MSC heterogeneity and increase both the MSC's expansion and chondrogenic differentiation capacity.

1.2 *In vitro* expansion of MSCs results in cellular senescence

In order to have enough MSCs for cartilage repair, *in vitro* expansion is necessary. Expanded MSCs can differentiate towards chondrocytes in the presence of TGF β 1 (**Figure 1.1**). However, like other primary cells, MSCs can be expanded for a limited number of cell divisions, referred to as the Hayflick limit, and eventually undergo cellular senescence (Hayflick and Moorhead 1961, Banfi, Bianchi *et al.* 2002). Senescence is a phenomenon by which cells irreversibly stop dividing and enter a state of permanent growth arrest, without undergoing cell death. Cellular senescence is a safety mechanism of the cell to prevent damaged cells to multiply. In damaged cells, cellular senescence is induced by different stress stimuli, such as telomere dysfunction, DNA damage and oncogene activation (Hernandez-Segura, Nehme *et al.* 2018). Cellular senescence alters the function of MSCs and could contribute to MSC heterogeneity and their reduced differentiation potential, therefore it is important to understand the consequence of MSC senescence for cartilage repair.

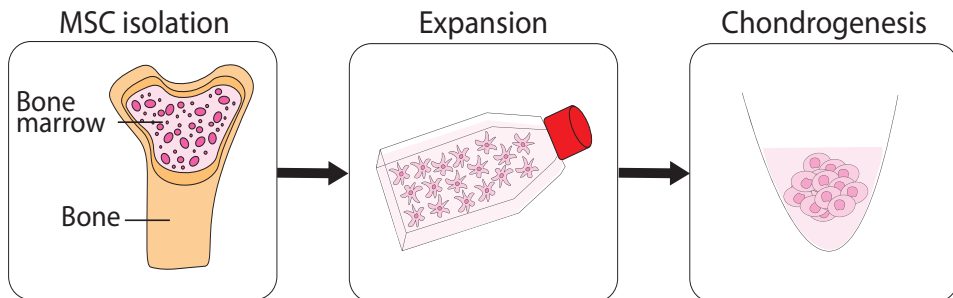


Figure 1.1 - *In vitro* chondrogenesis.

Mesenchymal Stem/Stromal Cells (MSCs) can be isolated from the bone marrow and can be expanded in monolayer cultures. To induce chondrogenesis, MSCs are cultured in a 3D culture in the presence of Transforming Growth Factor beta 1 (TGF β 1).

1.2.1 Hallmarks of MSC senescence

Senescent MSCs show cell cycle arrest, increased lysosomal activity and abnormalities in cell morphology and secretory phenotype (Li, Wu *et al.* 2017). These different characteristics of senescence are often used to identify cellular senescence in MSC populations.

Morphology and lysosomes

After isolation, MSCs generally have a uniform small size and a spindly-like shape, but during passaging in culture, the cell becomes enlarged, the morphology flattened and irregular, the nuclei compromised, and the cytoplasm granular (Wagner, Horn *et al.* 2008). However, due to variation in morphology between MSCs, cell morphology is not a specific marker for cellular senescence in MSCs. One of the most common markers to assess cellular senescence in cells is the increased expression of the lysosomal enzyme senescence-associated- β -galactosidase (SA- β -gal; **Figure 1.2**) (Dimri, Lee *et al.* 1995, Lee, Han *et al.* 2006). Lysosomal β -galactosidase catalyzes the cleavage of β -D-galactose in β -D-galactosides (de Mera-Rodríguez, Álvarez-Hernán *et al.* 2021). The consequence and molecular mechanism of this increased expression is, however, still unknown.

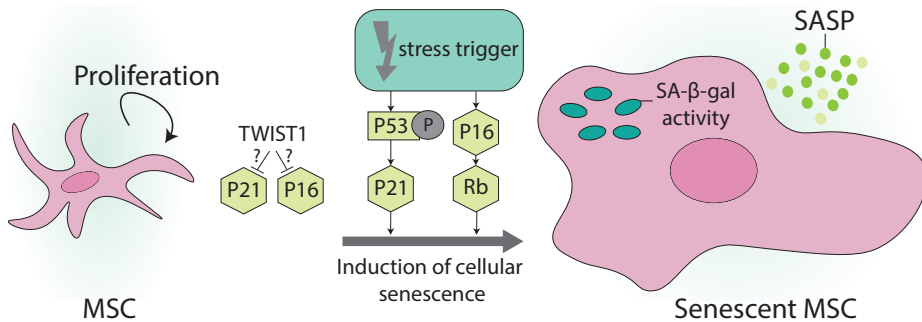


Figure 1.2 - Cellular senescence in mesenchymal stem/stromal cells (MSCs).

Various stress triggers can induce cellular senescence in MSCs. These stress triggers activate various cell signaling pathways, which lead to activation of the P53-P21 pathway and/or the P16-Rb pathway. P53 is activated via phosphorylation (P) and increases P21 expression, which induces cell cycle arrest. P16 also induces cell cycle arrest via Rb. It has been suggested that TWIST1 inhibits both P16 and P21. Senescent MSCs have an enlarged and flattened morphology, an increased senescence-associated beta galactosidase (SA- β -gal) activity in lysosomes and a senescence associated secretory phenotype (SASP).

Cell cycle arrest

Permanent growth arrest in senescent MSCs is regulated by cyclin-dependent kinase inhibitors P16^{INK4A} (CDKN2A, hereafter P16) and P21^{CIP} (CDKN1A, hereafter P21) (Shibata, Aoyama *et al.* 2007, Rodriguez, Rubio *et al.* 2009). Cell cycle arrest and the expression of P16 and P21 are often used

as markers to determine cellular senescence in MSCs. During *in vitro* culture, the expression of *P16* is increased in senescent MSCs, while knockdown of *P16* suppresses cellular senescence and enhances proliferation in MSCs (Shibata, Aoyama *et al.* 2007, Gu, Cao *et al.* 2012). *P16* mediates cell cycle arrest via the retinoblastoma (Rb) pathway (**Figure 1.2**) (Liu, Ding *et al.* 2020). A potential regulator of *P16* in MSCs is the transcription factor TWIST1. During *in vitro* culture of MSCs, downregulation of TWIST1 inhibits the expression of the transcription factor, E47, which induces *P16* expression (**Figure 1.2**) (Cakouros, Isenmann *et al.* 2012). Knockdown of P21 in MSCs increases cell proliferation and the expression of stemness markers *Oct-4* and *Nanog* (Yew, Chiu *et al.* 2011). P21 inhibits proliferation directly through binding to cyclin-dependent kinase complexes (Jung, Qian *et al.* 2010). The main regulator of P21 is P53, which is a sensor of cellular stresses and DNA damage (**Figure 1.2**) (Jung, Qian *et al.* 2010). In hypoxic MSC cultures, P21 is downregulated by TWIST1, indicating that TWIST1 might play a role in delaying senescence, at least under hypoxic conditions (**Figure 1.2**) (Tsai, Chen *et al.* 2011). Overall, these data suggest that TWIST1 might be a regulator of MSC senescence during *in vitro* culture.

Senescence associated secretory phenotype (SASP)

MSCs acquiring a senescence associated secretory phenotype (SASP) could have both positive and negative effects during tissue regeneration processes. Factors that are often secreted by MSCs with a SASP are IL-6, IL-8, IL-1, IL-10, VEGF, MMP-1, MMP-3 and MMP-13 (Lunyak, Amaro-Ortiz *et al.* 2017). The main driver of the SASP in senescent cells is the NF- κ B pathway (Salminen, Kauppinen *et al.* 2012). The presence of a SASP is often used to confirm cellular senescence in MSCs, however, the composition of the factors secreted can be heterogeneous. For example, senescent fibroblasts lacking some of the pro-inflammatory cytokines, such as IL-1, were recently identified. The senescent fibroblasts lacking the pro-inflammatory SASP had dysfunctional mitochondria, and were therefore referred to as mitochondrial dysfunction-associated senescence (MiDAS) (Wiley, Velarde *et al.* 2016), while irradiation induced senescent cells have a pro-inflammatory SASP.

1.2.2 Cellular senescence may limit MSC-based cartilage regeneration

The appearance of cellular senescence in MSCs can be a major limitation for cartilage tissue engineering. One of the limitations is that senescent MSCs are in permanent growth arrest, which prevents cell expansion and thus resulting in limited cells available to repair the damaged cartilage. Besides, in the early phases of differentiation, proliferation is required for *in vitro* chondrogenesis of MSCs (Dexheimer, Frank *et al.* 2012), suggesting that senescent MSCs may have a reduced chondrogenic differentiation potential. The effect of senescence on the chondrogenic differentiation capacity of MSCs remains largely unknown. It has been reported that the differentiation capacity of MSCs towards the adipogenic lineage is reduced during *in vitro* aging (Geissler, Textor *et al.* 2012). The effect of MSC senescence on the osteogenic differentiation capacity remains debated, since some studies show that senescent MSCs have a reduced mineralization potential compared to control MSCs after osteogenic differentiation (Geissler, Textor *et al.* 2012, Despars, Carbonneau *et al.* 2013), while others demonstrate that the osteogenic differentiation is increased in senescent MSCs compared to control MSCs (Wagner, Horn *et al.* 2008). This indicates that more research is necessary to better understand how cellular senescence affects the multilineage differentiation of MSCs.

Another limitation of the use of senescent MSCs is their paracrine effect. Senescent cells secrete SASP-related factors, such as pro-inflammatory cytokines and metalloproteases, which can negatively affect the neighboring tissue (Coppé, Patil *et al.* 2008, Gnani, Crippa *et al.* 2019). The SASP of senescent chondrocytes is suggested to contribute to tissue degeneration, including degradation of cartilage tissue and development of osteoarthritis (Jeon, David *et al.* 2018). Indeed, transplanted senescent cells in healthy knees of mice can induce an osteoarthritis-like condition (Xu, Bradley *et al.* 2017). Overall, these data suggest that senescent MSCs do not contribute to cartilage regeneration and could potentially even lead to cartilage degradation.

1.3 Signaling pathways involved in cartilage development and maintenance

To identify factors that prevent cellular senescence and enhance the chondrogenic capacity of MSCs, researchers often take inspiration from *in vivo* cartilage development and maintenance. Primordial cartilage is formed through condensation of mesenchymal progenitor cells, followed by differentiation into chondrocytes. The primordial cartilage will grow and form a cartilage template that starts to convert into bone in the center through a process called endochondral ossification (Mackie, Ahmed *et al.* 2008). At the joint site, the interzone appears and will gradually differentiate into articular cartilage and synovial joints (Pacifici, Koyama *et al.* 2006). At the epiphysis, a secondary ossification center is formed, which separates the growth plate cartilage and the articular cartilage. The cartilaginous region between the two ossifications centers forms the growth plate, while the region between the joint cavity and the secondary ossification centers forms the articular cartilage (**Figure 1.3**). Articular chondrocytes express many cartilage-specific genes such as *ACAN* and *PRG4* (Doerge, Sasaki *et al.* 1991, Flannery, Hughes *et al.* 1999). Upon aging, the synthesis of the cartilage-specific protein aggrecan declines and its structure alters in articular cartilage (Verbruggen, Cornelissen *et al.* 2000). As a consequence of these ECM related changes, the function of articular cartilage is declined during aging (Buckwalter, Roughley *et al.* 1994). Interestingly, a characteristic of aged articular cartilage is the increased number of senescent chondrocytes (Price, Waters *et al.* 2002, Martin and Buckwalter 2003), suggesting that senescent chondrocytes contribute to the pathophysiology of osteoarthritis (Price, Waters *et al.* 2002, Martin and Buckwalter 2003). In the next paragraphs we will describe how cartilage development and homeostasis is regulated by different transcription factors and growth factors.

1.3.1 Transcription factors

The classical function of transcription factors is to bind to enhancers and promoters and activate or repress gene expression. *SOX9* and *RUNX2/3*, are master regulators during chondrogenic differentiation (Liu, Samsa *et al.* 2017). These master regulators are supported by many other factors to control chondrogenic differentiation (*TWIST1*) (Reinhold, Kapadia *et al.* 2006), ECM production (*SOX5/6*) (Liu and Lefebvre 2015), and hypertrophic chondrocyte differentiation (*MEF2C*, *HIF* and *GLI*) (Arnold, Kim *et al.* 2007, Maes, Carmeliet *et al.* 2012, Alman 2015). In this thesis,

we focus on a subset of transcription factors that have a crucial role during chondrogenesis of mesenchymal progenitor cells.

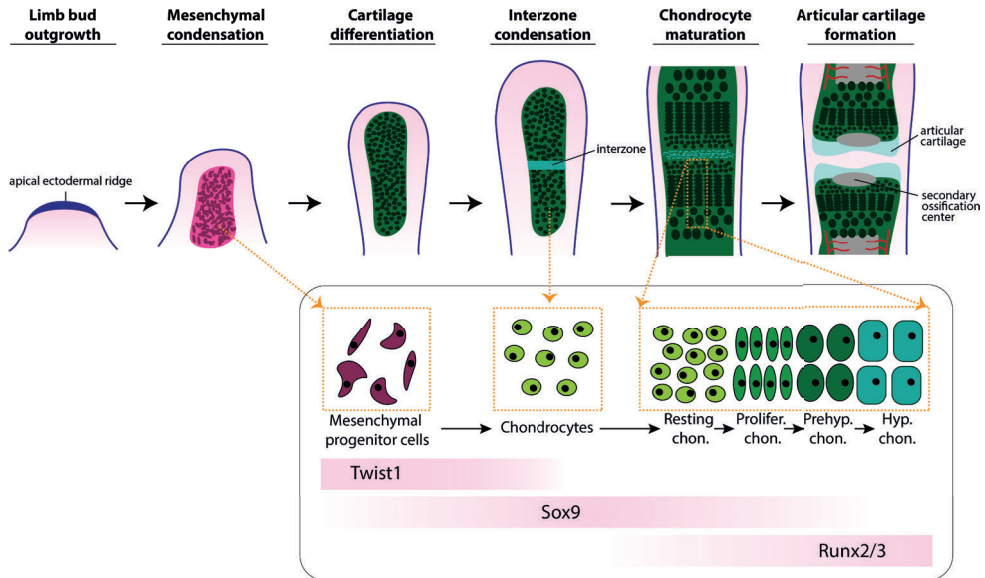


Figure 1.3 - Cartilage formation.

Schematic representation of the key steps during limb development and joint formation. Limb development starts with limb bud outgrowth and the formation of the apical ectodermal ridge. Limb bud outgrowth is followed by proliferation and migration of mesenchymal progenitor cells which express high levels of Twist1. Next, mesenchymal progenitor cells differentiate into chondrocytes via downregulation of Twist1 and upregulation of Sox9. At the joint side, a layer of condensed mesenchymal cells appears which forms the interzone. The cells in the interzone will give rise to the articular cartilage and synovial joints. Chondrocytes in the center of the growth plate undergo hypertrophy via upregulation of Runx2/3 and downregulation of Sox9 resulting in replacement of chondrocytes with endochondral bone. At the epiphyses a secondary ossification center is formed. This figure is adapted from Wang, Rigueur *et al.* 2014.

SOX transcription factors

The SOX (SRY-related HMG-box) proteins are a family of transcription factors that are essential during cell fate decisions in a wide variety of cell types including chondrocytes (Kamachi and Kondoh 2013). SOX9 is essential during chondrogenic differentiation and mutations in SOX9 cause a severe cartilage malformation syndrome named campomelic dysplasia

(Cameron and Sinclair 1997). During limb bud formation, Sox9 is already expressed in mesenchymal progenitor cells, where its function remains unknown, since Sox9 knockout mice show no defect in their early limb buds until the stage of cartilage differentiation (Akiyama, Chaboissier *et al.* 2002). During cartilage differentiation, Sox9 targets cartilage-specific genes including *Acan* and *Col2a1* (Ohba, He *et al.* 2015). Absence of Sox9 during chondrogenesis results in cell death of the mesenchymal progenitor cells and absence of cartilage (Bi, Deng *et al.* 1999, Akiyama, Chaboissier *et al.* 2002). Sox9 is still expressed in pre-hypertrophic chondrocytes where it prevents apoptosis and differentiation into osteoblasts (Ikegami, Akiyama *et al.* 2011). In hypertrophic chondrocytes Sox9 activity is reduced to stimulate osteoblast differentiation (**Figure 1.3**) (Dy, Wang *et al.* 2012). Postnatal absence of Sox9 resulted in the reduction of proteoglycans in the articular cartilage, indicating that Sox9 is necessary to keep articular chondrocytes healthy (Haseeb, Kc *et al.* 2021). The importance of SOX9 in articular cartilage homeostasis is further supported by the fact that SOX9 is downregulated in articular cartilage of late stage OA (Zhang, Ji *et al.* 2015).

Like Sox9, Sox5 and Sox6 are expressed in chondrocytes and bind to cartilage-specific super-enhancers (Lefebvre, Li *et al.* 1998, Liu and Lefebvre 2015). Double Sox5 and Sox6 knockout in mice results in a dead fetus with chondrodysplasia, while single knockout mice are born with only mild cartilage defects, indicating that Sox5 and Sox6 are redundant during chondrogenic differentiation (Smits, Li *et al.* 2001). It is suggested that SOX5 and SOX6 are also important for cartilage homeostasis, since the SOX5/6 together with SOX9 are downregulated in late stage osteoarthritic cartilage (Lee and Im 2011).

SOX8 is closely related to SOX9 and it is expressed in mesenchymal progenitor cells and chondrocytes (Schepers, Bullejos *et al.* 2000, Herlofsen, Høiby *et al.* 2014). However, its function during chondrogenesis remains unknown, since Sox8 knockout mouse show no cartilage malformations (Sock, Schmidt *et al.* 2001). Another group of Sox proteins are Sox4, Sox11 and Sox12 that are closely related to each other. They are expressed in mesenchymal progenitor cells and chondrocytes (Dy, Penzo-Méndez *et al.* 2008, Bhattaram, Penzo-Méndez *et al.* 2014), where they support cell survival and determine cell fate (Kato, Bhattaram *et al.* 2015).

RUNX2 and RUNX3 transcription factors

Runx2 and Runx3 are expressed in pre-hypertrophic and hypertrophic chondrocytes and are essential in chondrocyte maturation (**Figure 1.3**) (Yoshida, Yamamoto *et al.* 2004). Runx2 knockout mice show complete lack of ossification and delay in chondrocyte maturation, indicating that Runx2 promotes chondrocyte maturation (Komori, Yagi *et al.* 1997, Inada, Yasui *et al.* 1999). Runx3 knockout mice show a slight delay in endochondral ossification, while Runx2 and Runx3 double knockout mice show complete absence of pre-hypertrophic and hypertrophic chondrocytes, indicating that Runx2 and Runx3 are redundant (Yoshida, Yamamoto *et al.* 2004). Runx2 and Runx3 target hypertrophic markers such as *Col10a1*, *Mmp13* and *Ihh* (Yoshida, Yamamoto *et al.* 2004), and their binding sites are in close proximity of SOX5/6/9 binding sites in chondrocytes (Liu, Samsa *et al.* 2017). These data suggest that RUNX and SOX proteins interact during chondrogenesis (Liu, Samsa *et al.* 2017).

TWIST1 transcription factor

TWIST1 is a basic-helix-loop-helix transcription factor expressed in mesenchymal progenitor cells and controls mesenchymal cell proliferation and differentiation (Isenmann, Arthur *et al.* 2009, Boregowda, Krishnappa *et al.* 2016). Heterozygous mutations in *TWIST1* cause Seathre-Chatzen syndrome, that is associated with skeletal abnormalities such as craniosynostosis and short stature (el Ghouzzi, Le Merrer *et al.* 1997, Howard, Paznekas *et al.* 1997). Twist1 inhibits differentiation of mesenchymal progenitor cells into downstream cell lineages, including chondrocytes (**Figure 1.3**) (Reinhold, Kapadia *et al.* 2006, Goodnough, Chang *et al.* 2012). *TWIST1* expression is downregulated during chondrogenic differentiation, however during early chondrogenic differentiation of bone marrow derived MSCs, upregulation of *TWIST1* is necessary (Guzzo, Andreeva *et al.* 2011, Cleary, Narcisi *et al.* 2017). Twist1 regulates mesenchymal progenitor cell fate by interaction with the DNA binding site of other transcription factors including, Sox9, Runx2 and Runx3 and thereby inhibiting its function (Yousfi, Lasmole *et al.* 2002, Bialek, Kern *et al.* 2004, Gu, Boyer *et al.* 2012, Pham, Vincentz *et al.* 2012).

1.3.2 Growth factors

Besides transcription factors, growth factors play an essential role during chondrogenic differentiation and maintenance. FGF, TGF β and WNT signaling pathways are involved in different stages of chondrogenic differentiation.

FGF

FGF signaling plays an important role in various biological processes such as tissue regeneration and skeletal tissue formation (Ornitz and Itoh 2015). The FGF signaling pathway currently consists of twenty-three signaling molecules that can signal through four tyrosine kinase FGF receptors (fibroblast growth factor receptors; FGFRs). The importance of FGF in the formation of skeletal tissues is highlighted by the fact that mutations in the FGF receptors FGFR1, 2 and 3 can lead to skeletal dysplasia (Naski, Wang *et al.* 1996, Brodie, Kitoh *et al.* 1999, Passos-Bueno, Wilcox *et al.* 1999, Tsai, Tsai *et al.* 1999, Wilkie, Patey *et al.* 2002, Cho, Guo *et al.* 2004, White, Cabral *et al.* 2005, Heuertz, Le Merrer *et al.* 2006, Leroy, Nuytinck *et al.* 2007, Pollock, Gartside *et al.* 2007, Almeida, Campos-Xavier *et al.* 2009, Merrill, Sarukhanov *et al.* 2012, Wang, Sun *et al.* 2013).

In the early stage of cartilage development, Fgf10 and Fgfr1 are expressed in the lateral plate mesoderm and initiate the apical ectodermal ridge (AER) at the distal limb bud and initiate Fgf8 expression through Fgfr2 signaling (Crossley, Minowada *et al.* 1996, Vogel, Rodriguez *et al.* 1996, Deng, Bedford *et al.* 1997, Ohuchi, Nakagawa *et al.* 1997, Min, Danilenko *et al.* 1998, Xu, Weinstein *et al.* 1998, Arman, Haffner-Krausz *et al.* 1999, Sekine, Ohuchi *et al.* 1999, De Moerlooze, Spencer-Dene *et al.* 2000). Fgf8 promotes cell proliferation and maintains the undifferentiated state by inhibiting Sox9 expression (**Figure 1.4**) (ten Berge, Brugmann *et al.* 2008). Besides Fgf8, Fgf2 and Fgf4 are expressed at the AER and induce limb bud outgrowth (Niswander, Tickle *et al.* 1993, Fallon, López *et al.* 1994). During mesenchymal condensation, Fgfr1 is expressed in the limb mesenchyme and the periphery of the condensation, while Fgfr2 is expressed in the condensation (Orr-Urtreger, Givol *et al.* 1991, Peters, Werner *et al.* 1992, Delezoide, Benoist-Lasselín *et al.* 1998, Ornitz and Marie 2002, Goldring, Tsuchimochi *et al.* 2006, Hellingman, Koevoet *et al.* 2010).

At the onset of chondrogenic differentiation, *Fgfr3* is expressed at the center of the condensation (Hellingman, Koevoet *et al.* 2010). Later, *Fgfr3* is expressed in proliferating chondrocytes and suppresses chondrocyte proliferation and hypertrophic differentiation (Delezoide, Benoist-Lasselien *et al.* 1998, Sahni, Ambrosetti *et al.* 1999, Ornitz and Marie 2002), while *Fgfr1* is mainly expressed in hypertrophic chondrocytes (Goldring, Tsuchimochi *et al.* 2006, Hellingman, Koevoet *et al.* 2010). In articular cartilage, FGF2 and FGF18 regulate cartilage homeostasis. FGF2 signaling, via FGFR1, results in activation of the catabolic pathway, while signaling through FGFR3 leads to anabolic activation (Gonzalez, Gomez *et al.* 1991). FGF18 signals via FGFR3 and stimulates matrix synthesis (Ellman, An *et al.* 2008). Thus, FGF signaling is dynamic and crucial for proliferation and maintenance of mesenchymal cells for cartilage formation and maintenance.

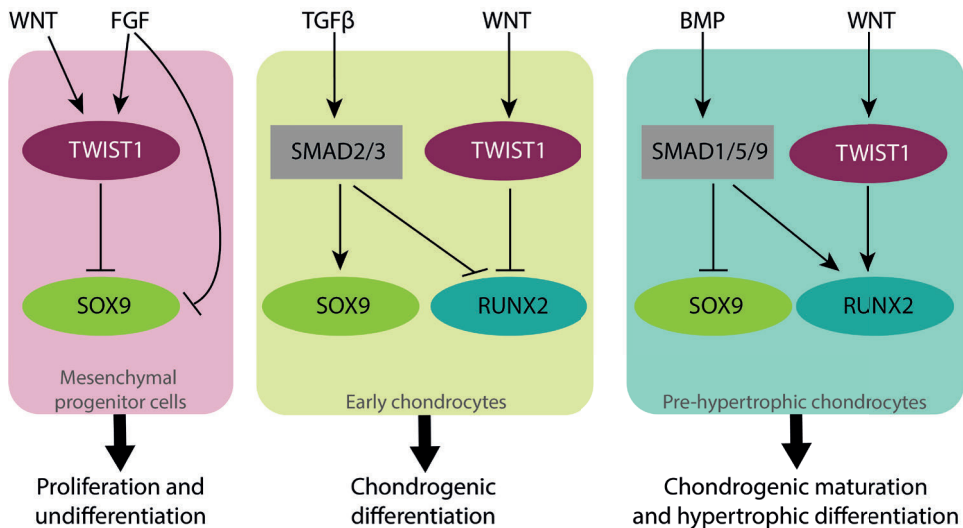


Figure 1.4 - Simplified hypothetical overview based on current literature of transcription factors and signaling pathways during mesenchymal stem/stromal cell differentiation.

In mesenchymal progenitor cells *Wnt3a* and FGF signaling are crucial to stimulate proliferation and inhibit differentiation via upregulation of *Twist1* and repression of *Sox9*. *TGFβ* and *Wnt5a* signaling stimulate chondrogenic differentiation through activation of *Sox9* and repression of *Runx2*. In pre-hypertrophic chondrocytes *Smad1/5/9* activation inhibits *Sox9* and activates *Runx2*. In addition *Wnt4* stimulates hypertrophic differentiation through an increased expression of *Runx2* and reduced expression of *Sox9*.

TGF β

The transforming growth factor (TGF) β signaling pathway plays an essential role during cartilage formation and maintenance (Wang, Rigueur *et al.* 2014). In mammals, the TGF β superfamily consists of multiple subfamilies, including TGF β s (1, 2, 3), bone morphogenic proteins (BMPs; 2, 4-10) (Weiss and Attisano 2013) and growth and differentiation factors (GDFs; 1-15) (Ducy and Karsenty 2000). Ligands of the TGF β superfamily can bind TGF β receptors and activate downstream SMAD pathways. The TGF β subfamily mainly signals via the SMAD2/3 pathway and the BMP subfamily mainly via the SMAD1/5/9 pathway (SMAD9 is also known as SMAD8), however TGF β s and BMPs can also crosstalk and signal through a SMAD independent pathway (Weiss and Attisano 2013). During all phases of chondrogenic differentiation in mice TGF β s, BMPs and GDFs are expressed and their coordination is essential for cartilage generation. TGF β signaling stimulates mesenchymal condensation via up-regulation of N-cadherin and fibronectin during mesenchymal condensation (Tuli, Tuli *et al.* 2003). In addition, TGF β signaling stimulates chondrogenic differentiation of mesenchymal progenitor cells through activation of Sox9 via Smad3 (Furumatsu, Ozaki *et al.* 2009), while it blocks chondrogenic maturation (Ballock, Heydemann *et al.* 1993, Zhang, Ziran *et al.* 2004). On the other hand, activation of Smad1/5/9 signaling is required for hypertrophic differentiation of chondrocytes. TGF β signaling regulates hypertrophic differentiation of chondrocytes via Runx2. Smad3 inhibits the function of Runx2 via direct binding (Alliston, Choy *et al.* 2001, Kang, Alliston *et al.* 2005, Chen, Thuillier *et al.* 2012), while Smad1/5-Runx2 interaction activates Runx2 (**Figure 1.4**) (Leboy, Grasso-Knight *et al.* 2001).

Another essential factor for cartilage formation is GDF5. *Gdf5* is an early marker for cells in the interzone during early joint development and there is a continuous influx of *Gdf5* positive cells during joint formation (Shwartz, Viukov *et al.* 2016). Lineage tracing experiments, show that *Gdf5* positive cells give rise to different tissues in the joint such a articular cartilage, synovium, menisci and ligaments (Rountree, Schoor *et al.* 2004).

WNT

Another family of secreted signaling molecules involved in cartilage development is the Wnt family (Ma, Landman *et al.* 2013). To date, 19 members of the Wnt family are identified, which can signal through canonical and non-canonical pathways (Miller 2002). Canonical Wnt signaling is mediated by frizzled receptors, which stabilize β -catenin and translocate to the nucleus, where it regulates gene transcription. β -catenin is degraded in the absence of Wnt signals (Dale 1998). The non-canonical pathway signals through multiple signaling pathways, including inositol triphosphate (IP3) and intercellular calcium (Semenov, Habas *et al.* 2007). During early limb development in mice, Wnt3a signaling interacts with Fgf10 signaling and induces AER formation (Kengaku, Capdevila *et al.* 1998, McQueeney, Soufer *et al.* 2002). Furthermore, Wnt3a inhibits chondrogenic differentiation via upregulation of Twist1 (**Figure 1.4**) (Reinhold, Kapadia *et al.* 2006). Later during chondrogenic differentiation, Wnt4, Wnt5a and Wnt5b are differently expressed; respectively in the joint regions, perichondrium and pre-hypertrophic chondrocytes (Hartmann and Tabin 2000, Church, Nohno *et al.* 2002). Each of these Wnt molecules has a different function during chondrogenesis. Wnt5a and Wnt5b promote early chondrogenesis through upregulation of Col2a1, while Wnt4 blocks chondrogenic differentiation and stimulates hypertrophic differentiation of chondrocytes (**Figure 1.4**) (Hartmann and Tabin 2000, Church, Nohno *et al.* 2002, Yang, Topol *et al.* 2003).

1.4 Aim and outline of this thesis

Human mesenchymal progenitor cells referred to as MSCs are a promising cell source to regenerate cartilage. The functional heterogeneity of MSCs among donors and within MSC populations, however, limits their clinical use. Moreover, their chondrogenic differentiation capacity is declined after *in vitro* expansion. Culture methods have been established to improve the proliferation capacity, while keeping their chondrogenic differentiation capacity. For example, FGF2 is a growth factor that is often added during expansion of MSCs, since it improves MSC proliferation and delays cellular senescence. However, MSCs eventually become senescent and gradually lose their chondrogenic differentiation capacity (Tsutsumi, Shimazu *et al.* 2001, Bianchi, Banfi *et al.* 2003). In recent work it was shown that addition of both WNT3A and FGF2 synergistically enhances MSC expansion while

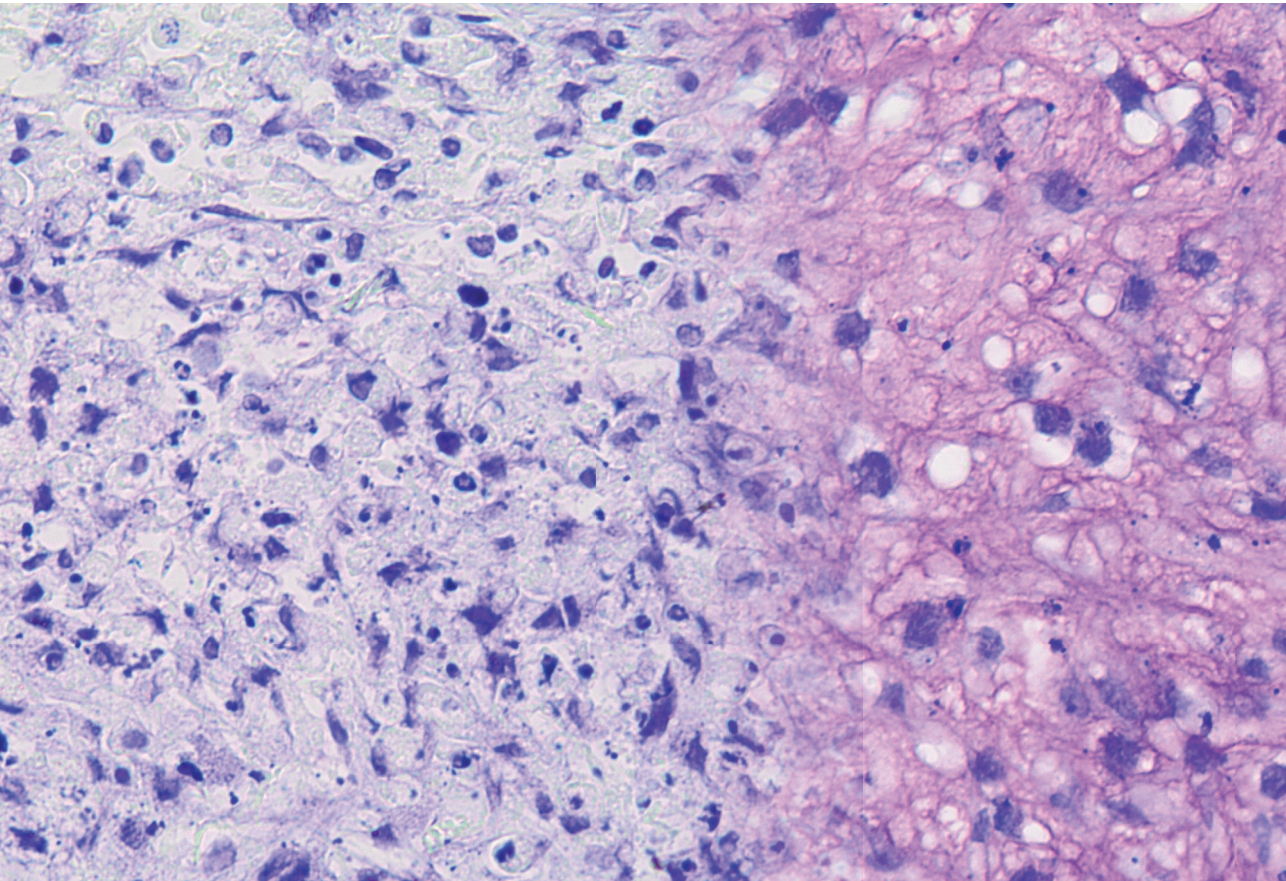
maintaining MSC characteristics such as a small cell morphology and a high *TWIST1* expression (Narcisi, Cleary *et al.* 2015). These data suggest that high *TWIST1* expression during the expansion phase of MSCs preserves the chondrogenic differentiation potential of MSCs via inhibition of cellular senescence (Lehmann, Narcisi *et al.* 2022). The main objective of this thesis is to *determine how MSCs can preserve their chondrogenic differentiation capacity during in vitro expansion*. The answers of the following questions contribute to the main objective:

- How does cellular senescence impact the differentiation capacity of MSCs?
- How does *TWIST1* expression during expansion affect MSC proliferation and chondrogenic differentiation?
- How can different expansion methods obtain MSCs with a high *TWIST1* expression?

In **chapter 2**, we study how MSC senescence affects the initiation of chondrogenic differentiation and maturation. Specifically, we investigate whether or not the senescence associated secretory phenotype (SASP) of MSCs plays a role. In **chapter 3**, we study how cellular senescence is regulated by *TWIST1* expression. We elucidate how *TWIST1* modulation in MSCs controls senescence, the SASP and the mitochondrial function of the cells.

To find novel strategies to improve the expansion and chondrogenic capacity of MSCs, we optimize a method that allows single cell detection of *TWIST1* mRNA levels in living MSCs using an RNA-based probe in **chapter 4**. Another strategy to increase chondrogenesis in MSCs is via direct modulation of *TWIST1* expression. Since *TWIST1* is upregulated by the pro-inflammatory cytokine TNF α (Hasei, Teramura *et al.* 2017), in **chapter 5** we determine the effect of different TNF α pre-treatment conditions on the chondrogenic differentiation potential of MSCs. Finally, in **chapter 6** we discuss the findings of this thesis in the light of further research on *TWIST1* and cellular senescence to improve MSCs for cartilage repair.

2



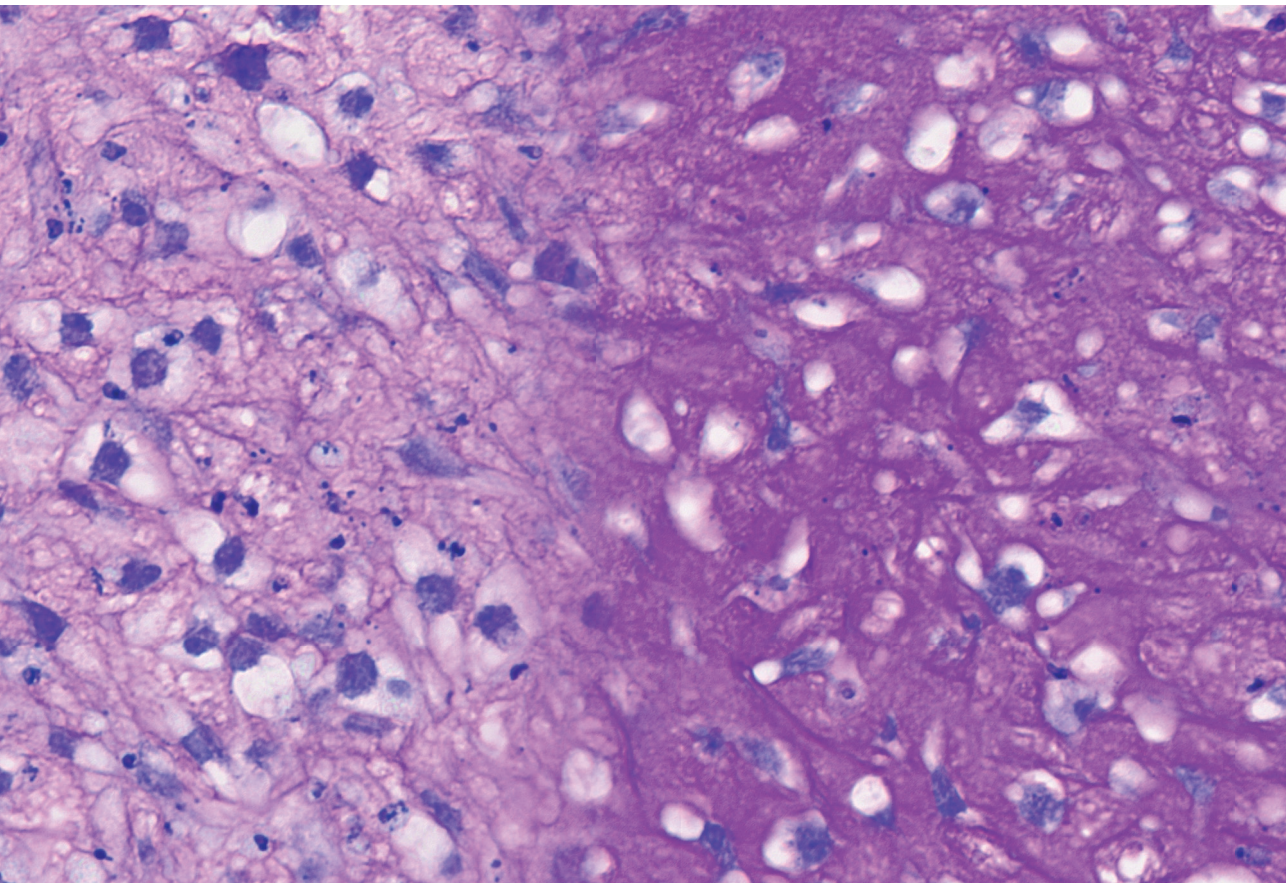
Chapter 2

Inducing senescence during early differentiation reduced the chondrogenic differentiation capacity of mesenchymal stem cells

Chantal Voskamp, Wendy J. L. M. Koevoet, Gerjo J.V.M. van Osch*, Roberto Narcisi*

*Contributed equally

Submitted



2.1 Abstract

Objective. Cellular senescence is a state characterized by stable cell cycle arrest, metabolic alterations, and substantial changes in the gene expression and secretory profile of the cell. Mesenchymal stem/stromal cells (MSCs) are progenitors known for their possible application in cartilage repair strategies, however the effect of senescence on chondrogenic differentiation of MSCs is still poorly investigated. The aim of this study was to investigate how senescence and the senescence associated phenotype (SASP) affect chondrogenic differentiation of MSCs.

Design. Senescence was induced in MSCs during monolayer and at different time points during chondrogenic pellet culture using gamma irradiation. Chondrogenesis was evaluated by (immuno)histochemistry, dimethylmethylene blue assay and RT-PCR. To investigate how the SASP affects cartilage generation, chondrogenic pellets were exposed to medium conditioned by senescent pellets. Western blot analysis on phosphorylated SMAD2 was performed to determine TGF β signaling activation.

Results. Senescent MSCs had a significant reduction in cartilage matrix, when senescence was induced during MSC expansion or at day-7 of differentiation. When senescence was induced at day-14 of differentiation, chondrogenesis was not significantly altered. Moreover, exposure to medium conditioned by senescent pellets had no significant effect on the expression of anabolic or catabolic cartilage markers in recipient chondrogenic pellets, suggesting a neglectable paracrine effect of senescence on cartilage generation in this model. Senescent MSCs had lower phosphorylated SMAD2 levels after stimulation with TGF β 1 than control MSCs.

Conclusions. This study demonstrated that chondrogenesis is reduced when senescence occurs early during MSC differentiation, possibly via a reduced responsiveness to the pro-chondrogenic factor TGF β 1.

2.2 Introduction

Articular cartilage is prone to damage and has a limited repair capability. Full-thickness loss of articular cartilage does not regenerate spontaneously and can lead to the degenerative joint disease osteoarthritis (OA) (Mankin 1982, Shapiro, Koide *et al.* 1993). Current treatment methods such as microfracture or autologous chondrocyte graft implantation have limitations and fail to prevent OA progression (Makris, Gomoll *et al.* 2015). An alternative strategy to repair damaged cartilage uses mesenchymal stem/stromal cells (MSCs). MSCs are progenitor cells that can be isolated from several tissues such as bone marrow, synovial membrane and adipose tissue and have the capacity to differentiate towards the chondrogenic lineage (Pittenger, Mackay *et al.* 1999, Sakaguchi, Sekiya *et al.* 2005).

To obtain enough MSCs to repair a cartilage defect, *in vitro* expansion is necessary. During extensive expansion, MSCs gradually lose their chondrogenic differentiation capacity (Banfi, Bianchi *et al.* 2002, Bonab, Alimoghaddam *et al.* 2006), limiting the applications of these cells. Expansion also triggers cellular senescence, a process leading to an irreversible cell cycle arrest, major metabolic changes and a senescence-associated secretory phenotype (SASP) (Hayflick and Moorhead 1961, Hernandez-Segura, Nehme *et al.* 2018). SASP factors produced by senescent cells include IL-6, IL-8, IL-1 β , TNF α , MMP3 and MMP13 (Philipot, Guérit *et al.* 2014, Basisty, Kale *et al.* 2020, Chung, Chen *et al.* 2020). It is known that these SASP factors can hamper tissue regeneration (Josephson, Bradaschia-Correa *et al.* 2019), for example exposure to TNF α and IL-1 β during *in vitro* chondrogenesis limit the chondrogenic differentiation capacity of MSCs (Wehling, Palmer *et al.* 2009). In addition, SASP factors such as TNF α and IL-1 β are known pro-inflammatory factors contributing to the pathophysiology of OA (Pelletier, Roughley *et al.* 1991, Greene and Loeser 2015). This is further supported by the fact that transplantation of senescent fibroblasts can lead to an OA-like phenotype, including cartilage erosion and delamination of the articular surface (Xu, Bradley *et al.* 2017). In addition, the SASP factors such as CCL2, IL-6, IGFBP4 and IGFBP7 have been suggested to contribute to the spread of cellular senescence in MSC (Severino, Alessio *et al.* 2013, Lehmann, Narcisi *et al.* 2022), known as paracrine senescence (Acosta, Banito *et al.* 2013).

It is known that cellular senescence alters the differentiation capacity of MSCs, especially the effects on the osteogenic and adipogenic lineages are studied. Loss of osteogenic and adipogenic potential has been demonstrated in senescent MSC (Bonab, Alimoghaddam *et al.* 2006), however it has also been reported that in late passaged MSCs the levels of mineralized matrix declines, while adipocyte differentiation increases (Stenderup, Justesen *et al.* 2003, Kim, Kim *et al.* 2012), indicating the complexity of this phenomena. Moreover, cartilage displays a decline in repair capacity with aging (Im, Jung *et al.* 2006), but little is known about the effect of cellular senescence on the chondrogenic differentiation capacity of MSCs. The aim of this study was therefore to determine how cellular senescence and their SASP affect chondrogenesis of MSCs.

2.3 Materials and methods

2.3.1 MSC isolation and expansion

Iliac crest bone chips were obtained from patients (9-13 years) undergoing alveolar bone graft surgery N=13. The tissue was procured as leftover/waste surgical material and it was reviewed and deemed exempt from full ethical review after ethical approval by the Erasmus Medical Ethical Committee (MEC-2014-16,). These pediatric MSCs have been previously characterized and used in this study because they exhibit a low number of senescent cells at early passages (Knuth, Kiernan *et al.* 2018, Lehmann, Narcisi *et al.* 2022). MSCs were isolated by rinsing bone chips twice with 10 mL alpha-MEM (Gibco brand ThermoFisher Scientific, Waltham, MA, USA) supplemented with 10% fetal calf serum (brand ThermoFisher Scientific; selected batch 41Q2047K), 1.5 µg/mL fungizone (Invitrogen brand ThermoFisher Scientific), 50 µg/ml gentamicin (Invitrogen brand ThermoFisher Scientific), 1 ng/mL FGF2 (R&D Systems, Minneapolis, MN, USA) and 0.1 mM ascorbic acid-2-phosphate (Sigma-Aldrich, Zwijndrecht, the Netherlands). The MSCs were plated in T175 flasks and after 24 hours the non-adherent cells were washed away. MSCs were trypsinized at sub-confluency and reseeded in a density of 2,300 cells/cm². MSCs between passage 3 and 6 were used for experiments.

2.3.2 Irradiation of MSCs in monolayer followed by chondrogenic differentiation

Senescence was induced in the cells using 20 Gy ionizing radiation by a RS320 X-Ray machine (X-Strahl, Camberley, UK) (Voskamp, Anderson *et al.* 2021). MSCs in monolayer were irradiated in a T175 flask (60-70% confluency) for 22 min (20 Gy). 24 hours post-irradiation the cells were trypsinized and seeded at a 9,600 cell/cm² density. Mock irradiated MSC were used as non-senescent controls and seeded at 2,300 cells/cm². 7 days post-irradiation, irradiated and non-irradiated MSCs were trypsinized, mixed (0, 25, 50, 75 and 100% irradiated versus non-irradiated cells) and centrifuged at 300 x g for 8 min to obtain pellets of 2x10⁵ cells. To induce chondrogenesis, cell pellets were cultured in chondrogenic medium, containing DMEM-HG medium (Invitrogen brand ThermoFisher Scientific), supplemented by 1% ITS (BD, Franklin Lakes, NJ, USA), 1.5 µg/mL fungizone (Invitrogen brand ThermoFisher Scientific), 50 µg/mL gentamicin (Invitrogen brand ThermoFisher Scientific), 1 mM sodium pyruvate (Invitrogen brand ThermoFisher Scientific), 40 µg/mL proline (Sigma-Aldrich), 10 ng/mL TGFβ1 (R&D Systems), 0.1 mM ascorbic acid-2-phosphate (Sigma-Aldrich) and 100 nM dexamethasone (Sigma-Aldrich) for 7, 14 or 21 days. The medium was renewed twice a week.

2.3.3 Senescence-associated beta-galactosidase staining

To confirm cellular senescence, 7 days post-irradiation, cells from each donor (N=5) were trypsinized and seeded in monolayer cultures in triplicates. Subconfluent cells were washed twice with PBS. Next, the cells were fixed with 0.5% glutaraldehyde and 1% formalin in Milli-Q water for 5 min at room temperature. Then the cells were washed twice with Milli-Q water and subsequently the cells were stained with freshly made X-gal solution containing 0.5% X-gal, 5 mM potassium ferricyanide, 5 mM potassium ferrocyanide, 2mM MgCl₂, 150mM NaCl, 7mM C₆H₈O₇ and 25mM Na₂HPO₄ incubated for 24 hours at 37°C. Cells were counterstained with 1:25 pararosaniline detected with bright field microscopy. Two independent researchers scored at least 100 cells as negative or positive as previously described (Voskamp, Anderson *et al.* 2021).

2.3.4 Irradiation of chondrogenic pellets and conditioned medium

To induce cellular senescence in chondrogenic pellets. Non-irradiated MSCs were cultured in chondrogenic medium and renewed twice a week. MSCs in pellets were irradiated at day 7 or 14 of chondrogenic differentiation in a 15 mL tube for 22 min (20 Gy). Chondrogenic medium was renewed 24 hours after irradiation, next the medium was renewed twice a week. Mock irradiated cells/pellets were used as controls. To determine the effect of SASP factors on chondrogenic differentiation, we generated two different sets of chondrogenic pellets from the same donor, medium donating pellets from irradiated MSCs and medium recipient pellets from non-irradiated MSCs. To determine the effect at different time points during chondrogenesis we analyzed the RNA expression of the medium recipient pellets at day 9 and at day 16.

First, to generate conditioned medium, the medium of the donating pellets was replaced by DMEM-HG medium supplemented with 1% ITS, 1.5 µg/mL fungizone (Invitrogen brand ThermoFisher Scientific), 50 µg/mL gentamicin (Invitrogen brand ThermoFisher Scientific), 1 mM sodium pyruvate (Invitrogen brand ThermoFisher Scientific) and 40 µg/mL proline 24-48 hours before harvesting. The medium from the donating pellets (N=2) was collected and pooled per donor and time point. To remove cell debris, the medium was centrifuged at 14,000 x g for 1 min. Next, medium was mixed with DMEM-HG medium supplemented with 1% ITS, 1.5 µg/mL fungizone (Invitrogen brand ThermoFisher Scientific), 50 µg/mL gentamicin (Invitrogen brand ThermoFisher Scientific), 1 mM sodium pyruvate (Invitrogen brand ThermoFisher Scientific) and 40 µg/mL proline at ratio 3:1, and 0.1 mM ascorbic acid-2-phosphate (Sigma-Aldrich) and 10 ng/ml TGFβ1 was added to the total volume.

The conditioned medium mixture was added to non-irradiated recipient MSCs pellets for 2 consecutive days, specifically at day 7- and 8 (timepoint 9 days), or at day 14- and 15 (timepoint 16 days) during chondrogenic differentiation. 24 h after the last addition of conditioned medium, at day 9 and day 16 respectively, the medium recipient pellets were lysed in RNA-STAT (Tel-Test, Friendswood, TX, USA) for mRNA expression analysis. Media from non-irradiated medium donating MSC pellets using cells from the same donor and at the same time points, were generated and used as a control conditioned media.

2.3.5 (Immuno)Histochemistry chondrogenic pellets

Pellets were fixed with 3.7% formaldehyde after 7, 14 or 21 days of chondrogenic induction. Next, pellets were embedded in paraffin and sectioned at 6 μm . To detect glycosaminoglycans, sections were stained with 0.04% thionine solution. To detect collagen type-2, sections were first treated with 0.1% Pronase (Sigma-Aldrich) in PBS for 30 min at 37°C, followed by 1% hyaluronidase (Sigma-Aldrich) in PBS for 30 min at 37°C. Sections were incubated with 10% normal goat serum (Sigma-Aldrich) and 1% bovine serum albumin (Sigma-Aldrich) in PBS for 30 min, followed by incubation with the collagen type-2 antibody (II-II 6B3, Developmental Studies Hybridoma Bank) for 1h. Then samples were incubated with a biotin-conjugated antibody (HK-325-UM, Biogenex) for 30 min, followed by incubation with alkaline phosphatase-conjugated streptavidin (HK-321-UK, Biogenex) for 30 min. New Fuchsin chromogen (B467, Chroma Gesellschaft) was used as a substrate. As a negative control an IgG1 isotype antibody (X0931, Dako Cytomation) was used. The positive area per pellet was determined using ImageJ software.

2.3.6 Osteogenic and adipogenic differentiation

To induce osteogenic differentiation, expanded MSCs were trypsinized, seeded at a density of 1.2×10^4 cells/cm² and cultured in DMEM HG medium (Gibco brand ThermoFisher Scientific) with 10% fetal calf serum (Gibco brand ThermoFisher Scientific), 1.5 $\mu\text{g}/\text{mL}$ fungizone (Invitrogen brand ThermoFisher Scientific), 50 $\mu\text{g}/\text{mL}$ gentamicin (Invitrogen brand ThermoFisher Scientific), 10 mM β -glycerophosphate (Sigma-Aldrich), 0.1 μM dexamethasone (Sigma-Aldrich) and 0.1 mM ascorbic acid-2-phosphate (Sigma-Aldrich) for 12-21 days. To detect calcium deposits the cultures were fixed in 3.7% formaldehyde, followed by hydration with Milli-Q water and incubation with 5% silver nitrate solution (Von Kossa; Sigma Aldrich) for 1 h in the presence of bright light. Next, the cultures were washed with distilled water followed by counterstaining with 0.4% thionine (Sigma-Aldrich). MSCs were used in triplicates (N=3 donors). To induce adipogenic differentiation, expanded MSCs were trypsinized, seeded in a density of 2×10^4 cells/cm² and cultured in DMEM HG (Gibco brand ThermoFisher Scientific) with 10% fetal calf serum (Gibco brand ThermoFisher Scientific), 1.5 $\mu\text{g}/\text{mL}$ fungizone (Invitrogen brand ThermoFisher Scientific), 50 $\mu\text{g}/\text{mL}$ gentamicin (Invitrogen brand ThermoFisher Scientific), 1.0 μM dexamethasone (Sigma-Aldrich), 0.2 mM indomethacin (Sigma-

Aldrich), 0.01 mg/mL insulin (Sigma-Aldrich) and 0.5 mM 3-isobutyl-1-methyl-xanthine (Sigma-Aldrich) for 21 days. To detect intracellular lipid accumulation, cells were fixed in 3.7% formaldehyde, followed by incubation with 0.3% Oil red O solution (Sigma-Aldrich) for 10 min and washes with distilled water. MSCs were used in triplicates (N=3 donors).

2.3.7 DNA and Glycosaminoglycan (GAG) Quantification

Pellets were digested at day 21 of chondrogenic differentiation using 1 mg/mL Proteinase K, 1 mM iodoacetamide, 10 µg/mL Pepstatin A in 50 mM Tris, 1 mM EDTA buffer (pH 7.6; all Sigma-Aldrich) for 16 h at 56°C, followed by Proteinase K inactivation at 100°C for 10 min. Afterwards, to determine the amount of DNA, cell lysates were treated with 0.415 IU heparin and 1.25 µg RNase for 30 min at 37°C followed by addition of 30 µL CYQUANT GR solution (Invitrogen). Samples were analyzed using a SpectraMax Gemini plate reader with an excitation of 480 nm and an emission of 520 nm. As a standard, DNA sodium salt from calf thymus (Sigma-Aldrich) was used. To determine the amount of GAG, cell lysates were incubated with 1,9-dimethylmethylene blue (DMB) as previously described by Ferndale *et al.* (Farndale, Buttle *et al.* 1986), and analyzed with an extinction of 590 nm and 530 nm. The 530:590 nm ratio was used to determine the glycosaminoglycan concentration. As a standard chondroitin sulfate sodium salt from shark cartilage (Sigma-Aldrich) was used.

2.3.8 mRNA Expression analysis

For both MSCs in pellet cultures and MSCs in monolayer cultures, the medium was renewed 24 hours before cell lysis. Pellets were washed twice with PBS, lysed in RNA-STAT (Tel-Test) and manually homogenized. Next, RNA was isolated using chloroform and purified using the RNeasy micro kit (Qiagen, Hilden, Germany) following the manufacturer's protocol. MSCs in monolayer were washed twice with PBS and RNA was isolated using RLT lysis buffer supplemented with 1% β-mercaptoethanol. Subsequently, RNA was purified using the RNeasy micro kit using the manufacturer's protocol. The RevertAid First Strand cDNA synthesis kit (Fermentas brand ThermoFisher Scientific) was used to reverse transcribe the RNA to cDNA. Next, real-time polymerase chain reactions were done with SYBR Green (Fermentas brand ThermoFisher Scientific) and TaqMan (Applied Biosystems brand ThermoFisher Scientific) MasterMix on a CFX96™ PCR machine (Bio-Rad, Hercules, CA, USA) using different primers listed in **Table 2.1**. Genes with a housekeeping function are

often used as reference genes for qPCR analysis, however senescent cells often have altered their housekeeping functions (Hernandez-Segura, Rubingh *et al.* 2019). Therefore, we tested four different housekeeping genes (*GAPDH*, *HPRT1*, *RPS27A* and *ACTB*) for each dataset and only used the genes that were stable across the different conditions as reference. Gene expression levels were calculated using the $2^{-\Delta C_t}$ formula.

2.3.9 Western blot

Irradiated MSCs and non-irradiated MSCs in monolayer were serum starved for 16 h in alpha-MEM (Invitrogen) supplemented with 1% BSA, 1.5 $\mu\text{g}/\text{mL}$ fungizone (Invitrogen) and 50 $\mu\text{g}/\text{mL}$ gentamicin (Invitrogen). Next, MSCs were stimulated with 0 or 10 ng/mL TGF β 1 for 30 min and subsequently, cells were lysed in MPER lysis buffer (ThermoFisher Scientific) with 1% Halt Protease Inhibitor (ThermoFisher Scientific) and 1% Halt Phosphatase Inhibitor (ThermoFisher Scientific). Protein samples, from MSCs from different donors (N=3 donors, in triplicates), were separated on a 4-12% SDS-PAGE gel (ThermoFisher Scientific) by electrophoresis using an equal amount of protein (5-12 μg) per sample. Proteins were transferred semi-wet from the SDS-PAGE gel on a nitrocellulose membrane (Millipore). The membrane was transferred to a 5% dry milk powder blocking solution in Tris-Buffered Saline with 0.1% Tween-20 (Millipore Sigma; TBST) for 3 h. Next, the membrane was incubated with the primary monoclonal rabbit antibody against phospho-SMAD2 Ser465/Ser467 (Cell Signaling technology; 3108S;) using a 1:1000 dilution in 5% BSA in TBST overnight at 4°C. Later, the membrane was incubated with a secondary anti-rabbit antibody conjugated with peroxidase (Cell Signaling, 7074S) using a 1:1000 dilution in 5% dry milk powder in TBST for 1.5 h at room temperature. Phospho-SMAD2 signal was detected with the SuperSignal Wester Pico Complete Rabbit IgG detection kit (ThermoFisher Scientific).

3.3.10 Data analysis

The Kolmogorov-Smirnov test was used to verify the normal (Gaussian) distribution of all the histology, RNA expression and western blot data. For statistical evaluation, a linear mixed model was applied, using the different conditions as fixed parameters and the donors as random factors. Bonferroni post-hoc test was used to correct for multiple comparisons. Data analysis was performed using PSAW statistics 20 software (SPSS Inc., Chicago, IL, USA). *p*-values less than 0.05 were considered as statistically significant.

Table 2.1- Primer sequences

Gene	Forward	Reverse	Probe	Method
<i>CDKN2A</i> (<i>P16</i>)	GATCCAGGTG- GGTAGAAGGTC	CCCCTG- CAAACCTTCGT- CCT	-	SYBR Green
<i>CDKN1A</i> (<i>P21</i>)	TGTCCGT- CAGGACCCA- TGC	AAAGTCGAAGT- TCCATCGCTC	-	SYBR Green
<i>IL6</i>	ACTCACCTCTT- CAGAACGAAT- TG	CCATCTTTG- GAAGGTTTCAG- GTTG	-	SYBR Green
<i>FABP4</i>	TGTCTCCAGT- GAAAACTTT- GATGATTA	CCATGCCAGC- CACTTTCC	-	SYBR Green
<i>PPARG</i>	AGGGCGATCT- TGACAGGAAA	TCTCCCATCA- TTAAGGAATT- CATG	ACAACAGA- CAAATCACCAT- TCGTTATCT	TaqMan
<i>RUNX2</i>	ACGTCCCCGTC- CATCCA	TGGCAGTGT- CATCATCT- GAAATG	ACTGGGCT- TCTTGCCATCA- CCGA	TaqMan
<i>ALPL</i>	GACCCTTGAC- CCCCACAAT	GCTCGTACTG- CATGTCCCCT	TGGACTACC- TATTGG- GTCTCTTCGAG- CCA	TaqMan
<i>COL2A1</i>	GGCAATAGCAG- GTTTCACGTACA	CGA- TAACAGTCTTG- CCCCACTT	CCGGTATGTTT- CGTGCAGCCA- TCCT	TaqMan
<i>ACAN</i>	TCGAGGACAG- CGAGGCC	TCGAGGGTG- TAGCGTGTAGA- GA	ATGGAACAC- GATGCCTTTCA- CCACGA	TaqMan
<i>SOX9</i>	TCCACGAAGG- GCCGC	CAACGCC- GAGCTCAGCA	TGGG- CAAGCTCTG- GAGACTTCT- GAACG	TaqMan
<i>MMP3</i>	TTTTGGCCA- TCTCTCCTT- CA	TGTGGATG- CCTCTTGGG- TATC	AACTTCATAT- GCGGCATCCA- CGCC	TaqMan
<i>MMP1</i>	CTCAATTT- CACTTCTGTTT- TCTG	CATCTCTGTCG- GCAAATTCGT	CACAACCTGC- CAAATGGGCTT- GAAGC	TaqMan
<i>MMP13</i>	AAGGAGCATG- GCGACTTCT	TGGCCCAG- GAGGAAAAGC	CCCTCTGG- CCTGCTGGCT- CA	TaqMan

(Continued on next page)

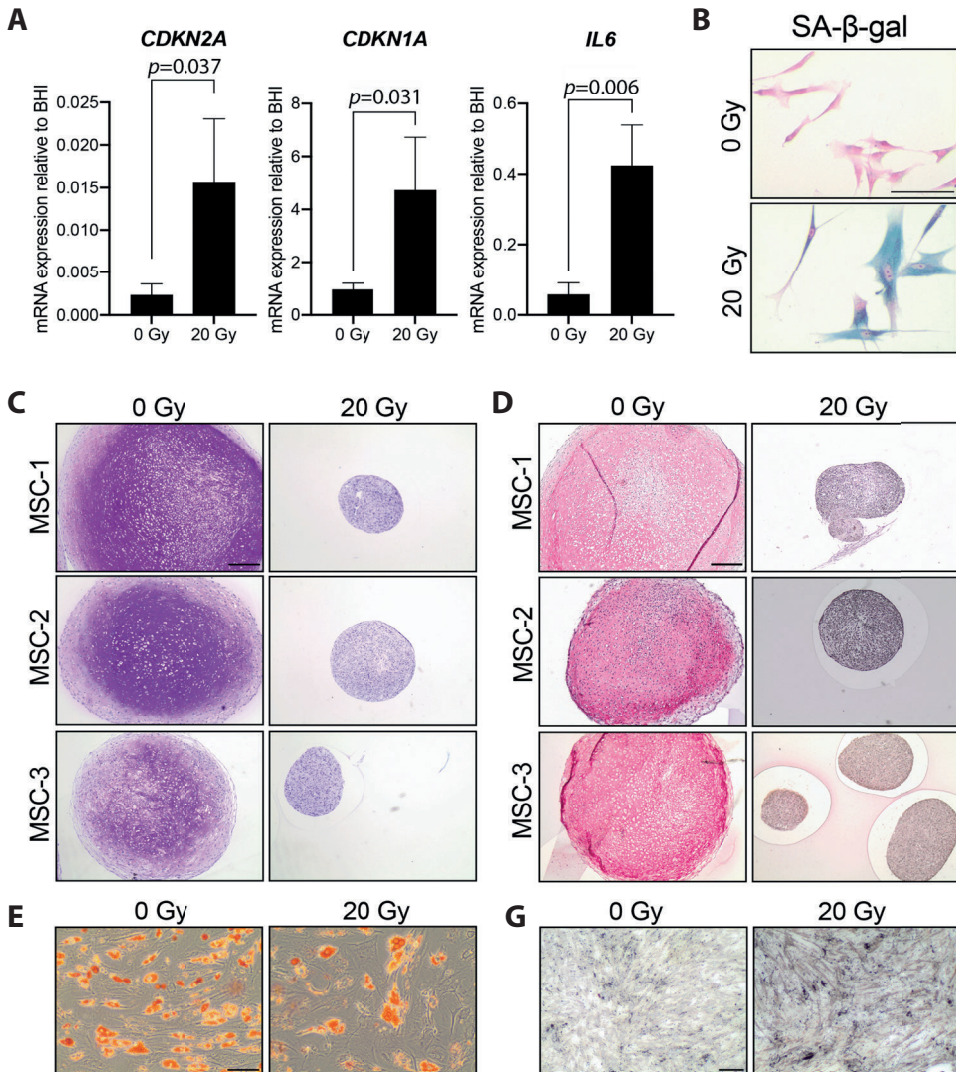
Continued

Gene	Forward	Reverse	Probe	Method
<i>ADAMTS4</i>	CAAGGTCCCAT- GTGCAACGT	CATCTGCCAC- CACCAGTGTCT	CCGAAGAGC- CAAGCGCTTT- GCTTC	TaqMan
<i>COL1A1</i>	CAGCCGCTT- CACCTACAGC	TTTTGTATT- CAATCACT- GTCTTGCC	CCGGTGTG- ACTCGTGCAG- CCATC	TaqMan
<i>COL10A1</i>	CAAGGCACCA- TCTCCAGGAA	AAAGGGTATT- TGTGGCAGCA- TATT	TCCAGCACG- CAGAATCCA- TCTGA	TaqMan
<i>RPS27A</i>	TGGCTGTCCT- GAAATATTA- TAAGGT	CCCCAGCAC- CACATTCATCA	-	SYBR Green
<i>GAPDH</i>	ATGGGGAAAG- GTGAAGGTCG	TAAAAGCAGC- CCTGGTGACC	CGCCCAATACG- ACCAAATCCGT- TGAC	TaqMan
<i>HPRT1</i>	TTATGGACAGG- ACTGAACGTCT- TG	GCACACAGAG- GGCTACCAT- GTG	AGATGTGAT- GAAGGAGATG- GGAGGCCA	TaqMan
<i>ACTB</i>	ACCGGGCA- TAGTGTTGGA	ATGGTACACG- GTTCTCAACA- TC	-	SYBR Green

2.4 Results**2.4.1 Cellular senescence impaired the chondrogenic capacity of MSCs**

Cellular senescence was induced in monolayer MSCs using gamma irradiation (20 Gy) and confirmed by an increased mRNA expression of cell-cycle dependent *CDKN2A* (6.9-fold) and *CDKN1A* (4.8-fold), a higher mRNA expression of the SASP associated gene *IL6* (8.6-fold) and a higher percentage of senescence associated β -galactosidase positive cells than the mock treated control MSCs (0 Gy; **Figure 2.1A-B**). After 21 days of chondrogenic induction, irradiated MSCs, had an impaired capacity to deposit the typical chondrogenic extracellular proteins GAG and COL2 (**Figure 2.1C-D**). To determine whether senescent MSCs have an overall reduced differentiation capacity or whether it was specific for the chondrogenic lineage, we assessed their osteogenic and adipogenic differentiation capacity. After adipogenic differentiation, the cells show lipid accumulation and expression of adipogenic

genes *PPRG* and *FABP4* in both the irradiated and non-irradiated cells, (**Figure 2.1E-F**) although for *FABP4* a reduced expression was detected compared to control MSCs. After osteogenic differentiation, irradiated and non-irradiated cells show no significant differences in the osteogenic markers *RUNX2* and *ALPL* (**Figure 2.1G-H**). Overall, these results indicate that senescent MSCs can differentiate towards the adipogenic and the osteogenic lineage, while a strong negative effect was detected specifically for the chondrogenic differentiation.



(Continued on next page)

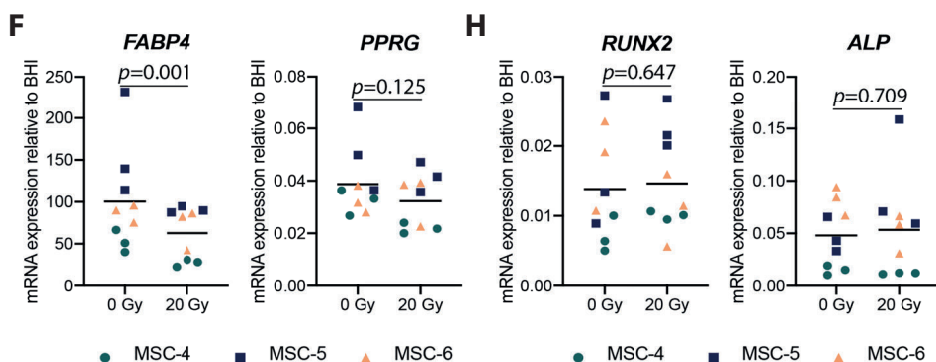


Figure 2.1 – Chondrogenic differentiation was impaired in senescent MSCs.

(A) MSCs that were gamma irradiated (20 Gy) or mock irradiated (0 Gy) after expansion. *CDKN2A* (*P16*), *CDKN1A* (*P21*) and *IL6* mRNA relative to the best housekeeping index (BHI; *GAPDH*, *HPRT*, *RPS27A* and *ACTB*). N=3 donors with 2-3 replicates per donor. Data show grand mean and standard deviation.

(B) Representative images of MSCs stained for senescence-associated β -galactosidase (SA- β -gal) activity. Scale bar represents 100 μ m. N=3 donors with 2-3 replicates per donor.

(C-D) Representative images of Thionine (C) and Collagen type 2 (D) staining of pellets of (mock-)irradiated MSCs that were chondrogenically differentiated for 21 days. Scale bar represents 250 μ m. N=3 donors with 3 pellets per donor.

(E) Representative images of Oil red O staining of (mock-)irradiated MSCs that were differentiated towards adipogenic lineage for 21 days. Scale bar represents 100 μ m, N=3 donors with 3 replicates per donor.

(F) *FABP4* and *PPARG* mRNA expression relative to the best housekeeping index (BHI; *GAPDH*, *RPS27A* and *ACTB*) of MSCs that were differentiated towards adipogenic lineage for 21 days. N=3 donors with 3 replicates per donor.

(G) Representative images of Von Kossa staining of (mock-)irradiated MSC that were differentiated towards osteogenic lineage for 14-21 days. Scale bar represents 200 μ m, N=3 donors with 3 replicates per donor.

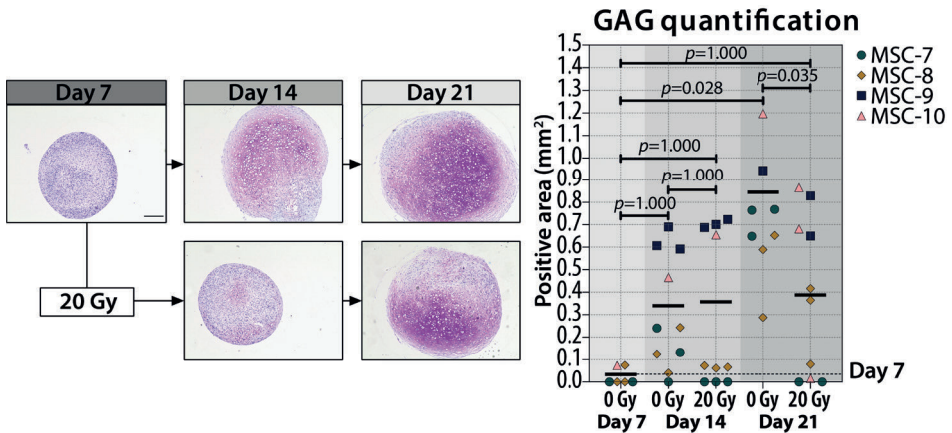
(H) *RUNX2* and *ALP* mRNA expression relative to the best housekeeping index (BHI; *GAPDH*, *RPS27A* and *ACTB*) of MSCs that were differentiated towards osteogenic lineage for 14-21 days. N=3 donors with 3 replicates per donor. Data show individual data points and grand mean. *p*-values were obtained with the linear mixed model, using the different irradiation conditions as fixed parameters and the donors as random factors.

2.4.2 Senescence during early MSC differentiation inhibited cartilage formation

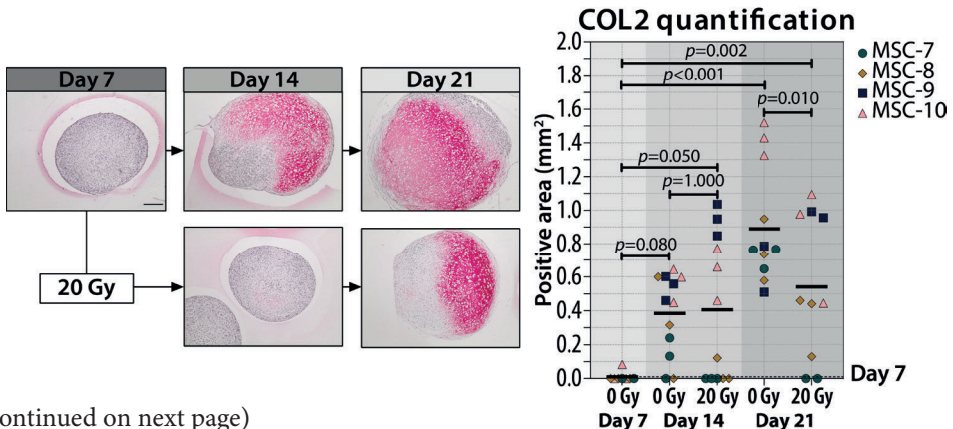
In order to understand whether cellular senescence is affecting chondrogenic differentiation only when induced in specific differentiation stages, we used non senescent MSCs to generate pellets and triggered senescence by irradiation during chondrogenic differentiation. Specifically, we induced senescence in pellet cultures by gamma irradiation (20 Gy) at 7 or 14 days of chondrogenesis, in a 21-day differentiation protocol. As expected, mock treated pellets (0 Gy) had

an increased GAG deposition over time and the deposition is highest at day 21 of chondrogenic differentiation ($p=0.028$ compared to day 7), while pellets treated with 20 Gy at day 7 of culture had an average of 1.6-fold reduction of GAG deposition at day 21 compared to controls (**Figure 2.2A** and Supplementary **Figure 2.1**; $p=0.035$). Immunostaining revealed an overall similar pattern between COL2 and GAG deposition, with a lower COL2 deposition detected at day 21 in day7-irradiated pellets compared to control pellets (**Figure 2.2B** and **Figure S2.2**; $p=0.010$). At gene expression level, *COL2A1* and *ACAN* significantly increased over time in both irradiated and control conditions, but at day 21 the day7-irradiated pellets showed a significant reduced expression compared to control (**Figure 2.2C**; *COL2A1* and *ACAN*). The transcription factor *SOX9* did not strongly increase over time and its expression was lower in day7-irradiated pellets compared to control at day 21 (**Figure 2.2C**; *SOX9*). Between day 14 and day 21 of chondrogenic differentiation, gene expression of *COL2A1*, *ACAN* and *SOX9* remained similar ($p=1.000$).

A



B



(Continued on next page)

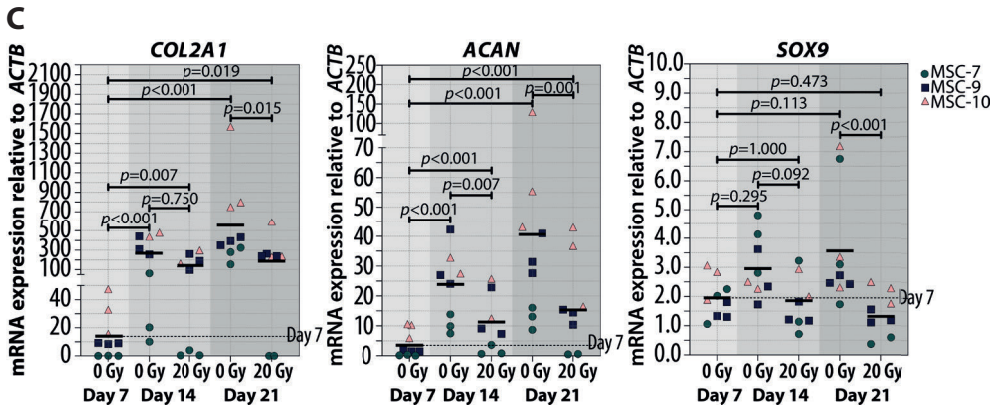
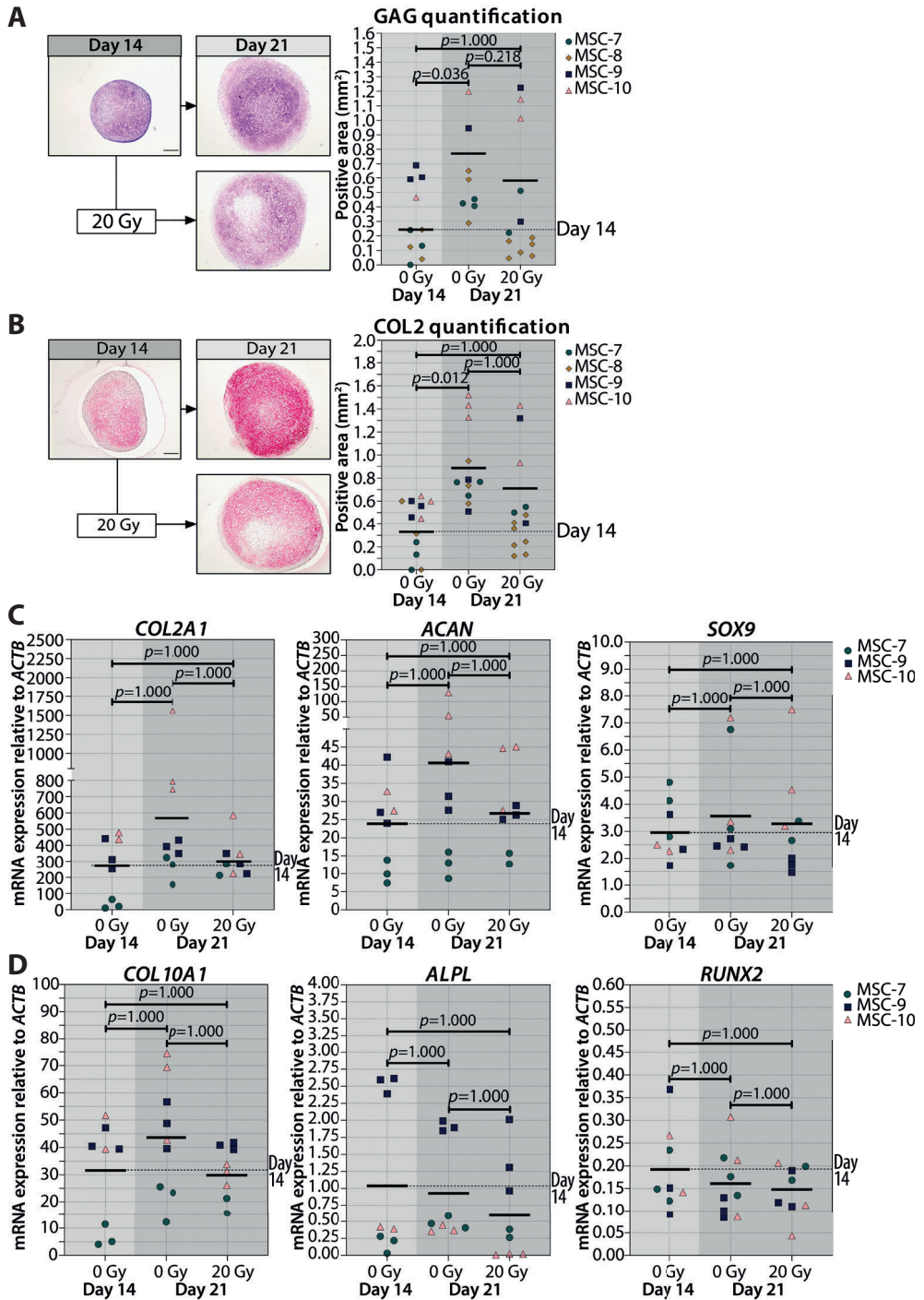


Figure 2.2 – 20 Gy irradiation at day 7 during MSC differentiation reduced chondrogenic markers at day 21.

(A-B; left panels) Representative images of (A) Thionine (GAG) and (B) Collagen type 2 (COL2) staining of MSC control pellets that were chondrogenically differentiated for 7, 14 and 21 days or MSC pellets that were irradiated at day 7 during chondrogenic differentiation and subsequently differentiated for 7 or 14 days. The scale bar represents 200 μm . (A-B; right panels) Quantification of (A) GAG or (B) COL2 positive area per condition in mm^2 . $N=4$ donors with 1-3 replicates per donor.

(C) Gene expression of chondrogenic markers in MSC control pellets that were chondrogenically differentiated for 7, 14 and 21 days or MSC pellets that were irradiated at day 7 during chondrogenic differentiation and subsequently differentiated for 7 and 14 days. Gene expression levels were normalized using *ACTB*. $N=3$ donors with 2-3 replicates per donor. Data show individual data points and grand mean. p -values were obtained with the linear mixed model, using the different irradiation conditions as fixed parameters and the donors as random factors.

Interestingly, when we irradiated the pellets at day14 the deposition of GAG and COL2 did not change compared to non-irradiated controls (**Figure 2.3A-B** and **Figure S2.3**). Similarly, *COL2A1*, *ACAN* and *SOX9* gene expression at day 21 were comparable between day-14 irradiated pellets and controls (**Figure 2.3C**). Overall, these data suggest that the chondrogenesis of MSCs was not negatively influenced by irradiation at day 14. To test whether there was at least an effect on the known hypertrophic tendency of MSCs during chondrogenesis, *COL10A1*, *ALPL* and *RUNX2* expression were analyzed. No differences in *COL10A1*, *ALPL* and *RUNX2* expression were observed between day14-irradiated and mock treated pellets (**Figure 2.3D**). Although with donor variation, these data suggest that senescence during early differentiation (day-7) inhibits chondrogenic maturation, while senescence during late chondrogenesis (day-14) has no evident effect.



(Legend on next page)

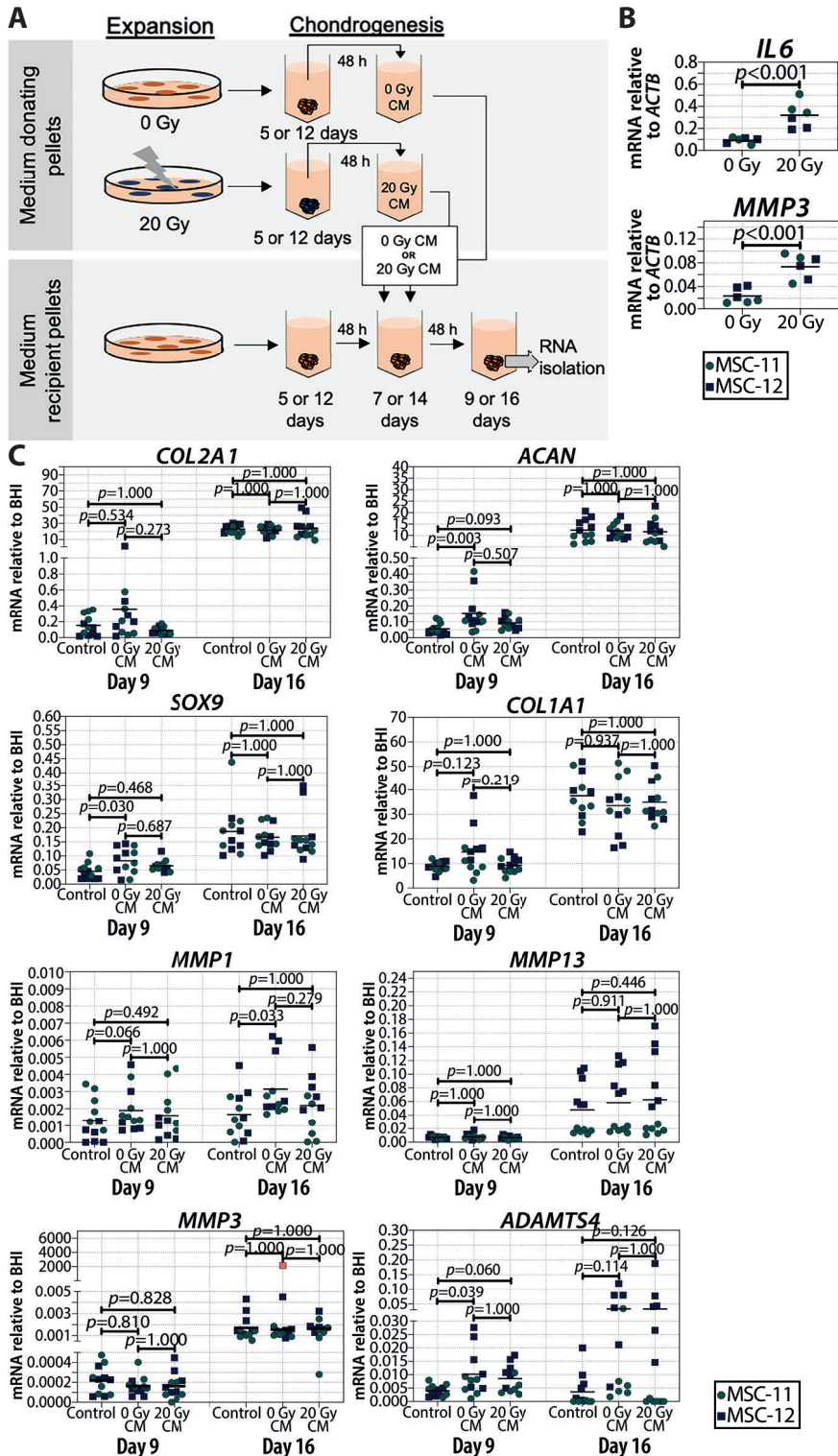
◀ **Figure 2.3 - Irradiation at day 14 during MSC differentiation did not alter chondrogenic markers at day 21.**

(A-B; left panels) Representative images of (A) Thionine (GAG) and (B) Collagen type 2 (COL2) staining of MSC control pellets that were chondrogenically differentiated for 14 and 21 days or MSC pellets that were irradiated at day 14 during chondrogenic differentiation and subsequently differentiated for 7. The scale bar represents 200 μm . (A-B; right panels) Quantification of (A) GAG or (B) COL2 positive area per condition in mm^2 . N=4 donors with 1-7 replicates per donor.

(C-D) Gene expression of (C) chondrogenic markers and (D) hypertrophic markers in MSC control pellets that were chondrogenically differentiated for 14 and 21 days or MSC pellets that were irradiated at day 14 during chondrogenic differentiation and subsequently differentiated for 7 days. Gene expression levels were normalized using *ACTB*. N=3 donors with 2-3 replicates per donor. Data show individual data points and grand mean. *p*-values were obtained with the linear mixed model, using the different irradiation conditions as fixed parameters and the donors as random factors.

2.4.3 Conditioned medium of senescent pellets had no major effect on cartilage formation

Senescent cells can affect their surrounding cells via the secretion of a SASP (Coppé, Desprez *et al.* 2010). To investigate whether or not the SASP contributes to reduced cartilage formation in chondrogenic pellets, conditioned medium of control and senescent pellets during chondrogenic differentiation (day 5-6 and day 12-13) was generated and added to non-irradiated recipient chondrogenic pellets at day 7 or day 14 (**Figure 2.4A**). First, we confirmed an increased expression of selected SASP factors *IL6* ($p < 0.001$) and *MMP3* ($p < 0.001$) in the irradiated pellets compared to non-irradiated control pellets (**Figure 2.4B**). Next, after exposition to the conditioned media of senescent pellets, we observed that *COL2A1*, *ACAN*, *SOX9* and *COL1A1* expression were not significantly different compared to the control pellets cultured in control conditioned media (**Figure 2.4C**), suggesting that factors secreted from senescent cells during chondrogenesis do not directly alter the expression of chondrogenic genes in recipient pellets in our experimental conditions. To understand whether the absence of changes in the expression of chondrogenic markers was influenced by an altered expression in catabolic genes, we analyzed the expression of *MMP13*, *MMP1*, *MMP3* and *ADAMTS4*. Pellets cultured in conditioned medium of irradiated pellets had similar expression of catabolic genes as pellets cultured in control conditioned medium at both day-9 and day-16 of chondrogenic differentiation (**Figure 2.4C**). Overall, these results suggest that the SASP-factors produced by senescent cells in the pellets have no major direct effect at different stages of cartilage formation.



(Legend on next page)

◀ **Figure 2.4 – Conditioned medium from pellets of senescent MSCs did not alter the expression of chondrogenic genes in recipient non-senescent pellets.**

(A) Schematic overview of experimental setup.

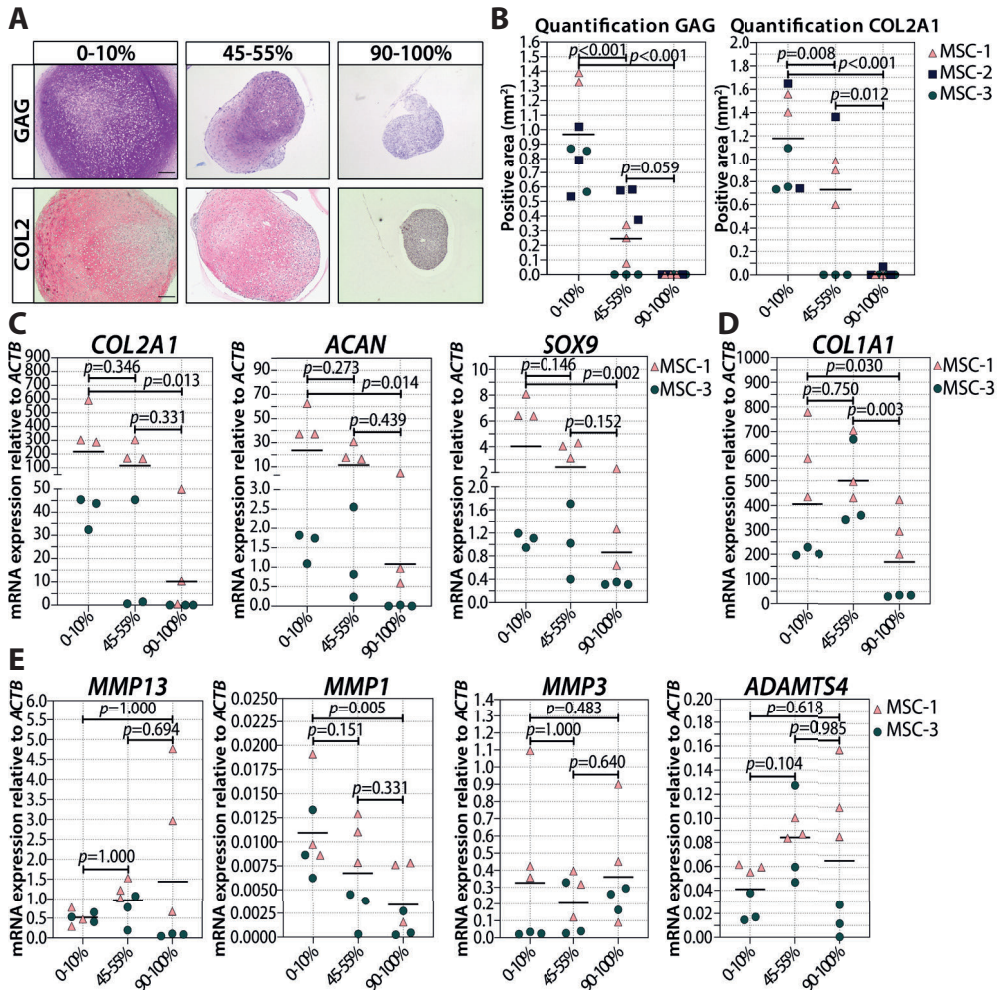
(B) mRNA expression of day 16 of chondrogenically differentiated pellets from 20 Gy gamma irradiated (during monolayer expansion) or not irradiated MSCs. N=2 donors with 3 replicates per donor.

(C) mRNA expression of MSC pellets that were chondrogenically differentiated for 9 or 16 days and treated with conditioned medium for the last 48 h. The conditioned medium was obtained from chondrogenic pellets from MSCs that were irradiated with 20 Gy or not irradiated during expansion. Gene expression levels were normalized using best housekeeping index (BHI; *GADPH*, *HPRT* and *RSP27A*). *MMP3* data shows one outlier in red. This value was excluded from the statistical analysis. N=2 donors with 6 replicates per donor. Data show individual data points and grand mean. *p*-values were obtained with the linear mixed model, using the different irradiation conditions as fixed parameters and the donors as random factors.

2.4.4 The number of senescent cells is associated with a reduced cartilage production

Next, we asked if the observed negative effect on chondrogenesis was dependent on the number of senescent cells present at the moment of pellet formation. To answer these questions, we generated pellets starting with a different ratio of irradiated and non-irradiated cells and we monitored their chondrogenic differentiation capacity. The number of irradiation-induced senescent cells prior to chondrogenic differentiation was indeed associated with a reduced GAG and COL2 deposition (**Figure 2.5A-B** and **Figure S2.4**) and both GAG and DNA content in chondrogenic pellets were negatively associated with the number of senescent MSCs (**Figure S2.4B-C**). MSC pellets with 20-30% senescent MSCs had an average of 42% lower GAG content than pellets with non-irradiated cells (**Figure S2.4**; $p=0.008$), suggesting that a low percentage of senescent cells already has a significant effect on the GAG deposition. MSC pellets with 45-55% senescent MSCs had, on average, 55% lower GAG/DNA than pellets with non-irradiated cells (**Figure S2.4**; $p=0.003$), indicating that the non-senescent MSCs were still able to deposit GAG in the mixed pellets. Histological analysis showed clearly reduced GAG and COL2 deposition in MSC pellets with 45-55% senescent MSCs compared to pellets with non-irradiated cells (**Figure 2.5A-B** and **Figure S2.5**). Furthermore, MSC pellets with 45-55% senescent MSCs had lower expression of *COL2A1*, *SOX9* and *ACAN* at day 21 of chondrogenic differentiation compared to non-senescent control MSCs, albeit not statistically significant (**Figure 2.5C**). MSC pellets with 70-80% senescent MSCs had a lower GAG content compared

to MSC pellets with 45-55% senescent MSCs, however these pellets still deposited GAG (**Figure S2.4**). On the other side, pellets with more than 90% senescent cells did not deposit GAG (**Figure 2.5A-B**). These pellets also had a low expression of *COL2A1* (97% reduced compared to non-senescent control MSCs; $p=0.013$), *SOX9* (75% reduced compared to non-senescent control MSCs, $p=0.002$) and *ACAN* (97% reduced compared to non-senescent control MSCs, $p=0.014$). No significant differences in the expression of *COL1A1* and the catabolic markers *MMP13*, *MMP1*, *MMP3*, *ADAMTS4* were observed between the different conditions (**Figure 2.5D-E**). These data may suggest that there is an inverse association between the number of senescent cells and the ability of generating cartilage.



(Legend on next page)

◀ **Figure 2.5 – Higher ratio of senescent to non-senescent MSC resulted in less cartilage markers.**

(A-B) Representative images of Thionine and Collagen type 2 staining of MSCs that were gamma irradiated during expansion with 0 or 20 Gy, mixed and subsequently chondrogenically differentiated for 21 days. Scale bar represents 200 μm . N=3 donor with 2-3 pellets per donor.

(C-E) mRNA expression of MSC pellets that were gamma irradiated during expansion with 0 or 20 Gy, mixed and subsequently chondrogenically differentiated for 21 days. Gene expression levels were normalized using *ACTB*. Data show individual data points and grand mean. *p*-values were obtained with the linear mixed model, using the experimental conditions as fixed parameters and the donors as random factors.

2.4.5 Senescent MSCs are less responsive to TGF β signaling

TGF β is the main driver of chondrogenesis in MSC. In order to understand the reason why senescent cells have a reduced capacity to differentiate towards the chondrogenic lineage, we analyzed the TGF β signaling activation by detecting the pSMAD2 levels in both irradiated MSCs (20 Gy) and control MSCs (0 Gy) upon TGF β 1 stimulation. In the presence of TGF β 1, pSMAD2 levels were higher in non-irradiated control MSCs compared to irradiated MSCs (**Figure 2.6A**; +TGF β and **Figure 2.6B**; 6.9-fold, $p=0.020$), while no detectable pSMAD2 levels were present in MSCs without TGF β 1 stimulation (**Figure 2.6A**; -TGF β). These data suggest that senescent MSCs are less responsive to TGF β 1, indicating that the reduced chondrogenic potential may be caused by a cell-intrinsic mechanism.

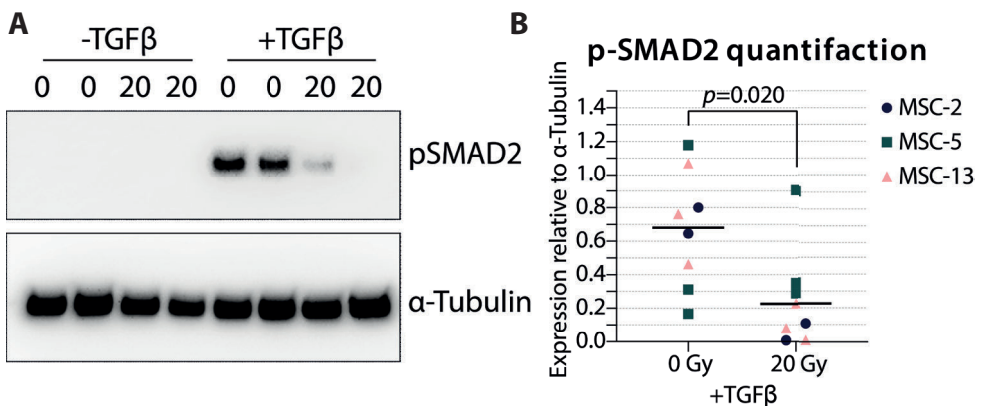


Figure 2.6 – Senescent MSCs had low TGF β induced phosphorylated SMAD2 levels.

(A) Western blot for phosphorylated SMAD2 (p-SMAD2).

(B) Quantification of western blot results relative to α -Tubulin. N=3 donors with 2-3 biological replicates per donor. Data show individual data points and grand mean. *p*-values were obtained with the linear mixed model, using the different experimental conditions as fixed parameters and the donors as random factors.

2.5 Discussion

MSCs are promising cells for cartilage tissue regeneration therapies. To obtain reproducible and safe clinical outcomes it is necessary to understand how the chondrogenic differentiation capacity in MSC populations is regulated. In this study, we demonstrated that cellular senescence impairs the chondrogenic differentiation capacity of MSCs, we showed there is an association between the number of senescent cells at the start of the culture and the reduced chondrogenic differentiation potential, and we observed that senescent cells have a reduced ability to respond to TGF β , the main factor responsible for chondrogenic differentiation of MSCs.

MSCs are a heterogeneous population of cells and the number of senescent cells varies between MSC cultures from different patients (Schellenberg, Stiehl *et al.* 2012) and, most importantly, with passaging *in vitro* (Bonab, Alimoghaddam *et al.* 2006, Lehmann, Narcisi *et al.* 2022). Here, we show for the first time that an increased number of senescent cells contribute to a reduced chondrogenic differentiation potential, indicating that the appearance of cellular senescence can contribute to heterogeneity in chondrogenic differentiation between MSC populations. This may be also linked with our previous observation that different MSC subtypes have a distinct differentiation capacity (Sivasubramaniyan, Ilas *et al.* 2018, Sivasubramaniyan, Koevoet *et al.* 2019). Furthermore, we show that in a mixed population with senescent MSCs, non-senescent MSCs are still able to differentiate towards the chondrogenic lineage and that the secretome of the senescent cells do not grossly influence the differentiation of neighboring non-senescent cells.

Our results suggest that senescent MSCs, while losing their chondrogenic differentiation potential, generally keep their osteogenic and adipogenic differentiation capacity. However, we identified some differences between gene expression and staining, specifically for the osteogenic assay. In fact, while mineral deposition seems slightly increased in irradiated MSCs, gene expression levels for osteogenic markers remain unaffected. This may explain why in the literature there is still no uniformed consensus on the effect of senescence in MSCs, with authors claiming minimal effect on osteogenic differentiation in late-passaged cells (Bonab, Alimoghaddam *et al.* 2006), others

claiming upregulation (Wagner, Horn *et al.* 2008) or even down-regulation of osteogenic differentiation (Geissler, Textor *et al.* 2012, Despars, Carbonneau *et al.* 2013) with passaging or senescence. This discrepancy might also be linked with the timing of senescence induction during the experiments or could possibly be due to the different ways to induce senescence. Indeed, we and others previously observed different senescence phenotypes depending on the way senescence was induced (Wiley, Velarde *et al.* 2016, Voskamp, Anderson *et al.* 2021), and we cannot exclude that this may have a different impact on MSC differentiation.

In this study we demonstrated that the effect of irradiation-induced cellular senescence is largest during the early phases of chondrogenic differentiation. It has been shown that proliferation during the early phase of chondrogenesis is essential for proper chondrogenic differentiation (Dexheimer, Frank *et al.* 2012). This indicates that impaired proliferation could be an explanation why MSCs failed to differentiate towards the chondrogenic lineage specifically when senescence is induced in monolayer or early during differentiation. Another explanation could be related to the differences we observed in the TGF β signaling pathway activation in senescent MSCs compared to non-senescent MSCs. The TGF β signaling has an important role in cartilage development and cartilage homeostasis (Thielen, van der Kraan *et al.* 2019). Particularly in the early phases of (re)differentiation, Smad2/3 phosphorylation is essential for chondrogenesis of MSCs (Hellingman, Davidson *et al.* 2011) and for re-differentiation of de-differentiated chondrocytes (Narcisi, Signorile *et al.* 2012). Here, we demonstrated that senescent MSCs have reduced pSMAD2 levels after TGF β 1 stimulation, compared to non-senescent control MSCs, suggesting that the canonical TGF β signaling is altered in senescent MSCs. However, other non-canonical TGF β pathways may be also involved in the process of cellular senescence and need further investigations.

It is known that senescent cells can affect the surrounding cells and tissues via their secretome. Previously, it has been shown that implantation of senescent cells can contribute to an OA-like phenotype in mice (Xu, Bradley *et al.* 2017). In order to safely use MSCs for cartilage repair strategies, it is crucial to understand whether the SASP factors released by senescence cells can limit chondrogenesis or even contribute to cartilage degeneration. In this study, we found that the conditioned medium of chondrogenic pellets of senescent MSCs had no direct effect on the expression of the chondrogenic

(*COL2A1*, *ACAN* and *SOX9*) or the catabolic (*MMP1*, *MMP13*, *MMP3* or *ADAMTS4*) markers in recipient pellet cultures. These data indicate that in our *in vitro* model, the SASP factors released from senescent MSCs have no negative effect on MSC chondrogenesis nor on the matrix degradation processes. Despite the absence of a direct effect on the MSCs exposed to the medium of senescent MSCs, we did find that senescent MSCs in the pellets had higher expression levels of inflammatory factors *IL6* and *MMP3*. The role of *IL6* in cartilage tissue is controversial, since it has been shown to stimulate both cartilage degeneration and synthesis (Porée, Kypriotou *et al.* 2008, Ryu, Yang *et al.* 2011, Tsuchida, Beekhuizen *et al.* 2012), and *MMP3* promotes cartilage loss via degradation of multiple extracellular matrix components (Murphy and Lee 2005), indicating that the SASP factors released by MSCs could thus also contribute to the pathophysiology of OA. On the other hand, the SASP factors have been shown to be essential for tissue regeneration via the recruitment of macrophages (Godwin, Pinto *et al.* 2013). Therefore, more studies specifically focused on the role of individual SASP factors are necessary to better understand their role in cartilage generation and degeneration as well as possible interventions to counteract these effects.

In this study we explored how senescence in MSCs affect the chondrogenesis process. We showed that the number of senescent cells in MSC cultures is associated with a reduced chondrogenic differentiation potential. Especially senescence in the early phase of chondrogenesis could be detrimental for MSC-based cartilage tissue engineering. Therefore strategies that prevent or abolish senescence in MSCs could be beneficial for MSC-based cartilage repair.

2.6 Supplemental Information

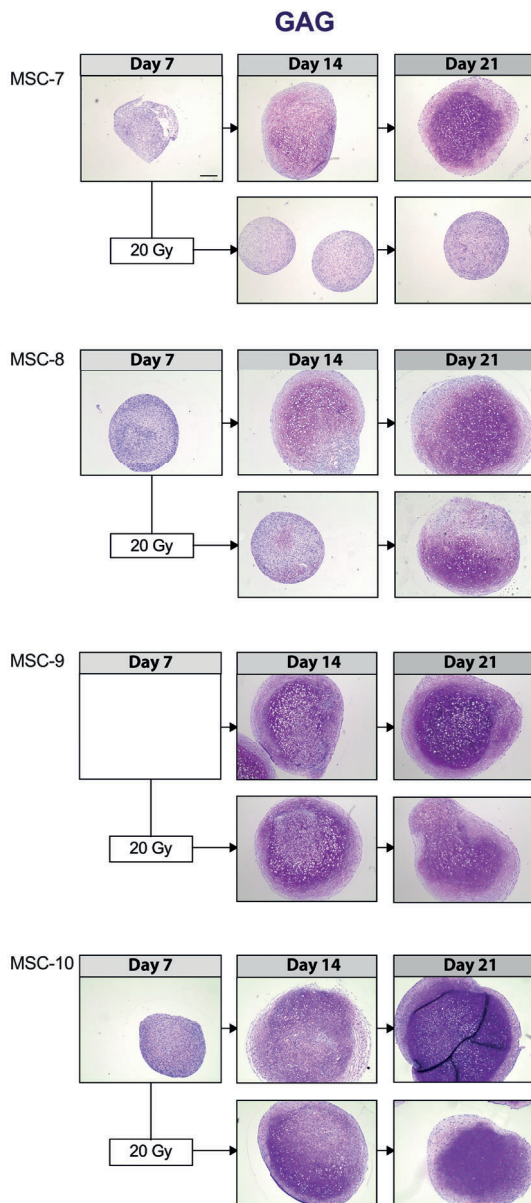


Figure S2.1 –Thionine staining of irradiated MSC pellets at day 7.

Images of Thionine (GAG) staining of MSC control pellets that were chondrogenically differentiated for 7, 14 and 21 days or MSC pellets that were irradiated at day 7 during chondrogenic differentiation and subsequently differentiated for 7 or 14 days. The day 7 pellets of donor MSC-9 are missing due to a technical issue during processing. The scale is the same in all images. Scale bar represents 200 μm and is indicated in the day 7 pellet of donor MSC-7. The images of donor MSC-8 are the same as depicted in Figure 2A. N=4 donors with 2-3 pellets per donor.

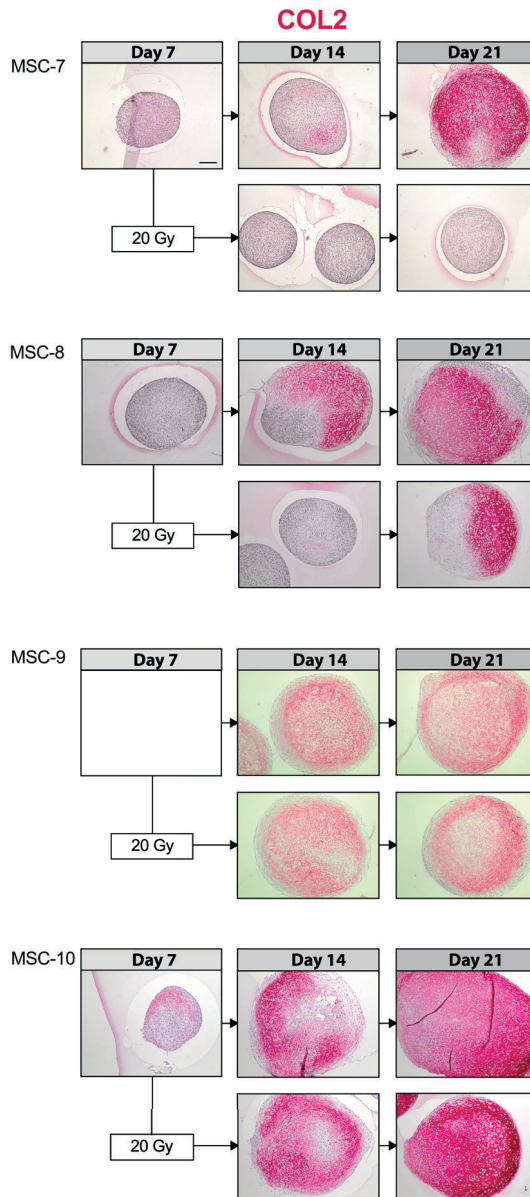
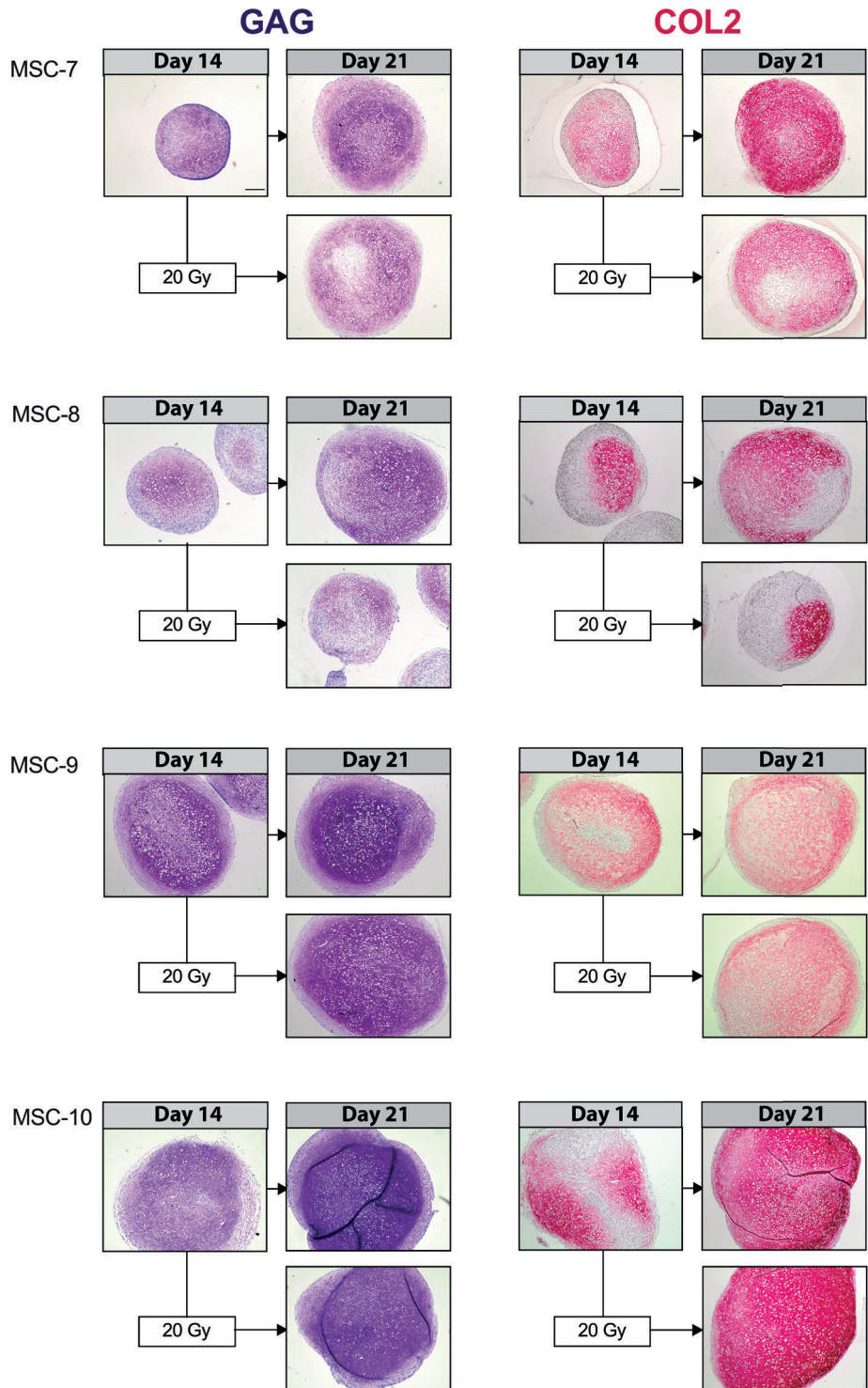


Figure S2.2 – Collagen type 2 staining of irradiated MSC pellets at day 7.

Images of Collagen type 2 (COL2) immunohistochemical staining of MSC control pellets that were chondrogenically differentiated for 7, 14 and 21 days or MSC pellets that were irradiated at day 7 during chondrogenic differentiation and subsequently differentiated for 7 or 14 days. Positive staining in red. The day 7 pellets of donor MSC-9 are missing due to a technical issue during processing. The scale is the same in all images. Scale bar represents 200 μ m and is indicated in the day 7 pellet of donor MSC-7. The images of donor MSC-8 are the same as depicted in Figure 2B. N=4 donors with 2-3 pellets per donor.



(Legend on next page)

◀ **Figure S2.3 – Thionine and Collagen type 2 staining of irradiated MSC pellets at day 14.** (Left panels) Images of Thionine (GAG) and (right panels) images of Collagen type 2 (COL2) staining of MSC control pellets that were chondrogenically differentiated for 14 and 21 days or MSC pellets that were irradiated at day 14 during chondrogenic differentiation and subsequently differentiated for 7. The scale bar represents 200 μm . The images of donor MSC-7 are the same as depicted in Figure 3A-B. N=4 donors with 2-3 pellets per donor.

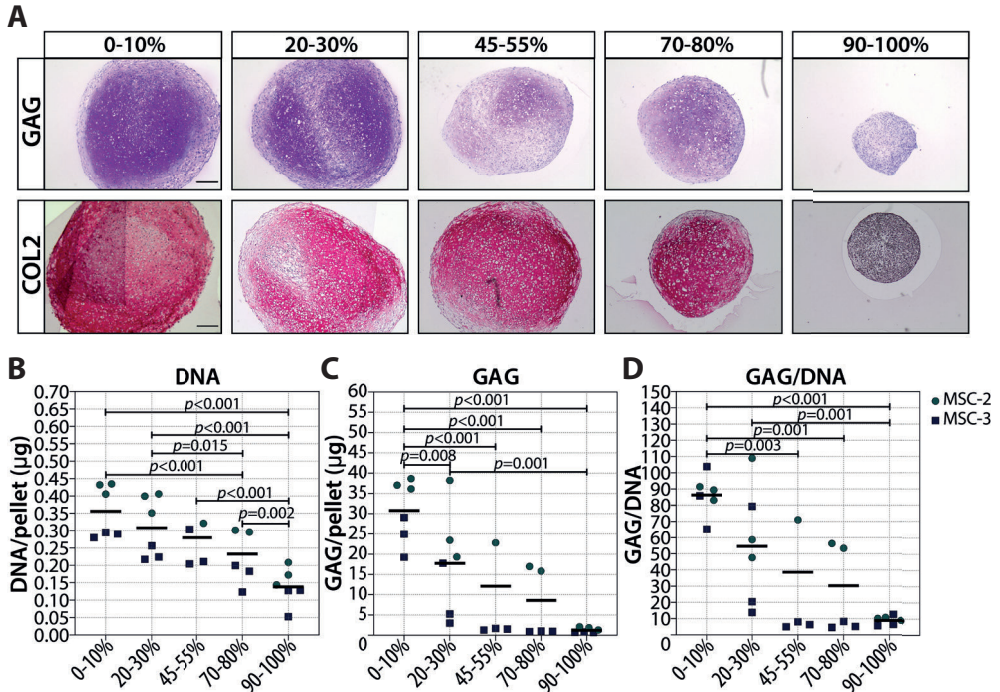


Figure S2.4 - GAG and DNA content in MSCs pellets with senescent and non-senescent cells mixed.

(A) Representative images of Thionine (GAG) and Collagen type-2 (COL2) staining of MSCs that were gamma irradiated during expansion with 0 or 20 Gy, mixed (percentages indicate the percentage of senescent MSCs) and subsequently chondrogenically differentiated for 21 days. Scale bar represents 200 μm . N=2 donors with 2-3 pellets per donor.

(B-D) GAG, DNA and GAG/DNA content of MSCs that were gamma irradiated during expansion with 0 or 20 Gy, mixed (percentages indicate the percentage of senescent MSCs) and subsequently chondrogenically differentiated for 21 days. N=2 donors with 2-3 pellets per donor. *p*-values were obtained with the linear mixed model, using the different experimental conditions as fixed parameters and the donors as random factors and Bonferroni post-hoc test was used to correct for multiple comparisons.

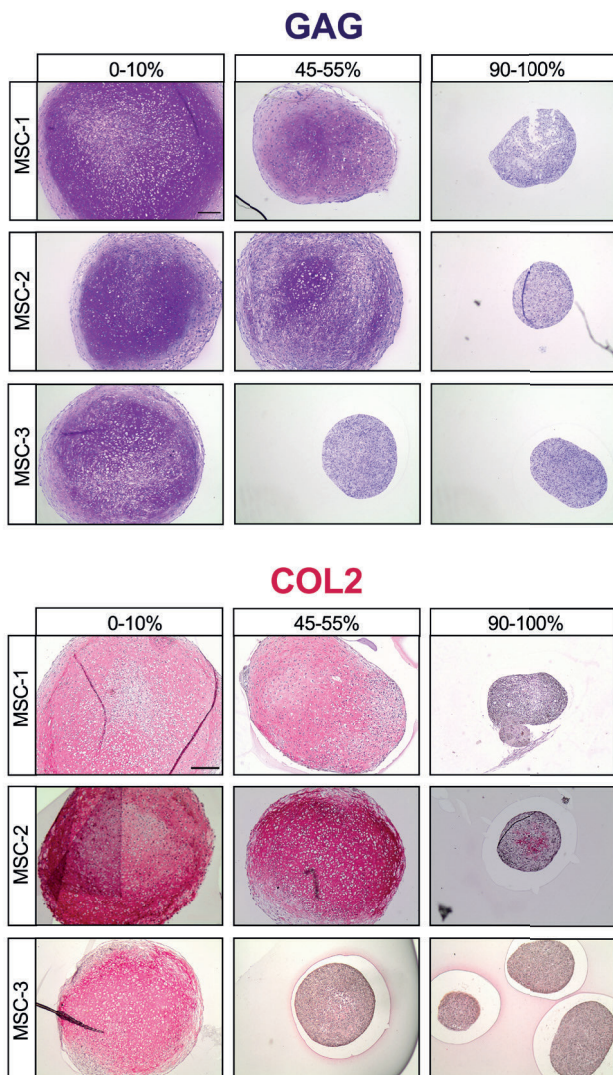


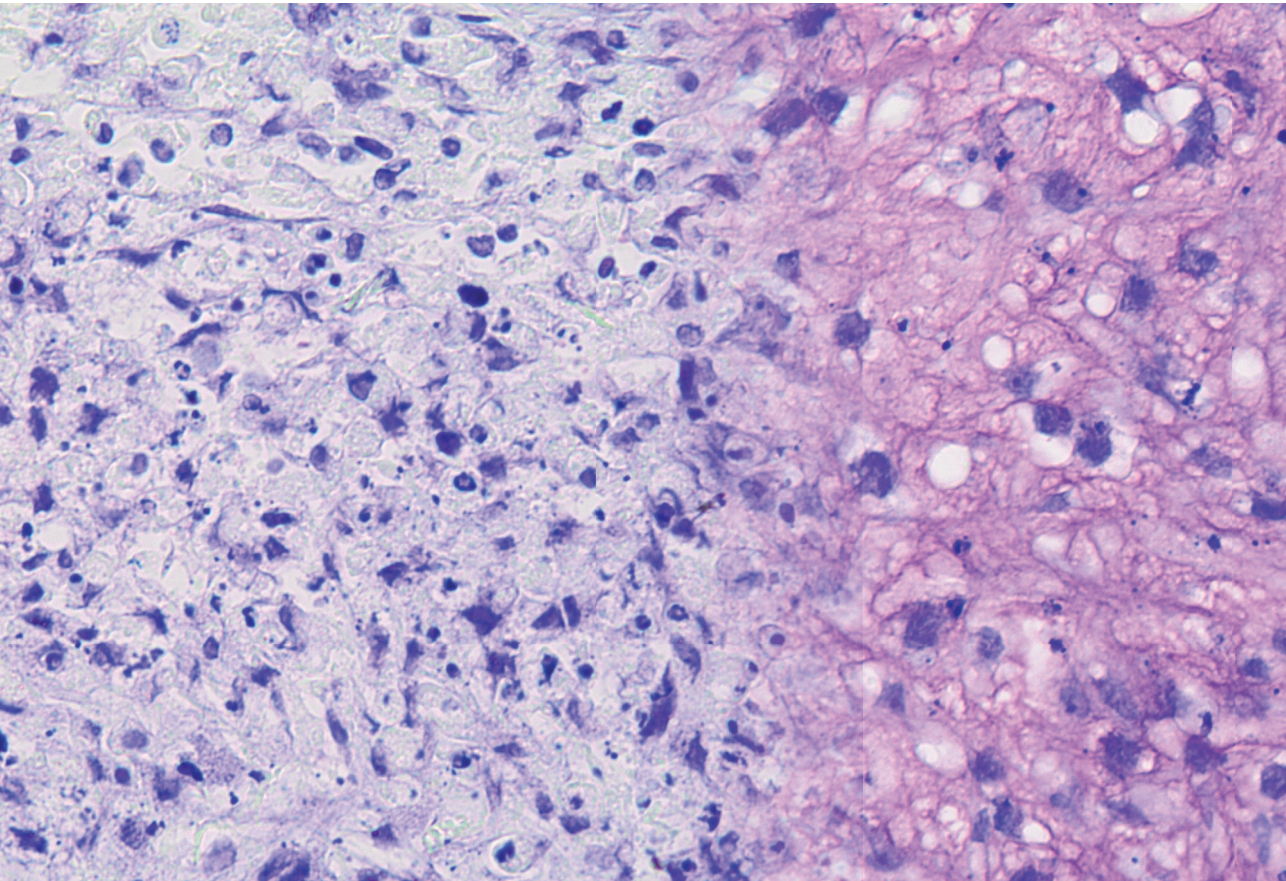
Figure S2.5 – Thionine and Collagen type 2 staining of MSC pellets with different ratios of senescent MSCs.

(A-B) Thionine (A) and Collagen type 2 (B) staining of MSCs that were gamma irradiated during expansion with 0 or 20 Gy, mixed and subsequently chondrogenically differentiated for 21 days. Representative images from different technical triplicates are depicted. Scale bar represents 200 μm . N=3 donors with 2-3 pellets per donor. The images of donor MSC-1 are the same as depicted in Figure 5A. The images of the Collagen type 2 staining with 0-10% and 90-100% senescent MSCs for donor MSC-1 and MSC-3 are the same as depicted in Figure 1D.

2.7 Acknowledgment of grant support

This research was financially supported by the Dutch Arthritis Society (ReumaNederland; 16-1-201) and by a TTW Perspectief grant from NWO (William Hunter Revisited; P15-23). This study is part of the Medical Delta RegMed4D program.

3

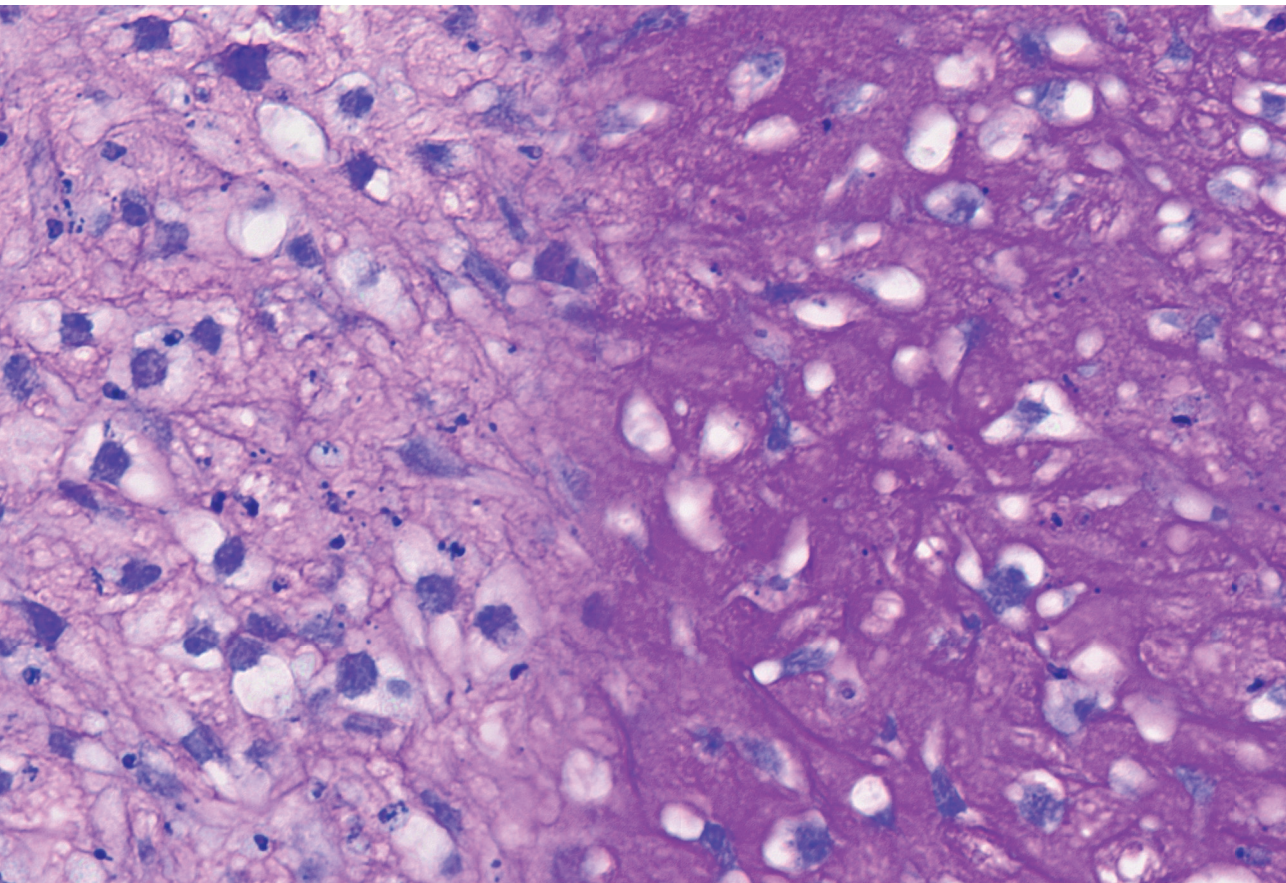


Chapter 3

***TWIST1* controls cellular senescence and energy metabolism in mesenchymal stem cells**

C. Voskamp, L.A. Anderson, W.J.L.M. Koevoet, S. Barnhoorn, P.G. Mastroberardino, G.J.V.M. van Osch, R. Narcisi

Eur Cell Mater. 2021 Nov 25;42:401-414



3.1 Abstract

Mesenchymal stem cells (MSCs) are promising cells for regenerative medicine therapies because they can differentiate towards multiple cell lineages. However, the occurrence of cellular senescence and the acquiring of the senescence-associated secretory phenotype (SASP) limit their clinical use. Since the transcription factor *TWIST1* influences expansion of MSCs, its role in regulating cellular senescence was investigated. The present study demonstrated that silencing of *TWIST1* in MSCs increased the occurrence of senescence, characterised by a SASP profile different from irradiation-induced senescent MSCs. Knowing that senescence alters cellular metabolism, cellular bioenergetics was monitored by using the Seahorse XF apparatus. Both *TWIST1*-silencing-induced and irradiation-induced senescent MSCs had a higher oxygen consumption rate compared to control MSCs, while *TWIST1*-silencing-induced senescent MSCs had a low extracellular acidification rate compared to irradiation-induced senescent MSCs. Overall, data indicated how *TWIST1* regulation influenced senescence in MSCs and that *TWIST1* silencing-induced senescence was characterised by a specific SASP profile and metabolic state.

3.2 Introduction

Regenerative medicine strategies aim to regenerate tissues that have been damaged by injury or pathology. A promising cell source for regenerative medicine therapies is the multipotent progenitor cell referred to as MSC. MSCs have the capacity to self-renew and differentiate towards multiple lineages (Pittenger, Mackay *et al.* 1999); moreover, they can be isolated from several tissues (Haynesworth, Goshima *et al.* 1992, Pittenger, Mackay *et al.* 1999, Erices, Conget *et al.* 2000, Halvorsen, Wilkison *et al.* 2000, Zuk, Zhu *et al.* 2001, Romanov, Svintsitskaya *et al.* 2003). However, a limitation that hinders the clinical use of MSCs is their inter- and intra-donor variability in differentiation capacity. This heterogeneity includes the occurrence of cellular senescence (Li, Wu *et al.* 2017). Cellular senescence is an irreversible state in which cells undergo permanent cell cycle arrest, while they are still metabolically active and can secrete pro-inflammatory factors. Senescence is generally induced by replicative exhaustion, DNA damage, oncogenes or mitochondrial dysfunction (Kumari and Jat 2021). The pool of factors secreted by senescent cells define the so called SASP (Lunyak, Amaro-Ortiz *et al.* 2017); their occurrence is linked to the metabolic state of the cell (Dörr, Yu *et al.* 2013, Wiley, Velarde *et al.* 2016) and to the kind of stressor responsible for inducing senescence (Kumari and Jat 2021). Typical SASP genes common to most senescent cells are *IL1B*, *IL6*, *MMPs*, *CCL2* and *VEGF*. Glycolysis, which breaks down glucose into pyruvate, ATP and NADH, has been demonstrated to be increased in senescent cells (Bittles and Harper 1984, James, Michalek *et al.* 2015). In addition, senescent fibroblasts can have an impaired mitochondrial metabolism (Wiley, Velarde *et al.* 2016).

Cellular senescence has been shown to reduce the differentiation capacity of umbilical-cord-derived MSCs (Cheng, Qiu *et al.* 2011) and could also be unsafe for regenerative medicine strategies, since senescent MSCs can promote tumour formation (Li, Xu *et al.* 2015, Hochane, Trichet *et al.* 2017). In addition, senescent cells are known to contribute to tissue degeneration, since senescent cells transplanted into a mouse knee joint can induce an osteoarthritis-like phenotype showing reduced cartilage content, osteophyte formation and subchondral bone structure alterations (Xu, Bradley *et al.* 2017). Safe and reproducible clinical use of MSCs requires a better understanding of the molecular mechanisms behind cellular senescence and their SASP profile.

MSC expansion has been associated with the expression of the transcription factor *TWIST1* (Isenmann, Arthur *et al.* 2009, Narcisi, Cleary *et al.* 2015, Voskamp, van de Peppel *et al.* 2020). Moreover, *TWIST1* can regulate the expression of the cellular senescence marker p21 in hypoxic MSC cultures (Tsai, Chen *et al.* 2011), and loss-of-function mutation of *TWIST1* in Saethre-Chotzen patient cells results in accelerated senescence (Cakouros, Isenmann *et al.* 2012). The present study showed that *TWIST1* overexpression in MSCs inhibited cellular senescence, while silencing of *TWIST1* induced cellular senescence. In addition, *TWIST1* could modulate the SASP and the bioenergetic profile in senescent MSCs, differently from senescence induced by irradiation. These results offered novel molecular insights in SASP and metabolism regulation and suggested that *TWIST1* could be a target to modulate cellular senescence.

3.3 Materials and Methods

3.3.1 Cell culture

MSCs were isolated from leftover iliac crest bone chip material (9-13 years old patients) as previously described (Knuth, Kiernan *et al.* 2018), in accordance with the Medical Ethical Commission of the Erasmus MC (protocol number MEC-2014-16). No morphological differences were observed between MSCs from different donors at passage 0 (P0). Cells from the selected donors represented a starting population of MSCs with a low number of senescent cells (< 10 % positivity for β -galactosidase, data not shown). MSCs were expanded in α MEM (Gibco) containing 10% fetal calf serum (Gibco, selected batch 41Q2047K), 1.5 μ g/mL fungizone (Invitrogen), 50 μ g/mL gentamicin (Gibco), 0.1 mmol/L ascorbic acid (Sigma-Aldrich) and 1 ng/mL FGF2 (Instruchemie, Delft Zijl, the Netherlands). MSCs were cultured at a density of 2,300 cells/cm² at 37 °C and 5 % CO₂. Cells were trypsinised and medium changed twice a week. Depending on the assay and the experimental plan, passage 3 (P3) to passage 7 (P7) cells were used. Cells at P3 (with high *TWIST1* expression) were used for the irradiation and silencing experiments to better appreciate the effect of *TWIST1* downregulation compared to control. Cells at P7 (with lower *TWIST1* expression) were used for the overexpression experiment to better appreciate the effect of *TWIST1* upregulation compared to controls.

3.3.2 TWIST1 silencing

To study whether silencing of *TWIST1* induced cellular senescence, low passage (P3-P4) MSCs were used. MSCs were seeded at a density of 2,300 cells/cm² and cultured for 24 h in standard expansion medium. Next, cells were either treated with 15 nmol/L TWIST1 (4390824, Ambion) or scramble (4390843, Ambion) siRNA in combination with Lipofectamine RNAMAX Transfection Reagent (1:1,150; Invitrogen) and optiMEM (1:6; Gibco) or left untreated. The treatment was repeated every 3-4 d for 13-14 d.

3.3.3 Lentiviral constructs and virus generation

To study the effect of *TWIST1* overexpression upon MSC senescence, tetracycline-inducible lentiviral constructs of TWIST1 and GFP were used. TWIST1 cDNA was cloned into a lentiviral construct under the control of the tetracycline operator. The GFP lentiviral vector was a gift from Marius Wernig's laboratory (Stanford School of Medicine, Stanford, CA, USA; Addgene plasmid #30130). An empty lentiviral construct was used as a control. Third generation lentiviral particles with a VSV-G coat were generated in HEK293T cells. HEK293T cells were cultured in DMEM HG GlutaMAX (Life Technologies) containing 10 % fetal calf serum, 1 mmol/L sodium pyruvate (Life Technologies) and 1:100 non-essential amino acids (Life Technologies) and seeded in poly-L-ornithine-coated plates at a density of 5×10^6 cells per 10 cm diameter dish. After 24 h, cells were transfected with one of the lentiviral packaging vectors PMDL (5 µg per 10 cm diameter dish), RSV (2.5 µg per 10 cm dish diameter) or VSV (2.5 µg per 10 cm diameter dish) and one of the experimental inserts rtTA, TWIST1, GFP or an empty vector (10 µg per 10 cm diameter dish) using polyethylenimine (1:166). Medium was changed 6 h post-transfection. Viral supernatants were filtered through a 0.45 µm filter 24 h after the last medium change and stored at -80°C until use.

3.3.4 Lentiviral transduction

To study whether TWIST1 overexpression inhibited cellular senescence, high passage (P7) MSCs were used. The transduction efficiency was determined by titration of the GFP lentivirus construct using different virus concentrations, 1:1:1, 1:1:3 and 1:1:8 of GFP:rtTA:MSC expansion medium. After transduction for 16 h, cells were washed with PBS and fresh expansion medium supplemented with 2 µg/mL doxycycline (Sigma-Aldrich) was added. The transduction efficiency was assessed by analysis of

the percentage of GFP positive cells using fluorescent microscopy and flow cytometry. For flow cytometry analysis, GFP-transduced MSCs were fixed in 2% formaldehyde (Fluka) and filtered through 70 μm filters. Untransduced MSCs were used as a negative control. Samples were analysed by flow cytometry using a BD LSRFortessa™ Cell Analyzer (BD Biosciences). Data were analysed using FlowJo V10 software.

3.3.5 mRNA analysis

For each experiment involving RNA evaluation, the medium was changed 24 h before cell harvesting. MSCs were washed with PBS and lysed in RLT buffer containing 1% β -mercaptoethanol. Subsequently, RNA was isolated from the cells using the RNeasy micro kit (Qiagen) according to the manufacturer's instructions. cDNA was synthesised using the RevertAid First-Strand cDNA Synthesis Kit (Thermo Fisher Scientific). Real-time polymerase chain reactions were performed using TaqMan™ Universal PCR MasterMix (FAM + TAMRA chemistry; Applied Biosystems) or SYBR Green MasterMix (Fermentas) using a CFX96™ PCR detection system (Bio-Rad). The following thermal protocol was used: 10 min at 95°C + 40 cycles consisting of 15 s at 95°C followed by 1 min at 60°C as annealing step, except for *CDKN2A* (*P16*), *CDKN1A* (*P21*) and *CCL2*, which needed an annealing temperature of 61.5°C. The melting curve protocol consisted of ramping from 65°C to 95°C with an increase of 0.5°C/min. Primers are listed in **Table 3.1** and housekeeping genes *GAPDH*, *HPRT1* and *RPS27A* were chosen for their stable expression in MSCs. The BHI, the geometric mean of the three housekeeping genes, was calculated according to the $(\text{Ct}^{\text{GAPDH}} \times \text{Ct}^{\text{HPRT}} \times \text{Ct}^{\text{RPS27A}})^{1/3}$ formula (Pfaffl, Tichopad *et al.* 2004). Each primer used was validated to generate a unique melting peak. Data were visualised based on the $2^{-\Delta\text{Ct}}$ method.

3.3.6 Irradiation-induced senescence

Irradiation-induced senescence of MSCs was performed by a 20 Gray protocol (20 Gy) using ionising radiation by a RS320 X-Ray machine (X-Strahl, Camberley, UK). P3 MSCs at 60-70 % confluence in T175 flasks were used for the irradiation protocol. Cells were exposed for 22 min. After irradiation, cells were left in the flask for 48 h, trypsinised, seeded at 9,600 nc/cm^2 and cultured for another 3-5 d to allow for senescence to occur. At day 7 post irradiation β -galactosidase staining was performed. Control cells underwent the same protocol and were exposed to a 0 Gy irradiation. Following

trypsinisation, they were re-seeded at 2,300 nc/cm².

Table 3.1- Primer sequences

Gene	Forward	Reverse	Probe	Method
<i>TWIST1</i>	5'-GTCCG-CAGTCTTAC-GAGGAG-3'	5'-CCAGCTT-GAGGGTCT-GAATC-3'	-	SYBR Green
<i>CDKN2A (P16)</i>	5'-GATCCAGGT-GGGTAGAAG-GTC-3'	5'-CCCCTG-CAA-ACTTCGT-CCT-3'	-	SYBR Green
<i>CDKN1A (P21)</i>	5'-TGTCCGT-CAGGACCCAT-GC-3'	5'-AAAGTC-GAAGTTCCAT-CGCTC-3'	-	SYBR Green
<i>IL6</i>	5'-ACTCA-CCTCTTCA-GAACGAATTG-3'	5'-CCATCTTTG-GAAGGTTTCAG-GTTG-3'	-	SYBR Green
<i>CXCL8 (IL8)</i>	5'-TTTTT-GAAGAGGGCT-GAGAATTC-3'	5'-ATGAAGTGT-TGAAGTAGATT-TGCTTG-3'	-	SYBR Green
<i>CCL2</i>	5'-GAGCCAGAT-GCAATCAATG-CC-3'	5'-TGGAATCCT-GAACCCACT-TCT-3'	-	SYBR Green
<i>IL1B</i>	5'-CCTAAACA-GATGAAGTGCT-CCTT-3'	5'-GTAGTCG-GATGCCGC-CAT-3'	-	SYBR Green
<i>VEGFA</i>	5'-CTTGCCT-TGCTGCTC-TACC-3'	5'-CACACAG-GATGGCTT-GAAG-3'	-	SYBR Green
<i>MMP13</i>	5'-AAGGAGCA-TGGCGACT-TCT-3'	5'-TGGCC-CAGGAG-GAAAAGC-3'	5'-CCCTCTGG-CCTGCTGGCT-CA-3'	TaqMan
<i>GAPDH</i>	5'-ATGGGGAAG-GTGAAGGT-CG-3'	5'-TAAAAGCAG-CCCTGGTG-ACC-3'	5'-CGCCCAAT-ACGACCAAATC-CGTTGAC-3'	TaqMan
<i>RPS27A</i>	5'-TGGCTGT-CCTGAAATAT-TATAAGGT-3'	5'-CCCCAGCA-CCACATTCAT-CA-3'	-	SYBR Green
<i>HPRT1</i>	5'-TTATGG-ACAGGACT-GAACGTCTTG-3'	5'-GCACACA-GAGGGCTAC-CATGTG-3'	5'-AGATGTGAT-GAAGGAGATG-GGAGGCCA-3'	TaqMan

3.3.7 SA- β -gal staining

Cells were washed twice with PBS and fixed with 0.5% glutaraldehyde and 1% formalin in Milli-Q water. Then, cells were washed with Milli-Q water and incubated for 24 h at 37 °C with freshly made X-gal solution (0.5% X-gal, 5 mmol/L potassium ferricyanide, 5 mmol/L potassium ferrocyanide, 2mmol/L MgCl_2 , 150mmol/L NaCl, 7mmol/L $\text{C}_6\text{H}_8\text{O}_7$, 25 mmol/L Na_2HPO_4). Cells were counterstained with pararosaniline (1:25 in Milli-Q water) and imaged using a bright-field microscopy. For each condition, two independent researchers blinded to the experimental plan scored at least 300 cells as negative, low positive or high positive.

3.3.8 Bioenergetics assays

Mitochondrial respiration was measured as OCR using a XF-24 Extracellular Flux Analyzer (Seahorse Bioscience) as previously described (Milanese, Bombardieri *et al.* 2019). MSCs were seeded at a density of 3×10^4 cells/well on Seahorse plates. Optimal cell densities were determined experimentally to ensure a proportional response to FCCP (oxidative phosphorylation uncoupler). 24 h after cell seeding, the medium was changed to unbuffered DMEM (XF Assay Medium, Agilent Technologies) supplemented with 2 mmol/L glutamine, 10 mmol/L glucose and 1 mmol/L sodium pyruvate and incubated for 1 h at 37 °C in the absence of CO_2 . Three baseline measurements were performed, followed by subsequent measurements after injections of mitochondrial toxins, 1.0 $\mu\text{mol/L}$ oligomycin (ATP-synthase inhibitor), 2.0 $\mu\text{mol/L}$ FCCP and 1 $\mu\text{mol/L}$ antimycin A (complex III inhibitor). Medium and reagents were adjusted to pH 7.4 according to manufacturer's instructions. Non-mitochondrial respiration, basal respiration, proton leak, ATP production, maximal respiration and spare capacity were calculated. The non-mitochondrial respiration was defined as the average OCR values after antimycin A injection. Basal respiration was calculated as the difference between basal respiration and respiration measured after antimycin A injection. Proton leak was calculated as the difference between respiration measured after oligomycin and after antimycin A injections. ATP production was calculated as the difference between baseline respiration and respiration measured after oligomycin injection. Maximal respiration was calculated as the difference between respiration measured after FCCP and after antimycin A injections. Spare capacity was defined as the difference between respiration measured after FCCP injection and baseline respiration (**Figure 3.5A**).

3.3.9 Data analysis

Results were statistically analysed using PSAW statistics 20 software (SPSS Inc., Chicago, IL, USA). The normal distribution of the data was determined using the Kolmogorov-Smirnov test. When necessary, data were Log-transformed to meet the normal distribution criteria. A linear mixed model was applied; in this model the conditions were considered as fixed parameters and the donors as random factors. $p < 0.05$ was considered statistically significant. The grand mean was determined by calculating the mean of the donor means, with 2-6 replicates per donor.

3.4 Results

3.4.1 TWIST1 expression was negatively associated with cellular senescence in MSCs

To determine whether *TWIST1* expression was involved in cellular senescence in human MSCs, its expression was analysed in irradiation-induced senescent MSCs, a commonly used experimental setup to induce senescence. Cellular senescence was induced in MSCs by gamma irradiation (20 Gy) and confirmed by SA- β -gal staining (**Figure 3.1A**). *TWIST1* expression was overall significantly reduced in irradiation-induced senescent MSCs compared to mock-irradiated MSCs; although only ~15 % reduction was observed for donor MSC-2 (**Figure 3.1B**; $p = 0.022$), indicating that *TWIST1* expression was negatively associated with cellular senescence in MSCs. Following this observation, the study hypothesis was that high expression of *TWIST1* was able to delay the entrance into the senescence state during passaging *in vitro*. To test this hypothesis, *TWIST1* was overexpressed in MSCs by a lentiviral-based approach. Transduction was determined by the percentage of GFP positive cells (> 65 % transduced cells; data not shown) and overexpression confirmed by qPCR analysis (103-fold increase compared to empty vector control; **Figure 3.1C**). Then, control and *TWIST1*-overexpressing P7 MSCs were serially passaged for 11 d (up to P10), followed by SA- β -gal analysis (**Figure 3.1D**), when the cells were divided into negative, low positive or high positive (**Figure 3.1E**). *TWIST1*-overexpressing MSCs showed an average of 15 % SA- β -gal low positive cells and 0.4 % SA- β -gal high positive cells, while empty vector control cells had an average of 52 % SA- β -gal low positive cells ($p < 0.001$) and 2 % high positive cells ($p = 0.052$; **Figure 3.1F**). Overall, these results suggested that *TWIST1* expression could inhibit cellular senescence in MSCs.

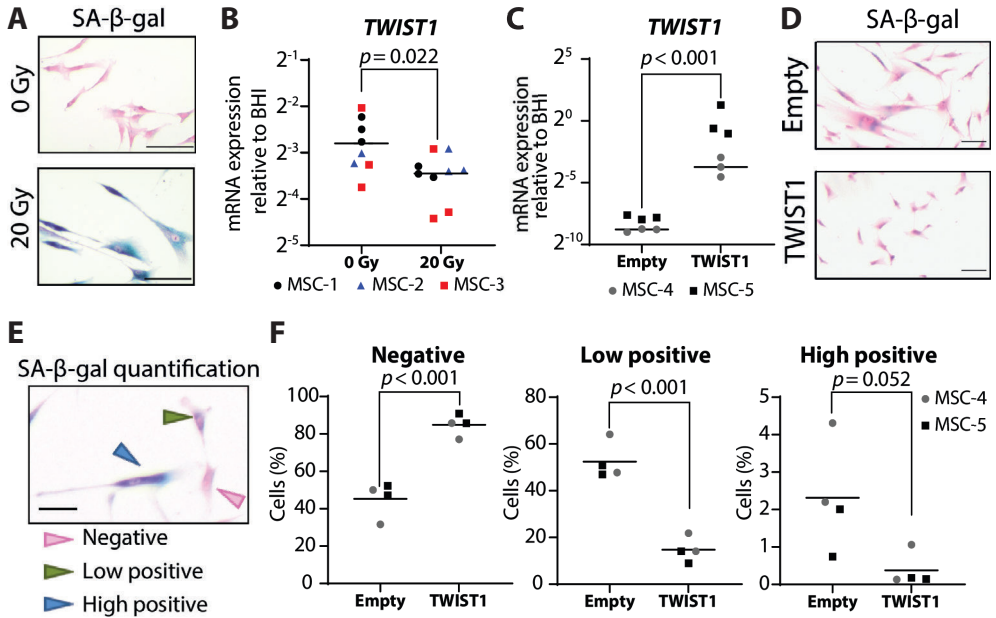


Figure 3.1 - *TWIST1* expression was negatively associated with SA-β-gal.

(A) Representative images of SA-β-gal staining counterstained with pararosaniline of MSCs 7 d after gamma irradiation with 0 or 20 Gy. Scale bar: 100 μm.

(B) *TWIST1* mRNA levels of MSCs 7 d after gamma irradiation with 0 or 20 Gy. Data show individual data points and grand mean with N=8 (0 Gy) or N=9 (20 Gy), 3 donors with 2-3 replicates per donor, linear mixed model.

(C) *TWIST1* mRNA levels of MSCs transduced with an empty overexpression lentiviral construct (Empty) or a *TWIST1* overexpression lentiviral construct (*TWIST1*) after 11d of expansion. Data show individual data points and grand mean with N=6, 2 donors with 3 replicates per donor, linear mixed model.

(D) Representative images of SA-β-gal staining counterstained with pararosaniline of MSCs transduced with an empty overexpression lentiviral control construct (Empty) or a *TWIST1* overexpression lentiviral construct (*TWIST1*) after 11 d of expansion. Scale bar: 100 μm.

(E) MSCs were categorised as negative for SA-β-gal staining if no blue staining was detected in the cells (pink arrow). MSCs were categorised as low positive for SA-β-gal staining if cells showed partial cytoplasmic staining (green arrow). MSCs were categorised as high positive for SA-β-gal staining if cells showed complete cytoplasmic staining (blue arrow). Scale bar: 50 μm.

(F) SA-β-gal quantification of MSCs transduced with an empty overexpression lentiviral construct (Empty) or a *TWIST1* overexpression lentiviral construct (*TWIST1*) after 11 d of expansion. Data show individual data points and grand mean with N=4, 2 donors with 2 replicates per donor, linear mixed model.

3.4.2 TWIST1 silencing induced cellular senescence with a specific SASP in MSCs

To elucidate whether cellular senescence could be induced by *TWIST1* modulation, *TWIST1* expression was silenced in MSCs (si*TWIST1*-MSCs) using an siRNA approach. After 24 h, *TWIST1* mRNA levels in si*TWIST1*-MSCs were reduced by 53 % ($p=0.035$) compared to scramble controls (**Figure 3.2A**), with an increased expression of the cell cycle inhibitor and senescence marker *CDKN2A* (1.8-fold; $p=0.015$; **Figure 3.2B**) and no difference in *CDKN1A* (another commonly used senescence marker) expression (**Figure 3.2C**). Additionally, SA- β -gal analysis revealed no statistically significant difference in the number of cells negative or positive for this senescence marker 24 h after *TWIST1* silencing (**Figure 3.2D**), while following 2 passages, si*TWIST1*-MSCs become increasingly highly positive for SA- β -gal (**Figure 3.3**).

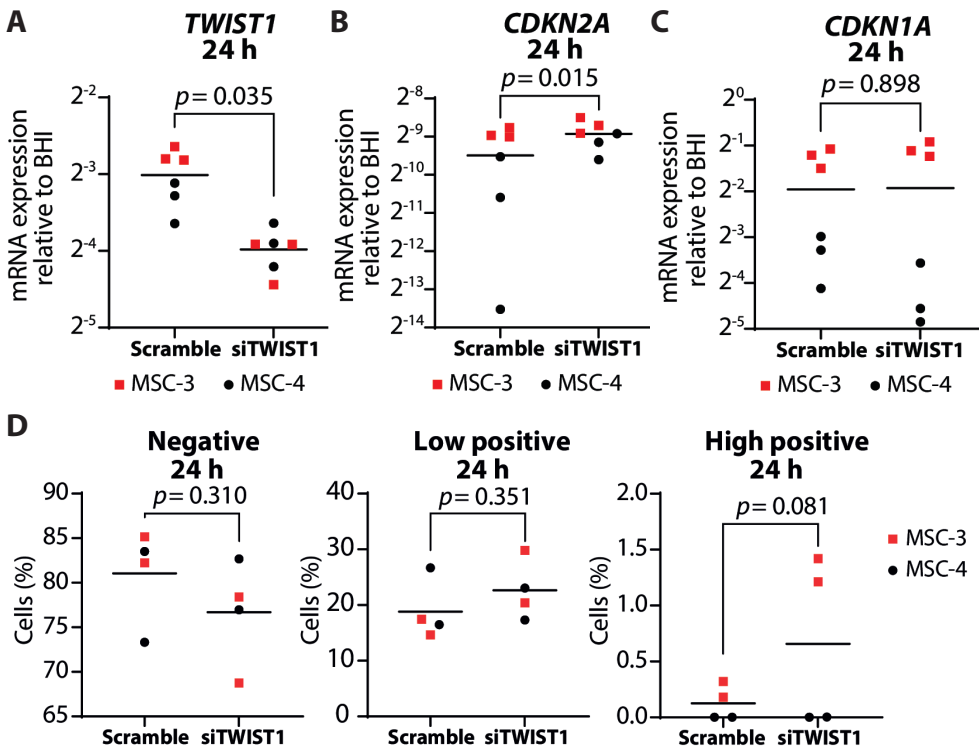


Figure 3.2 - Senescence markers expression after 24 h of *TWIST1* silencing treatment in MSCs.

(A-C) *TWIST1* (A), *CDKN2A* (B) and *CDKN1A* (C) mRNA levels in MSCs treated for 24 h with scramble siRNA (Scramble) or siRNA against *TWIST1* (si*TWIST1*). N=6, 2 donors with 3 replicates per donor, linear mixed model. Graphs show individual data points and

◀ grand mean.

(D) SA-β-gal quantification of MSCs treated for 24 h with scramble siRNA (Scramble) or siRNA against *TWIST1* (si*TWIST1*). N=4, 2 donors with 2 replicates per donor, linear mixed model. Graphs show individual data points and grand mean of percentage of SA-β-gal negative (left), low positive (middle panel) and high positive (right panel) cells.

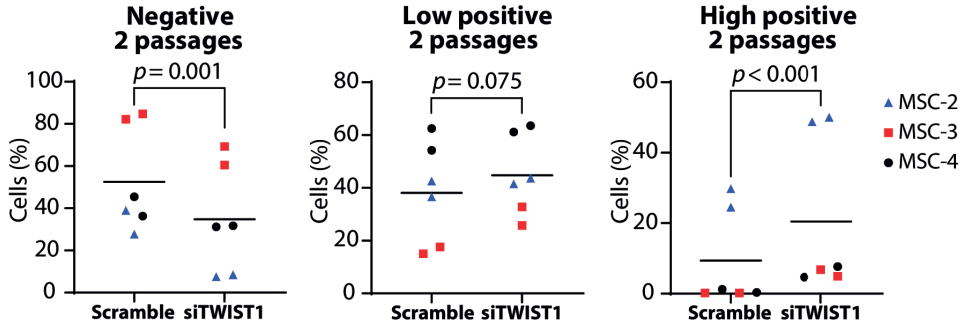
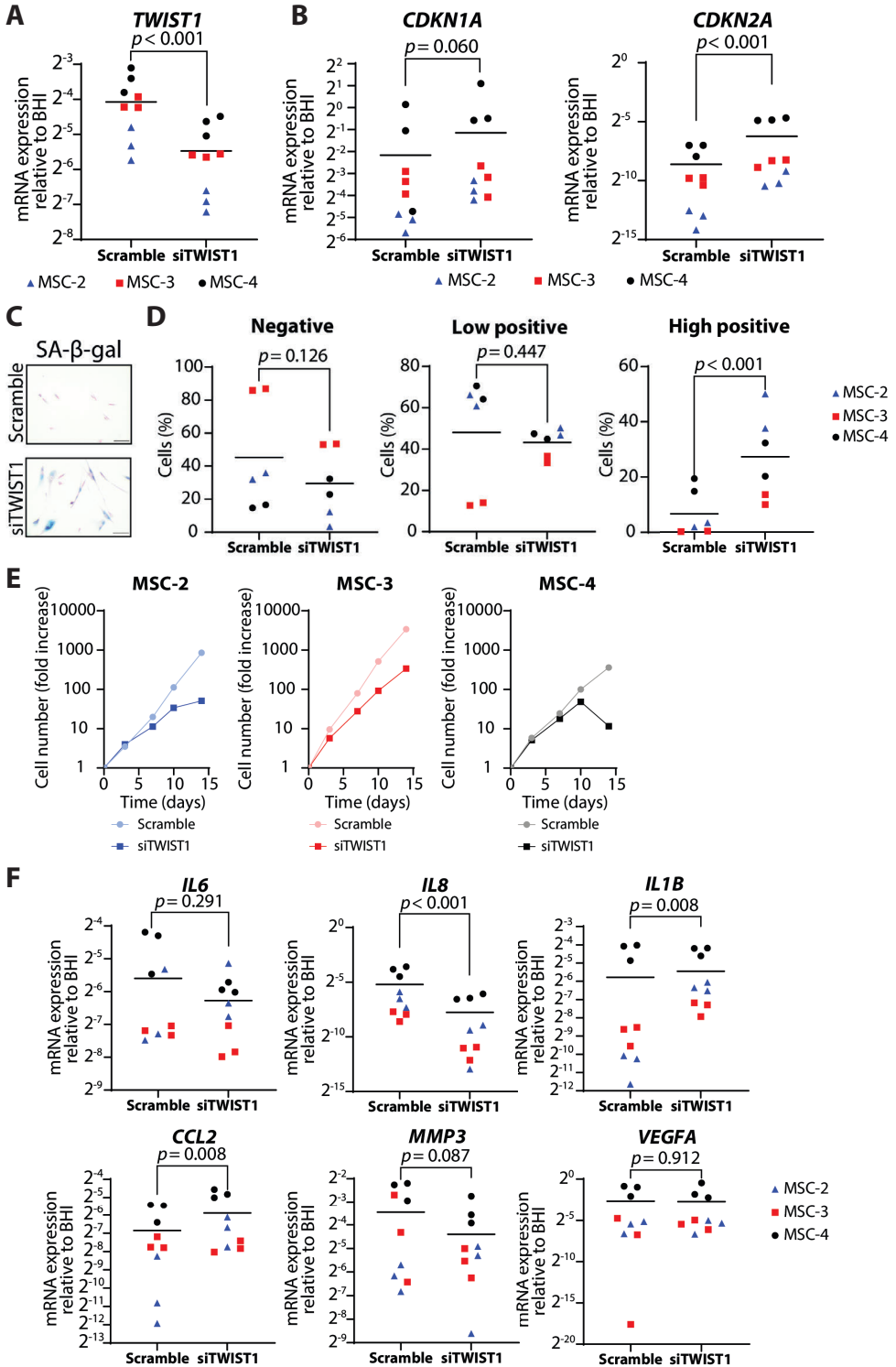


Figure 3.3 - Senescence markers expression after 2 passages of *TWIST1* silencing treatment in MSCs.

SA-β-gal quantification of MSCs treated for 2 passages with scramble siRNA (Scramble) or siRNA against *TWIST1* (si*TWIST1*). N=6, 3 donors with 2 replicates per donor, linear mixed model. Graphs show individual data points and grand mean of percentage of SA-β-gal negative (left), low positive (middle panel) and high positive (right panel) cells.

After 4 passages, si*TWIST1*-MSCs showed an average of 64 % knockdown of *TWIST1* mRNA levels ($p < 0.001$; **Figure 3.4A**) and *TWIST1* silencing increased the expression of *CDKN2A* (6.5-fold, $p < 0.001$) and *CDKN1A* (2.1-fold, $p = 0.060$; **Figure 3.4B**). In addition, after 4 passages, *TWIST1* silencing increased SA-β-gal activity in MSCs (**Figure 3.4C-D**) and decreased cell expansion rate (**Figure 3.4E**), overall indicating that *TWIST1* knockdown induced senescence-associated growth arrest. Since the SASP can drive chronic inflammation and thereby contribute to age-related diseases such as osteoarthritis and cancer (as reviewed by Zhu, Armstrong *et al.* 2014 and Loeser, Collins *et al.* 2016), the expression of the SASP related genes *IL6*, *IL1B*, *MMP3*, *IL8*, *CCL2* and *VEGFA* was determined in si*TWIST1*-MSCs. Interestingly, si*TWIST1*-MSCs expressed higher levels of *CCL2* and *IL1B* compared to control condition, although the effect was donor dependent (3.3-fold $p = 0.008$, 7.4-fold $p = 0.008$, respectively; **Figure 3.4F**). Moreover, the expression of *IL6*, *MMP3* and *VEGFA* was not significantly affected and *IL8* expression was even significantly decreased ($p = 0.291$, $p = 0.077$, $p = 0.087$, $p = 0.912$, $p < 0.001$, respectively; **Figure 3.4F**). These results indicated that senescence was induced in MSCs by *TWIST1* knockdown but generating a non-classical SASP profile.



(Legend on next page)

◀ **Figure 3.4 - *TWIST1* silencing induced cellular senescence in MSCs with a specific SASP mRNA expression profile.**

(A) *TWIST1* mRNA levels in MSCs treated for 4 passages with scramble siRNA (Scramble) or siRNA against *TWIST1* (si*TWIST1*). N=9, 3 donors with 3 replicates per donor, linear mixed model.

(B) *CDKN2A* and *CDKN1A* mRNA levels in MSCs treated for 4 passages with scramble siRNA (Scramble) or siRNA against *TWIST1* (si*TWIST1*). N=9, 3 donors with 3 replicates per donor, linear mixed model.

(C) Representative images of SA-β-gal staining counter stained with pararosaniline of MSCs treated for 4 passages with scramble siRNA (Scramble) or siRNA against *TWIST1* (si*TWIST1*). Scale bar: 100 μm.

(D) SA-β-gal quantification of MSCs treated for 4 passages with scramble siRNA (Scramble) or siRNA against *TWIST1* (si*TWIST1*). N=6, 3 donors with 2 replicates per donor, linear mixed model. Graphs show individual data points and grand mean of percentage of SA-β-gal negative (left), low positive (middle panel) and high positive (right panel) cells.

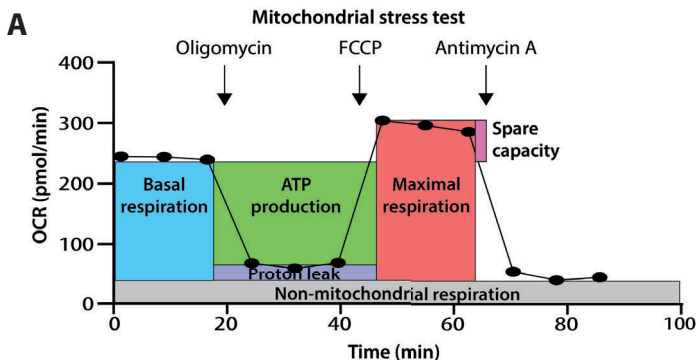
(E) Cell number data during expansion of MSCs treated with scramble siRNA (Scramble) or siRNA against *TWIST1* (si*TWIST1*) at day 0, 3, 7, 10 and 14 of treatment, N = 3 donors.

(F) *IL6*, *IL8*, *IL1B*, *CCL2*, *MMP3* and *VEGFA* mRNA levels in MSCs treated for 4 passages with scramble siRNA (Scramble) or siRNA against *TWIST1* (si*TWIST1*). N=9, 3 donors with 3 replicates per donor, linear mixed model. Graphs show individual data points and grand mean.

3

3.4.3 *TWIST1* silencing altered MSC bioenergetics

Since the expression of the SASP is associated with the metabolic state of the cell (Dörr, Yu *et al.* 2013, Wiley, Velarde *et al.* 2016, Lunyak, Amaro-Ortiz *et al.* 2017), the bioenergetic profile in si*TWIST1*-MSCs was monitored using a Seahorse XF-24 Extracellular Flux Analyzer. The OCR reflecting cellular respiration was measured followed by subsequent measurement after injection of mitochondrial toxins: oligomycin, FCCP and antimycin A (see Materials and Methods and **Figure 3.5A**). First, optimal cell density (30,000 cells/well; **Figure 3.5B**) and the ideal concentration of FCCP (2.0 μmol/L; **Figure 5C**) to detect OCR in human MSCs were identified.



(Continued on next page)

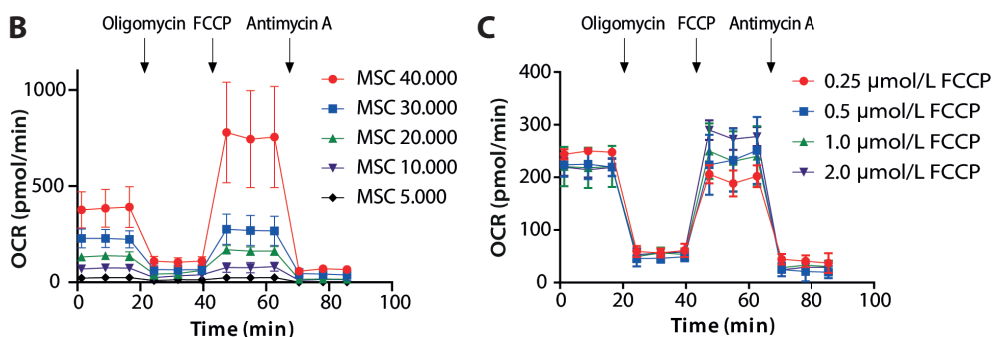


Figure 3.5 - Optimisation of the cell number and FCCP concentration for the mitochondrial stress test using Seahorse technology.

(A) The OCR in MSCs was measured using Seahorse technology followed by subsequent measurements after injection of mitochondrial toxins: oligomycin, FCCP and antimycin A. This assay used the built-in injection ports on Seahorse XF sensor cartridges to add the mitochondrial toxins (modulators of respiration) into cell wells during the assay to reveal the key parameters of mitochondrial function. Specifically, using the mitochondrial stress test basal OCR, ATP production, maximum OCR, spare capacity, non-mitochondrial respiration and proton leak were determined.

(B) Mitochondrial stress test with different MSC densities per well (5,000, 10,000, 20,000, 30,000 and 40,000) using 1.0 µmol/L FCCP.

(C) Mitochondrial stress test with 30,000 MSCs per well using different concentrations of FCCP (0.25, 0.5, 1.0 and 2.0 µmol/L). N=5-7, 1 donor with 5-7 replicates per donor. Graphs represent mean with SD. A detailed explanation of the mitochondrial stress test is provided in Materials and Methods.

Then, a significant increase in basal respiration levels was observed in siTWIST1-MSCs compared to scramble controls ($p=0.011$; **Figure 3.6A-C**). In addition, siTWIST1-MSCs showed higher values for maximum OCR, proton leak, ATP production and spare respiratory capacity compared to scramble control cells ($p=0.001$, $p=0.006$, $p=0.002$ and $p=0.001$, respectively; **Figure 3.6D-G**). No differences in non-mitochondrial respiration were observed between scramble control and siTWIST1-MSCs ($p=0.251$; **Figure 3.6H**). Overall, these data indicated that *TWIST1* silencing induced changes in the MSC mitochondrial function, although in one of the two donors (MSC-6) the effect of the silencing was less pronounced. SASP expression was different between *TWIST1*-silencing-induced senescent MSCs and irradiation-induced senescent MSCs (**Figure 3.4**). Therefore, possible differences in their metabolic profile were investigated.

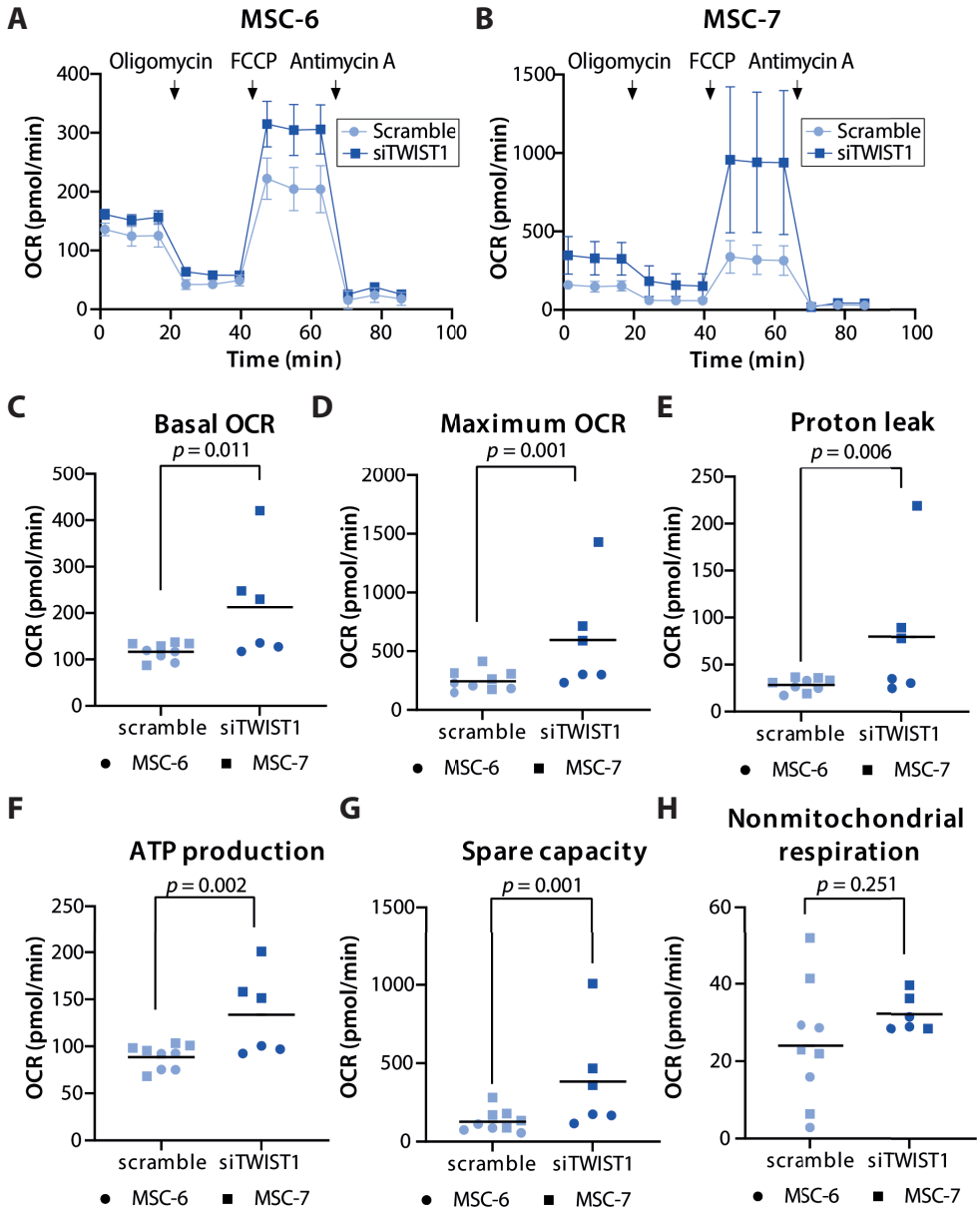
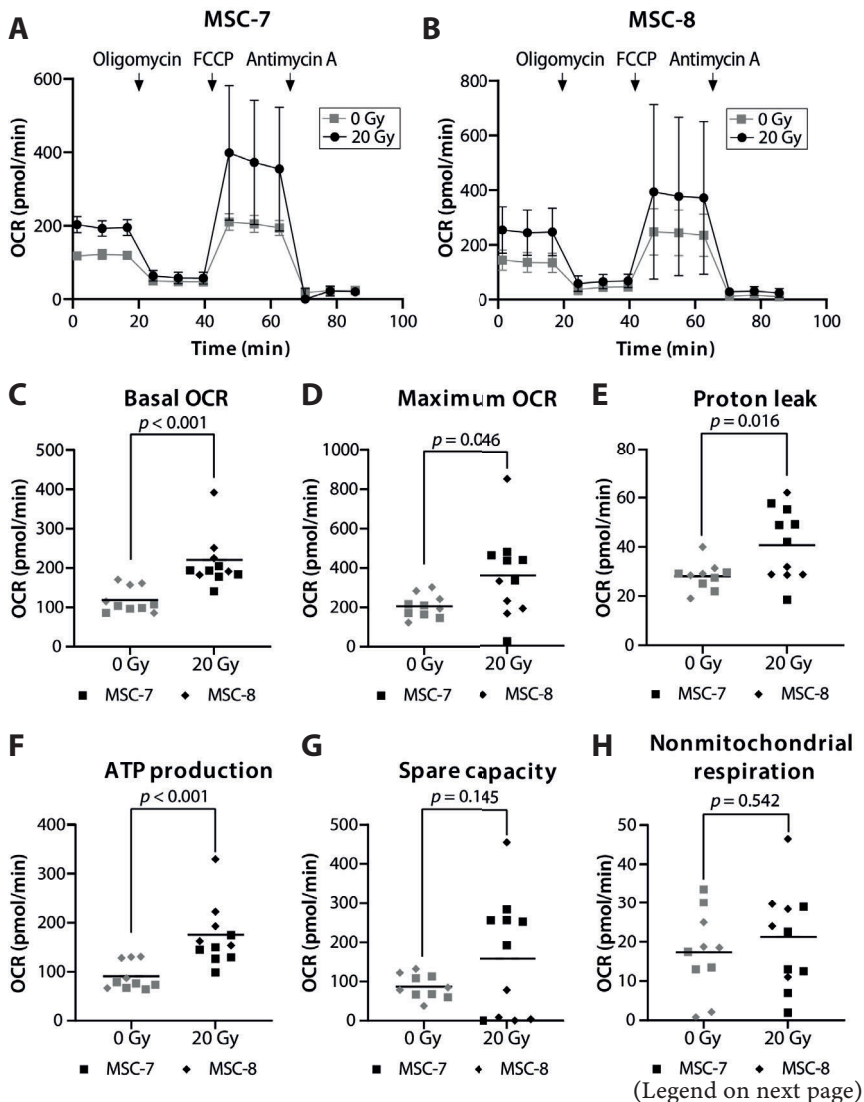


Figure 3.6 - Increased oxygen consumption rate (OCR) in *TWIST1*-silenced MSCs.

(A-B) Graphs show the OCR in MSCs treated with a scramble or *TWIST1* siRNA at basal level and after addition of oligomycin, FCCP and antimycin A in two different donors, (A) MSC-6 and (B) MSC-7. Values represent mean with SD, N=3-5 replicates per donor.

(C-H) Graphs show calculated values for (C) basal OCR, (D) maximum OCR, (E) proton leak, (F) ATP production, (G) spare capacity and (H) non-mitochondrial respiration in MSCs treated with scramble or *TWIST1* siRNA. N=6-9, 2 donors with 3-5 replicates per donor, linear mixed model. Graphs show individual data points and grand mean.

As a measure of mitochondrial respiration, the OCR value of siTWIST1-MSCs was compared to irradiation-induced senescent MSCs. Similarly to siTWIST1-MSCs, irradiation-induced senescent MSCs showed higher values for basal OCR, maximum OCR, proton leak and ATP production compared to non-irradiated control cells ($p < 0.001$, $p = 0.046$, $p = 0.016$ and $p < 0.001$, respectively; **Figure 3.7A-F**). Moreover, no overall differences were observed in spare respiratory capacity – due to an opposite response of the two donors tested – and in non-mitochondrial respiration compared to controls ($p = 0.256$; **Figure 3.7G-H**). These data suggested that both siTWIST1-MSCs and irradiation-induced senescent MSCs had a similar increased OCR to non-senescent MSCs.

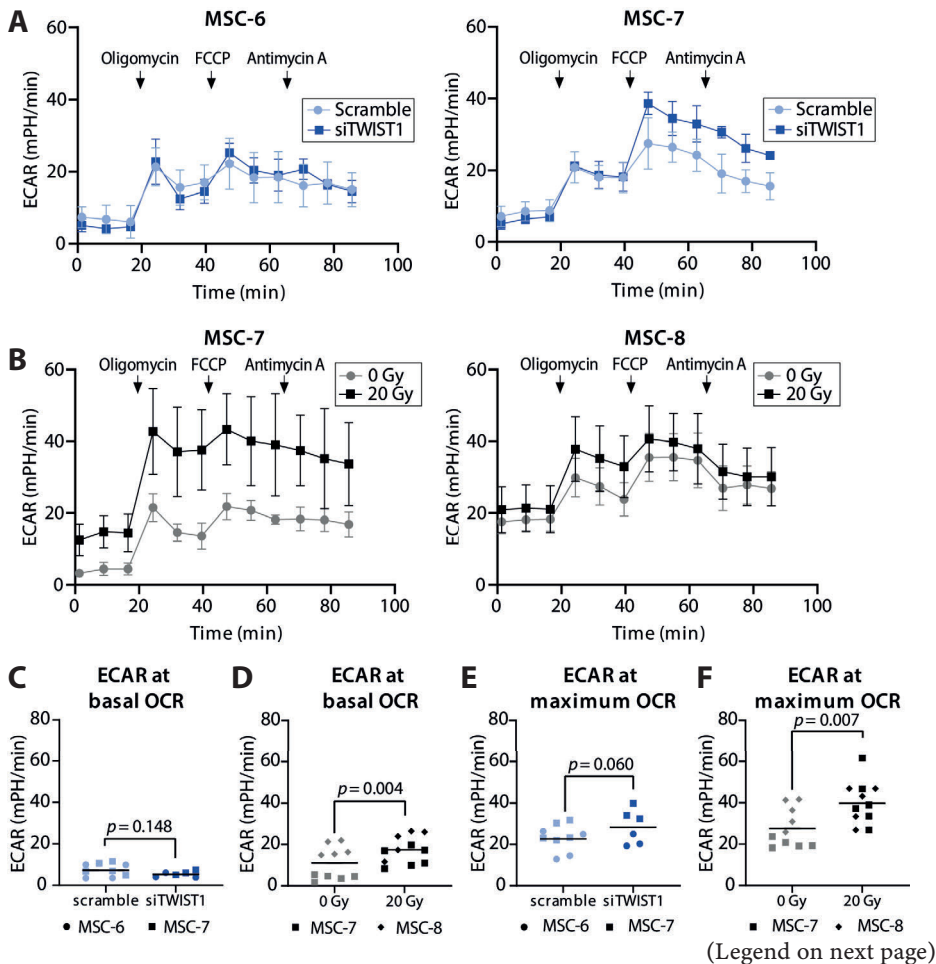


◀ **Figure 3.7 - Increased oxygen consumption rate (OCR) in irradiated MSCs.**

(A-B) Graphs show the OCR in MSCs irradiated with 0 or 20 Gy after addition of oligomycin, FCCP and antimycin A in two different donors, (A) MSC-7 and (B) MSC-8. Values represent mean with SD, N=5-6 replicates per donor.

(C-H) Graphs show calculated values for (C) basal OCR, (D) maximum OCR, (E) proton leak, (F) ATP production, (G) spare capacity and (H) non-mitochondrial respiration in MSCs irradiated with 0 or 20 Gy. N=11, 2 donors with 5-6 replicates per donor, linear mixed model. Graphs show individual data points and grand mean.

As a measure of glycolytic flux, the ECAR in si*TWIST1*-MSCs and irradiated MSCs was analysed. Irradiated MSCs had a higher ECAR compared to control MSCs, while no significant differences in ECAR were observed between scramble control cells and si*TWIST1*-MSCs, indicating that *TWIST1* silencing did not alter the glycolytic flux in MSCs (**Figure 3.8**). This suggested that, in contrast to irradiation-induced senescent MSCs, the glycolytic capacity was unaltered in si*TWIST1*-MSCs compared to untreated controls.



◀ **Figure 3.8 - *TWIST1* silencing did not increase extracellular acidification rate (ECAR) in MSCs.**

(A) Graphs show the ECAR in MSCs treated with a scramble or *TWIST1* siRNA at basal level and after addition of oligomycin, FCCP and antimycin A in two different donors, MSC-6 and MSC-7. Values represent mean with SD, N=3-5 replicates per donor.

(B) Graphs show the ECAR in MSCs irradiated with 0 or 20 Gy after addition of oligomycin, FCCP and antimycin A in two different donors, MSC-7 and MSC-8. Values represent mean with SD, N=5-6 replicates per donor.

(C,E) Graphs show ECAR values for (C) basal oxygen consumption rate (OCR) and (E) maximum OCR in MSCs treated with scramble or *TWIST1* siRNA. N=8, 2 donors with 3-5 replicates per donor, linear mixed model. Graphs show individual data points and grand mean.

(D,F) Graphs show ECAR values for (D) basal OCR and (F) maximum OCR in MSCs irradiated with 0 or 20 Gy. N=11, 2 donors with 5-6 replicates per donor, linear mixed model. Graphs show individual data points and grand mean.

3.5 Discussion

TWIST1 expression has been associated with rapid cell growth and a high proliferation capacity of MSCs (Isenmann, Arthur *et al.* 2009, Boregowda, Krishnappa *et al.* 2016, Voskamp, van de Peppel *et al.* 2020). High *TWIST1* expression levels in MSC are associated with enhanced differentiation capacity, especially towards the adipogenic and chondrogenic lineage (Narcisi, Cleary *et al.* 2015, Cleary, Narcisi *et al.* 2017). The present study showed that enforced *TWIST1* expression suppressed MSC senescence and increased their proliferation capacity. On the other hand, the study demonstrated that *TWIST1* silencing in MSCs induced cellular senescence with a non-classical SASP profile, lacking *IL6* and *IL8* expression. The expression of SASP is regulated by mitochondria and *TWIST1* plays an essential role in the mitochondrial metabolism of cancer cells and adipocytes, since downregulation of *TWIST1* promotes mitochondrial dysfunction (Seo, Kim *et al.* 2014, Lu, Wang *et al.* 2018). Mitochondrial dysfunction can induce cellular senescence with a different SASP profile, referred to as MiDAS (Wiley, Velarde *et al.* 2016). Cells with MiDAS have a SASP expression profile similar to si*TWIST1*-MSCs (Wiley, Velarde *et al.* 2016), suggesting that *TWIST1* silencing might induce cellular senescence in MSCs through mitochondrial dysfunction.

Both mitochondrial dysfunction and cellular senescence are hallmarks of ageing and senescent cells have an altered mitochondrial biogenesis. The

present study showed that both *TWIST1*-silencing-induced and irradiation-induced senescent MSCs had an increased proton leak, indicating that senescent MSCs have dysfunctional mitochondria. Dysfunctional mitochondria can trigger cellular senescence (Wiley, Velarde *et al.* 2016) and removal of mitochondria in senescent cells has been shown to reduce the senescence phenotype (Correia-Melo, Marques *et al.* 2016), suggesting that dysfunctional mitochondria are essential for the senescence phenotype. Dysfunctional mitochondria are associated with altered mitochondrial bioenergetics and increased mitochondrial mass. Indeed, senescent MSCs had an increased OCR, which could be the results of either increased mitochondrial respiration or increased mitochondrial mass. An increase in mitochondrial mass has been reported before for senescent fibroblasts (Lee, Yin *et al.* 2002, Correia-Melo, Marques *et al.* 2016). In addition, dysfunctional mitochondria produce enhanced levels of reactive oxygen species, which stimulate the induction of cellular senescence (Brookes 2005, Nelson, Kucheryavenko *et al.* 2018). Dysfunctional mitochondria can modulate the SASP through complex mechanisms (Chapman, Fielder *et al.* 2019). Despite the difference in the SASP, both *TWIST1*-silencing-induced and irradiation-induced senescent MSCs showed a similar increase in mitochondrial respiration.

In addition to mitochondrial respiration, glycolysis plays an important role in MSC energy metabolism (Pattappa, Heywood *et al.* 2011). Cellular senescence has been associated with an increased glycolytic capacity after *in vitro* expansion in fibroblasts (Bittles and Harper 1984). The present study showed that irradiation-induced senescent MSCs had an increased ECAR compared to control MSCs, confirming earlier published data in fibroblasts (James, Michalek *et al.* 2015). However, *TWIST1*-silencing-induced senescent MSCs did not show significant differences in ECAR compared to control MSCs. These data suggested that the glycolytic capacity was unaltered in si*TWIST1*-MSCs and showed that senescent MSCs could have a different bioenergetic profile depending on the inducer of senescence.

It is of note that SASP factors are not only known to play a role in senescence but they are also involved in development and tissue repair (Rhinn, Ritschka *et al.* 2019). For example, cells transiently exposed to the SASP have enhanced expression of classical stem cell markers and regenerative capacity, while prolonged exposure induces cell-intrinsic senescence arrest (Ritschka,

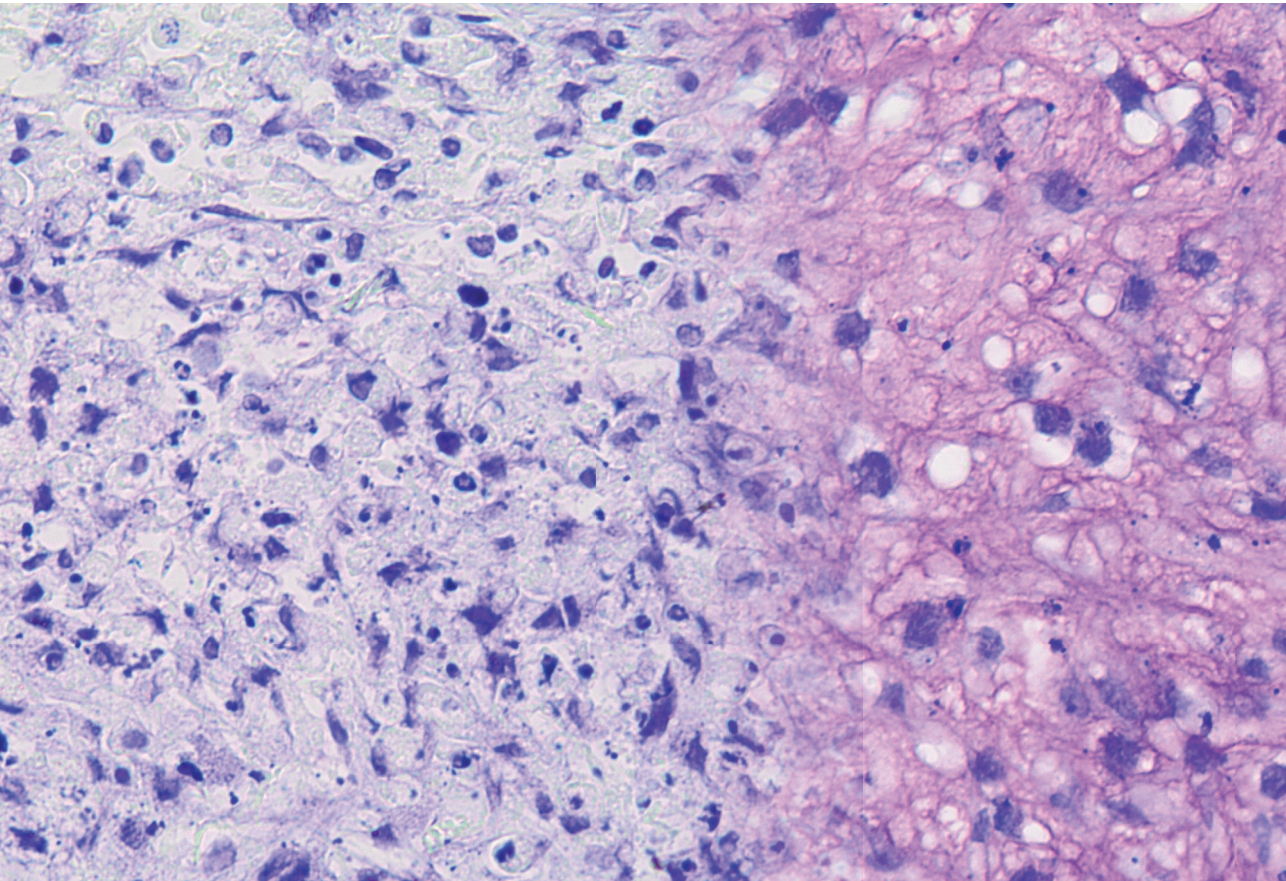
Storer *et al.* 2017). This indicates that these factors can play different roles depending on the exposition time of the cell to the stimuli. However, very little is known about how different kinds of senescent cells and SASP contribute to the induction of senescence or tissue regeneration, for example by transiently or permanently changing the metabolic state of the cells. A better understanding of these processes could contribute to develop new tools that may be used in regenerative medicine.

In summary, the present study provided novel insights in the function of *TWIST1* in regulating cellular senescence in MSCs, suggesting that reduction in *TWIST1* expression might drive the ageing phenotypes of MSCs. Furthermore, the phenotype of these si*TWIST1*-induced senescent MSCs differs from irradiation-induced senescent cells regarding their expression of the SASP and their bioenergetics, highlighting that senescent MSCs can manifest in different ways.

3.6 Acknowledgements

The authors would like to thank Andrea Lolli for advice on the *TWIST1* silencing protocol, Eric Farrell and Janneke Witte-Bouma for access to their source of MSCs, Nicole Kops and Arielle Molina Rakos for technical assistance with the senescence-associated β -galactosidase staining and quantification, Marius Wernig's laboratory (Stanford School of Medicine, Sandford, CA, USA) for providing the GFP overexpression construct and the lentiviral packaging constructs, the FACS sorting facility at the Erasmus MC for support with the BD LSRFortessaTM Cell Analyzer. This research was financially supported by the Dutch Arthritis Society (ReumaNederland; 16-1-201) and by a TTW Perspectief grant from NWO (William Hunter Revisited; P15-23). This study is part of the Medical Delta RegMed4D program and the Erasmus Postgraduate School Molecular Medicine. The authors have no conflict of interest to declare.

4

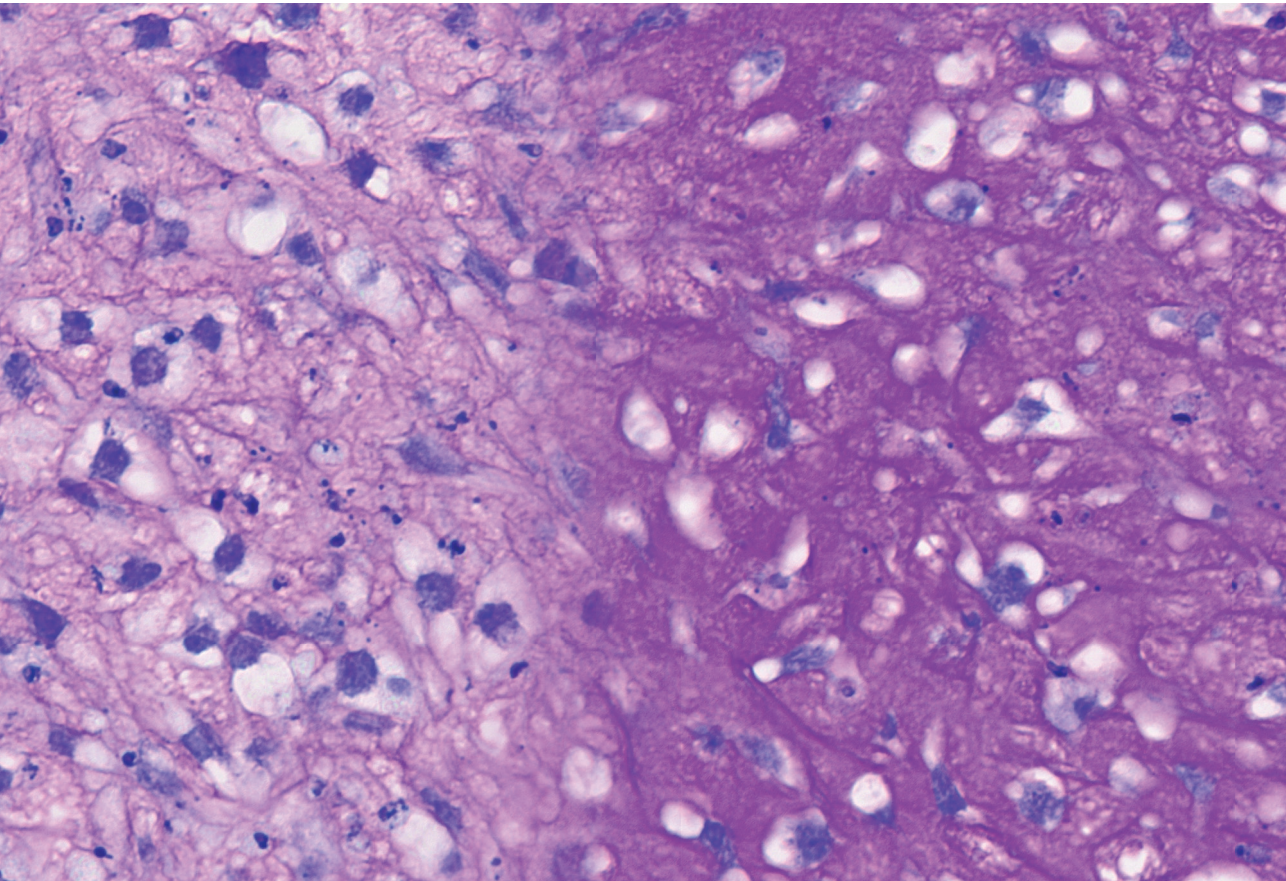


Chapter 4

Sorting living mesenchymal stem cells using a TWIST1 RNA-based probe depend on incubation time and uptake capacity

Chantal Voskamp, Jeroen van de Peppel, Simona Gasparinia, Paolo Giannoni, Johannes P.T.M. van Leeuwen, Gerjo J.V.M. van Osch, Roberto Narcisi

Cytotechnology. 2020 Feb;72(1):37-45



4.1 Abstract

Bone marrow derived mesenchymal stromal cells (BMSCs) are multipotent progenitors of particular interest for cell-based tissue engineering therapies. However, one disadvantage that limits their clinical use is their heterogeneity. In the last decades a great effort was made to select BMSC subpopulations based on cell surface markers, however there is still no general consensus on which markers to use to obtain the best BMSCs for tissue regeneration. Looking for alternatives we decided to focus on a probe-based method to detect intracellular mRNA in living cells, the SmartFlare technology. This technology does not require fixation of the cells and allows us to sort living cells based on gene expression into functionally different populations. However, since the technology is available it is debated whether the probes specifically recognize their target mRNAs. We validated the *TWIST1* probe and demonstrated that it specifically recognizes *TWIST1* in BMSCs. However, differences in probe concentration, incubation time and cellular uptake can strongly influence signal specificity. In addition we found that *TWIST1*^{high} expressing cells have an increased expansion rate. The SmartFlare probes recognize their target gene, however for each probe and cell type validation of the protocol is necessary.

4.2 Introduction

Multipotent progenitor cells from bone marrow aspirates can differentiate into chondrocytes, osteoblasts and adipocytes (Pittenger, Mackay *et al.* 1999). These progenitor cells, often referred to as bone marrow-derived mesenchymal stem or stromal cells (BMSCs), are appealing for cell-based tissue engineering purposes. Unfortunately, their limited expansion capacity and their heterogeneity, hinder their clinical use (Banfi, Muraglia *et al.* 2000, Chen, Sotome *et al.* 2005, Bonab, Alimoghaddam *et al.* 2006, Li, Liu *et al.* 2011). Several studies investigated cell surface molecules to identify specific subpopulations of BMSCs (Buhring, Battula *et al.* 2007, Sacchetti, Funari *et al.* 2007, Delorme, Ringe *et al.* 2008, Sivasubramaniyan, Harichandan *et al.* 2013, Alvarez-Viejo, Menendez-Menendez *et al.* 2015, Cleary, Narcisi *et al.* 2016). However, despite the great effort, there is still no general consensus on the surface markers that need to be used to define or select the best BMSC subset for tissue engineering. One drawback of surface markers is that their function is often unknown, so alternative markers are necessary to select cells according to their function (Clevers and Watt 2018).

Recently, a probe-based method to detect intracellular mRNA in living single cells has been developed, the SmartFlare technology (Seferos, Giljohann *et al.* 2007, Prigodich, Seferos *et al.* 2009). The SmartFlare technique is a promising tool to sort BMSCs into functionally different populations. The SmartFlare probes are taken up by the cells via endocytosis and if the target mRNA is present, the probes bind to the target mRNA and fluorescent reporters are released and detectable (**Figure S4.1A**). Since the SmartFlare technology is available, this technique already successfully identified cancer cells (Kronig, Walter *et al.* 2015, McClellan, Slamecka *et al.* 2015) and pluripotent stem cells (Lahm, Doppler *et al.* 2015). Additionally it was applied to investigate a *Nodal* expressing subpopulation of melanoma cells (Seftor, Seftor *et al.* 2014), and to study a subpopulation of human BMSCs with an enhanced osteogenic potential (Li, Menzel *et al.* 2016). However, other studies did not find a correlation between the SmartFlare fluorescence intensity and mRNA expression measured by RT-PCR (Czarnek and Bereta 2017, Yang, Anholts *et al.* 2018). In addition, Czarnek *et al.* found that the SmartFlare signal intensity correlates with the probe uptake ability of the cells (Czarnek and Bereta 2017).

To assess if the SmartFlare technique can be used to sort different populations of BMSCs based on gene expression, we focused on the validation of a probe for *TWIST1*. *TWIST1* is a transcription factor that is involved in the regulation of BMSC proliferation (Isenmann, Arthur *et al.* 2009, Goodnough, Chang *et al.* 2012, Tian, Xu *et al.* 2015) and differentiation (Isenmann, Arthur *et al.* 2009, Narcisi, Cleary *et al.* 2015, Boregowda, Krishnappa *et al.* 2016, Narcisi, Arikan *et al.* 2016, Cleary, Narcisi *et al.* 2017). In the present study, we evaluated the SmartFlare protocol in order to detect a specific probe signal in our culture conditions and illustrated that the SmartFlare fluorescence intensity is associated with probe concentration, incubation time and cellular uptake capacity.

4.3 Materials and methods

4.3.1 Isolation and culture of human adult bone marrow mesenchymal stem cells

Human adult bone marrow aspirates were obtained from femoral biopsies of 8 patients (22-79 years) undergoing total hip replacement (MEC 2015-644, MEC 2004-142: Erasmus Medical Center, Rotterdam; MEC 2011.07 Albert Schweitzer Hospital, Dordrecht), after obtaining informed consent and full ethical approval by the Erasmus MC and Albert Schweitzer ethics committee. Human BMSCs were isolated, seeded at the density of 2,300 cells/cm² and cultured as previously described in standard expansion media, containing 10% FCS (Lonza, Verviers, Belgium; selected batch:1S016) and 1 ng/mL FGF2 (AbD Serotech, Kidlington, United Kingdom) (Narcisi, Arikan *et al.* 2016). The medium was refreshed twice a week. BMSCs expanded for 3 to 6 passages were used for experiments.

4.3.2 SmartFlare probes

Cells were treated with the SmartFlare probe when they were sub-confluent. SmartFlare probes *TWIST1*-Cy3 (the only label available for *TWIST1*), Uptake-Cy5, and GAPDH-Cy5 were purchased from Merck. The probes were resuspended in 50 μ L sterile nuclease free water, 1:20 prediluted in PBS (Lonza) and added to the cells with a final concentration of 50 pM or 100 pM. The cells were incubated for 6 or 16 hrs at 37°C and 5% CO₂ and analyzed using flow cytometry. To assure a broad range of *TWIST1* gene expression during the validation of the *TWIST1*-Cy3 probe, BMSCs from

two different donors were mixed and treated with the TWIST1-Cy3 probe.

4.3.3 Flow cytometry and FACS

Flow cytometry analysis was performed using a BD Fortessa and the data was analyzed using FlowJo V10 software. The cells were sorted using a BD Biosciences FACS Aria and the data was analyzed using BD FACS Diva 8.0.1 software. Cell debris were excluded from the population through forward scatter (FSC)/ side scatter (SSC) gate and doublets were excluded using FSC-A/FSC-H gate (**Figure S4.2A**). To confirm effective sorting, the sorted populations were reanalyzed (**Figure S4.2B**). Mean fluorescent intensity (MFI) was measured using FlowJo V10 software. The two different gates $TWIST1^{high}$ and $TWIST1^{low}$ were established based on the TWIST1-Cy3 fluorescence intensity, 15-25% of the extremes or two different gates $TWIST1/Uptake^{high}$ and $TWIST1/Uptake^{low}$ were established based on the TWIST1-Cy3 fluorescence intensity, 15% of the extremes with a comparable Uptake-Cy5 fluorescence intensity. The sorted cells were collected in PBS with 1% FCS and reseeded with a density of 2,300 cells per cm^2 or used for RNA isolation.

4.3.4 Real time PCR analysis

Post-sorting, 200,000 BMSCs per sample were spun down and treated on ice with RLT lysis buffer (Qiagen, Hilden, Germany) with 1% β -mercaptoethanol. BMSCs in monolayer were washed with PBS and treated on ice with RLT lysis buffer (Qiagen) with 1% β -mercaptoethanol. A range of 0.25-1.00 μ g of purified RNA (RNeasy Micro Kit; Qiagen) was reverse transcribed into cDNA (RevertAid First Strand cDNA Synthesis Kit; MBI Fermentas, St. Leon-Rot, Germany). RT-PCR was performed using an annealing temperature of 60 °C on a C1000 Touch™ Thermal Cycler using SybrGreen (Eurogentec, Seraing, Belgium). The data were normalized to the housekeeper gene *RPS27A*. The relative expression was calculated according to the $2^{-\Delta\Delta Ct}$ formula. The primers used for RT-PCR are listed in (**Table S4.1**).

4.3.5 Data Analysis

Linear correlation was analyzed with GraphPad Prism Software 5.00 assuming a normal distribution of the data.

4.4 Results

4.4.1 *TWIST1* SmartFlare detect *TWIST1* mRNA after 6 hours using a concentration of 50 pM in human BMSCs

SmartFlare probes enter the cell via endocytosis and this process can vary between different cell types (Choi, Hao *et al.* 2013). The probe incubation time and concentration which is suggested by the manufacturer is 16 hours and 100 pM. However we also included a 6 hours timepoint and a concentration of 50 pM in order to verify whether or not it was possible to further optimize the SmartFlare protocol for *TWIST1* in BMSCs. Interestingly, already after 6 hours with a probe concentration of 50 pM, 98.5% of the cells were positive for *TWIST1* SmartFlare signal (**Figure 4.1A**; lowest panel). No major differences in SmartFlare signal intensity were observed between the different probe concentrations and incubation times (**Figure 4.1A**).

To study *TWIST1*-Cy3 signal specificity, BMSCs were treated with *TWIST1*-Cy3 probe for 16 hours or 6 hours, sorted based on the *TWIST1*-Cy3 signal by FACS and subsequently tested by RT-PCR. Our FACS gating strategy consisted of sorting 15% of the BMSCs with the lowest *TWIST1*-Cy3 signal and 15% of the BMSCs with the highest *TWIST1*-Cy3 signal (*TWIST1*^{low} vs *TWIST1*^{high}; **Figure 4.1B**). To our surprise no difference in relative *TWIST1* gene expression was detected between *TWIST1*^{low} and *TWIST1*^{high} cells after 16 hours of probe incubation (**Figure 4.1C**). This indicates that although we observe a *TWIST1* SmartFlare signal after 16 hours, this signal is probably not specific for *TWIST1* gene expression. However after 6 hours incubation we confirmed that *TWIST1*^{high} BMSCs have a higher *TWIST1* gene expression than the *TWIST1*^{low} population (6.25-fold difference; **Figure 4.1C**).

These data show that the *TWIST1* probe specifically detects *TWIST1* gene expression in this population of BMSCs already after 6 hours incubation with a concentration of 50 pM probe. In addition, we observed that more than 97.3% of cells were positive for the Uptake control probe, a probe which is always fluorescent without binding to a target (**Figure S4.3**), with 50 pM after 6 hours of incubation.

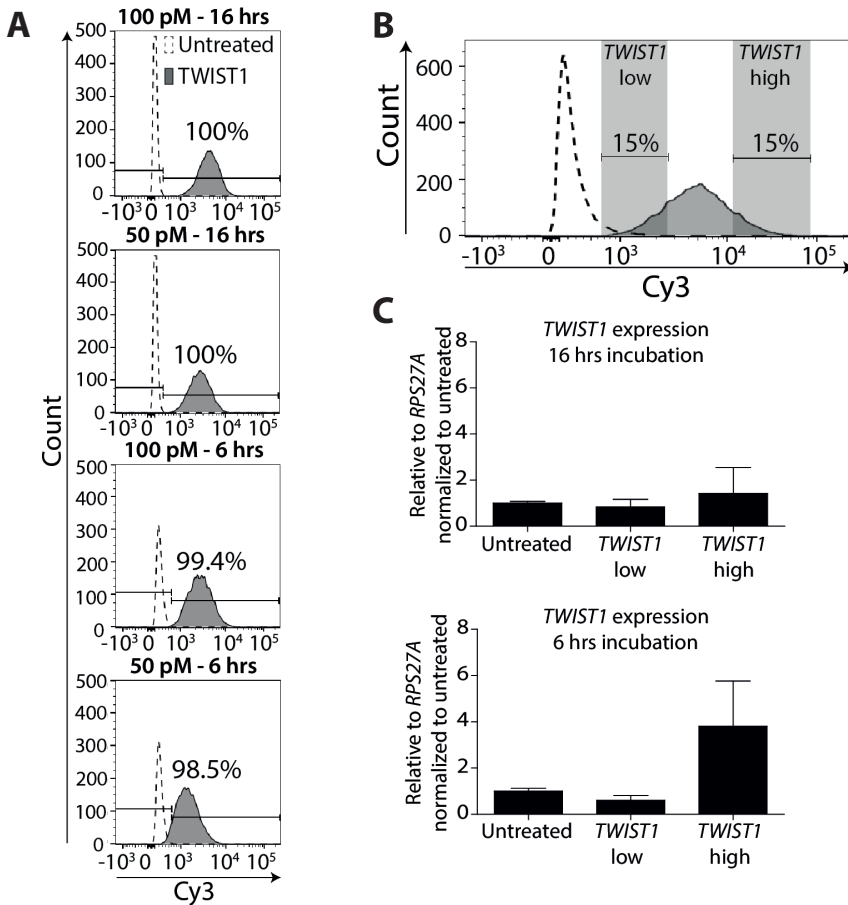


Figure 4.1- *TWIST1* SmartFlare probes are efficiently taken up by BMSCs after 6 hours. (A) Flow cytometry histogram of untreated BMSCs and BMSCs with 100 pM or 50 pM *TWIST1*-Cy3 probe incubated for 16 or 6 hours, % shows percentage Cy5 positive cells. (B) Gating strategy based on *TWIST1*-Cy3 intensity. The dotted graph represents unstained BMSCs and the gray graph represents BMSCs with *TWIST1*-Cy3 probes. (C) BMSCs were sorted based on *TWIST1*-Cy3 intensity after 16 and 6 hours of probe incubation. *TWIST1* transcripts were analysis by RT-PCR. Values represent the mean \pm SD from duplicates or quadruplicate.

To further determine the signal specificity of the *TWIST1* probe after 6 hours, we analyzed the correlation between the *TWIST1*-Cy3 signal intensity and *TWIST1* expression by RT-PCR. *TWIST1* probe signal intensity from two BMSC populations (referred to as donor 1 and donor 2) was measured using flow cytometry, showing a higher intensity in donor 2 difference in *TWIST1* expression between the two donors, showing a higher expression in donor 2 (8775 vs 5645 MFI; **Figure 4.2A**). Transcript analysis confirmed the

difference in *TWIST1* expression between the two donors, showing a higher expression in donor 2 (**Figure 4.2B**). We therefore repeated the analysis in four other donors showing a positive and consistent correlation between *TWIST1*-Cy3 probe intensity and *TWIST1* gene expression ($r^2=0.997$; **Figure 4.2C**). These data again confirms that the *TWIST1* probe specifically targets the *TWIST1* mRNA after 6 hours of incubation.

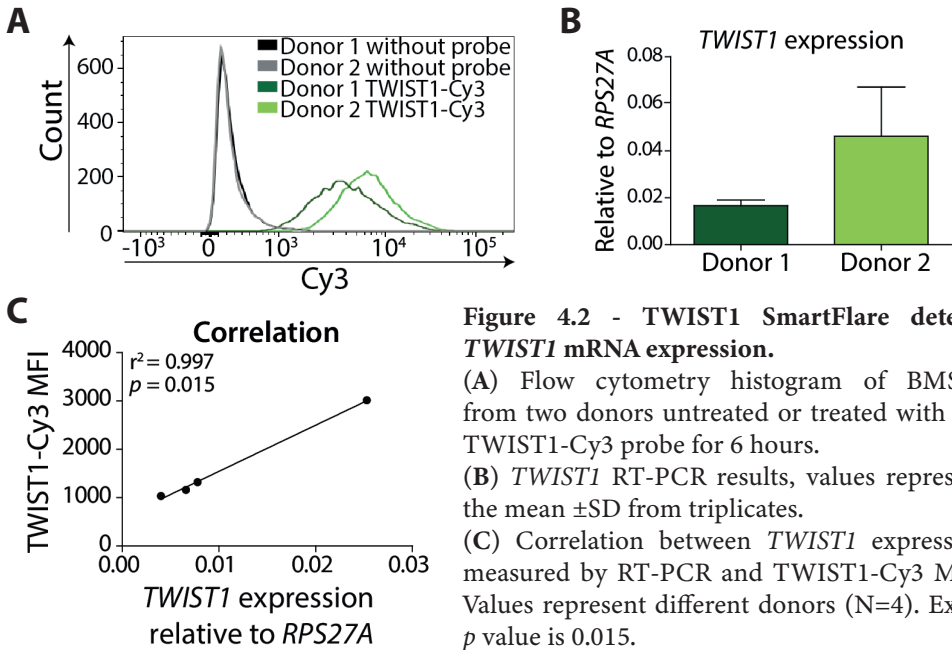


Figure 4.2 - *TWIST1* SmartFlare detects *TWIST1* mRNA expression.

(A) Flow cytometry histogram of BMSCs from two donors untreated or treated with the *TWIST1*-Cy3 probe for 6 hours.

(B) *TWIST1* RT-PCR results, values represent the mean \pm SD from triplicates.

(C) Correlation between *TWIST1* expression measured by RT-PCR and *TWIST1*-Cy3 MFI. Values represent different donors (N=4). Exact p value is 0.015.

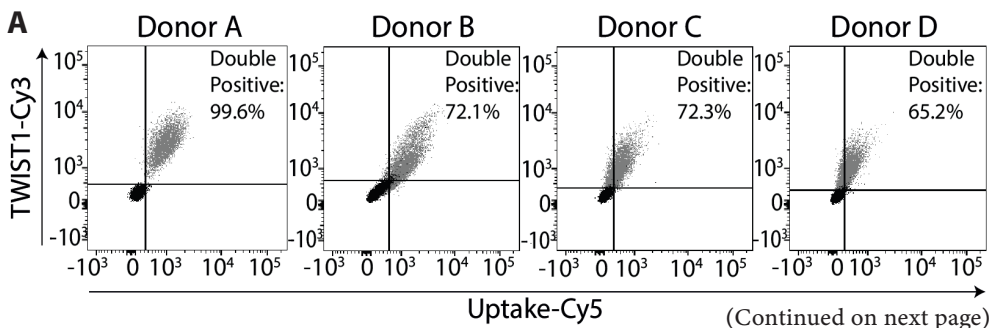
4.4.2 Correction for cellular probe uptake improves *TWIST1* gene detection

When we repeated the sorting experiment with other donors not always differences in *TWIST1* expression by RT-PCR were observed between *TWIST1*^{low} and *TWIST1*^{high} sorted cells (**Figure S4.4**). Given that, and considering that Czarnek *et al.* recently showed that uptake capacity can influence the SmartFlare signal specificity (Czarnek and Bereta 2017), we decided to carefully monitor uptake in our BMSC populations.

To evaluate the effect of cellular uptake on the *TWIST1* signal, BMSCs from 4 different donors were double labeled with *TWIST1*-Cy3 and Uptake-Cy5 probes (**Figure S4.1B**). At least 65% of the BMSCs were able to take up both the *TWIST1*-Cy3 and Uptake-Cy5 probe (**Figure 4.3A**) and we demonstrated

that BMSCs from different donors have a different uptake capacity (**Figure S4.5**). Moreover, it is clear from the FACS analysis that there is a general positive correlation between Uptake-Cy5 signal and TWIST1-Cy3 signal (the higher the *TWIST1* signal, the higher the Uptake signal), although with variation between donors (**Figure 4.3A** and **Figure S4.5**). This indicates that in BMSCs from different donors the TWIST1-Cy3 signal can be affected by the cellular uptake capacity, with a degree that depends on the individual uptake capacity of the cells in the BMSC population.

To determine whether or not the detected differences in cellular uptake have an effect on *TWIST1* gene detection, BMSCs with a high variation in Uptake-Cy5 fluorescence intensity were treated with both TWIST1-Cy3 and Uptake-Cy5 probes and were sorted by FACS using two different sorting strategies or left unsorted. In the first gating strategy, similar to that previously used, 15% of the BMSCs with the lowest TWIST1-Cy3 signal and 15% of the BMSCs with the highest TWIST1-Cy3 signal (*TWIST1*^{high}) were sorted (**Figure 4.3B**; left panel). In the second gating strategy we corrected for the uptake signal (**Figure 4.3C**; left panel) by sorting *TWIST1*^{high} and *TWIST1*^{low} cells with a minimal uptake variation. Gene expression analysis showed no differences between *TWIST1*^{low} and *TWIST1*^{high} populations in the absence of uptake correction (**Figure 4.3B**; left middle panel), while a strong difference (13.3-fold) was detected between the subpopulations where the *TWIST1* signal was corrected for the uptake (**Figure 4.3C**; left middle panel). These data indicate that differences in cellular uptake can strongly influence *TWIST1* detection using SmartFlare. In addition, we observed that the sorted populations of BMSCs corrected for cellular uptake had a similar cellular granularity (**Figure 4.3B-C**; right middle panel) and cell size (**Figure 4.3B-C**; right panel) compared to the populations sorted without uptake correction.



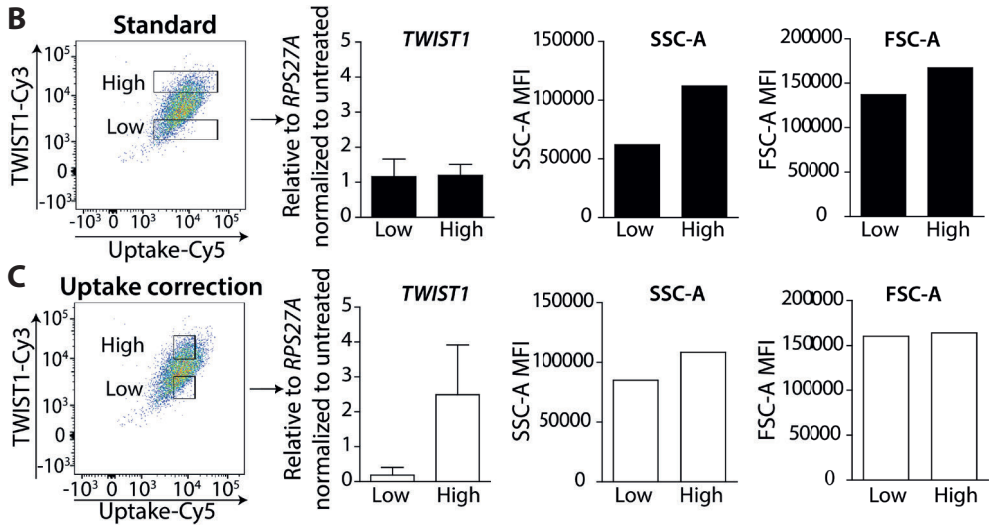


Figure 4.3- Correction for cellular probe uptake improves *TWIST1* gene detection.

(A) Flow cytometry plots of BMSCs of four donors treated with both *TWIST1*-Cy3 and Uptake-Cy5 probe for 6 hours (grey). The perpendicular lines represent the unstained control (black) for each donor. % shows percentage Cy3 and Cy5 double positive cells.

(B-C) FACS gating strategies using *TWIST1*-Cy3 and Uptake-Cy5 probes for 6 hours and *TWIST1* RT-PCR results, values represent the mean \pm SD from duplicates. SSC-A MFI and FSC MFI of Standard and Uptake correction low vs high.

4.4.3 *TWIST1*^{high} BMSCs have a high expansion capacity

In order to further validate our sorting strategy and prove for the first time the pro-proliferative role of *TWIST1* in a subpopulation of BMSCs, we sorted *TWIST1*^{high} and *TWIST1*^{low} cells and we compared their expansion capacity post-sorting. RT-PCR confirmed that *TWIST1*^{high} BMSCs had a higher relative *TWIST1* gene expression than *TWIST1*^{low} BMSCs (1.6-fold difference; **Figure 4.4A**). No evident differences in morphology between *TWIST1*^{low} and *TWIST1*^{high} were observed 5 days post sorting, while 16 days post sorting *TWIST1*^{low} BMSCs appeared more enlarged compared to the *TWIST1*^{high} BMSCs (**Figure 4.4B**). Moreover, *TWIST1*^{high} BMSCs showed a higher expansion capacity than the *TWIST1*^{low} population (**Figure 4.4C**; 1.5 fold difference after 3 passages) and, 16 days post sorting, the *TWIST1*^{low} BMSCs stop growing while the *TWIST1*^{high} BMSCs were still expanding (data not shown). This indicates that within the same population of BMSCs, the *TWIST1*^{high} expressing cells have a higher expansion rate compared to the *TWIST1*^{low} expressing cells.

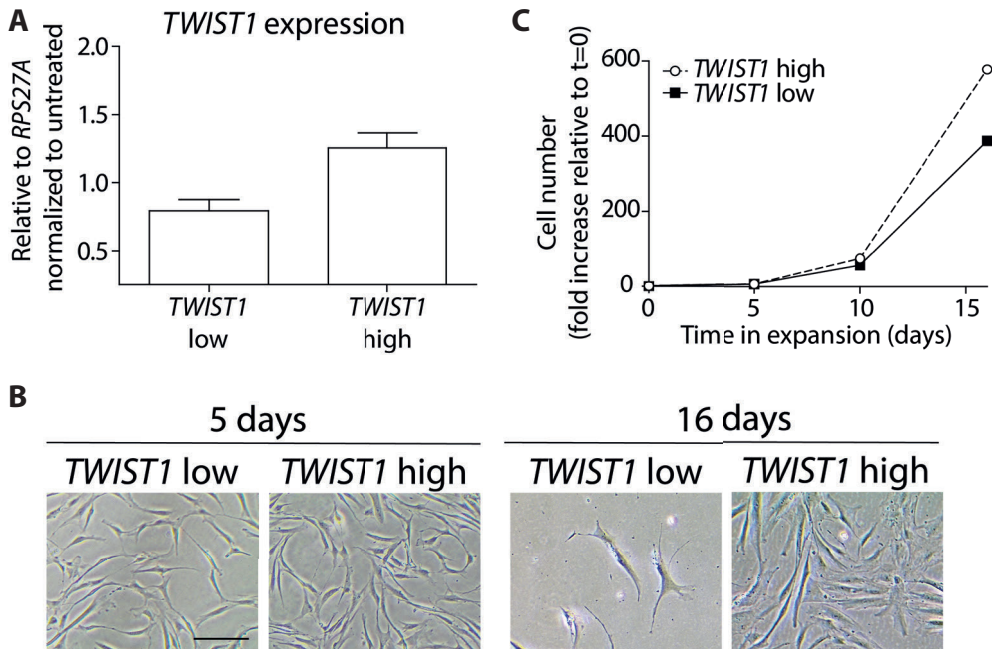


Figure 4.4- *TWIST1*^{high} BMSCs have a high proliferation capacity.

- (A) *TWIST1* RT-PCR results of Untreated, *TWIST1*^{low} and *TWIST1*^{high} populations, values represent the mean \pm SD from duplicates.
- (B) Morphology of BMSCs 5 days and 16 days after being sorted. Scale bar represents 100 μ m.
- (C) Cell numbers relative to t=0 of Untreated, *TWIST1*^{low} and *TWIST1*^{high} were passaged and counted on day 0, day 5, day 10 and day 16.

4.5 Discussion

In this study, we evaluated the SmartFlare technique to detect *TWIST1* expression at a single cell level in living BMSCs. Multiple studies successfully detected mRNA expression with the SmartFlare technique (Seftor, Seftor *et al.* 2014, Kronig, Walter *et al.* 2015, Lahm, Doppler *et al.* 2015, McClellan, Slamecka *et al.* 2015, Li, Menzel *et al.* 2016). However, two recent studies showed that different SmartFlare probes were not able to specifically detect their target mRNAs in cell lines and monocytes (Czarnek and Bereta 2017, Yang, Anholts *et al.* 2018). However, here we show that SmartFlare is an effective tool to detect *TWIST1* gene expression in living BMSCs, but differences in probe concentration, incubation time and cellular uptake can influence the SmartFlare sensitivity and possibly lead to misinterpretation of the results.

We observed that specific detection of *TWIST1* mRNA expression in BMSCs is possible already after 6 hours of incubation with a concentration of 50 pM, *TWIST1*-Cy3 probe. While most of the studies used 16 hours (Seftor, Seftor *et al.* 2014, McClellan, Slamecka *et al.* 2015, Li, Menzel *et al.* 2016, Czarnek and Bereta 2017) or even 24 hours (Kronig, Walter *et al.* 2015, Lahm, Doppler *et al.* 2015, Czarnek and Bereta 2017) as optimal incubation time, we were not able to specifically detect *TWIST1* after 16 hours incubation (**Figure S4.4**). The SmartFlare technology was recently applied in BMSCs (Li, Menzel *et al.* 2016), but never for the detection of *TWIST1* expression. In our study a different protocol was needed compared to the *RUNX2* and the *SOX9* probes used by Li *et al.* (Li, Menzel *et al.* 2016). Possible explanations could be ascribed to differences in culture conditions, origin of BMSCs or binding efficiency of the probe to the target.

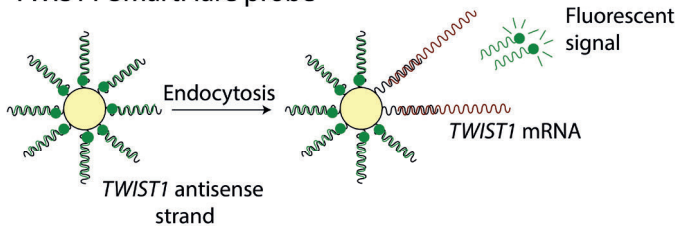
In addition, our data illustrates that BMSCs can have a high difference in probe uptake. We observed that these differences strongly influence the *TWIST1* SmartFlare specificity. This confirms a previous report where SmartFlare intensity was affected by cellular uptake in 293T cells (Czarnek and Bereta 2017). The differences in uptake capacity can be explained by differences in cell cycle stage between the BMSCs, since endocytosis is reduced during mitosis (Fielding, Willox *et al.* 2012). Here, we were able to overcome this problem by correcting *TWIST1* detection for the cellular uptake based on Uptake probe intensity during sorting. Next, we demonstrate that *TWIST1*^{high} expressing BMSCs have a higher expansion capacity than *TWIST1*^{low} expressing BMSCs derived from the same donor. A population of BMSCs with a high *TWIST1* expression and a high proliferation rate have already been reported by us and others (Isenmann, Arthur *et al.* 2009, Narcisi, Cleary *et al.* 2015, Cleary, Narcisi *et al.* 2017). Here, we show for the first time that within the BMSCs of the same donor, the subpopulation of *TWIST1*^{high} expressing BMSCs have a higher expansion capacity than the *TWIST1*^{low} expressing BMSCs. In a previous report the ratio between two functional markers, *RUNX2* and *SOX9*, was used (Li, Menzel *et al.* 2016). This is a possible alternative to correct for uptake, since this approach would automatically take into account differences in uptake, as these would not change the ratio, but only the intensity of the individual signals.

4.6 Conclusion

In summary, our data indicate that for each probe and cell type, a validation of the SmartFlare protocol is necessary. Given that we were able to successfully use the TWIST1 probe to detect *TWIST1* mRNA in living cells and that we were able to sort *TWIST1*^{high} cells, SmartFlare is a promising tool to divide a heterogeneous population of cells based on gene expression in functionally different populations.

4.7 Supplemental Information

A TWIST1 SmartFlare probe



B

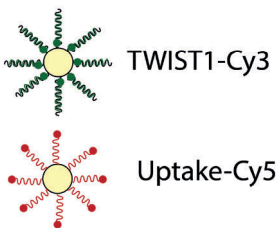


Figure S4.1 – Schematic overview of detection of *TWIST1* expression by the SmartFlare probe.

Figure S4.1 is based on the figures in the SmartFlare manufacture user guide.

(A) The *TWIST1* SmartFlare probe exists of a gold particle with a *TWIST1* antisense strand attached to it. To this antisense strand a fluorescent reporter is bound, which is quenched by the gold particle. The probes enter the cells via endocytosis and if there is *TWIST1* mRNA in the cells, the fluorescent probe will be released and fluorescent.

(B) The *TWIST1*-Cy3 probe is designed for specific detection of *TWIST1* mRNA. The Uptake-Cy5 is a control probe which is permanent fluorescent. The uptake-Cy5 fluorophore is not quenched because the fluorophore is located far from the gold particle.

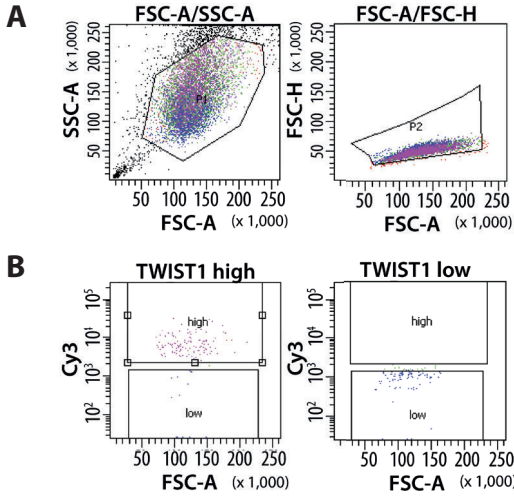


Figure S4.2 – FACS gating strategy to exclude cell debris and cell doublets.
 (A) Cell debris are excluded by plotting FSC-A versus SSC-A (P1). Cell doubles are excluded by plotting FSC-A versus FSC-H (P2).
 (B) Sorted populations were reanalyzed to test effective sorting.

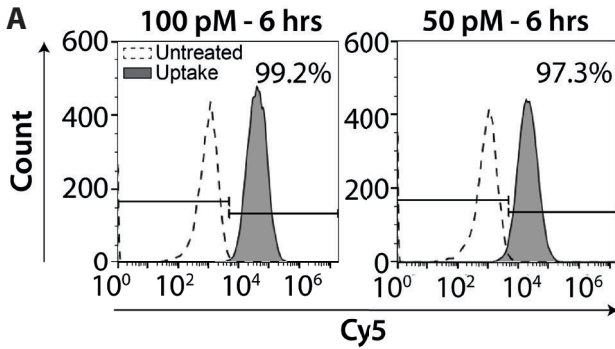


Figure S4.3 – SmartFlare probes are taken up by BMSCs after 6 hours.
 (A) Uptake flow cytometry histograms of untreated BMSCs and BMSCs with 100 pM or 50 pM Uptake-Cy5 probe incubated for 6 hours. % shows percentage of Cy5 positive cells.

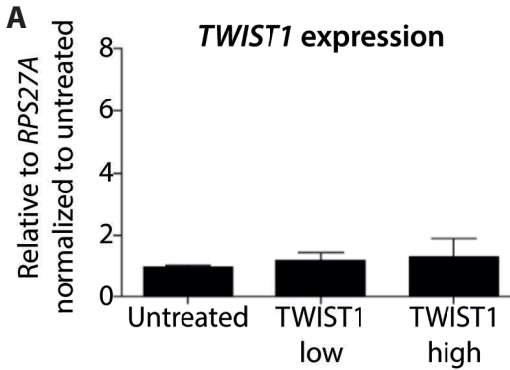


Figure S4.4 – RT-PCR results of *TWIST1*^{high} and *TWIST1*^{low} sorted BMSCs.
 (A) BMSCs are treated for 6 hours with 50 pM *TWIST1*-Cy3 probe and sorted based on *TWIST1*-Cy3 intensity (15% of the extremes) or left untreated. RT-PCR results, values represent the mean \pm SD from triplicates.

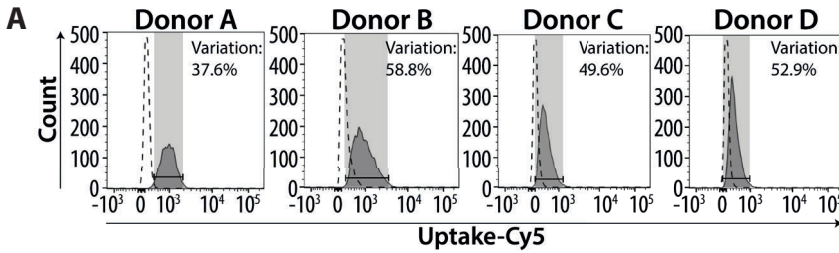


Figure S4.5– Different MSC donors have a different probe uptake capacity.

(A) Flow cytometry plots of BMSCs of four donors treated with Uptake-Cy5 probe and TWIST1-Cy3 probe for 6 hours show uptake variation (indicated in grey). Variation is coefficient of variation of the Uptake-Cy5 signal.

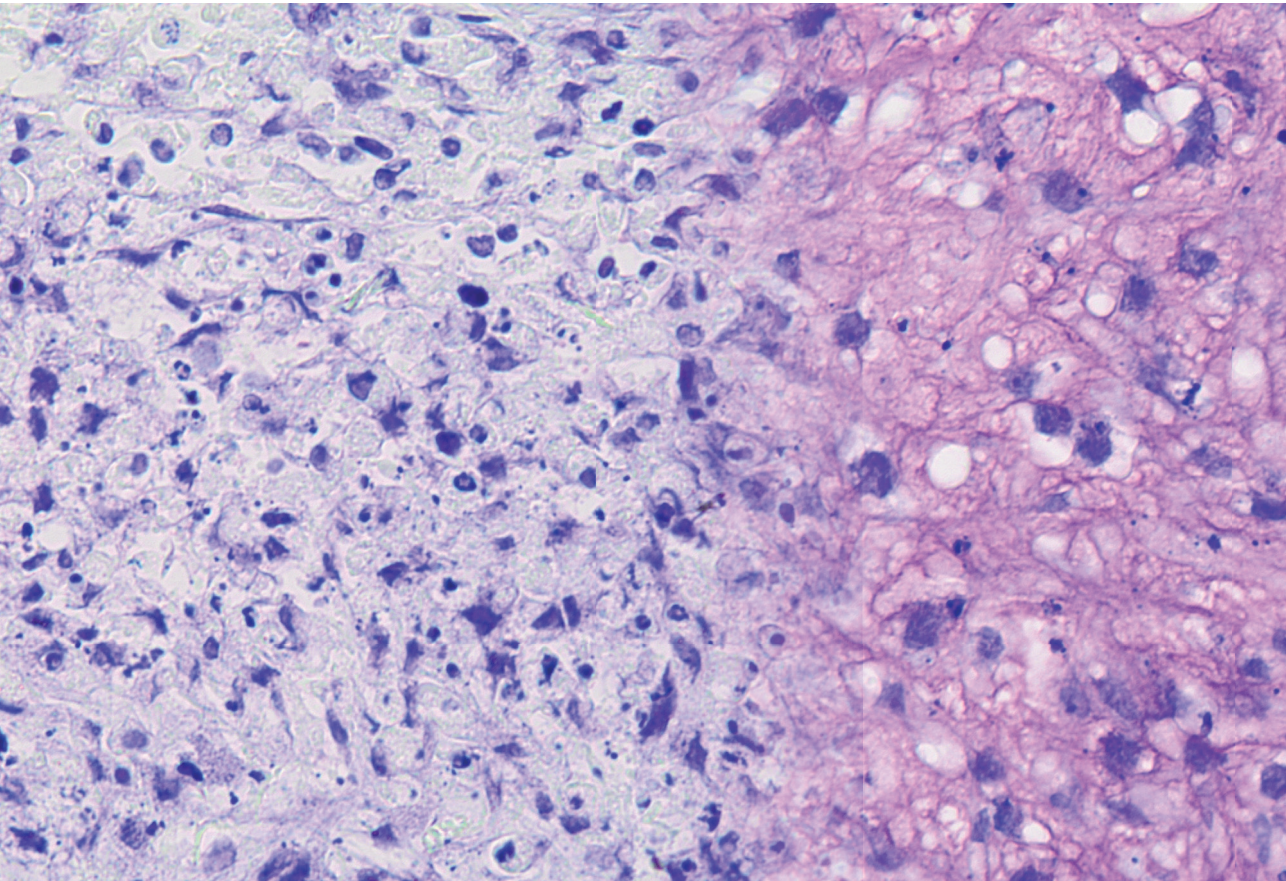
Table S4.1- RT-PCR primers

Gene	Primers
<i>TWIST1</i>	Fw: 5'- GTCCGCAGTCTTACGAGGAG-3' Rv: 5'- CCAGCTTGAGGGTCTGAATC-3'
<i>RPS27A</i>	Fw: 5'-TGGCTGTCCTGAAATATTATAAGGT-3' Rv: 5'-CCCCAGCACCACATTCATCA-3'

4.8 Acknowledgements

J.L.M. Koevoet, A.L.M. Vriends, T.W. Kan, P. van Geel, G. Kremers are acknowledged for technical assistance. We are thankful to the Erasmus MC FACS sorting facility for support with FACS machines This work was financially supported by the Dutch Arthritis Foundation (16-1-201), and R.N. was further supported by a Veni grant from NWO (13659).

5

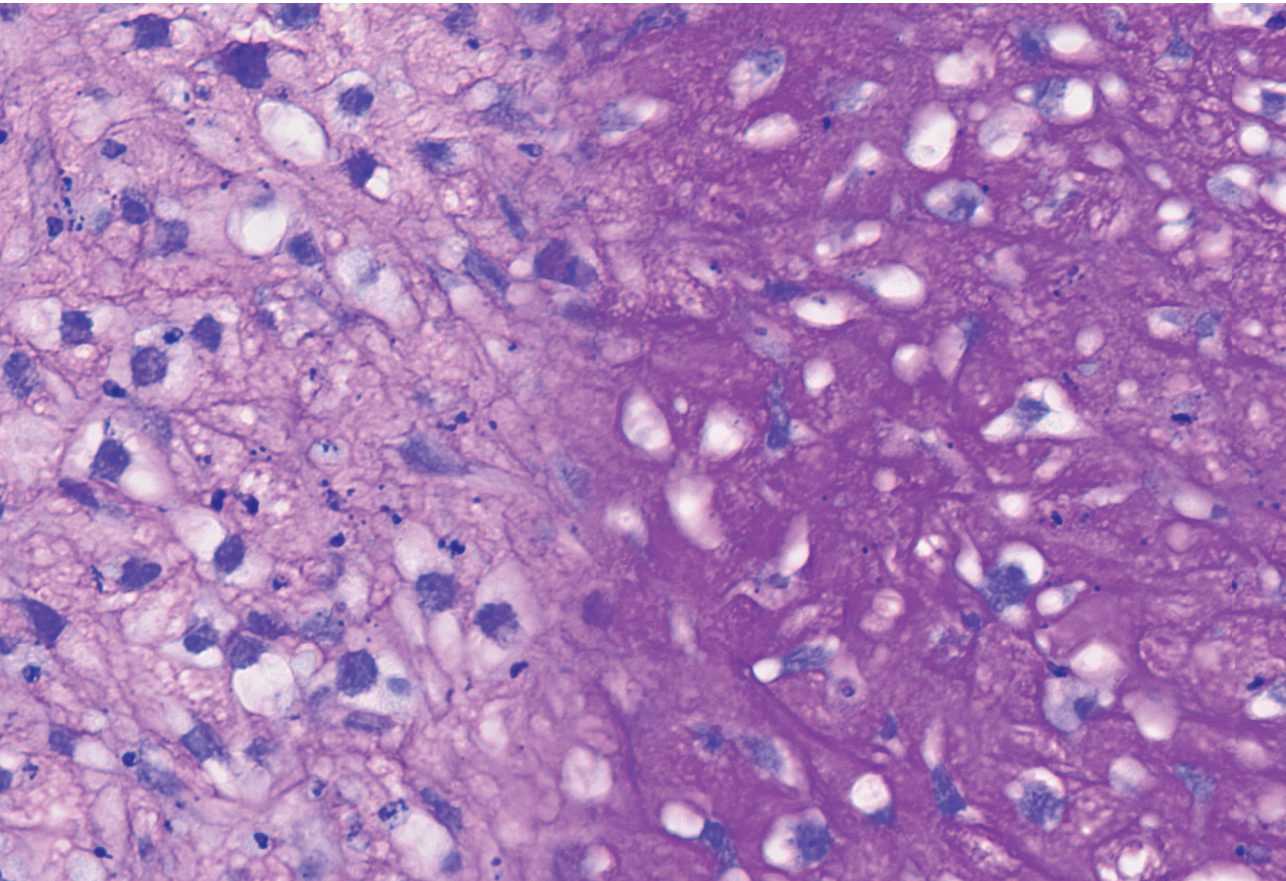


Chapter 5

Enhanced Chondrogenic Capacity of Mesenchymal Stem Cells After TNF α Pre-treatment

Chantal Voskamp, Wendy J L M Koevoet, Rodrigo A Somoza, Arnold I Caplan, Véronique Lefebvre, Gerjo J V M van Osch, Roberto Narcisi

Front Bioeng Biotechnol. 2020 Jun 30;8:658



5.1 Abstract

Mesenchymal stem cells (MSCs) are promising cells to treat cartilage defects due to their chondrogenic differentiation potential. However, an inflammatory environment during differentiation, such as the presence of the cytokine TNF α , inhibits chondrogenesis and limits the clinical use of MSCs. On the other hand, it has been reported that exposure to TNF α during *in vitro* expansion can increase proliferation, migration and the osteogenic capacity of MSCs and therefore can be beneficial for tissue regeneration. This indicates that the role of TNF α on MSCs may be dependent on the differentiation stage. To improve the chondrogenic capacity of MSCs in the presence of an inflamed environment, we aimed to determine the effect of TNF α on the chondrogenic differentiation capacity of MSCs. Here, we report that TNF α exposure during MSC expansion increased the chondrogenic differentiation capacity regardless of the presence of TNF α during chondrogenesis and that this effect of TNF α during expansion was reversed upon TNF α withdrawal. Interestingly, pre-treatment with another pro-inflammatory cytokine, IL-1 β , did not increase the chondrogenic capacity of MSCs indicating that the pro-chondrogenic effect is specific for TNF α . Finally, we show that TNF α pre-treatment increased the levels of SOX11 and active β -catenin suggesting that these intracellular effectors may be useful targets to improve MSC-based cartilage repair. Overall, these results suggest that TNF α pre-treatment, by modulating SOX11 levels and WNT/ β -catenin signaling, could be used as a strategy to improve MSC-based cartilage repair.

5.2 Introduction

Cartilage has a limited repair capacity and, if left untreated after damage, it will often undergo progressive, irreversible degeneration. The treatment of cartilage defects still remains challenging and novel regenerative medicine strategies are needed. Mesenchymal stem cells (MSCs) are promising cells for cell-based cartilage regeneration approaches (Caplan 1991, Caplan and Dennis 2006) because ease of isolation, chondrogenic potential (Johnstone, Hering *et al.* 1998, Pittenger, Mackay *et al.* 1999) and anti-inflammatory properties (Kinnaird, Stabile *et al.* 2004, Caplan and Dennis 2006, Ren, Zhang *et al.* 2008, van Buul, Villafuertes *et al.* 2012). These properties can be affected by factors present in the microenvironment, such as pro-inflammatory cytokines. TNF α is one of the pro-inflammatory cytokines that can be present in symptomatic cartilage defects (Tsuchida, Beekhuizen *et al.* 2014), osteoarthritic cartilage and synovium (Chu, Field *et al.* 1991, Kapoor, Martel-Pelletier *et al.* 2011, Tsuchida, Beekhuizen *et al.* 2014) and that contributes to the pathophysiology of osteoarthritis (reviewed by Fernandes, Martel-Pelletier *et al.* 2002, Goldring and Otero 2011).

Exposure to TNF α during MSC chondrogenesis *in vitro* reduces the chondrogenic capacity (Wehling, Palmer *et al.* 2009), increasing the expression of aggrecanases and decreasing expression of proteoglycans (Markway, Cho *et al.* 2016). However TNF α is known to be involved in several biological processes such as apoptosis, proliferation and cell survival (Brenner, Blaser *et al.* 2015, Cheng, Li *et al.* 2019). In addition, there is also evidence that TNF α can promote tissue regeneration since it can increase osteogenesis (Daniele, Natali *et al.* 2017) and MSC proliferation and migration (Bocker, Docheva *et al.* 2008, Bai, Xi *et al.* 2017, Shioda, Muneta *et al.* 2017). It has been shown that MSCs primed with TNF α *in vitro* survive better than control MSCs when transplanted *in vivo* (Giannoni, Scaglione *et al.* 2010). Overall these data suggest that the effect of TNF α may depend on the dynamics of exposure and that its effect may be beneficial for MSC-based tissue regeneration. Specifically, the effect on chondrogenesis of TNF α administration during MSC expansion has been incompletely investigated whether in the presence or absence of an inflamed environment during the subsequent phase of cell differentiation.

In order to increase the chondrogenic capacity of MSCs under inflammatory conditions, we hypothesized that TNF α administration during cell expansion (pre-treatment) would have a beneficial effect on the subsequent chondrogenesis performed in the presence of TNF α . Here we demonstrated that TNF α pre-treatment increases MSC chondrogenesis regardless of the presence of TNF α during differentiation and that the effect of TNF α on the chondrogenic capacity is reversible. This pro-chondrogenic effect could not be obtained by pre-treatment with interleukin 1 β (IL-1 β) another pro-inflammatory cytokine involved in local inflammation in the joint (Goldring and Otero 2011). Finally, to identify a possible TNF α target pathway in the pre-treated MSCs, we investigated the levels of the SOXC protein (SOX4 and SOX11), this group of SRY-related transcription factors was previously described to be stabilized by TNF α and involved in cartilage primordia and growth plate formation (Bhattaram, Muschler *et al.* 2018); (Kato, Bhattaram *et al.* 2015). In addition, we also analyzed active β -catenin levels, since SOXC can increase β -catenin protein levels (Bhattaram, Penzo-Méndez *et al.* 2014) and WNT/ β -catenin signaling can increase the chondrogenic potential of MSCs (Narcisi, Cleary *et al.* 2015).

5.3 Materials and Methods

5.3.1 MSC isolation and expansion

MSCs were isolated from human bone marrow aspirates from patients (17-73 years old, Table S1) undergoing total hip replacement after informed consent and with approval of the ethics committee (MEC 2015-644: Erasmus MC, Rotterdam). Patients with radiation therapy in the hip area, hematologic disorders and mental retardation or dementia were excluded from our study population. MSCs were isolated by plastic adherence and the day after seeding the non-adherent cells were washed away with PBS with 1% fetal calf serum (Gibco, selected batch 41Q2047K). They were cultured in alpha-MEM (Invitrogen), with 10% fetal calf serum, 1.5 μ g/ml fungizone (Gibco), 50 μ g/mL gentamicin (Invitrogen), 1 ng/mL FGF2 (AbD Serotec) and 0.1 mM ascorbic acid-2-phosphate (Sigma-Aldrich). After 10-12 days, the MSCs were trypsinized and re-seeded at a density of 2,300 cells/cm². MSCs in our study were selected based on their capacity to chondrogenically differentiate, their MSC morphology (small elongated and spindle-shaped cells) and expansion capacity (cells with less than 0.15 doublings/day were excluded).

To investigate whether exposure to TNF α during expansion prior to chondrogenic differentiation (pre-treatment) could inhibit the negative effect of TNF α , MSCs were pre-treated with different concentrations of TNF α (0, 1, 10 or 50 ng/mL TNF α , PeproTech) for different exposure times 24 h, 4-6 days (1 passage) or 8-10 days (2 passages) and then chondrogenically differentiated in the presence of 0 or 1 ng/mL TNF α . When indicated, MSCs were first treated with TNF α for 1 passage (4 days) followed by removal of TNF α for 1 passage (4 days) and subsequently chondrogenically differentiated in the presence of 1 ng/mL TNF α . To investigate the effect of IL-1 β pre-treatment on the chondrogenic differentiation, MSCs were pre-treated for 1 passage with different concentrations of IL-1 β (0, 0.1, 1, 10 and 50 ng/mL, PeproTech), followed by chondrogenic differentiation in the absence of IL-1 β . MSCs from different donors are indicated as donor 1, 2, 4, 5, 6, 7, 8, or 9.

5.3.2 Chondrogenic differentiation

To obtain a 3D pellet culture, 2×10^5 MSCs were centrifuged at $300 \times g$ for 8 min in polypropylene tubes. To induce chondrogenesis, the pelleted cells were cultured in DMEM-HG (Invitrogen), 1% ITS (B&D), 1.5 μ g/mL fungizone (Invitrogen), 50 μ g/mL gentamicin (Invitrogen), 1mM sodium pyruvate (Invitrogen), 40 μ g/mL proline (Sigma-Aldrich), 10 ng/mL TGF β 1 (R&D Systems), 0.1 mM ascorbic acid 2-phosphate (Sigma-Aldrich), and 100 nM dexamethasone (Sigma-Aldrich), referred to as chondrogenic medium (Johnstone, Hering *et al.* 1998). After 24 h, the medium was renewed with chondrogenic medium with or without 1 ng/mL TNF α , as indicated. Afterwards the medium was renewed two times per week for a period of 4 weeks.

5.3.3 COL2A1 reporter assays

Cultures of human bone marrow-derived MSCs from healthy de-identified adult volunteer donors (31-33 years old, **Table S5.1**) were established as previously described (Lennon and Caplan 2006) after informed consent. The bone marrow was collected using a procedure reviewed and approved by the University Hospitals of Cleveland Institutional Review Board (IRB# 09-90-195). MSCs from different donors are indicated as donor 3 or 10. Lentiviral constructs for the *COL2A1* promoter were placed upstream of the Gaussia luciferase reporter gene. MSCs were transduced with the *COL2A1* reporter lentivirus as previously described for a *SOX9* reporter (Correa *et al.*, 2018).

MSCs with the *COL2A1* luciferase reporter were expanded as indicated above. At different time points during chondrogenesis, medium of MSCs with the *COL2A1* reporter was harvested 48 h after the last medium renewal. Per condition, 50 μ L of the medium was transferred to a white 96-well plate and 20 μ M coelenterazine substrate (NanoLight technology) was injected into the wells. The Gaussia Luciferase (Gluc) activity was measured using a GloMax-96 Microplate Luminometer (Promega) in technical duplicates.

5.3.4 CD marker analysis

Per condition, 2×10^5 MSCs were re-suspended in 500 μ L FACSFlow solution (BD Biosciences) and stained with antibodies against human CD45-APC (368515, BioLegend), CD90-APC (FAB2067A, R&D Systems), CD73-PE (550257, BD Biosciences) or CD105-FITC (FAB10971F, R&D Systems), following the manufacturer's guidelines. Afterwards, the cells were fixed using 2% formaldehyde (Fluka) and were filtered through 70- μ M filters. Unstained cells were used as a negative control. Samples were analyzed by flow cytometry using a BD Fortessa machine (BD Biosciences). The data were analyzed using FlowJo V10 software.

5.3.5 Apoptosis analysis

Per condition, 5×10^5 MSCs were re-suspended in 1x Binding Buffer and stained with Annexin V and Propidium Iodide using manufacturer's instructions (all products from eBioscience, San Diego, USA). Samples were analyzed by flow cytometry using a BD Fortessa machine (BD Biosciences) and analyzed using FlowJo V10 software.

5.3.6 (Immuno)Histochemistry

After 4 weeks of chondrogenic induction, pellets were fixed with 3.8% formaldehyde, embedded in paraffin and sectioned (6 μ m). Glycosaminoglycans (GAG) were stained with 0.04% thionine solution and collagen type-2 was immunostained using a collagen type-2 primary antibody (II-II 6B3, Developmental Studies Hybridoma Bank). Antigen retrieval was performed with 0.1% Pronase (Sigma-Aldrich) in PBS for 30 min at 37°C, followed by incubation with 1% hyaluronidase (Sigma-Aldrich) in PBS for 30 min at 37°C to improve antibody penetration. The slides were pre-incubated with 10% normal goat serum (Sigma-Aldrich) in PBS with 1% bovine serum albumin (BSA; Sigma-Aldrich). Next, the slides were incubated for 1 h with collagen type-2 primary antibody, and then with a

biotin-conjugated secondary antibody (HK-325-UM, Biogenex), alkaline phosphatase-conjugated streptavidin (HK-321-UK, Biogenex), and the New Fuchsin chromogen (B467, Chroma Gesellschaft). An IgG1 isotype antibody (X0931, Dako Cytomation) was used as negative control.

5.3.7 DNA and glycosaminoglycan (GAG) quantification

After chondrogenic induction for 28 days, pellets were digested using 250 μ L digestion solution containing in 1 mg/mL Proteinase K, 1 mM iodoacetamide, 10 μ g/mL Pepstatin A in 50 mM Tris, 1mM EDTA buffer (pH 7.6; all Sigma-Aldrich) for 16 h at 56°C. Next, Proteinase K was inactivated at 100°C for 10 min. To determine the DNA content, 50 μ L cell lysate was treated with 100 μ L heparin solution (8.3 IU/mL) and 50 μ L RNase (0.05 mg/mL) solution for 30 min at 37°C. Next 50 μ L ethidium bromide (25 μ g/mL) was added and the samples were analyzed on a Wallac 1420 Victor2 plate reader (Perkin-Elmer) using an excitation of 340 nm and an emission of 590 nm. In case the amount of DNA was lower than 1 μ g per mL, 50 μ L cell lysate was treated with 50 μ L heparin solution and 25 μ L RNase for 30 min at 37°C. After incubation, 30 μ L CYQUANT GR solution (Invitrogen) was added and samples were analyzed on a SpectraMax Gemini plate reader using an excitation of 480 nm and an emission of 520 nm. DNA sodium salt from calf thymus was used as a standard (Sigma-Aldrich). GAG content was determined using the 1,9-dimethylmethylene blue (DMB) assay, as previously described (Farndale, Buttle *et al.* 1986). In short, 100 μ L cell lysate, containing up to 5 μ g GAG, was incubated with 200 μ L DMB solution and analyzed using an extinction of 590 nm and 530 nm. Chondroitin sulfate sodium salt from shark cartilage was used as a standard (Sigma-Aldrich).

5.3.8 mRNA expression analysis

After chondrogenic induction for 14 or 28 days, pellets were lysed in RNA-Bee (TEL-TEST) and manually homogenized. RNA was extracted using chloroform and purified using the RNeasy Kit (Qiagen), following manufacturer's guidelines. RNA was reverse-transcribed with a RevertAid First Strand cDNA synthesis kit (MBI Fermentas). Real-time polymerase chain reactions were performed with TaqMan Universal PCR MasterMix (Applied Biosystems) or SYBR Green MasterMix (Fermentas) using a CFX96™ PCR detection system (Bio-Rad). Primers are listed in **Table S5.2** and the genes *GAPDH*, *RPS27A* and *HPRT1* were used as housekeeping genes. The best housekeeping index (BHI) was calculated using the formula $(Ct^{GAPDH} * Ct^{RPS27A} * Ct^{HPRT1})^{1/3}$. Relative mRNA levels were

calculated using the formula $2^{-\Delta\Delta Ct}$.

5.3.9 Adipogenic differentiation

To induce differentiation towards the adipogenic lineage, 2×10^4 cells/cm² were seeded and cultured in DMEM HG (Invitrogen) with 10% fetal calf serum (Gibco), 1.5 μ g/mL fungizone (Invitrogen), 50 μ g/mL gentamicin (Invitrogen), 1.0 μ M dexamethasone (Sigma-Aldrich), 0.2 mM indomethacin (Sigma-Aldrich), 0.01 mg/mL insulin (Sigma-Aldrich) and 0.5 mM 3-isobutyl-1-methyl-xanthine (Sigma-Aldrich) for 14 days. In order to visualize intracellular lipid accumulation, cells were fixed in 3.8% formaldehyde, treated with 0.3% Oil red O solution (Sigma-Aldrich) for 10 min and then washed with distilled water. In addition, *PPARG* mRNA expression was analyzed as indicated above.

5.3.10 Osteogenic differentiation

To induce differentiation towards the osteogenic lineage, 3×10^3 cells/cm² were seeded and cultured in DMEM HG (Invitrogen) with 10% fetal calf serum (Gibco), 1.5 μ g/mL fungizone (Invitrogen), 50 μ g/mL gentamicin (Invitrogen), 10 mM β -glycerophosphate (Sigma-Aldrich), 0.1 μ M dexamethasone (Sigma-Aldrich) and 0.1 mM ascorbic acid-2-phosphate (Sigma-Aldrich) for 14-18 days. For the detection of calcium deposits (Von Kossa staining), cells were fixed in 3.8% formaldehyde, hydrated with distilled water, treated with 5% silver nitrate solution (Sigma-Aldrich) for 60 min in the presence of bright light and then washed with distilled water followed by counterstaining with 0.4% thionine (Sigma-Aldrich). In addition, *ALPL* mRNA expression was analyzed as indicated above.

5.3.11 Western Blot

To test for SMAD2 activation, MSC monolayers were pre-treated for 4 days with 0 or 50 ng/mL TNF α in standard MSC growth medium, followed by serum starvation overnight (16 h) in DMEM-HG (Invitrogen) containing 1% ITS (B&D), 1.5 μ g/mL fungizone (Invitrogen), 50 μ g/mL gentamicin (Invitrogen), 1mM sodium pyruvate (Invitrogen), 40 μ g/mL proline (Sigma-Aldrich) and 0 or 50 ng/mL TNF α . Next, MSCs were stimulated for 30 min with 0 or 10 ng/mL TGF β 1 in the presence or absence of 1 ng/mL TNF α . To assess the SOXC proteins (SOX11 and SOX4), and (active) β -catenin levels, MSCs were pre-treated for 4 days with 0 or 50 ng/mL TNF α in standard MSC medium. 24 h prior to harvest, the medium was renewed with

standard MSC growth medium containing 0 or 50 ng/mL TNF α . Western blot were made using MSC lysates prepared using M-PER lysis buffer containing 1% Halt Protease Inhibitor and 1% Halt Phosphatase Inhibitor (Thermo Scientific). Total protein concentration was determined using a BCA assay (Thermo Scientific). 8-10 μ g protein was electrophoresed on a 4-12% gradient SDS-PAGE gel. Proteins were transferred to a nitrocellulose membrane (Millipore) by semi-wet transfer, followed by blocking with 5% milk powder dissolved in Tris-buffered saline containing 0.1% Tween (TBST) for 3 h. Membranes were incubated overnight at 4°C with primary antibody according to **Table S5.3** in 5% BSA in TBST, followed by incubation at room temperature for 1.5 h with peroxidase-conjugated anti-rabbit secondary antibody (Cell Signaling, 7074S) in 5% dry milk in TBST. Proteins were detected using the SuperSignal Wester Pico Complete Rabbit IgG detection kit (ThermoFisher scientific) following manufacturer's instructions.

5.3.12 Statistical Analysis

Data were analyzed using SPSS software (IBM SPSS statistics 25). Normal distribution was tested using the Kolmogorov-Smirnov test. Since the Kolmogorov-Smirnov test showed that the *COL2A1* reporter data was not normally distributed a Mann-Whitney U test was applied to analyze these data. All other data were normally distributed and a linear mixed model, with the different conditions considered as fixed parameters and the donors as random parameters was applied. Bonferroni post-hoc tests were performed to correct for multiple comparisons. *p*-values less than 0.05 were considered statistically significant.

5.4 Results

5.4.1 MSCs pre-treated with TNF α had an increased chondrogenic potential when subsequently maintained under stimulation by TNF α during differentiation

To study if TNF α exposure during MSCs expansion (pre-treatment) could inhibit the negative effect of TNF α during chondrogenic differentiation, MSCs were pre-treated with different concentrations of TNF α and incubation time prior to chondrogenic differentiation in the presence of 1 ng/mL TNF α (**Figure S5.1A**). First, we confirmed that the presence of 1 ng/mL TNF α during the chondrogenic phase reduced the ability of MSCs to differentiate

(**Figure S5.1B-D**; condition 0/0 versus 0/1). Pre-treatment for 1 passage increased GAG deposition in MSC pellets after chondrogenic induction in the presence of TNF α (**Figure S5.1C**), with the larger effect occurring when the pre-treatment was performed with 10 and 50 ng/mL TNF α (**Figure S5.1C**; condition 0/1 vs 10/1 and 50/1). Pre-treatment with TNF α for 24 h and 2 passages did not have a clear effect on chondrogenesis (**Figure S5.1B and D**; 0/1 versus 1/1, 10/1 and 50/1). Given these observations, we performed the rest of the experiments using TNF α pre-treatment for 1 passage (**Figure 5.1A**).

Next, we analyzed MSCs from four other donors and observed that chondrogenic pellets of MSCs pre-treated for 1 passage with 50 ng/mL TNF α had a higher GAG content after 28 days of chondrogenic induction in the presence of TNF α compared to MSCs without TNF α pre-treatment (**Figure 5.1B and Figure S5.2A**; 0/1 versus 50/1, $p=0.003$), while no effect on DNA content was observed (**Figure S5.2A**). Moreover, GAG staining demonstrated an increased GAG content in the TNF α pre-treated MSCs at day 28 (**Figure 5.1C**; 0/1 versus 50/1). Staining for collagen type-2 did not show differences (**Figure 5.1D**). No increase in GAG content was observed after pre-treatment for 1 passage with 10 ng/mL TNF α (**Figure 5.1B-C**). In order to determine whether the effect of 50 ng/mL TNF α is due to an acceleration of chondrogenic differentiation, first a non-destructive luciferase-based method was validated as a proxy for endogenous *COL2A1* expression in pellet cultures (**Figure S5.3**) and then applied to assess *COL2A1* promoter activation at day 3 and day 7 of chondrogenic differentiation. However, no significant differences were observed in *COL2A1* promoter activation at day 3 and day 7 (**Figure S5.4A**) of chondrogenesis, suggesting that TNF α pre-treatment did not increase the rate of chondrogenesis during the first week of differentiation. Subsequent analysis performed by RT-PCR on *SOX9*, *COL2A1* and *ACAN* showed no significant differences at day 14 and 28 during chondrogenesis between the conditions (**Figure S5.4A-B**).

Overall, these data indicate that pre-treatment of MSC monolayers with 50 ng/mL TNF α significantly increases the chondrogenic potential of MSCs when exposed to 1 ng/mL TNF α during differentiation, but without prompting the onset of chondrocyte marker expression. For this reason, the following experiments were performed using 50 ng/mL TNF α pre-treatment.

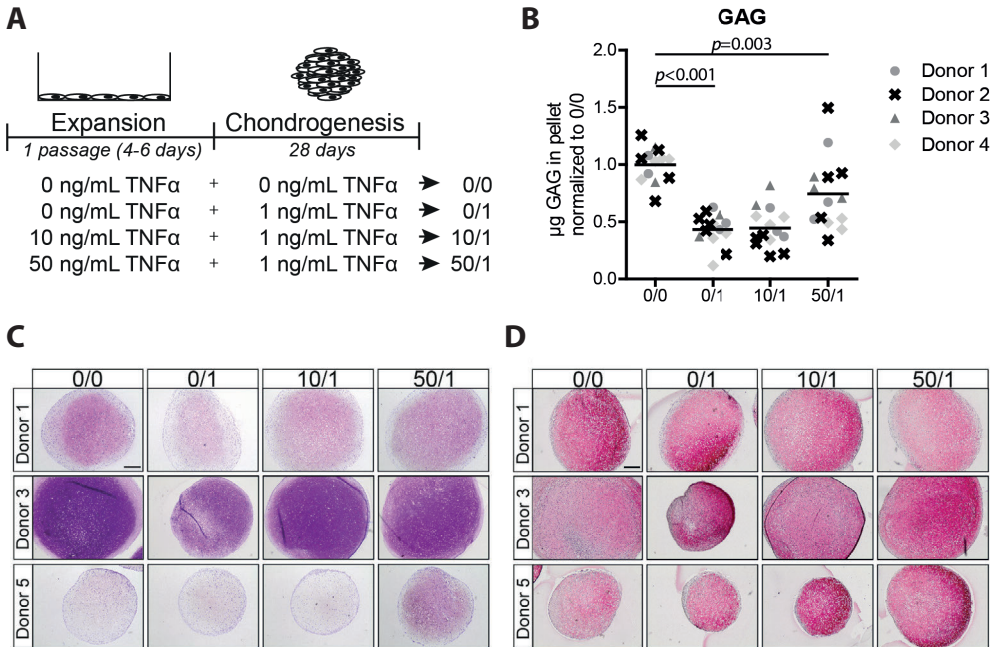


Figure 5.1 - Pre-treatment of MSC monolayers with 50 ng/mL TNF α reduced the inhibitory effect of the cytokine in subsequent chondrogenic conditions.

(A) Schematic overview of the experiment.

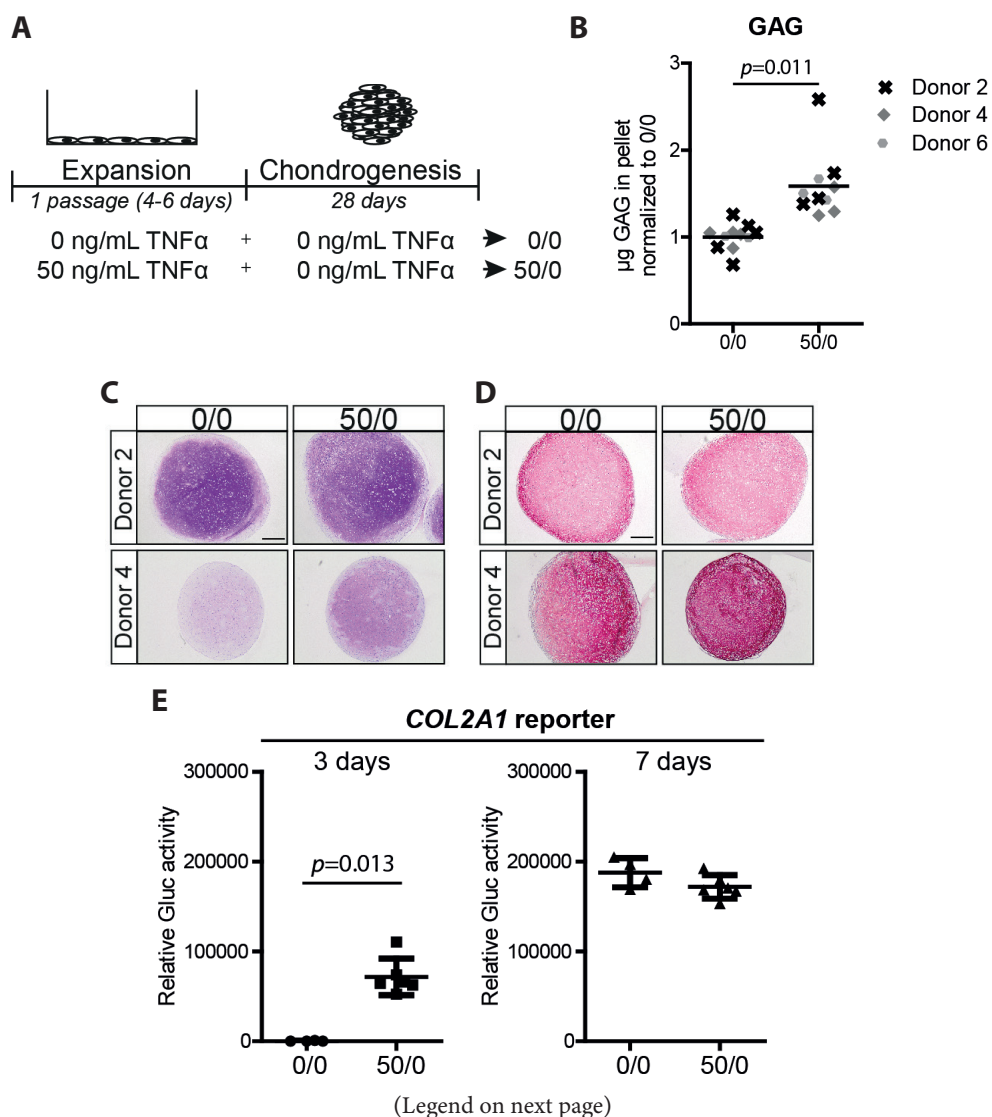
(B) GAG content of MSC pellets after 28 days of chondrogenic induction. N=4 donors with 2-5 pellets per donor.

(C-D) Representative images of pellets stained for GAG with (C) thionine and (D) COL2A1 after 28 days of chondrogenic induction. N=5 donors with 2-3 pellets per donor. Scale bar represents 250 μm .

5.4.2 Pre-treatment with TNF α increased the chondrogenic potential of MSCs regardless the presence of the cytokine during chondrogenic differentiation

Next, we tested whether the effect of TNF α pre-treatment on the chondrogenic potential of MSCs was dependent on the presence of the cytokine during the differentiation phase. MSCs were pre-treated during expansion with 0 and 50 ng/mL TNF α , followed by chondrogenic induction in the absence of TNF α (**Figure 5.2A**). Biochemical assays determined that chondrogenic pellets of MSCs pre-treated with TNF α had a higher GAG concentration ($p=0.011$; **Figure 5.2B** and **Figure S5.2B**) and DNA content (**Figure S5.2B**). Histological staining confirmed increased GAG accumulation (**Figure 5.2C**), while no clear effect on collagen type-2 content was observed after chondrogenic induction (**Figure 5.2D**).

To further investigate the effect of TNF α pre-treatment on the speed of chondrogenic induction in the absence of TNF α , we determined *COL2A1* promoter activation over time using a *COL2A1* luciferase reporter system. Analysis on 3-day pellet cultures indicated that TNF α pre-treated MSCs had enhanced luciferase activity, while no differences between the conditions were observed at day 7 (**Figure 5.2E**). These data suggest that TNF α pre-treatment accelerates chondrogenic differentiation probably via an early induction of *COL2A1* expression among other genes. These data indicate that TNF α pre-treatment increases the chondrogenic potential of the MSCs regardless of the presence of TNF α during chondrogenesis.



◀ **Figure 5.2 - Pre-treatment with 50 ng/mL TNF α increased the chondrogenic potential.**
(A) Schematic overview of the experiment.
(B) GAG content of MSC pellets after 28 days of chondrogenic induction. N=3 donors with 2-4 pellets per donor.
(C-D) Representative images of pellets stained for (C) GAG with thionine and (D) COL2A1 after 28 days of chondrogenic induction. N=4 donors with 2-3 pellets per donor. Scale bar represents 250 μ m.
(E) Relative secreted Gaussia Luciferase (Gluc) activity of medium from MSC pellets containing the *COL2A1* promoter reporter after 3 and 7 days of chondrogenic induction. Values represent the mean \pm SD with 4-6 pellets.

To better understand the effect of the TNF α pre-treatment on MSCs and the specificity for the chondrogenic lineage, we determined if TNF α increased apoptosis, expansion and multilineage differentiation potential. No clear effect on apoptotic rates was observed after 24 h or 5 days of exposure to TNF α (**Figure S5.5A-B**), but a slight increase in MSC expansion capacity was detected after pre-treatment for 1 passage (1.4-fold difference; **Figure S5.5C**). Adipogenically induced MSCs pre-treated with TNF α showed less lipid accumulation compared to control MSCs ($p=0.039$; **Figure S5.5D**) and a reduced *PPARG* expression, which codes for a transcription factor involved in the adipogenic differentiation process (**Figure S5.5E**). No statistically significant effect of TNF α pre-treatment on the osteogenic differentiation capacity was observed although, on average, mineralization and *ALPL* expression slightly increased (**Figure S5.5F-G**). Overall, these data suggest that TNF α pre-treatment specifically enhances the chondrogenic potential of the MSCs.

5.4.3 IL-1 β pre-treatment did not increase the chondrogenic potential of MSCs

We then investigated whether the effect of pre-treatment on the chondrogenic potential of MSCs was specific for TNF α or whether IL-1 β another pro-inflammatory cytokine can have a similar effect (**Figure 5.3A**). No differences in GAG deposition were observed after pre-treatment with different concentrations of IL-1 β , based on histology (**Figure 5.3B**), indicating that in contrast to TNF α , IL-1 β pre-treatment for 1 passage does not increase the chondrogenic potential of the MSCs. These data suggest distinct effects of TNF α and IL-1 β pretreatments on MSCs.

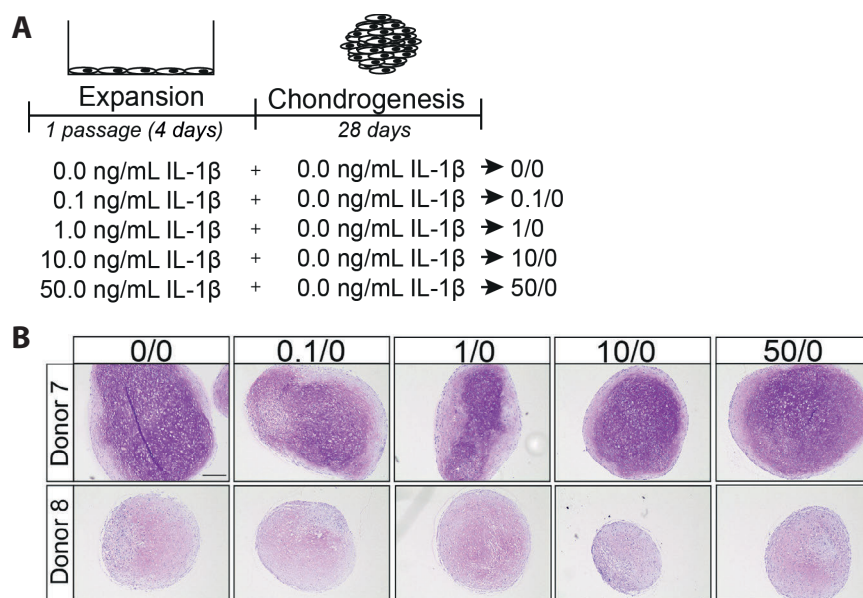


Figure 5.3 - IL-1 β pretreatment did not increase the chondrogenic differentiation capacity of MSCs.

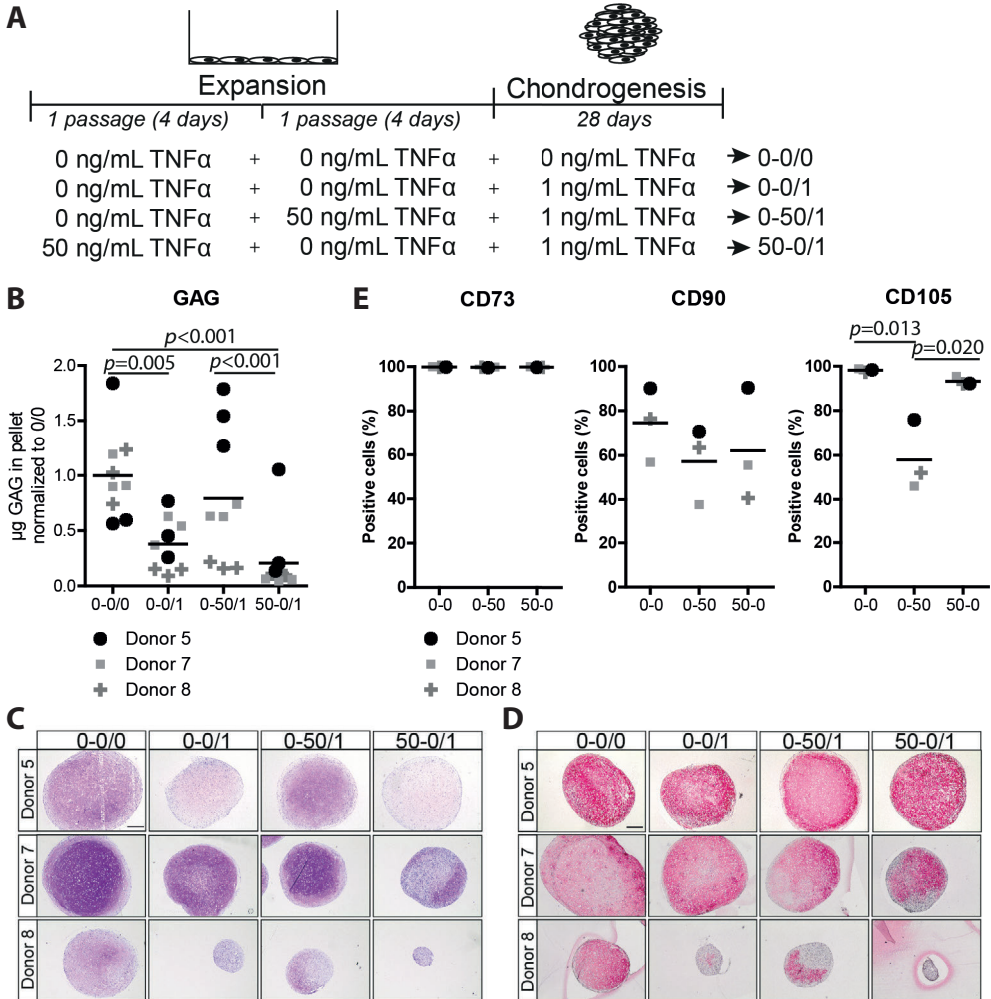
(A) Schematic overview of experiment.

(B) GAG staining with thionine of MSCs pellets after 28 days culture in chondrogenic medium. Representative image of MSC pretreated for 1 passage with different concentrations IL-1 β . N=2 donors with 3 pellets per donor. Scale bar represents 250 μ m.

5.4.4 The effect of TNF α pre-treatment on the chondrogenic capacity and expression of MSC marker CD105 was reversible

To study whether the effect of TNF α is reversible, MSCs were pre-treated with TNF α for one passage followed by TNF α withdrawal for one additional passage and subsequently subjected to chondrogenic differentiation (**Figure 5.4A**). Interestingly, GAG staining and biochemical assays showed that the positive effect of TNF α on the amount of GAG was lost after TNF α withdrawal ($p < 0.001$; **Figure 5.4B-C**, **Figure S5.2C**). No consistent effect on DNA content and collagen type-2 expression was observed after chondrogenic induction (**Figure 5.4D** and **Figure S5.2C**). To further characterize the MSCs after TNF α pre-treatment, we analyzed the expression of the MSC markers CD73, CD90 and CD105 (Dominici *et al.*, 2006) together with the negative MSC marker CD45 (hematopoietic marker). In the control condition without TNF α pre-treatment, more than 97% of the MSCs expressed CD73 and CD105, on average 77% of the cells expressed CD90 (**Figure 5.4E**), while no cells expressed CD45 (data not shown). TNF α administration had no

effect on the expression of CD73 and CD90, but it significantly decreased the number of CD105 positive MSCs ($p=0.013$; **Figure 5.4E**), indicating that TNF α can modulate the MSC phenotype. Interestingly, the number of CD105 positive cells returned back to control levels after TNF α withdrawal for one passage ($p=0.020$; **Figure 5.4E**). These data indicate that the effect of TNF α pre-treatment on MSC chondrogenic capacity and phenotype is reversible.



(Legend on next page)

◀ **Figure 5.4. The effect of TNF α pre-treatment on chondrogenesis and MSC marker expression was reversible after TNF α withdrawal.**

(A) Schematic overview of the experiment.

(B) GAG content of MSC pellets after 28 days of chondrogenic induction. N=3 donors with 3 pellets per donor.

(C-D) Representative images of pellets stained for (C) GAG with thionine and (D) COL2A1 after 28 days of chondrogenic induction. N=3 donors with 3 pellets per donors. Scale bar represents 250 μ m.

(E) Flow cytometry analysis of surface markers CD73, CD90 and CD105. The values represent the percentage of positive cells for the indicated surface marker, N=3 donors.

5.4.5 TNF α pre-treatment increased SOX11 and active β -catenin expression in MSCs

To elucidate how TNF α pre-treatment increases the chondrogenic differentiation capacity of MSCs we first evaluated effects on the TGF β 1 signaling pathway, since exposure to TNF α reduced the expression of the TGF β co-receptor CD105 (**Figure 5.4E**). MSCs were then stimulated by 10 ng/mL TGF β 1 for 30 min in the presence or absence of 1 ng/mL TNF α . TGF β 1 increased pSMAD2 levels, however the levels were not altered by TNF α pre-treatment (0/1 vs 50/1 and 0/0 vs 50/0; **Figure S5.6A-B**). These data suggested that TNF α pre-treatment does not alter the canonical TGF β 1/SMAD2 signaling pathway in MSCs.

We next studied the effect of TNF α pre-treatment on SOXC proteins, SOX11 and SOX4 in MSCs. The level of SOX11 protein was significantly increased (6.5-fold; $p < 0.001$; **Figure 5.5A**), while no significant effect was observed for SOX4 ($p = 0.983$; **Figure 5.5A**). Finally, since SOXC proteins can stabilize β -catenin (Bhattaram, Penzo-Méndez *et al.* 2014), we analyzed the level of active β -catenin in the TNF α pre-treated MSCs. Interestingly, the amount of active β -catenin was increased after TNF α pre-treatment in MSCs (2.0-fold; $p = 0.003$; **Figure 5.5A**). This suggests that TNF α pre-treatment increased canonical WNT signaling in MSCs, possibly via SOXC stabilization, and thereby enhanced the chondrogenic potential (**Figure 5.5B**).

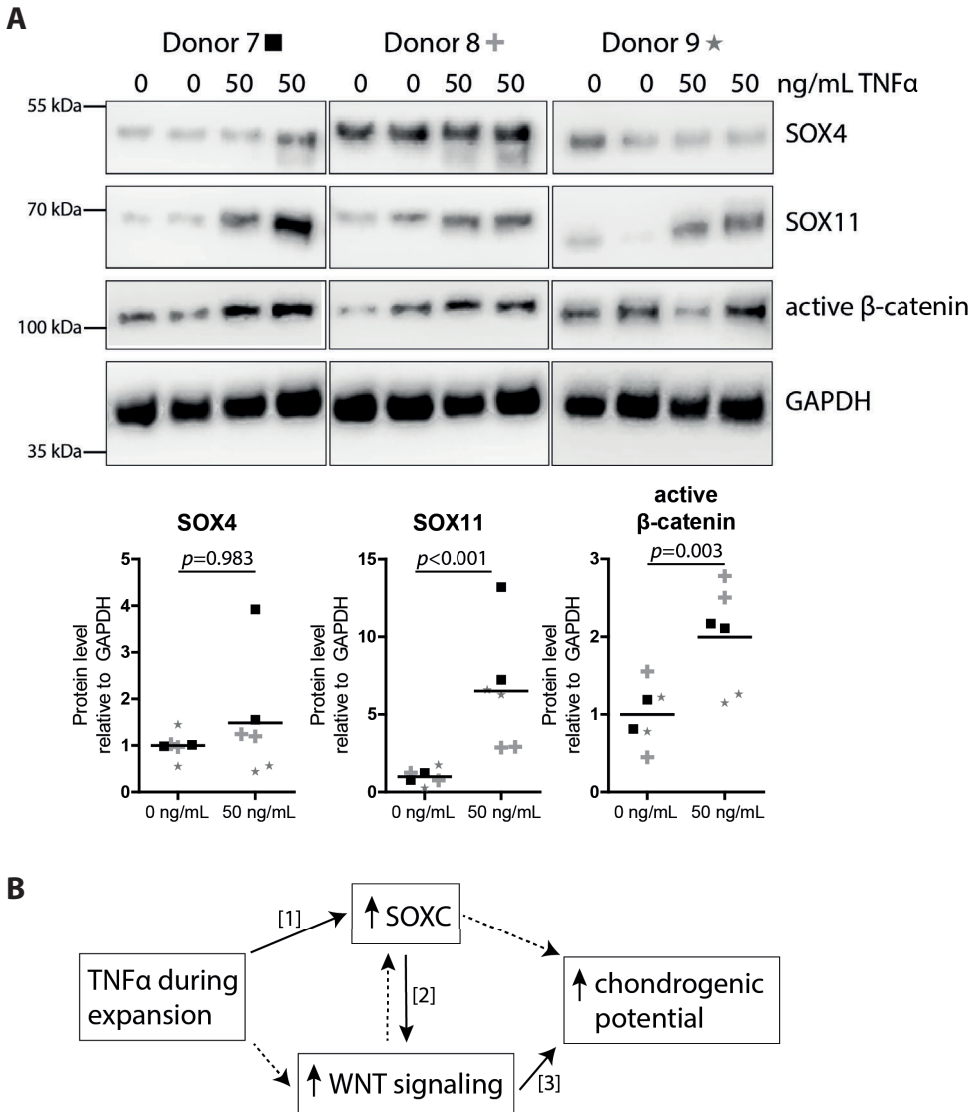


Figure 5.5. TNF α pre-treatment increased SOXC and active β -Catenin expression in MSCs.

(A) Western blot for SOXC (SOX11 and SOX4, pan-SOXC antibody) and non-phospho (active) β -Catenin (Ser33/37Thr41). Below: quantification of western blot results relative to GAPDH and normalized to 0 ng/mL TNF α pre-treatment. N=3 donors with biological duplicates per donor.

(B) Possible working mechanism of TNF α pre-treatment on the chondrogenic potential of MSC. Solid lines show known interactions, [1] Bhattaram, P. *et al.* Arthritis Rheumatol 2018. [2] Bhattaram, P *et al.* J Cell Biol 2014. [3] Narcisi, R. *et al.* Stem Cell Reports 2015. Dotted lines indicate unknown interactions.

5.5 Discussion

In this study, we demonstrated that TNF α pre-treatment of MSCs in monolayers reduced the inhibitory effect of TNF α during chondrogenic differentiation by boosting the chondrogenic capacity of these cells. This pro-differentiation effect was both temporal and specific for the chondrogenic lineage and possibly mediated by SOX11 and WNT signaling. SOX11 is a SOXC protein which TNF α is known to stabilize in fibroblast-like synoviocytes (Bhattaram, Muschler *et al.* 2018). SOXC genes play a crucial role in mesenchymal progenitor cell fate during skeletal development (reviewed in (Lefebvre and Bhattaram 2016)). In addition, SOXC proteins are known to synergize with canonical WNT signaling via stabilization of β -catenin (Bhattaram, Penzo-Méndez *et al.* 2014). WNT signaling has been shown before to play a role in stem cell fate (ten Berge, Brugmann *et al.* 2008). We previously showed that induction of WNT signaling during monolayer increases the expansion and chondrogenic potential of MSCs (Narcisi, Cleary *et al.* 2015, Narcisi, Arikan *et al.* 2016). A link between SOX11 and WNT signaling has been suggested before in a study with rat MSCs where Sox11 overexpression also increased the β -catenin level and resulted in improved cartilage defect repair (Xu, Shunmei *et al.* 2019). The results of the current study suggest that SOX11 may play a role during chondrogenesis of human MSCs. Furthermore, we show that the expression of SOX11 in MSCs can be modulated by TNF α .

MSCs are a heterogeneous population of cells with known intra and inter-donor phenotypic and potency variability. This is what we also observed in our study where we used MSCs from both healthy donors and from patients undergoing total hip replacements. In addition, MSCs from patients with a broad age range were used for which we cannot exclude a possible effect of unknown underlying conditions. The differences in the chondrogenic capacity of MSCs in our study could be due to differences in cell subpopulations, since the bone marrow houses MSC subpopulations with different chondrogenic capacities (Sivasubramaniyan, Ilas *et al.* 2018). In addition the age of the donor can have an effect on the chondrogenic capacity of MSCs (Payne, Didiano *et al.* 2010). Although differences in chondrogenic potential were observed between MSCs from different patients, a similar effect after TNF α stimulation was detected in all cases, indicating that TNF α increases the chondrogenic potential of MSCs regardless of their chondrogenic capacity before TNF α pre-treatment.

Immunophenotyping of MSC is often used to characterize the cells (Dominici, Le Blanc *et al.* 2006), even though it is a topic of discussion. We here demonstrated a clear difference in the expression of CD105, a surface marker commonly associated with the MSC phenotype (Haynesworth, Goshima *et al.* 1992, Dominici, Le Blanc *et al.* 2006), after pre-treatment with TNF α . In line with our previous work (Cleary, Narcisi *et al.* 2016), we further confirmed that CD105 is not a good marker to predict the chondrogenic potential of bone marrow-derived MSCs and, on the contrary, its expression was inversely associated with the chondrogenic capacity of MSCs. In addition, we show that the expression of CD105 can be strongly influenced by inflammatory environmental changes. This could be an explanation for contradictory published results regarding CD105 and MSCs (Majumdar, Banks *et al.* 2000, Kastrinaki, Andreakou *et al.* 2008, Jiang, Liu *et al.* 2010, Asai, Otsuru *et al.* 2014, Cleary, Narcisi *et al.* 2016). In addition, a reduced adipogenic differentiation was observed after TNF α pre-treatment. It is known that TNF α can reduce the adipogenic differentiation in 3T3-L1 pre-adipocytes by preventing *Pparg* and *Cebpa* expression (Cawthorn, Heyd *et al.* 2007), which is in line with the reduction of PPARG gene expression levels that we found after TNF α pre-treatment. In agreement with other studies (Daniele, Natali *et al.* 2017), we observed that TNF α pre-treatment slightly increased the osteogenic differentiation capacity of MSCs. Overall, these data suggest that TNF α pre-treatment changes the immunophenotype and multipotency of MSCs.

In this study, we tested three different concentrations and incubation times and found that pre-treatment with 50 ng/mL TNF α for 1 passage (4-6 days) increased the chondrogenic capacity in a more reproducible way than the other conditions. Since a previous study indicated that 50 ng/mL TNF α can induce apoptosis in MSC (Cheng, Li *et al.* 2019), we investigated apoptosis. No large effect on apoptosis was observed after addition of TNF α . Given the fact that our apoptosis rates are relatively low, we assume that the pro-chondrogenic effect of TNF α on MSCs is not due to an increased apoptotic rate. In addition TNF α can activate several transduction pathways, among which are the NF- κ B, ERK and JNK pathways (Lu, Chen *et al.* 2016, Bai, Xi *et al.* 2017). Since a 24-h pre-treatment was not sufficient to observe an effect on chondrogenesis, we assume that the effect of TNF α on the chondrogenic capacity of MSCs was not mediated via direct induction of these pathways, since they are already activated after 24 h (van Buul, Villafuertes *et al.* 2012).

In addition, TNF α pre-treatment for 2 passages (8-10) did not increase the chondrogenic potential suggesting that long-term exposure to TNF α during expansion does not improve the chondrogenic capacity of MSCs. Moreover, no increase in chondrogenic differentiation was observed after pre-treatment with 0.1, 1, 10 and 50 ng/mL IL-1 β for 1 passage. Similar to TNF α , IL-1 β is involved in joint inflammation (Goldring and Otero 2011). This suggests that TNF α induces the pro-chondrogenic effect in MSCs via an intracellular pathway that is not activated by IL-1 β . As far as we know, no previous research has investigated whether IL-1 β can increase SOXC and WNT levels in human MSCs. Overall, these data indicate that not all pro-inflammatory cytokines can increase the chondrogenic potential of MSCs and that the effect seems to be specific for TNF α .

As previously reported, TNF α exposure during the chondrogenic differentiation phase reduces chondrogenesis of MSCs (Markway, Cho *et al.* 2016). Although the TNF α concentrations used during chondrogenic differentiation in this *in vitro* study are higher than the TNF α concentrations in post-traumatic and OA joints (4-24 pg/mL, (Sward, Frobell *et al.* 2012, Tsuchida, Beekhuizen *et al.* 2014, Imamura, Ezquerro *et al.* 2015, Alonso, Bravo *et al.* 2020), our data indicate that *in vitro* pre-treatment with 50 ng/mL TNF α can be beneficial for cartilage regeneration in an inflamed environment. In addition we found an association between TNF α pre-treatment and SOX11 and β -catenin activation in MSCs, therefore regulation of these pathways might improve cartilage repair in the presence of TNF α . Overall, the results of our study suggest that exposure to TNF α during the expansion phase of MSCs could improve cartilage regeneration approaches.

5.6 Supplemental Information

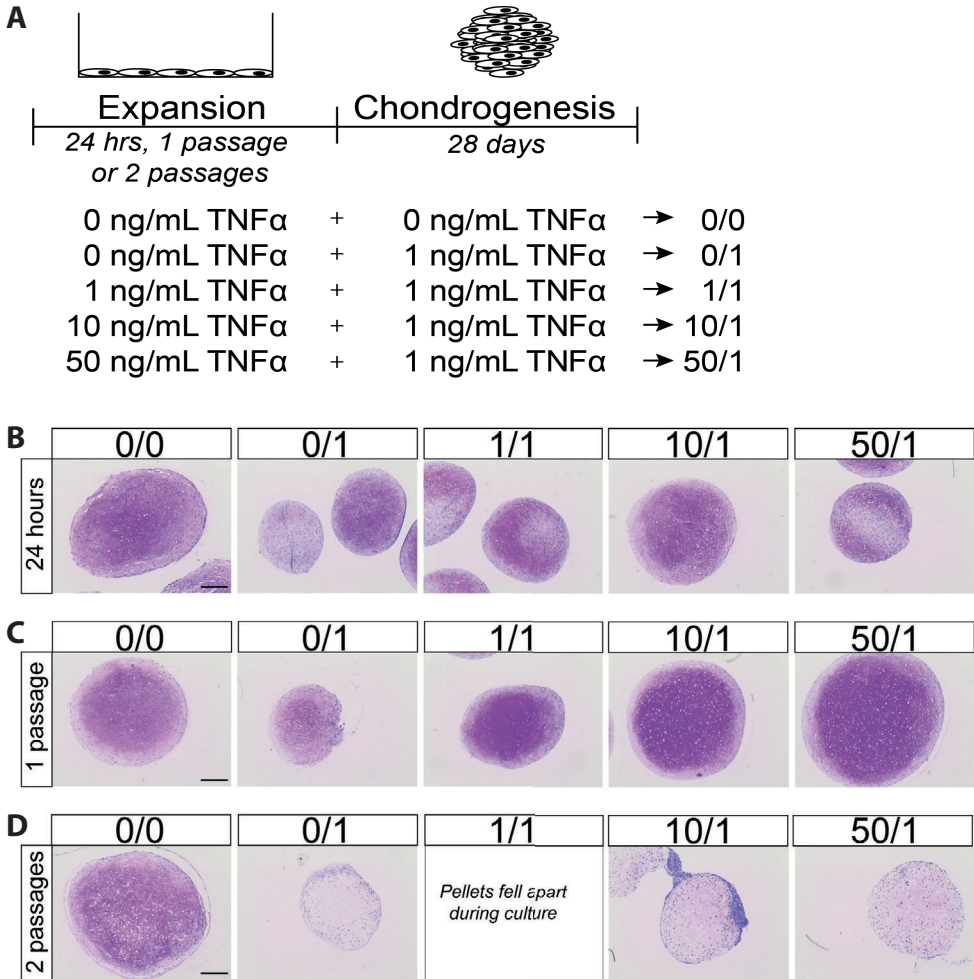


Figure S5.1 - The effect of TNF α pre-treatment of MSCs on chondrogenesis is time- and dose- dependent.

(A) Schematic overview of the experiment.

(B-D) GAG staining with thionine of MSC pellets after pre-treatment in monolayer with different concentrations TNF α followed by 28 days in chondrogenic medium. Representative images of MSCs pretreated for 24 h; N=1 donor with 3 pellets per donor (B), for 1 passage (4-6 days); N=5 donors with biological triplicates (C), for 2 passages (8-10 days); N=2 donors with biological triplicates (D). Scale bar represents 250 μ m.

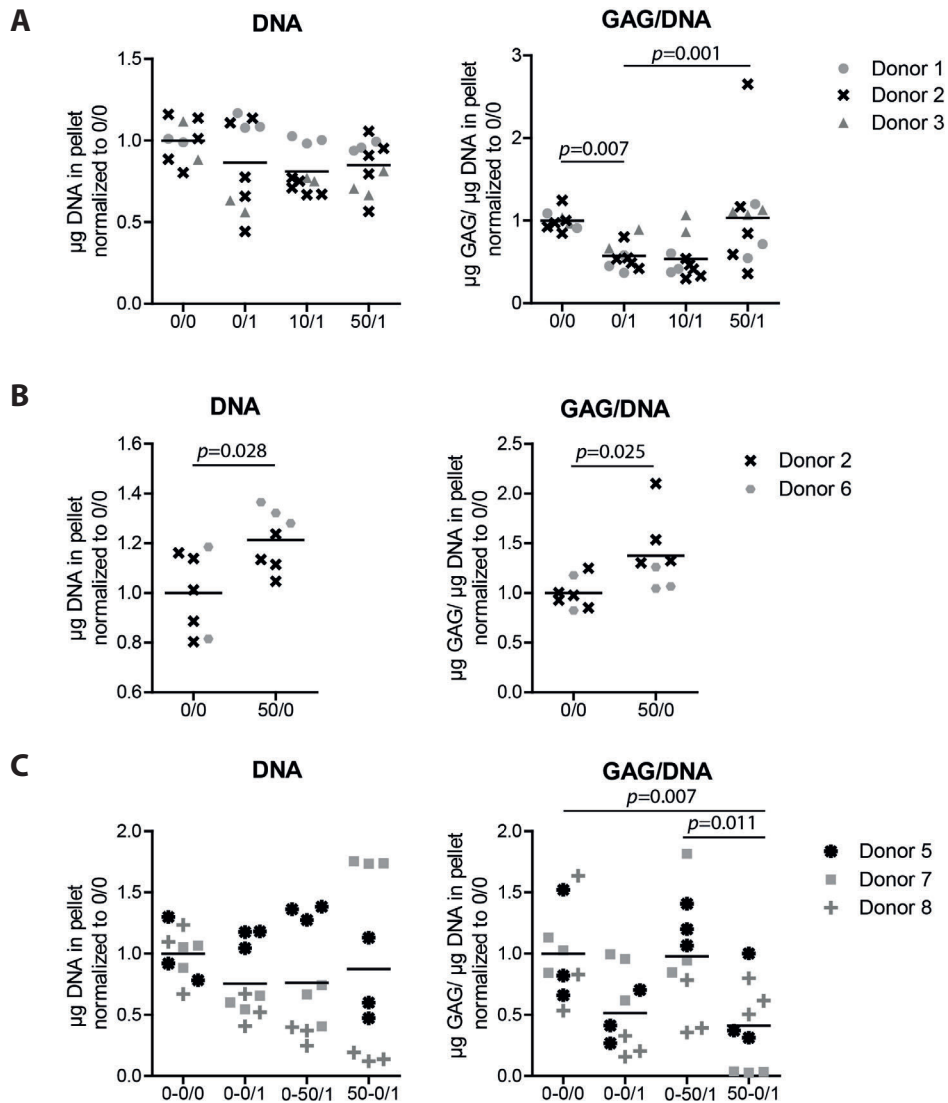


Figure S5.2 - DNA and GAG/DNA of MSC pellets after 28 days of culture in chondrogenic medium.

(A) Effect of TNF α pre-treatment on DNA and GAG/DNA content in cell pellets after chondrogenic differentiation in the presence of TNF α . N=3 donors with duplicates-quintuplicates per donor.

(B) Effect of TNF α pre-treatment on DNA and GAG/DNA content in cell pellets after chondrogenic differentiation in the absence of TNF α . N=2 donors with biological duplicates-quintuplicates per donor.

(C) Effect of TNF α withdrawal after pre-treatment on DNA and GAG/DNA content in the pellet after chondrogenic differentiation in the presence of TNF α . N=3 donors with biological triplicates per donor.

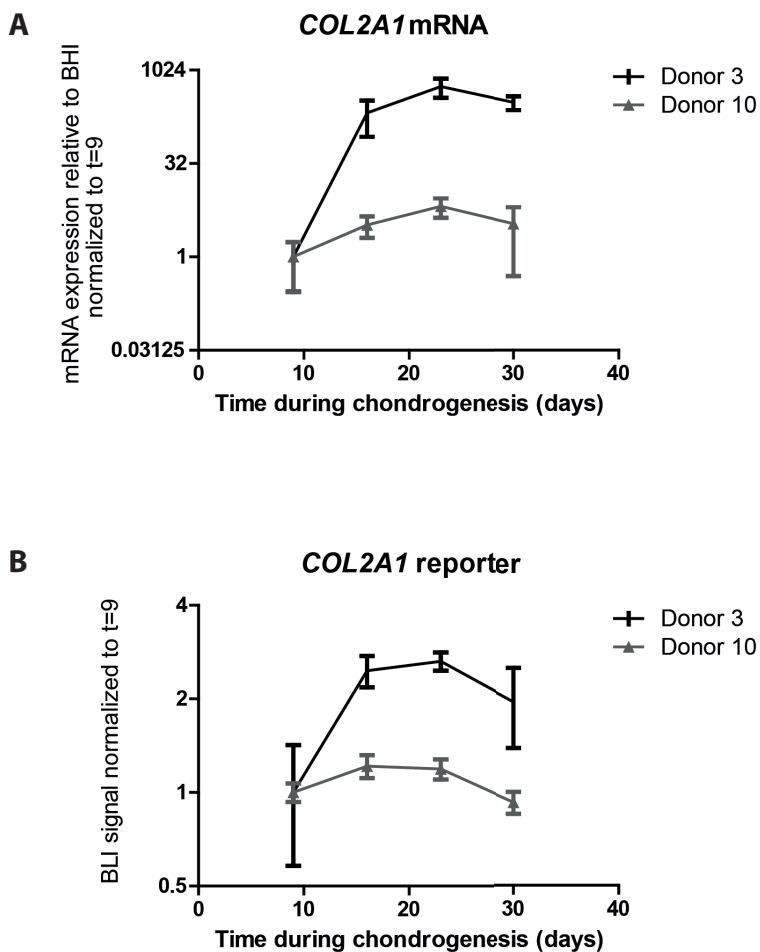


Figure S5.3 - Validation *COL2A1* reporter in pellets during chondrogenesis.

(A) mRNA expression relative to best housekeeper index (BHI) of pellets at t=9, t=16, t=23 and t=30 during chondrogenic differentiation. Values represent the mean \pm SD, triplicates.

(B) Relative *Gussia* Luciferase (*Gluc*) activity of medium from *COL2A1* reporter transduced pellets at various days. Values represent the mean \pm SD from quintuplicates.

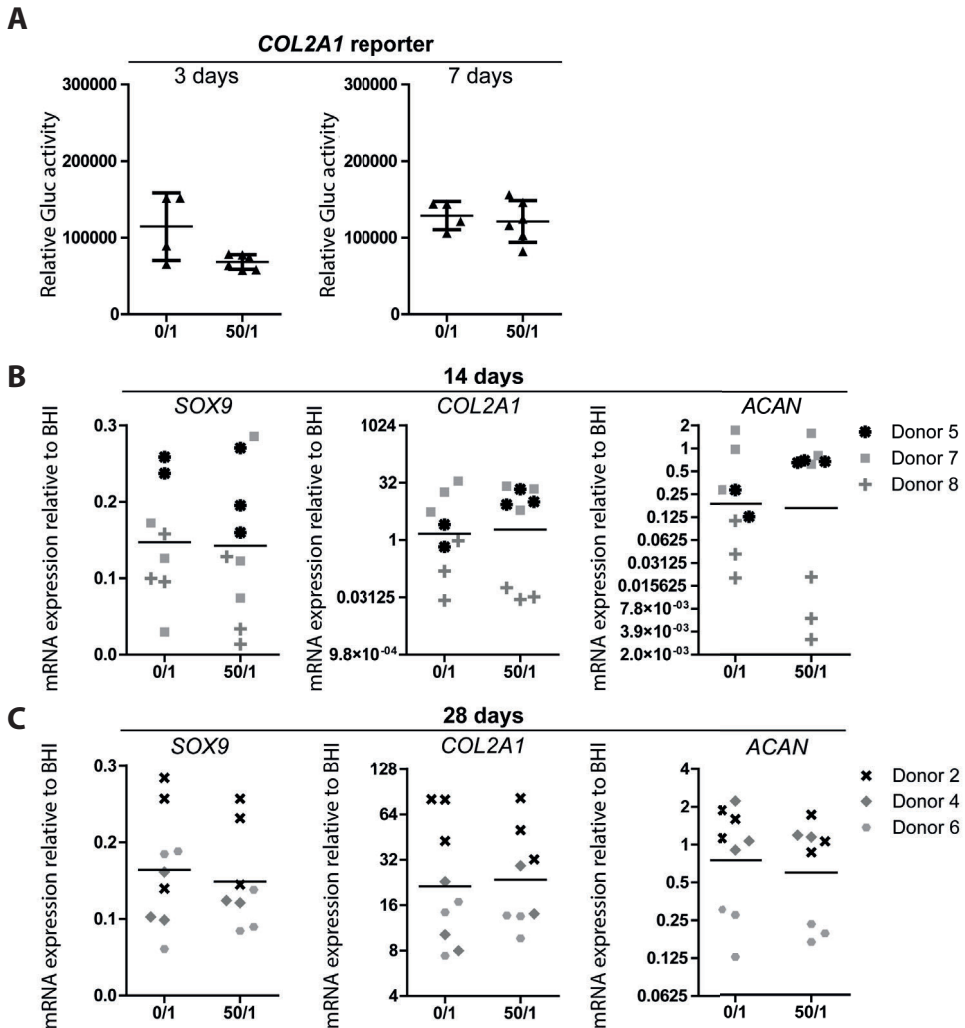


Figure S5.4 - 50 ng/mL pre-treatment with TNF α did not alter the expression of chondrogenic genes after chondrogenic induction in TNF α environment.

(A) Relative Gaussia Luciferase (Gluc) activity of medium from MSC pellets containing the COL2A1 reporter gene after 3 and 7 days of chondrogenic induction. Values represent the mean \pm SD with 4-6 pellets.

(B-C) COL2A1, ACAN, SOX9 mRNA expression relative to best housekeeping index (BHI) of pellets at t=14 (B) and t=28 (C). N=3 donors with 2-3 pellets per donor.

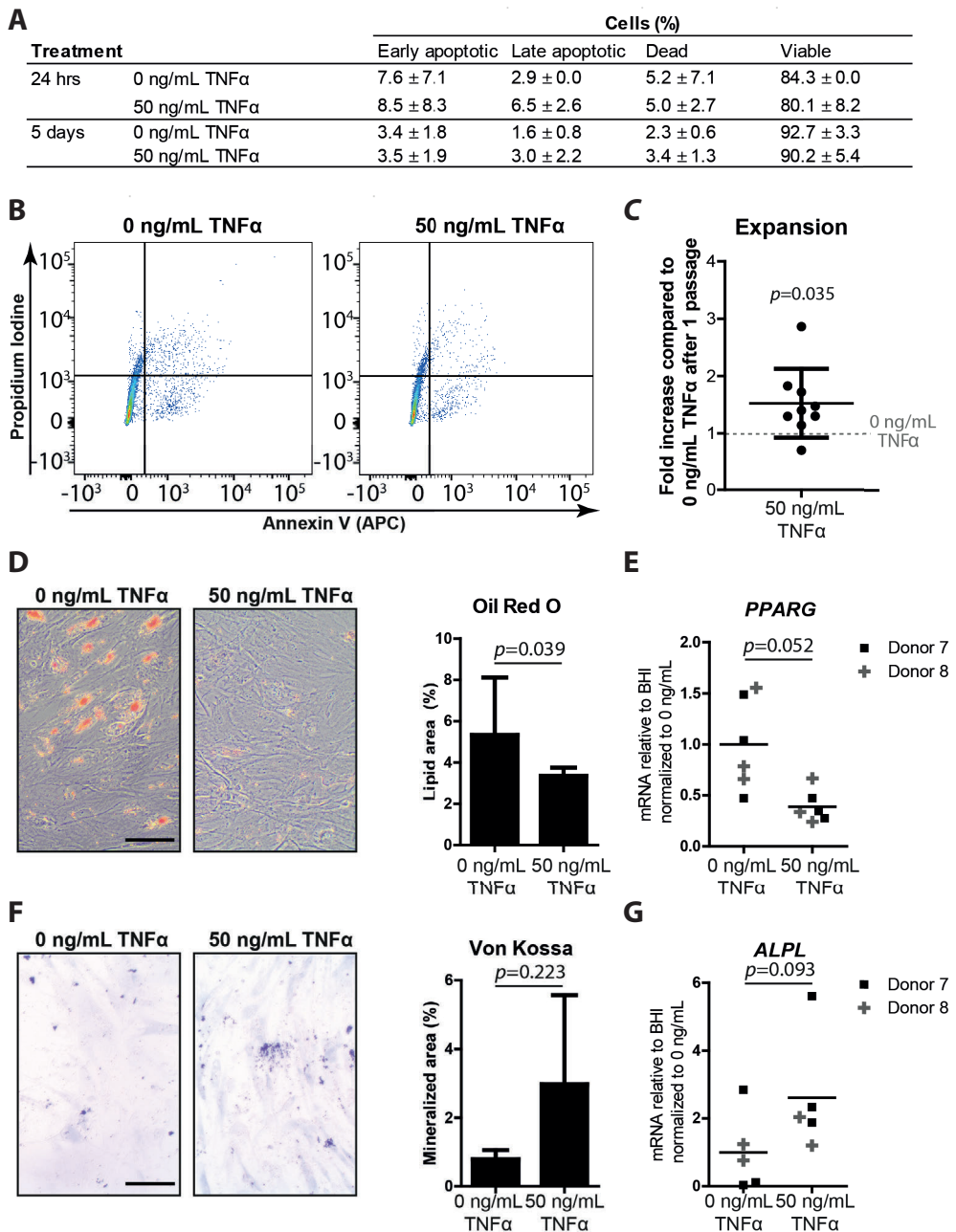


Figure S5.5 - TNF α pre-treatment affected the multi-potency, increased expansion and did not affect apoptosis of MSCs.

(A) Percentages of apoptotic cells determined by Annexin V and Propidium Iodide (PI) using flow cytometry. Early apoptotic cells are Annexin V/PI $^{+/-}$, Late apoptotic cells are Annexin V/PI $^{+/+}$, Dead cells are Annexin V/PI $^{-/+}$, Viable cells are Annexin V/PI $^{-/-}$.

- ◀
- (B) Representative graph of MSCs incubated for 24 hours with 0 or 50 ng/mL TNF α followed by Annexin V and PI staining and flow cytometry analysis.
- (C) Cell number data during expansion after 1 passage with 0 or 50 ng/mL TNF α . N=9 donors.
- (D) Representative image of Oil red O staining of MSCs 21 days after adipogenic differentiation. Scale bar represents 100 μ m. Right, quantification of Oil red O positive (lipids) area. N=2 donors with biological triplicates per donor.
- (E) *PPARG* mRNA expression of MSCs after 21 days of adipogenic differentiation. N=2 donors with three replicates per donor.
- (F) Representative image of Von Kossa staining of MSCs 21 days after osteogenic differentiation. Scale bar represents 100 μ m. Right, quantification of Von Kossa positive (mineralized) area. N=2 donors with biological singlicate-triplicates per donor.
- (G) *ALPL* mRNA expression of MSCs 21 days after osteogenic differentiation. N=2 donors with 2-3 replicates per donor.

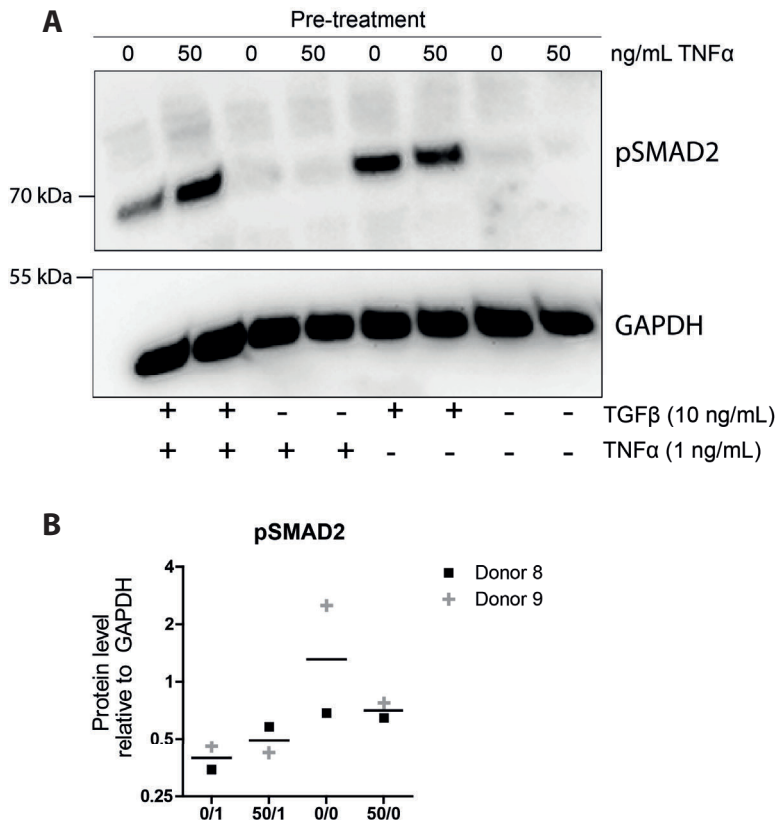


Figure S5.6 - TNF α pre-treatment did not alter SMAD2 activation after TGF β 1 exposure.

- (A) Representative western blot showing the expression levels of phospho-SMAD2 of MSCs pre-treated for 4 days with 0 or 50 ng/mL TNF α followed by 30 min 10 ng/ml TGF β 1 and/or 1 ng/mL TNF α stimulation, N=2 donors.
- (B) Quantification of western blot results relative to GAPDH, N=2 donors.

Table S5.1. List of MSC donors

Donor	Sex	Age (years)	Donor source
1	F	17	Total hip replacement patients
2	F	55	Total hip replacement patients
3	M	33	Healthy volunteers
4	M	42	Total hip replacement patients
5	F	20	Total hip replacement patients
6	F	73	Total hip replacement patients
7	M	23	Total hip replacement patients
8	M	50	Total hip replacement patients
9	F	29	Total hip replacement patients
10	M	31	Healthy volunteers

Table S5.2. List of primers used to detect mRNA levels by qRT-PCR

Gene	Forward primer	Reverse primers	
<i>GAPDH</i>	5'-ATGGGGAAGGT-GAAGGTCG-3'	5'-TAAAAGCAGCCCT-GGTGACC-3'	TaqMan
<i>RPS27A</i>	5'-TGGCTGTCCT-GAAATATTATAAGGT-3'	5'-CCCCAGCACCACA-TTCATCA-3'	SYBR Green
<i>HPRT1</i>	5'-TTATGGACAGG-ACTGAACGTCTTG-3'	5'-GCACACAGAGGGC-TACCATGTG-3'	TaqMan
<i>COL2A1</i>	5'-GGCAATAGCAGGT-TCACGTACA-3'	5'-CGATAACAGTCTT-GCCCCACTT-3'	TaqMan
<i>ACAN</i>	5'-TCGAGGACAGC-GAGGCC-3'	5'-TCGAGGGTGTAG-CGTGTAGAGA-3'	TaqMan
<i>SOX9</i>	5'-TCCACGAAGGGC-CGC-3'	5'-CAACGCCGAGCT-CAGCA-3'	TaqMan
<i>ALPL</i>	5'-GACCCTTGACCCC-CACAAT-3'	5'-GCTCGTACTGCAT-GTCCCCT-3'	TaqMan
<i>PPARG</i>	5'-AGGGCGATCTTGA-CAGGAAA-3'	5'-TCTCCCATCAT-TAAGGAATTCATG-3'	TaqMan

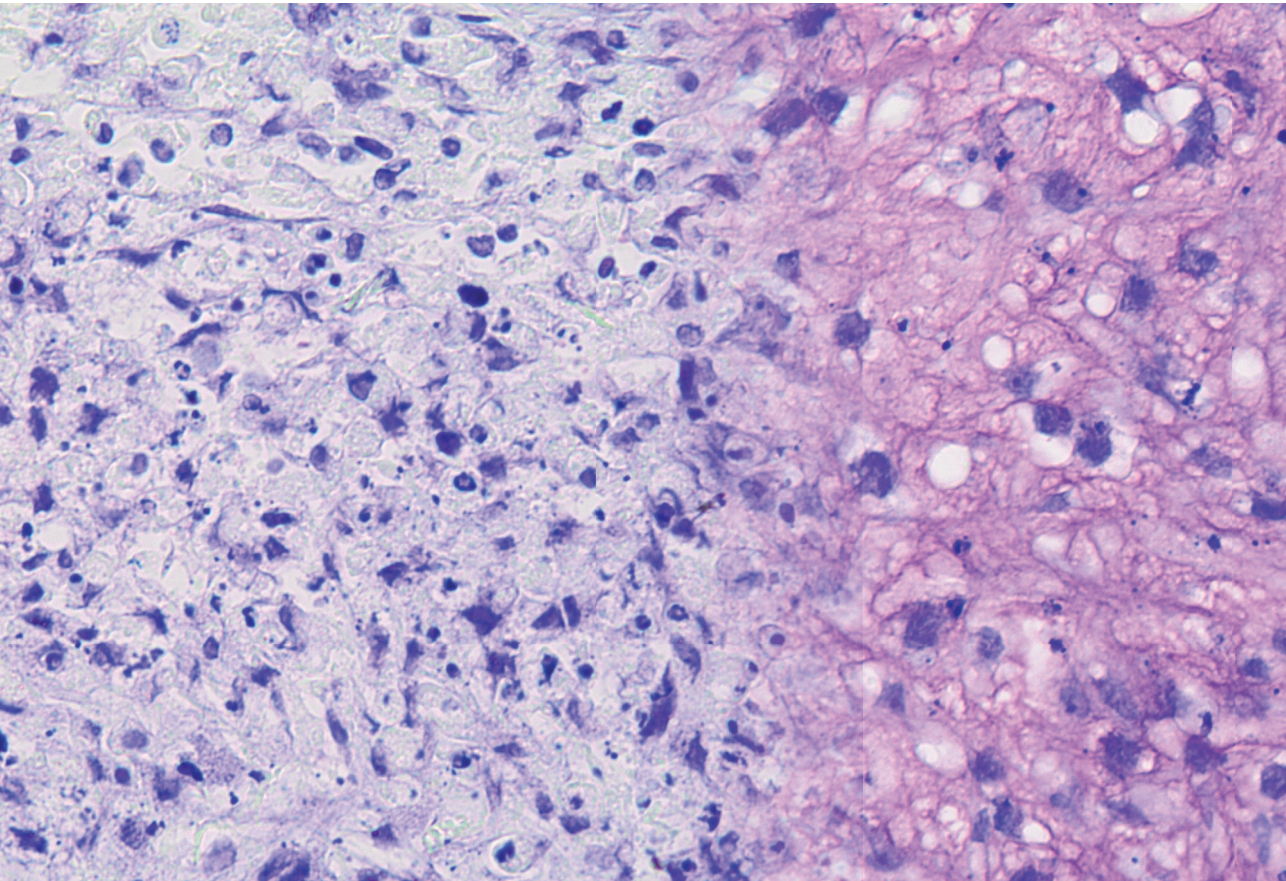
Table S5.3. List of antibodies used to detect specific proteins in Western blots

Protein	Antibody	Dilution	Catalog
Pan-SOXC (Sold as SOX11), binds SOX11 more efficiently than SOX4 and SOX12 (Bhattaram, <i>et al.</i> 2018)	Rabbit, polyclonal	1/1000	Atlas antibodies, HPA000536
Non-phospho (Active) β -catenin (Ser33/37/Thr41)	Rabbit, monoclonal	1/1000	Cell Signaling technology, 8814S
GAPDH	Rabbit, monoclonal	1/1000	Cell Signaling technology, 2118S
Phospho SMAD2 (Ser465/Ser467)	Rabbit, monoclonal	1/1000	Cell Signaling technology, 3108S

5.7 Acknowledgements

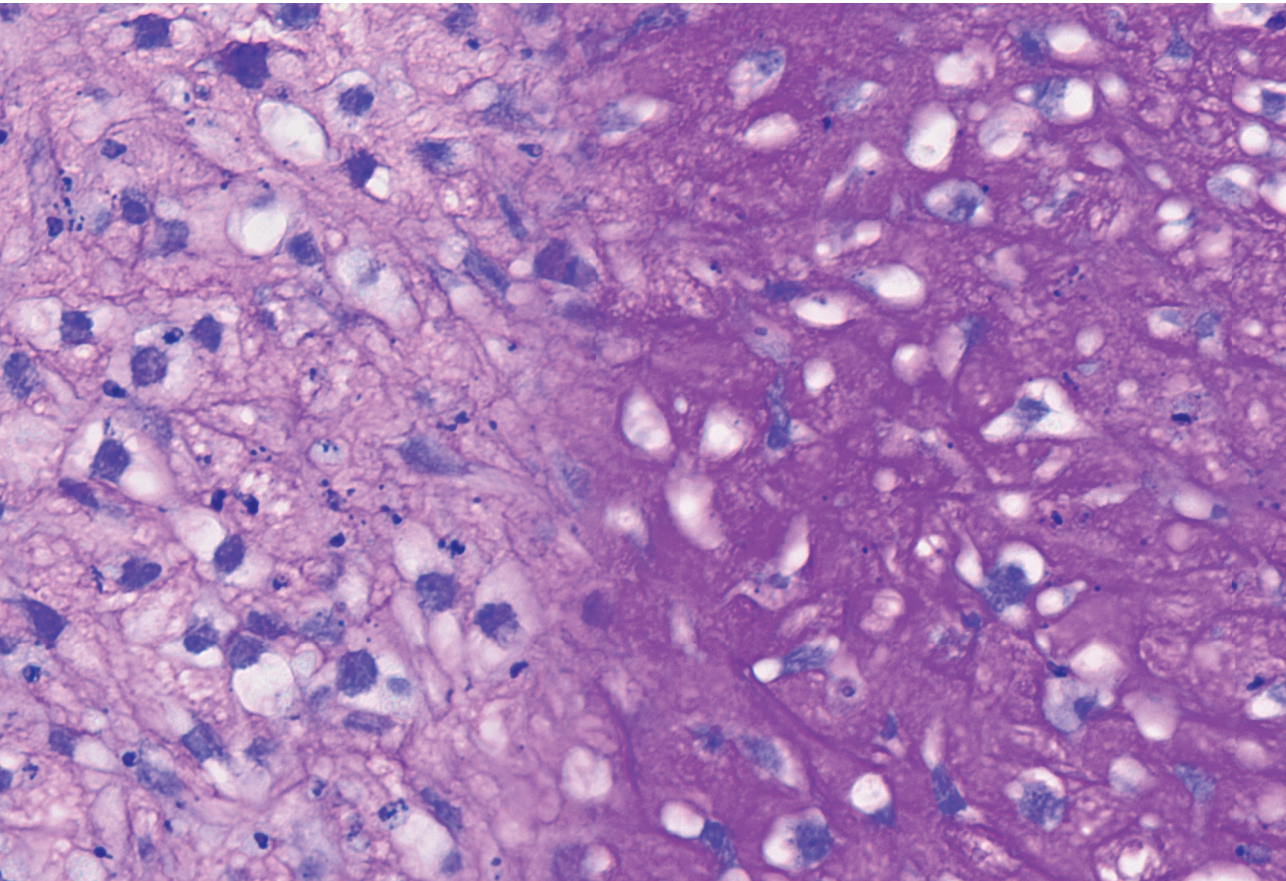
The authors would like to thank Sascha Schmidt and Janneke Witte-Bouma for technical assistance with the Gaussia luciferase activity measurements and the FACS sorting facility at the Erasmus MC for support with the BD Fortessa machine. The monoclonal antibody II-II 6B3 deposited by Linsenmayer, T.F. was obtained from the Developmental Studies Hybridoma Bank created by the NICHD of the NIH and maintained at The University of Iowa, Department of Biology, Iowa City, IA 52242. This study is part of the Medical Delta RegMed4D program.

6



Chapter 6

General discussion



6.1 Discussion

Articular cartilage has a limited regeneration capacity and if left untreated after damage it can lose its functional properties, eventually leading to the development of osteoarthritis (OA) (Mankin 1982, Shapiro, Koide *et al.* 1993). Mesenchymal progenitor cells referred to as mesenchymal stem or stromal cells (MSCs) have emerged as a promising cell source for cartilage regenerative purposes. Despite several clinical trials, currently there is no robust and routine clinical application using MSCs for cartilage repair. One of the challenges for MSC-based cartilage regeneration strategies is the fact that MSCs lose their chondrogenic differentiation potential during *in vitro* expansion. *In vitro* expansion is necessary to obtain enough cells to repair the cartilage defect (Bonab, Alimoghaddam *et al.* 2006). However, during expansion of MSCs, accumulation of senescent cells occurs and it is largely unknown how senescent MSCs affect the chondrogenic differentiation capacity of the MSC population and how this is influencing its neighboring cells. Notably, the expression of the transcription factor *TWIST1*, which is known to play a role in cell proliferation and differentiation, is downregulated during *in vitro* expansion (Narcisi, Cleary *et al.* 2015). These data suggest that both cellular senescence and *TWIST1* expression alter the chondrogenic differentiation potential of MSCs. In this thesis we aimed to determine the effect of cellular senescence and *TWIST1* expression on MSC fate. In addition, we aimed to establish culture methods to improve MSC expansion and chondrogenesis via *TWIST1* modulation. The following paragraphs discuss the implications of cellular senescence, inflammatory cytokines, *TWIST1* and *in vitro* expansion methods for MSC-based cartilage repair.

6.1.1 Cellular senescence: good or bad for cartilage repair?

In 1961, Hayflick and Moorehead were the first to describe the accumulation of senescent cells after *in vitro* expansion (Hayflick and Moorhead 1961, Hayflick 1965). Besides that, senescent cells accumulate in different tissues during aging, including cartilage and bone (Farr, Fraser *et al.* 2016, Diekman, Sessions *et al.* 2018). In addition, it is known that senescent cells are present in the joint tissue of patients with OA, suggesting that senescent cells drive, or are at least linked, to the development of OA (Jeon, David *et al.* 2018). In line with this hypothesis, it has been observed that transplantation of senescent fibroblasts into the knee of mice resulted in an OA-like phenotype

with articular cartilage damage and osteophyte formation (Xu, Bradley *et al.* 2017). At the same year, it has been reported that clearance of senescent cells, using the senolytic molecule XBX0101, reduced the development of post-traumatic OA (Jeon, Kim *et al.* 2017). Together these results suggest that the use of senescent MSCs for cartilage repair may be detrimental for cartilage regeneration. On the other hand, several studies have discovered that senescence can favor tissue regeneration (Rhinn, Ritschka *et al.* 2019). For example, senescent cells are induced during cutaneous wound healing and the senescence-associated secretory phenotype (SASP) factor PDGF-A stimulates optimal wound closure (Demaria, Ohtani *et al.* 2014). In addition, senescent cells induce the expression of stem cell markers in skin cells (Ritschka, Storer *et al.* 2017). Furthermore, cellular senescence is induced during limb regeneration in salamanders (Yun, Davaapil *et al.* 2015), and occurs in mice during embryonic development in limbs (Storer, Mas *et al.* 2013), and during puberty in long bones (Li, Chai *et al.* 2017). All these findings combined indicate that the senescent MSCs can be both detrimental and beneficial for joint tissue homeostasis.

Cellular senescence impairs chondrogenic differentiation via cell-intrinsic mechanisms

Studies focusing on senescent MSCs mainly focused on the adipogenic and osteogenic differentiation potential. The outcome of these studies is controversial, so it remains debated whether the osteogenic and adipogenic differentiation potential of senescent MSCs is decreased, unaltered or even increased (Stolzing, Jones *et al.* 2008, Wagner, Horn *et al.* 2008, Geissler, Textor *et al.* 2012). In this thesis, we show that senescent MSCs have an impaired chondrogenic differentiation capacity (**chapter 2**). Moreover, we show that the chondrogenic differentiation capacity was reduced in a dose dependent way by the number of senescent MSCs prior to chondrogenic induction. These data are in line with the fact that MSCs reduce their chondrogenic differentiation potential during *in vitro* expansion (Bonab, Alimoghaddam *et al.* 2006). How senescence in MSCs reduces their differentiation potential remains unknown. One of the main characteristics of senescent cells is the absence of proliferation and it is known that proliferation is required in the early stage of *in vitro* chondrogenesis of MSCs (Dexheimer, Frank *et al.* 2012). Another characteristic of senescent cells is increased oxidative stress (Coryell, Diekman *et al.* 2021). In **chapter 3**, we show that indeed senescent MSCs have an increased oxidative consumption rate. It is known that oxidative stress can

modulate the ability of transcription factors to bind the DNA via disulfate post-translational modifications (O'Brian and Chu 2005). So, it can be speculated that oxidative stress in senescent cells alter the function of key transcription factors such as SOX9 and TWIST1 during chondrogenesis. Furthermore, we show that TGF β signaling activation is altered in senescent MSCs (**chapter 2**). TGF β signaling stimulates chondrogenic differentiation via Sox9 (Furumatsu, Ozaki *et al.* 2009). Overall, these data suggest that elimination of senescent MSCs prior to chondrogenic differentiation can increase the chondrogenic differentiation capacity and might reduce chondrogenic heterogeneity.

The effect of senescence associated secretory factors on cartilage regeneration may be factor, time and dose dependent

Besides growth arrest, another hallmark of senescent cells is the release of high levels of chemokines (such as CCL2), cytokines (such as IL6, IL8, IL10, IL1 and TNF) proteases (such as MMP1, MMP3, MMP13 and ADAMTS5) and growth factors (such as TGF β and VEGF), known as the SASP. These SASP factors are elevated in cartilage tissue of patients with symptomatic cartilage defects and in synovial fluid of patients with OA and can induce a variety of different physiological and pathological responses in cartilage tissue (Tsuchida, Beekhuizen *et al.* 2014, Coryell, Diekman *et al.* 2021). Therefore, it is crucial to understand how the SASP of senescent MSCs affect the cartilage tissue. For example, Ccl2 knockout mice had reduced endogenous cartilage after injury (Jablonski, Leonard *et al.* 2019), suggesting that Ccl2 contribute to cartilage regeneration. On the other hand, Ccl2 knockout mice had reduced pain after destabilization of the medial meniscus (DMM) (Miotla Zarebska, Chanalaris *et al.* 2017). Furthermore, it is known that CCL2 inhibits chondrogenesis of synovial MSCs (Harris, Seto *et al.* 2013). Cytokines IL1 β and TNF α are known to induce matrix degradation and reduce the differentiation potential of MSCs (Wehling, Palmer *et al.* 2009, Markway, Cho *et al.* 2016). In **chapter 5**, however, we show that MSCs pre-treated with the SASP factor TNF α had an increased chondrogenic differentiation capacity *in vitro*. Suggesting that TNF α can have a beneficial role during early cartilage repair. IL10 induces chondrocyte proliferation and hypertrophic differentiation (Jung, Kim *et al.* 2013). Additionally, matrix metalloproteinases (MMPs) can contribute to extracellular matrix degradation (Murphy and Lee 2005). All these findings, indicate that the effect of SASP factors on cartilage regeneration is complex and may be factor, dose and time dependent.

In **chapter 3**, we show that *TWIST1*-silencing-induced senescent MSCs and irradiation induced senescent MSCs have a different SASP profile, highlighting the complexity of the SASP in MSCs. In this thesis, we showed that the secretome of senescent MSCs, in a three-dimensional pellet, did not alter the expression of chondrogenic markers, *COL2A1*, *SOX9* and *ACAN* during chondrogenic differentiation of MSCs (**chapter 2**). Based on these findings it could be suggested that the SASP factors of senescent MSCs have no effect on cartilage formation during chondrogenesis of MSCs *in vitro*. However, more studies are necessary to fully exclude that SASP factors from senescent MSCs have no effect on chondrogenic differentiation. As highlighted in **chapter 3**, the composition of the SASP of MSCs could be heterogeneous and, depending on the composition, it might have a different effect on surrounding tissues. For optimal cartilage regeneration and safe MSC-based cartilage tissue engineering, it is important to understand the effect of the SASP on cartilage and synovium tissues in the joints. Chondrocytes and synoviocytes lose their functional properties upon exposure to inflammatory cytokines (Benito, Veale *et al.* 2005, Sutton, Clutterbuck *et al.* 2009, Goldring, Otero *et al.* 2011). A next step would be to determine the composition of SASP factors produced by senescent MSCs and study the dose and time dependent effects on different joint tissues, such as chondrocytes and synovial membrane cells *in vivo*.

Chondrocyte senescence and osteoarthritis

Senescent chondrocytes are present in cartilage tissue from OA patients (Price, Waters *et al.* 2002). Aging chondrocytes have reduced anabolic activity, while increasing their catabolic activity (Forsyth, Cole *et al.* 2005). One of the catabolic markers that was elevated in aging chondrocytes was the SASP factor MMP13 (Forsyth, Cole *et al.* 2005). It has been hypothesized that senescent chondrocytes contribute to the development of OA (Price, Waters *et al.* 2002). This is further supported by the fact that cartilage from patients with OA had high expression levels of MMP13 (Wang, Manner *et al.* 2004). During the progression of OA, chondrocytes become hypertrophic leading to mineralization of the cartilage tissue (von der Mark, Kirsch *et al.* 1992). Hypertrophic chondrocytes share some of the markers of senescent chondrocytes, such as MMP13 and VEGF (Rim, Nam *et al.* 2020). These results suggest that chondrocyte hypertrophy and senescence might be linked. One striking result in this thesis is the fact that induction of cellular senescence during chondrogenesis did not alter the expression of hypertrophic markers compared to non-irradiated control pellets (**chapter 5**).

These findings suggest that the occurrence of cellular senescence during chondrogenesis has no direct effect on hypertrophic marker expression *in vitro*. Whether chondrocyte hypertrophy and senescence are causality linked, remains to be determined. Techniques such as single-cell RNA sequencing identified different subpopulations in chondrocytes from OA patients (Ji, Zheng *et al.* 2019), and is a promising tool to provide new insights on how cellular senescence affects the cartilage tissue.

Modulation of cellular senescence in MSCs to improve chondrogenic differentiation

Since senescent MSCs had an impaired chondrogenic differentiation capacity (**chapter 2**), the next step would be to eliminate senescent cells from the cultures. Senolytic molecules appear as promising drugs since they specially kill senescent cells (Kirkland and Tchkonja 2020). Only a limited number of studies have been performed to test the effect of senolytics on MSC cultures. The senolytic drugs quercetin, nicotinamide riboside, and danazol did not specifically kill senescent MSCs during *in vitro* culture (Grezella, Fernandez-Rebollo *et al.* 2018). However, ABT-263 reduced the number of SA- β -gal positive MSCs, but did not increase the expansion capacity (Grezella, Fernandez-Rebollo *et al.* 2018). Another senolytic molecule, dasatinib, reduces the expression of the senescence associated genes in MSCs (Suvakov, Cubro *et al.* 2019). Overall, these data show that senolytic molecules are promising to eliminate senescent cells in MSCs cultures. It remains to be determined whether senolytic molecules have a positive effect on chondrogenic differentiation. Another strategy to reduce cellular senescence in MSC populations, is to develop culture methods that prevent induction of cellular senescence such as addition of the signaling protein WNT3A (Lehmann, Narcisi *et al.* 2022), or hypoxia (Tsai, Chen *et al.* 2011). More studies are necessary to find the best treatment to eliminate senescent MSC.

6.1.2 TWIST1 as a marker to select chondrogenic MSC

In this thesis we show that the transcription factor TWIST1 has an important role in MSCs and that it is involved in MSC expansion, senescence and metabolism.

TWIST1 regulates cell fate in MSCs

TWIST1 plays an essential role in MSC expansion and maintenance (Isenmann, Arthur *et al.* 2009). It has been shown that enforced expression of TWIST1 in MSCs increases the population doubling level (Isenmann, Arthur *et al.* 2009). During expansion, TWIST1 expression levels are downregulated, suggesting that high TWIST1 expression stimulates MSC growth (Isenmann, Arthur *et al.* 2009, Cakouros, Isenmann *et al.* 2012, Narcisi, Cleary *et al.* 2015). In addition, TWIST1 inhibits chondrogenic and osteogenic differentiation of MSCs (Reinhold, Kapadia *et al.* 2006, Isenmann, Arthur *et al.* 2009). It has been hypothesized that TWIST1 inhibits MSCs differentiation via direct binding to the DNA-binding domain of SOX9 and RUNX2 via its C-terminal transactivation domain (Bialek, Kern *et al.* 2004, Gu, Boyer *et al.* 2012). Indeed, TWIST1 expression is downregulated during chondrogenic differentiation of MSCs (Cleary, Narcisi *et al.* 2017). However, TWIST1 silencing does not improve chondrogenic differentiation and TWIST1 is upregulated at day 1 of chondrogenic differentiation (Cleary, Narcisi *et al.* 2017). These data suggest that TWIST1 is required during early chondrogenic differentiation of MSCs. What the function is of TWIST1 during early chondrogenic differentiation remains to be determined. Based on these data one might hypothesize that TWIST1 is necessary for the upregulation of chondrogenic genes. This hypothesis is supported by the fact that TWIST1 can bind and activate the intronic *COL2A1* regulatory element in MC3T3 and HEK293T cells (Chakraborty, Wirrig *et al.* 2010).

To further study if TWIST1 is a good marker to select chondrogenic MSCs, in **chapter 4** we selected MSCs based on *TWIST1* levels using an RNA-based probe. We showed that *TWIST1* expression is heterogenous and that the subpopulation of MSCs with a high *TWIST1* expression has increased expansion capacity compared to the subpopulation of MSCs with a low *TWIST1* expression. These data highlight the role of *TWIST1* as a possible marker to select MSCs with a high expansion capacity. This is further supported by the fact that *TWIST1* expression levels can be used to predict donor variation of MSCs (Boregowda, Krishnappa *et al.* 2016). MSCs with a high *TWIST1* expression were more likely to differentiate towards chondrocytes compared to MSCs

with a low *TWIST1* expression (Boregowda, Krishnappa *et al.* 2016). Overall, it could be speculated that MSCs with a high *TWIST1* expression keep their chondrogenic differentiation potential upon *in vitro* expansion.

TWIST1 silencing alters the metabolic state of MSCs

TWIST1 is known to play an important role in different metabolic pathways, since it can alter the glycolysis and the mitochondrial function in different cell types (Pan, Fujimoto *et al.* 2009, Lu, Wang *et al.* 2018, Wang, Yin *et al.* 2020, Wang, Yin *et al.* 2021). In tumor cells, TWIST1 stimulates aerobic glycolysis, also known as the Warburg effect, via direct promoter activation of glycolytic genes such as *SLC2A1*, *HK2*, *ENO1* and *PKM2* (Wang, Yin *et al.* 2020). Moreover, TWIST1 can regulate several proteins involved in mitochondrial function (Pan, Fujimoto *et al.* 2009, Lu, Wang *et al.* 2018, Wang, Yin *et al.* 2021). PGC-1 α is such a protein that can stimulate mitochondrial biogenesis and Twist1 can inhibit its transcription activity via direct binding (Pan, Fujimoto *et al.* 2009). Loss of Twist1 in hematopoietic stem cells resulted in increased Ca²⁺ and ROS levels, suggesting that Twist1 is necessary for a proper mitochondrial function (Wang, Yin *et al.* 2021). The role of TWIST1 in MSC energy metabolism is less studied. In **chapter 3**, we show that *TWIST1* silencing in MSCs resulted in an increased oxygen consumption rate without altering the extracellular acidification rate, indicating that *TWIST1* plays an important role in the regulation of the oxygen consumption rate of MSCs. It remains to be determined whether *TWIST1* silencing directly or indirectly alters the metabolic flux towards an increased oxygen consumption in MSCs and what the effect is of the altered oxygen consumption on the differentiation capacity of MSCs. It is suggested that the metabolic flux of MSCs plays a crucial role during chondrogenic differentiation, since it is a highly energy demanding process and the cartilage tissue is anaerobic. This is supported by the fact that MSCs cultured under hypoxic condition have an increased chondrogenic capacity (Markway, Tan *et al.* 2010). Furthermore, during chondrogenic differentiation of MSCs, the oxygen consumption was reduced (Carroll, Buckley *et al.* 2021). Overall, it could be hypothesized that downregulation of the oxygen consumption support chondrogenic differentiation and that TWIST1 plays a role in this process.

TWIST1 suppresses senescence

TWIST1 expression is downregulated during *in vitro* expansion (Narcisi, Cleary *et al.* 2015). In **chapter 3**, we show that overexpression of TWIST1 increases the expansion capacity of MSCs and reduces the number of β -gal positive cells. Furthermore, *TWIST1^{high}* expressing MSCs have an increased expansion capacity compared to *TWIST1^{low}* expressing MSCs (**chapter 4**). These data suggest that TWIST1 regulates cellular senescence in MSCs. This is further supported by the fact that MSCs with a loss of function mutation in *TWIST1* have an increased number of β -gal positive cells compared to control MSCs (Cakouros, Isenmann *et al.* 2012). In addition, we showed in **chapter 3** that TWIST1 silencing upregulated the expression of *CDKN2A* (*P16*) and *CDKN1A* (*P21*), induced growth arrest and increased the number of β -SA-gal positive cells. These data indicate that TWIST1 suppresses cellular senescence in MSCs. However, the molecular mechanism how TWIST1 controls cellular senescence has not been fully understood. It has been shown that TWIST1 inhibits E2A transcription (Tsai, Chen *et al.* 2011), and E2A activates the cyclin-dependent kinases inhibitor p21 (Harper, Adami *et al.* 1993, Prabhu, Ignatova *et al.* 1997), therefore it is reasonable to hypothesize that TWIST1 inhibits activation of p21 via E2A. Furthermore, TWIST1 can reduce the levels of E47, an inducer of p16 transcription (Cakouros, Isenmann *et al.* 2012). Overall, these results indicate that TWIST1 controls cellular senescence in MSCs via indirect regulation of the cyclin-dependent kinases p21 and p16. Besides upregulation of p21 and p16, TWIST1-silencing induced senescent MSCs had a non-classical SASP, lacking the expression of *IL6*, *IL8* and *MMP3* (**chapter 3**). In adipocytes, it has been shown that Twist1 can bind to the IL-6 promoters, suggesting that TWIST1 can directly modulate the expression of IL-6 (Pettersson, Laurencikiene *et al.* 2010). However, the regulation of the SASP is complex and remains to be completely understood. It has been shown before in fibroblasts and epithelial cells that the SASP can be heterogenous and that it is dependent on the cell type and senescent inducer (Wiley, Velarde *et al.* 2016, Basisty, Kale *et al.* 2020). The data in this thesis indicate that TWIST1 directly or indirectly modulates the expression of SASP genes in MSCs, so it could be speculated that TWIST1 could be a new target to modulate the SASP in MSCs.

Although the modulation of TWIST1 activity might be challenging due to the lack of defined small-molecule binding pockets of transcription factors, several promising chemical biology approaches to target transcription factors are emerging (Wiedemann, Weisner *et al.* 2018, Henley and Koehler

2021, Su and Henley 2021). There are strategies that focus on inhibition of transcription factor activity via (1) inhibiting gene expression, (2) binding to the DNA-binding domain (3) disrupting protein-protein interactions or (4) binding to the DNA responsive element (Fontaine, Overman *et al.* 2015). In order to develop a strategy to modulate *TWIST1* expression in MSCs, it is crucial to fully understand which genes are targeted by *TWIST1* during both cellular senescence and MSC differentiation.

6.1.3 Culture methods to reduce MSC heterogeneity and improve chondrogenic capacity

It is known that the addition of FGF2 and WNT3A during expansion can increase the chondrogenic differentiation capacity of MSCs, however inter-donor variation remains a problem (Narcisi, Cleary *et al.* 2015). MSCs expanded in the presence of FGF2 and WNT3A have higher *TWIST1* levels compared to MSCs cultured in the presence of FGF2 alone (Narcisi, Cleary *et al.* 2015). In this thesis we show that MSCs with a high *TWIST1* expression had a higher expansion capacity compared to MSCs with a low *TWIST1* expression, indicating that *TWIST1* is a promising MSC marker for cartilage tissue regeneration. It could be hypothesized that boosting *TWIST1* expression in MSCs or selecting MSCs with a high *TWIST1* expression can improve the clinical outcome for cartilage repair. In this thesis we used two approaches to obtain expanded MSCs with high *TWIST1* expression to reduce heterogeneity and improve chondrogenesis: 1) MSC selection and 2) MSCs priming.

Selecting MSCs based on function rather than phenotype

In the last decade, researchers tried to select chondrogenic MSCs based on surface marker selection. In 2006, the Mesenchymal and Tissue Stem Cell Committee of the International Society for Cellular Therapy proposed the minimal criteria to define MSCs (Dominici, Le Blanc *et al.* 2006). One of the criteria is that human MSCs should express the surface markers CD105, CD73 and CD90, and do not express CD45, CD34, CD14 or CD11b, CD79 α or CD19 and HLA-DR surface molecules (Dominici, Le Blanc *et al.* 2006). Some of these surface molecules have been found to be associated with a higher chondrogenic differentiation potential (Arufe, De la Fuente *et al.* 2010, Asai, Otsuru *et al.* 2014), however inconsistencies were found among researchers (Lv, Tuan *et al.* 2014, Cleary, Narcisi *et al.* 2016).

CD105 is such a surface molecule that has been associated with an increased chondrogenic differentiation potential in MSCs (Fan, Li *et al.* 2016). However, Cleary *et al.* found that CD105 does not predict the chondrogenic differentiation capacity on expanded MSCs (Cleary, Narcisi *et al.* 2016). A potential reason why the studies on surface markers are contradictory, is the fact that MSCs are cultured using different culture methods. This hypothesis is supported by the fact that exposure to TNF α can reduce CD105 expression of MSCs while these MSCs have an increased chondrogenic differentiation potential compared to MSCs without exposure to TNF α (**chapter 5**).

As an alternative to surface markers, new methods to select MSCs based on functional characteristics are necessary. The fact that functional markers, such as TWIST1, are expressed intracellular is an obstacle that makes it difficult to select living MSCs based on expression. In **chapter 4**, we show that it is possible to select MSCs based on *TWIST1* expression using a SmartFlare RNA-based probe. The selected cells had an increased expansion capacity. It remains, however, to be determined whether high *TWIST1* expressing cells have a high chondrogenic differentiation potential. These RNA based probes (NanoFlares) were designed and developed by the group of Prof. dr. Chad Merkin and commercialized under the name SmartFlares (Giljohann, Seferos *et al.* 2007, Prigodich, Seferos *et al.* 2009). At the moment, SmartFlares are no longer commercially available. Unfortunately, this prevented us from studying the chondrogenic differentiation capacity of *TWIST1*^{high} MSCs.

Besides the fact that the RNA-based probes are no longer commercially available, the use of RNA-based probes for cell selection does have more limitations. One of the limitations is that the protocol needs to be optimized for each target gene and each cell type. In addition, other researchers found that serum can increase the uptake capacity of SmartFlare probes in primary human T cells (Golab, Krzystyniak *et al.* 2020), highlighting the importance to determine the uptake capacity of RNA probes for each culture method. The high variation in probe uptake, makes the RNA-based probes unsuitable for clinical use. After appropriate validation, however, RNA-based probes have a high potential for a wide variety of research fields, since it allows us to study RNA expression in living cells.

Expansion methods that boost TWIST1 expression in MSCs to increase chondrogenesis

Besides MSC selection, another strategy to reduce heterogeneity and increase

the chondrogenic differentiation potential is via MSC pre-treatment/priming. Based on the results in this thesis one might speculate that boosting TWIST1 expression during expansion could be beneficial for MSC proliferation and chondrogenic differentiation. TWIST1 can be upregulated by several different growth factors. FGF2 and WNT3A are such growth factors which upregulate TWIST1 expression in MSCs (Narcisi, Cleary *et al.* 2015, Boregowda, Krishnappa *et al.* 2016). Indeed, pre-treatment with FGF2 and WNT3A increases the proliferation and chondrogenic differentiation capacity of MSCs (Tsutsumi, Shimazu *et al.* 2001, Bianchi, Banfi *et al.* 2003, Narcisi, Cleary *et al.* 2015).

Another method to stimulate TWIST1 expression is via low oxygen tension (hypoxia) (Yang, Wu *et al.* 2008). Hypoxia regulates cellular responses via the expression of the transcription factor HIF-1 α which directly target the expression of TWIST1 (Yang, Wu *et al.* 2008). Expansion of MSCs in a hypoxic environment increases the chondrogenic differentiation capacity of MSCs. Furthermore, hypoxia reduces the expression of senescence markers (Tsai, Chen *et al.* 2011). These data suggest that hypoxia can reduce cellular senescence during MSC expansion via TWIST1 expression.

Another method to upregulate TWIST1 expression in MSCs is via mechanical cyclical stretch stimulation (Guo, Liu *et al.* 2020). Mechanical stimulation of MSCs, such as compression load, increased expression of chondrogenic markers (Fahy, Alini *et al.* 2018).

In **chapter 5**, we show that TNF α during expansion increased the expansion rate and chondrogenic differentiation potential. TNF α can increase the expression of TWIST1 in chondrocytes (Hasei, Teramura *et al.* 2017), hypothesizing that TNF α upregulated TWIST1 in MSCs. In addition, TNF α increased active β -catenin and SOXC protein levels. The SOXC protein, Sox12, can transactivate Twist1 expression (Huang, Chen *et al.* 2015). On the other hand, addition of TNF α during chondrogenesis can reduce the chondrogenic differentiation potential of MSCs, induce cytokine secretion and cellular senescence, upregulate ROS levels and increase DNA damage in cells (Beyne-Rauzy, Recher *et al.* 2004, Wehling, Palmer *et al.* 2009, Kandhaya-Pillai, Miro-Mur *et al.* 2017, Li, Gan *et al.* 2017). It could be speculated that TNF α activates multiple pathways in MSCs which can be both beneficial and detrimental for chondrogenesis. In **chapter 5**, we show that pre-treatment with TNF α during monolayer can make the MSCs better resistant against the negative results of TNF α during chondrogenesis (**chapter 5**). This makes TNF α pre-treatment promising for MSC-based

cartilage tissue engineering purposes, since post-traumatic joints have elevated levels of pro-inflammatory cytokines, including TNF α (Sward, Frobell *et al.* 2012, Tsuchida, Beekhuizen *et al.* 2014, Imamura, Ezquerro *et al.* 2015, Alonso, Bravo *et al.* 2020).

6.2 Future perspectives

MSCs are a promising cells source for cartilage tissue regeneration. In this thesis we show how cellular senescence impairs chondrogenic differentiation of MSCs and that TNF α during the expansion phase of MSCs can increase their chondrogenic capacity. Moreover, we highlight the importance of TWIST1 during MSC expansion. In order to regenerate high quality articular cartilage using MSCs, there are still some hurdles to overcome.

6.2.1 Develop methods to generate stable cartilage

In this thesis, we show that TNF α can increase the chondrogenic differentiation potential of MSCs (**chapter 5**). These differentiated chondrocytes have the tendency to differentiate into hypertrophic chondrocytes and eventually the formed cartilage will be remodeled into bone (Farrell, Both *et al.* 2011). Therefore, it is crucial to understand the molecular mechanism behind the differentiation process. The transcription factors TWIST1, SOX9 and RUNX2/3 play an important role in cell fate determination during chondrogenic differentiation of MSCs. TWIST1 can interact with the DNA binding sites of SOX9, RUNX2 and RUNX3 (Yousfi, Lasmoles *et al.* 2002, Bialek, Kern *et al.* 2004, Gu, Boyer *et al.* 2012, Pham, Vincentz *et al.* 2012). However, the target genes of TWIST1, SOX9 and RUNX2/3 during the different stages of MSC differentiation remain to be determined. Chromatin immunoprecipitation sequencing (ChIP-seq) assays have become the standard to determine DNA-binding sites of transcription factors. Recently, Cleavage Under Targets and Release Using Nuclease (CUT&RUN) technology was developed as an alternative method to ChIP-seq (Skene and Henikoff 2017, Skene, Henikoff *et al.* 2018). An advantage of CUT&RUN technology over ChIP-seq is that this method is suitable for low cell input. This is a major advantage which allows us to study transcription factor binding during chondrogenic differentiation of MSCs. Understanding which genes are targeted by TWIST1, SOX9 and RUNX2/3 during the different stages of chondrogenesis might help us to identify new targets to stimulate chondrogenesis and block hypertrophic differentiation.

6.2.2 Endogenous MSCs to repair cartilage tissue

A strategy to repair cartilage is using freshly isolated MSCs followed by *in vitro* expansion, chondrogenic differentiation and transplantation into the cartilage defect. The advantage of *in vitro* expansion of MSCs is that the cells proliferate and increase in cell number. However, a disadvantage of MSC expansion is that it can induce cellular senescence and reduce their chondrogenic differentiation potential. An alternative strategy to repair cartilage with MSCs is via the recruitment of endogenous MSCs towards the cartilage defect. Chemokines, growth factors and platelet -rich plasma can stimulate MSC migration, however the perfect dosage, timing and selection of the chemo-attractants needs to be determined to use as treatment for cartilage defects (Yang, Li *et al.* 2020). TWIST1 can mediate cell migration in different cell types (Matsuo, Shiraha *et al.* 2009, Lee and Yutzey 2011, Wang, Lin *et al.* 2020), so TWIST1 might be an interesting factor to target in MSCs in order to recruit MSCs towards the cartilage damage. Both *in vitro* expansion and endogenous recruitment of MSCs have advantages and disadvantages and it remains to be determined which method is the best to repair articular cartilage. It could be speculated that patient specific factors such as age, lifestyle and the size of the cartilage defect contribute to decide which treatment approach is best.

6.2.3 Single cell technologies to advance the understanding of MSC chondrogenesis

Intra- and inter-donor variation in differentiation potential of MSCs brings major challenges and limits the clinical use of MSCs. It is still not fully understood which factors contribute to this heterogeneity. In the recent years, novel methods have been developed that allow us to study RNA expression, protein levels and chromatin accessibility at a single cell level (Chan, Gulati *et al.* 2018). For example, single cell RNA-sequencing data in MSCs identified novel surface markers and identified a population of PDPN+CD146-CD73+CD164+ cells, known as the human skeletal stem cell (Chan, Gulati *et al.* 2018). However, the expression of surface markers changes upon *in vitro* expansion, therefore additional knowledge at single cell level is necessary during chondrogenic differentiation of MSCs to identify functional markers.

Since the surface markers change upon *in vitro* expansion, another strategy is to directly isolate the chondroprogenitor cells from the bone marrow using surface markers. Bone marrow cells that are FACS enriched for CD271+CD56+

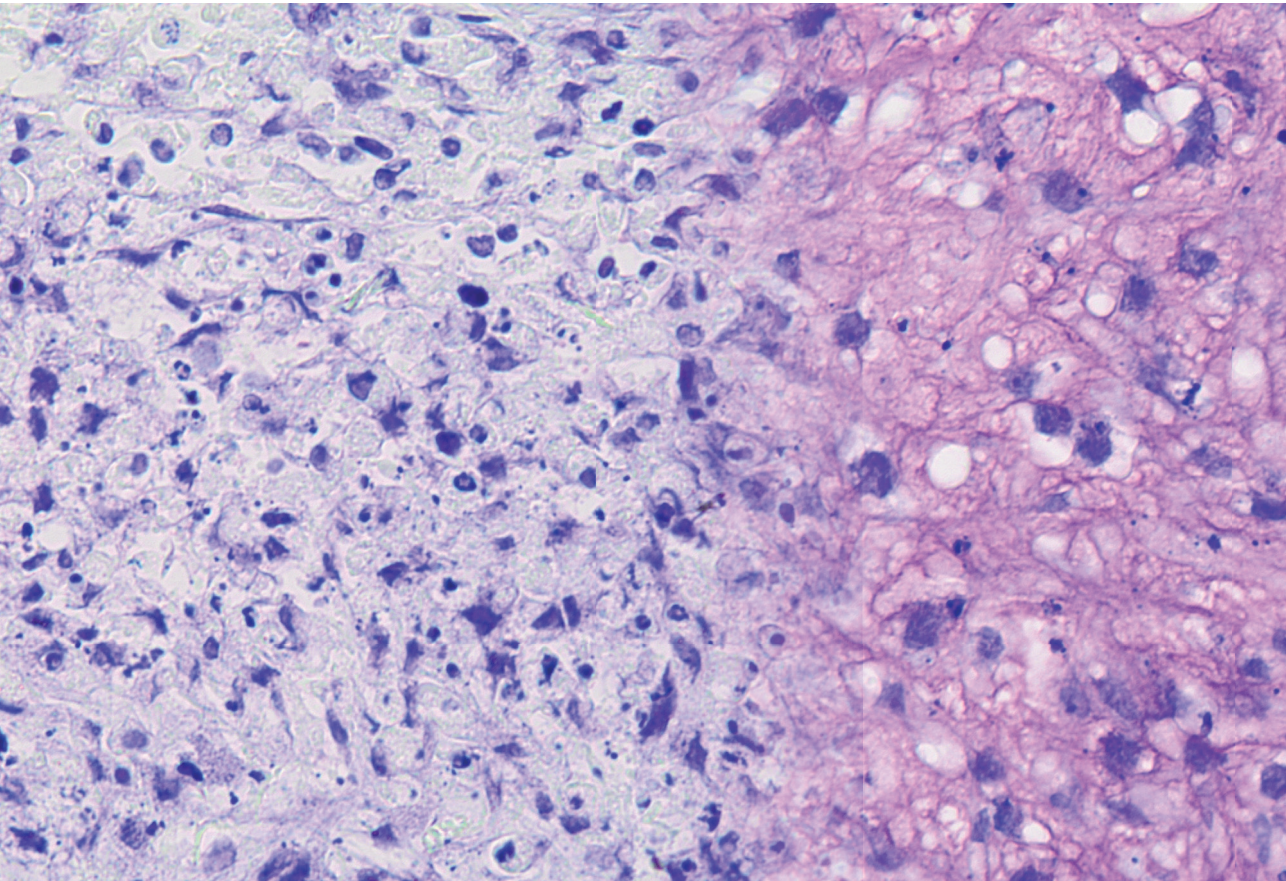
have a higher chondrogenic differentiation potential compared to cells that are FACS enriched for CD271+CD56- (Battula, Treml *et al.* 2009). The percentage of CD271+CD56+chondroprogenitor cells is higher in bone marrow cells after rasping compared to bone marrow aspiration with a Jamshidi needle, indicating that the harvesting technique has an impact on the isolation of the different mesenchymal progenitor subpopulations (Sivasubramaniyan, Ilas *et al.* 2018). It would be interesting to compare the transcriptomes from different mesenchymal progenitor cell populations, with a different chondrogenic differentiation potential, to understand which pathways are involved in functional heterogeneity of MSCs. Furthermore, it could be hypothesized that the different mesenchymal progenitor cells populations have different TWIST1 levels, a different metabolic state and respond different to TNF α . Based on the results of this thesis it could be speculated that the chondroprogenitor cell population might have high expression profiles of TWIST1, low oxygen consumption and extracellular acidification rate and an active TNF α signaling pathway.

The possibilities of single cell technology have expanded and improved rapidly over the last years and therefore they became a major research tool in different research fields. It is likely that single cell technologies will progress in the coming years and that these technologies will be essential to fully understand and tackle heterogeneity in MSC populations.

6.2.4 Concluding remarks

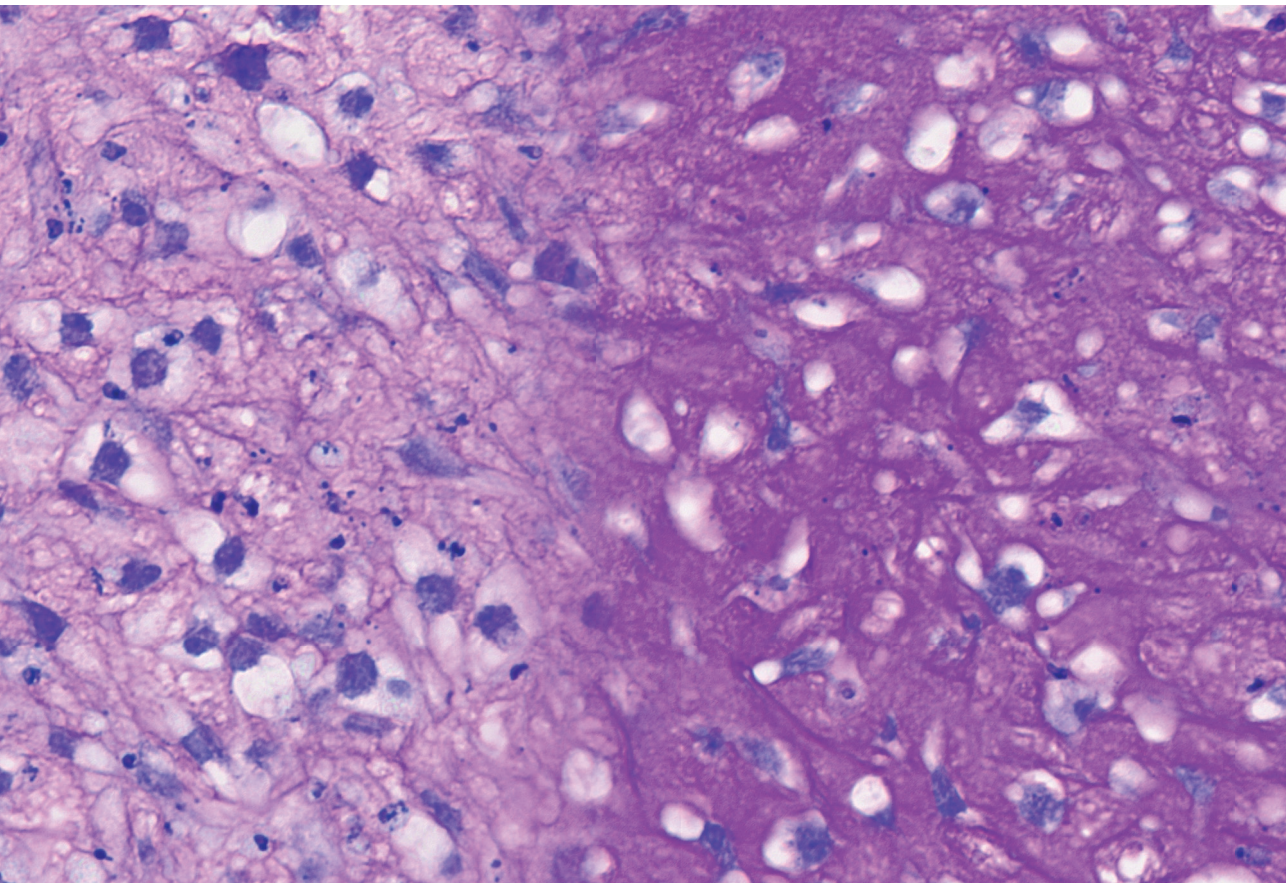
The number of publications on MSCs is growing and both fundamental and clinical studies give more and more information to solve the puzzle how MSCs can preserve their chondrogenic differentiation potential and how they can be used to regenerate articular cartilage. However, more knowledge is needed to fully understand the cartilage regeneration potential of MSCs. In addition, a collaborative effort between different research fields such as tissue engineering, cell biology, single cell transcriptomics, bioinformatics and clinical research is crucial to solve this complex puzzle.

7



Chapter 7

Summary



7.1 Summary

Focal articular cartilage defects occur often during knee trauma. Articular cartilage has a limited repair capacity, so it is necessary to repair these cartilage defects to prevent further degeneration of the knee joint. Mesenchymal progenitor cells, often referred to as mesenchymal stem or stromal cells (MSCs) are promising cells for cartilage tissue engineering strategies. However, the chondrogenic differentiation capacity of MSCs declines with *in vitro* expansion. The overall aim of this thesis was to determine how MSCs can preserve their chondrogenic differentiation potential during *in vitro* expansion.

In **chapter 2**, we determined how cellular senescence influences the differentiation capacity of MSCs. Therefore, cellular senescence was induced during monolayer and at different time points during chondrogenesis using gamma irradiation. When cellular senescence was induced during expansion or during early chondrogenic differentiation, the cells had a reduced chondrogenic differentiation capacity. When senescence was induced later during chondrogenic differentiation, no significant changes in the chondrogenic markers were observed. To investigate the effect of paracrine senescence, we treated non-senescent pellets with medium conditioned by senescent pellets. After 48 h of exposure, no significant effect on the expression of anabolic or catabolic markers was determined in recipient pellets. Finally, we showed that senescent MSCs had a reduced ability to respond to TGF β 1, one of the key factors to induce chondrogenic differentiation. In conclusion, the results in **chapter 2** indicated that the occurrence of cellular senescence in MSCs inhibited early processes of chondrogenic differentiation and thereby the capacity of MSCs to generate cartilage.

High MSC expansion was previously associated with high TWIST1 levels. To better understand how TWIST1 levels affect MSC expansion and senescence, we silenced *TWIST1* using siRNAs (**chapter 3**). Silencing of *TWIST1* increased the percentage of senescent MSCs. Surprisingly, *TWIST1*-silencing-induced senescent MSCs had a non-classical senescence-associated secretory phenotype (SASP) lacking the expression of *IL-6* and *IL-8*, in contrast to irradiation-induced senescent cells. It is known that senescence and their SASP are associated to the metabolic state of the cells. Indeed, when we determined

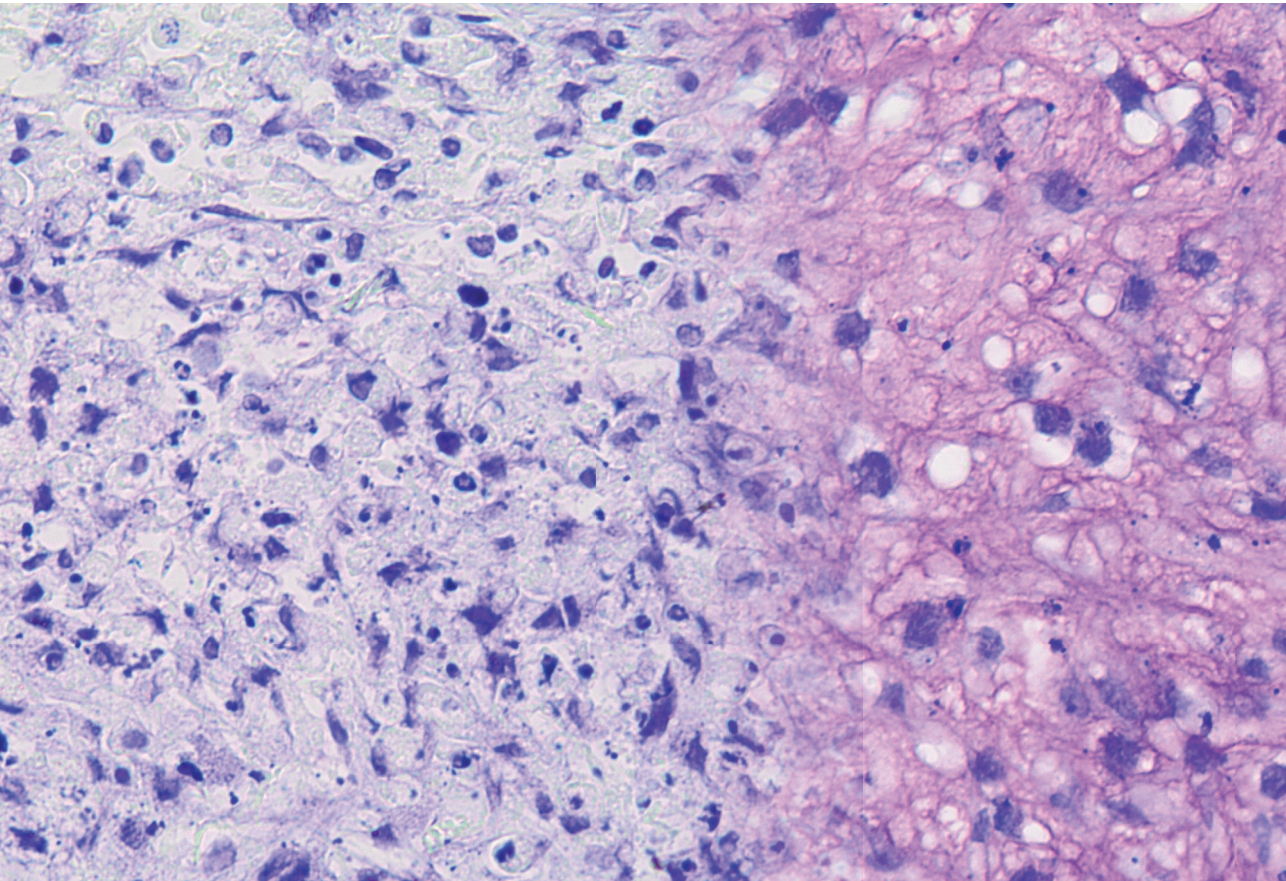
the bioenergetic state, the *TWIST1*-silencing-induced and irradiation-induced senescent cells had a different energetic state. Both types of senescent cells had an increased oxygen consumption rate compared to control non-senescent MSCs, but *TWIST1*-silencing-induced senescent MSCs had a lower extracellular acidification rate, compared to irradiation-induced senescent MSCs. In **chapter 4**, we used a fluorescent probe-based method (SmartFlare) that has the benefit that it does not require fixation of the cells, allowing to sort living cells based on *TWIST1* RNA expression. First, we validated the *TWIST1* probe and demonstrated that the probe specifically recognized *TWIST1* in MSCs. Next, *TWIST1*^{high} and *TWIST1*^{low} expressing MSCs were sorted. *TWIST1*^{high} expressing MSCs had an increased expansion rate compared to *TWIST1*^{low} expressing MSCs. In conclusion, the results of **chapter 3** and **chapter 4** demonstrated that high *TWIST1* expressing MSCs had a higher expansion rate compared to low *TWIST1* expressing MSCs. Furthermore, using methods to silence *TWIST1* we demonstrated that low *TWIST1* levels induced cellular senescence in MSCs and that these senescent cells had a specific SASP profile and metabolic state.

In **chapter 5**, we aimed to determine how different culture methods can influence the expansion and chondrogenic capacity of MSCs. It had been reported that exposure to TNF α , during *in vitro* expansion, could be potentially beneficial for tissue regeneration. Therefore, we treated the MSCs with TNF α during MSC expansion and showed that the treatment increased the chondrogenic differentiation capacity of the cells. Furthermore, treatment with TNF α during expansion reduced the inhibitory effect of the cytokine during subsequent chondrogenic differentiation. Finally, we show that TNF α pre-treatment increased the levels of SOXC proteins and active β -catenin. In conclusion, the results of **chapter 5** revealed that that TNF α pre-treatment could potentially be used as a strategy to improve MSC-based cartilage repair.

7.2 Concluding remarks

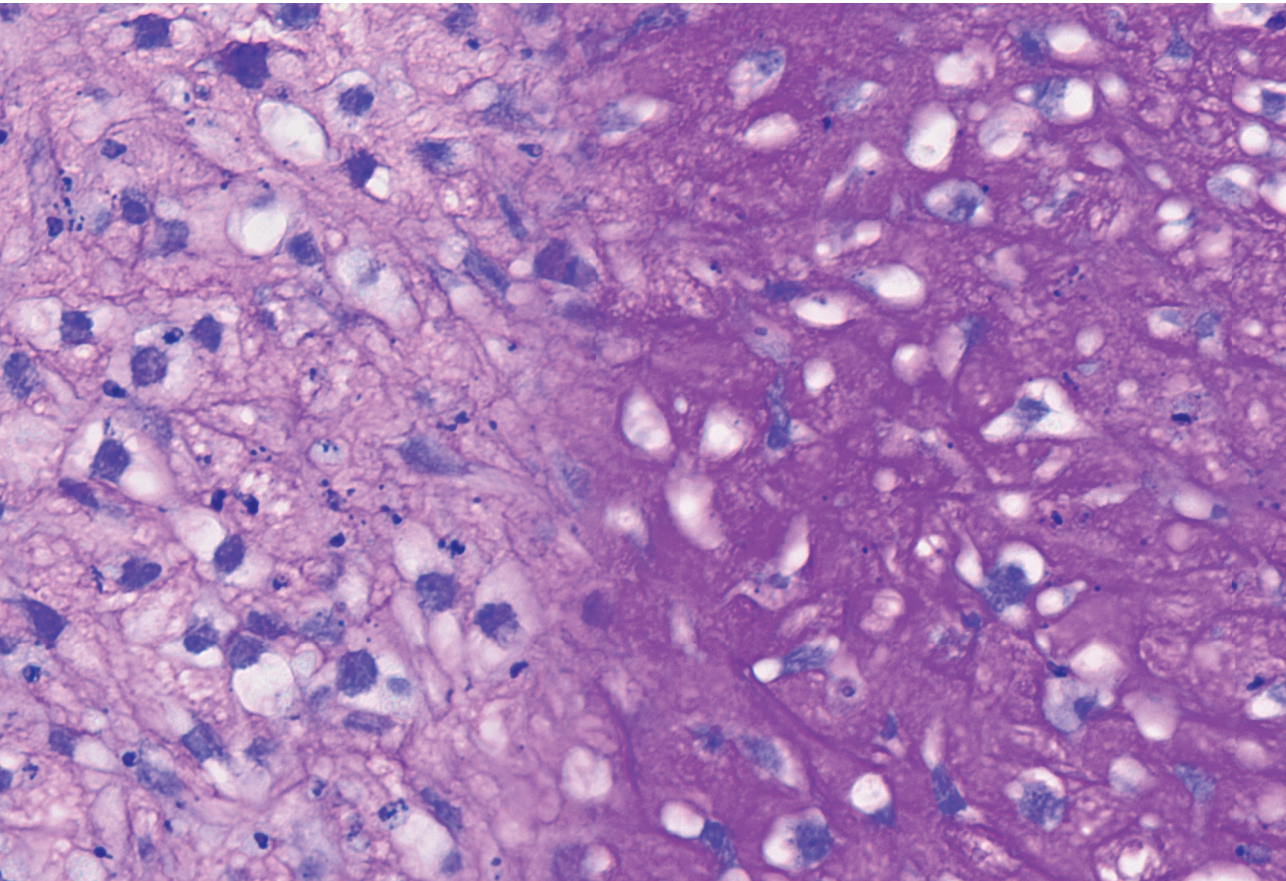
To conclude, this thesis showed that different aspects such as 1) low percentage of senescent cells, 2) high expression level of *TWIST1*, and 3) exposure to TNF α , during the expansion phase of MSCs could be beneficial for their chondrogenic differentiation potential. The knowledge of this thesis can be applied to further improve MSC-based therapies to repair cartilage defects.

8



Chapter 8

References



- Acosta, J. C., A. Banito, T. Wuestefeld, A. Georgilis, P. Janich, J. P. Morton, D. Athineos, T. W. Kang, F. Lasitschka, M. Andrulis, G. Pascual, K. J. Morris, S. Khan, H. Jin, G. Dharmalingam, A. P. Snijders, T. Carroll, D. Capper, C. Pritchard, G. J. Inman, T. Longerich, O. J. Sansom, S. A. Benitah, L. Zender and J. Gil (2013). "A complex secretory program orchestrated by the inflammasome controls paracrine senescence." *Nat Cell Biol* 15(8): 978-990.
- Akiyama, H., M. C. Chaboissier, J. F. Martin, A. Schedl and B. de Crombrughe (2002). "The transcription factor Sox9 has essential roles in successive steps of the chondrocyte differentiation pathway and is required for expression of Sox5 and Sox6." *Genes Dev* 16(21): 2813-2828.
- Alliston, T., L. Choy, P. Ducy, G. Karsenty and R. Derynck (2001). "TGF-beta-induced repression of CBFA1 by Smad3 decreases cbfa1 and osteocalcin expression and inhibits osteoblast differentiation." *Embo J* 20(9): 2254-2272.
- Alman, B. A. (2015). "The role of hedgehog signalling in skeletal health and disease." *Nat Rev Rheumatol* 11(9): 552-560.
- Almeida, M. R., A. B. Campos-Xavier, A. Medeira, I. Cordeiro, A. B. Sousa, M. Lima, G. Soares, M. Rocha, J. Saraiva, L. Ramos, S. Sousa, J. P. Marcelino, A. Correia and H. G. Santos (2009). "Clinical and molecular diagnosis of the skeletal dysplasias associated with mutations in the gene encoding Fibroblast Growth Factor Receptor 3 (FGFR3) in Portugal." *Clin Genet* 75(2): 150-156.
- Alonso, B., B. Bravo, L. Mediavilla, A. R. Gortazar, F. Forriol, J. Vaquero and M. C. Guisasola (2020). "Osteoarthritis-related biomarkers profile in chronic anterior cruciate ligament injured knee." *Knee* 27(1): 51-60.
- Alvarez-Viejo, M., Y. Menendez-Menendez and J. Otero-Hernandez (2015). "CD271 as a marker to identify mesenchymal stem cells from diverse sources before culture." *World J Stem Cells* 7(2): 470-476.
- Arman, E., R. Haffner-Krausz, M. Gorivodsky and P. Lonai (1999). "Fgfr2 is required for limb outgrowth and lung-branching morphogenesis." *Proc Natl Acad Sci U S A* 96(21): 11895-11899.
- Arnold, M. A., Y. Kim, M. P. Czubryt, D. Phan, J. McAnally, X. Qi, J. M. Shelton, J. A. Richardson, R. Bassel-Duby and E. N. Olson (2007). "MEF2C transcription factor controls chondrocyte hypertrophy and bone development." *Dev Cell* 12(3): 377-389.
- Arufe, M. C., A. De la Fuente, I. Fuentes, F. J. de Toro and F. J. Blanco

- (2010). "Chondrogenic potential of subpopulations of cells expressing mesenchymal stem cell markers derived from human synovial membranes." *J Cell Biochem* 111(4): 834-845.
- Asai, S., S. Otsuru, M. E. Candela, L. Cantley, K. Uchibe, T. J. Hofmann, K. Zhang, K. L. Wapner, L. J. Soslowsky, E. M. Horwitz and M. Enomoto-Iwamoto (2014). "Tendon progenitor cells in injured tendons have strong chondrogenic potential: the CD105-negative subpopulation induces chondrogenic degeneration." *Stem Cells* 32(12): 3266-3277.
- Bai, X., J. Xi, Y. Bi, X. Zhao, W. Bing, X. Meng, Y. Liu, Z. Zhu and G. Song (2017). "TNF-alpha promotes survival and migration of MSCs under oxidative stress via NF-kappaB pathway to attenuate intimal hyperplasia in vein grafts." *J Cell Mol Med* 21(9): 2077-2091.
- Ballock, R. T., A. Heydemann, L. M. Wakefield, K. C. Flanders, A. B. Roberts and M. B. Sporn (1993). "TGF-beta 1 prevents hypertrophy of epiphyseal chondrocytes: regulation of gene expression for cartilage matrix proteins and metalloproteases." *Dev Biol* 158(2): 414-429.
- Banfi, A., G. Bianchi, R. Notaro, L. Luzzatto, R. Cancedda and R. Quarto (2002). "Replicative aging and gene expression in long-term cultures of human bone marrow stromal cells." *Tissue Eng* 8(6): 901-910.
- Banfi, A., A. Muraglia, B. Dozin, M. Mastrogiacomo, R. Cancedda and R. Quarto (2000). "Proliferation kinetics and differentiation potential of ex vivo expanded human bone marrow stromal cells: Implications for their use in cell therapy." *Exp Hematol* 28(6): 707-715.
- Basisty, N., A. Kale, O. H. Jeon, C. Kuehnemann, T. Payne, C. Rao, A. Holtz, S. Shah, V. Sharma, L. Ferrucci, J. Campisi and B. Schilling (2020). "A proteomic atlas of senescence-associated secretomes for aging biomarker development." *PLoS Biol* 18(1): e3000599.
- Battula, V. L., S. Treml, P. M. Bareiss, F. Gieseke, H. Roelofs, P. de Zwart, I. Müller, B. Schewe, T. Skutella, W. E. Fibbe, L. Kanz and H. J. Bühring (2009). "Isolation of functionally distinct mesenchymal stem cell subsets using antibodies against CD56, CD271, and mesenchymal stem cell antigen-1." *Haematologica* 94(2): 173-184.
- Benito, M. J., D. J. Veale, O. FitzGerald, W. B. van den Berg and B. Bresnihan (2005). "Synovial tissue inflammation in early and late osteoarthritis." *Ann Rheum Dis* 64(9): 1263-1267.
- Beyne-Rauzy, O., C. Recher, N. Dastugue, C. Demur, G. Pottier, G. Laurent, L. Sabatier and V. Mansat-De Mas (2004). "Tumor necrosis factor

- alpha induces senescence and chromosomal instability in human leukemic cells." *Oncogene* 23(45): 7507-7516.
- Bhattaram, P., G. Muschler, V. Wixler and V. Lefebvre (2018). "Inflammatory Cytokines Stabilize SOXC Transcription Factors to Mediate the Transformation of Fibroblast-Like Synoviocytes in Arthritic Disease." *Arthritis Rheumatol* 70(3): 371-382.
- Bhattaram, P., A. Penzo-Méndez, K. Kato, K. Bandyopadhyay, A. Gadi, M. M. Taketo and V. Lefebvre (2014). "SOXC proteins amplify canonical WNT signaling to secure nonchondrocytic fates in skeletogenesis." *J Cell Biol* 207(5): 657-671.
- Bi, W., J. M. Deng, Z. Zhang, R. R. Behringer and B. de Crombrughe (1999). "Sox9 is required for cartilage formation." *Nat Genet* 22(1): 85-89.
- Bialek, P., B. Kern, X. Yang, M. Schrock, D. Sasic, N. Hong, H. Wu, K. Yu, D. M. Ornitz, E. N. Olson, M. J. Justice and G. Karsenty (2004). "A twist code determines the onset of osteoblast differentiation." *Dev Cell* 6(3): 423-435.
- Bianchi, G., A. Banfi, M. Mastrogiacomo, R. Notaro, L. Luzzatto, R. Cancedda and R. Quarto (2003). "Ex vivo enrichment of mesenchymal cell progenitors by fibroblast growth factor 2." *Exp Cell Res* 287(1): 98-105.
- Bittles, A. H. and N. Harper (1984). "Increased glycolysis in ageing cultured human diploid fibroblasts." *Biosci Rep* 4(9): 751-756.
- Bocker, W., D. Docheva, W. C. Prall, V. Egea, E. Pappou, O. Rossmann, C. Popov, W. Mutschler, C. Ries and M. Schieker (2008). "IKK-2 is required for TNF-alpha-induced invasion and proliferation of human mesenchymal stem cells." *J Mol Med* 86(10): 1183-1192.
- Bonab, M. M., K. Alimoghaddam, F. Talebian, S. H. Ghaffari, A. Ghavamzadeh and B. Nikbin (2006). "Aging of mesenchymal stem cell in vitro." *BMC Cell Biol* 7: 14.
- Boregowda, S. V., V. Krishnappa, C. L. Haga, L. A. Ortiz and D. G. Phinney (2016). "A Clinical Indications Prediction Scale Based on TWIST1 for Human Mesenchymal Stem Cells." *EBioMedicine* 4: 62-73.
- Brenner, D., H. Blaser and T. W. Mak (2015). "Regulation of tumour necrosis factor signalling: live or let die." *Nat Rev Immunol* 15(6): 362-374.
- Brodie, S. G., H. Kitoh, R. S. Lachman, L. M. Nolasco, P. B. Mekikian and W. R. Wilcox (1999). "Platyspondylic lethal skeletal dysplasia, San Diego type, is caused by FGFR3 mutations." *Am J Med Genet* 84(5): 476-

480.

- Brookes, P. S. (2005). "Mitochondrial H(+) leak and ROS generation: an odd couple." *Free Radic Biol Med* 38(1): 12-23.
- Buckwalter, J. A. and H. J. Mankin (1998). "Articular cartilage: tissue design and chondrocyte-matrix interactions." *Instr Course Lect* 47: 477-486.
- Buckwalter, J. A., P. J. Roughley and L. C. Rosenberg (1994). "Age-related changes in cartilage proteoglycans: quantitative electron microscopic studies." *Microsc Res Tech* 28(5): 398-408.
- Buhring, H. J., V. L. Battula, S. Treml, B. Schewe, L. Kanz and W. Vogel (2007). "Novel markers for the prospective isolation of human MSC." *Ann NY Acad Sci* 1106: 262-271.
- Cakouros, D., S. Isenmann, L. Cooper, A. Zannettino, P. Anderson, C. Glackin and S. Gronthos (2012). "Twist-1 induces Ezh2 recruitment regulating histone methylation along the Ink4A/Arf locus in mesenchymal stem cells." *Mol Cell Biol* 32(8): 1433-1441.
- Cameron, F. J. and A. H. Sinclair (1997). "Mutations in SRY and SOX9: testis-determining genes." *Hum Mutat* 9(5): 388-395.
- Caplan, A. I. (1991). "Mesenchymal stem cells." *J Orthop Res* 9(5): 641-650.
- Caplan, A. I. and J. E. Dennis (2006). "Mesenchymal stem cells as trophic mediators." *J Cell Biochem* 98(5): 1076-1084.
- Carroll, S. F., C. T. Buckley and D. J. Kelly (2021). "Measuring and Modeling Oxygen Transport and Consumption in 3D Hydrogels Containing Chondrocytes and Stem Cells of Different Tissue Origins." *Front Bioeng Biotechnol* 9: 591126.
- Cawthorn, W. P., F. Heyd, K. Hegyi and J. K. Sethi (2007). "Tumour necrosis factor-alpha inhibits adipogenesis via a beta-catenin/TCF4(TCF7L2)-dependent pathway." *Cell Death Differ* 14(7): 1361-1373.
- Chakraborty, S., E. E. Wrigg, R. B. Hinton, W. H. Merrill, D. B. Spicer and K. E. Yutzey (2010). "Twist1 promotes heart valve cell proliferation and extracellular matrix gene expression during development in vivo and is expressed in human diseased aortic valves." *Dev Biol* 347(1): 167-179.
- Chan, C. K. F., G. S. Gulati, R. Sinha, J. V. Tompkins, M. Lopez, A. C. Carter, R. C. Ransom, A. Reinisch, T. Wearda, M. Murphy, R. E. Brewer, L. S. Koepke, O. Marecic, A. Manjunath, E. Y. Seo, T. Leavitt, W. J. Lu, A. Nguyen, S. D. Conley, A. Salhotra, T. H. Ambrosi, M. R. Borrelli, T. Siebel, K. Chan, K. Schallmoser, J. Seita, D. Sahoo, H. Goodnough, J. Bishop, M. Gardner, R. Majeti, D. C. Wan, S.

- Goodman, I. L. Weissman, H. Y. Chang and M. T. Longaker (2018). "Identification of the Human Skeletal Stem Cell." *Cell* 175(1): 43-56.e21.
- Chapman, J., E. Fielder and J. F. Passos (2019). "Mitochondrial dysfunction and cell senescence: deciphering a complex relationship." *FEBS Lett* 593(13): 1566-1579.
- Chen, C. G., D. Thuillier, E. N. Chin and T. Alliston (2012). "Chondrocyte-intrinsic Smad3 represses Runx2-inducible matrix metalloproteinase 13 expression to maintain articular cartilage and prevent osteoarthritis." *Arthritis Rheum* 64(10): 3278-3289.
- Chen, J., S. Sotome, J. Wang, H. Orii, T. Uemura and K. Shinomiya (2005). "Correlation of in vivo bone formation capability and in vitro differentiation of human bone marrow stromal cells." *J Med Dent Sci* 52(1): 27-34.
- Cheng, H., L. Qiu, J. Ma, H. Zhang, M. Cheng, W. Li, X. Zhao and K. Liu (2011). "Replicative senescence of human bone marrow and umbilical cord derived mesenchymal stem cells and their differentiation to adipocytes and osteoblasts." *Mol Biol Rep* 38(8): 5161-5168.
- Cheng, S., X. Li, Z. Jia, L. Lin, J. Ying, T. Wen, Y. Zhao, Z. Guo, X. Zhao, D. Li, W. Ji, D. Wang and D. Ruan (2019). "The inflammatory cytokine TNF-alpha regulates the biological behavior of rat nucleus pulposus mesenchymal stem cells through the NF-kappaB signaling pathway in vitro." *J Cell Biochem* 120(8): 13664-13679.
- Cho, J. Y., C. Guo, M. Torello, G. P. Lunstrum, T. Iwata, C. Deng and W. A. Horton (2004). "Defective lysosomal targeting of activated fibroblast growth factor receptor 3 in achondroplasia." *Proc Natl Acad Sci U S A* 101(2): 609-614.
- Choi, C. H., L. Hao, S. P. Narayan, E. Auyeung and C. A. Mirkin (2013). "Mechanism for the endocytosis of spherical nucleic acid nanoparticle conjugates." *Proc Natl Acad Sci U S A* 110(19): 7625-7630.
- Chu, C. Q., M. Field, M. Feldmann and R. N. Maini (1991). "Localization of tumor necrosis factor alpha in synovial tissues and at the cartilage-pannus junction in patients with rheumatoid arthritis." *Arthritis Rheum* 34(9): 1125-1132.
- Chung, Y. P., Y. W. Chen, T. I. Weng, R. S. Yang and S. H. Liu (2020). "Arsenic induces human chondrocyte senescence and accelerates rat articular cartilage aging." *Arch Toxicol* 94(1): 89-101.

- Church, V., T. Nohno, C. Linker, C. Marcelle and P. Francis-West (2002). “Wnt regulation of chondrocyte differentiation.” *J Cell Sci* 115 (Pt 24): 4809-4818.
- Cleary, M. A., R. Narcisi, A. Albiero, F. Jenner, L. M. G. de Kroon, W. Koevoet, P. A. J. Brama and G. van Osch (2017). “Dynamic Regulation of TWIST1 Expression During Chondrogenic Differentiation of Human Bone Marrow-Derived Mesenchymal Stem Cells.” *Stem Cells Dev* 26(10): 751-761.
- Cleary, M. A., R. Narcisi, K. Focke, R. van der Linden, P. A. Brama and G. J. van Osch (2016). “Expression of CD105 on expanded mesenchymal stem cells does not predict their chondrogenic potential.” *Osteoarthritis Cartilage* 24(5): 868-872.
- Clevers, H. and F. M. Watt (2018). “Defining Adult Stem Cells by Function, not by Phenotype.” *Annu Rev Biochem* 87: 1015-1027.
- Coppé, J. P., P. Y. Desprez, A. Krtolica and J. Campisi (2010). “The senescence-associated secretory phenotype: the dark side of tumor suppression.” *Annu Rev Pathol* 5: 99-118.
- Coppé, J. P., C. K. Patil, F. Rodier, Y. Sun, D. P. Muñoz, J. Goldstein, P. S. Nelson, P. Y. Desprez and J. Campisi (2008). “Senescence-associated secretory phenotypes reveal cell-nonautonomous functions of oncogenic RAS and the p53 tumor suppressor.” *PLoS Biol* 6(12): 2853-2868.
- Correia-Melo, C., F. D. Marques, R. Anderson, G. Hewitt, R. Hewitt, J. Cole, B. M. Carroll, S. Miwa, J. Birch, A. Merz, M. D. Rushton, M. Charles, D. Jurk, S. W. Tait, R. Czapiewski, L. Greaves, G. Nelson, Y. M. Bohlooly, S. Rodriguez-Cuenca, A. Vidal-Puig, D. Mann, G. Saretzki, G. Quarato, D. R. Green, P. D. Adams, T. von Zglinicki, V. I. Korolchuk and J. F. Passos (2016). “Mitochondria are required for pro-ageing features of the senescent phenotype.” *Embo J* 35(7): 724-742.
- Coryell, P. R., B. O. Diekman and R. F. Loeser (2021). “Mechanisms and therapeutic implications of cellular senescence in osteoarthritis.” *Nat Rev Rheumatol* 17(1): 47-57.
- Crossley, P. H., G. Minowada, C. A. MacArthur and G. R. Martin (1996). “Roles for FGF8 in the induction, initiation, and maintenance of chick limb development.” *Cell* 84(1): 127-136.
- Czarnek, M. and J. Bereta (2017). “SmartFlares fail to reflect their target transcripts levels.” *Sci Rep* 7(1): 11682.

- Dale, T. C. (1998). "Signal transduction by the Wnt family of ligands." *Biochem J* 329 (Pt 2): 209-223.
- Daniele, S., L. Natali, C. Giacomelli, P. Campiglia, E. Novellino, C. Martini and M. L. Trincavelli (2017). "Osteogenesis Is Improved by Low Tumor Necrosis Factor Alpha Concentration through the Modulation of Gs-Coupled Receptor Signals." *Mol Cell Biol* 37(8).
- de Mera-Rodríguez, J. A., G. Álvarez-Hernán, Y. Gañán, G. Martín-Partido, J. Rodríguez-León and J. Francisco-Morcillo (2021). "Is Senescence-Associated β -Galactosidase a Reliable in vivo Marker of Cellular Senescence During Embryonic Development?" *Front Cell Dev Biol* 9: 623175.
- De Moerlooze, L., B. Spencer-Dene, J. M. Revest, M. Hajihosseini, I. Rosewell and C. Dickson (2000). "An important role for the IIIb isoform of fibroblast growth factor receptor 2 (FGFR2) in mesenchymal-epithelial signalling during mouse organogenesis." *Development* 127(3): 483-492.
- Delezoide, A. L., C. Benoist-Lasselin, L. Legeai-Mallet, M. Le Merrer, A. Munnich, M. Vekemans and J. Bonaventure (1998). "Spatio-temporal expression of FGFR 1, 2 and 3 genes during human embryo-fetal ossification." *Mech Dev* 77(1): 19-30.
- Delorme, B., J. Ringe, N. Gallay, Y. Le Vern, D. Kerboeuf, C. Jorgensen, P. Rosset, L. Sensebe, P. Layrolle, T. Haupl and P. Charbord (2008). "Specific plasma membrane protein phenotype of culture-amplified and native human bone marrow mesenchymal stem cells." *Blood* 111(5): 2631-2635.
- Demaria, M., N. Ohtani, S. A. Youssef, F. Rodier, W. Toussaint, J. R. Mitchell, R. M. Laberge, J. Vijg, H. Van Steeg, M. E. Dollé, J. H. Hoeijmakers, A. de Bruin, E. Hara and J. Campisi (2014). "An essential role for senescent cells in optimal wound healing through secretion of PDGF-AA." *Dev Cell* 31(6): 722-733.
- Deng, C., M. Bedford, C. Li, X. Xu, X. Yang, J. Dunmore and P. Leder (1997). "Fibroblast growth factor receptor-1 (FGFR-1) is essential for normal neural tube and limb development." *Dev Biol* 185(1): 42-54.
- Dennis, J. E., A. Merriam, A. Awadallah, J. U. Yoo, B. Johnstone and A. I. Caplan (1999). "A quadripotential mesenchymal progenitor cell isolated from the marrow of an adult mouse." *J Bone Miner Res* 14(5): 700-709.
- Despars, G., C. L. Carbonneau, P. Bardeau, D. L. Coutu and C. M.

- Beauséjour (2013). “Loss of the osteogenic differentiation potential during senescence is limited to bone progenitor cells and is dependent on p53.” *PLoS One* 8(8): e73206.
- Dexheimer, V., S. Frank and W. Richter (2012). “Proliferation as a requirement for in vitro chondrogenesis of human mesenchymal stem cells.” *Stem Cells Dev* 21(12): 2160-2169.
- Diekman, B. O., G. A. Sessions, J. A. Collins, A. K. Knecht, S. L. Strum, N. K. Mitin, C. S. Carlson, R. F. Loeser and N. E. Sharpless (2018). “Expression of p16(INK) (4a) is a biomarker of chondrocyte aging but does not cause osteoarthritis.” *Aging Cell* 17(4): e12771.
- Dimri, G. P., X. Lee, G. Basile, M. Acosta, G. Scott, C. Roskelley, E. E. Medrano, M. Linskens, I. Rubelj, O. Pereira-Smith and *et al.* (1995). “A biomarker that identifies senescent human cells in culture and in aging skin in vivo.” *Proc Natl Acad Sci U S A* 92(20): 9363-9367.
- Doerge, K. J., M. Sasaki, T. Kimura and Y. Yamada (1991). “Complete coding sequence and deduced primary structure of the human cartilage large aggregating proteoglycan, aggrecan. Human-specific repeats, and additional alternatively spliced forms.” *J Biol Chem* 266(2): 894-902.
- Dominici, M., K. Le Blanc, I. Mueller, I. Slaper-Cortenbach, F. Marini, D. Krause, R. Deans, A. Keating, D. Prockop and E. Horwitz (2006). “Minimal criteria for defining multipotent mesenchymal stromal cells. The International Society for Cellular Therapy position statement.” *Cytotherapy* 8(4): 315-317.
- Dörr, J. R., Y. Yu, M. Milanovic, G. Beuster, C. Zasada, J. H. Däbritz, J. Lisec, D. Lenze, A. Gerhardt, K. Schleicher, S. Kratzat, B. Purfürst, S. Walenta, W. Mueller-Klieser, M. Gräler, M. Hummel, U. Keller, A. K. Buck, B. Dörken, L. Willmitzer, M. Reimann, S. Kempa, S. Lee and C. A. Schmitt (2013). “Synthetic lethal metabolic targeting of cellular senescence in cancer therapy.” *Nature* 501(7467): 421-425.
- Ducy, P. and G. Karsenty (2000). “The family of bone morphogenetic proteins.” *Kidney Int* 57(6): 2207-2214.
- Dy, P., A. Penzo-Méndez, H. Wang, C. E. Pedraza, W. B. Macklin and V. Lefebvre (2008). “The three SoxC proteins--Sox4, Sox11 and Sox12--exhibit overlapping expression patterns and molecular properties.” *Nucleic Acids Res* 36(9): 3101-3117.
- Dy, P., W. Wang, P. Bhattaram, Q. Wang, L. Wang, R. T. Ballock and V. Lefebvre (2012). “Sox9 directs hypertrophic maturation and

- blocks osteoblast differentiation of growth plate chondrocytes." *Dev Cell* 22(3): 597-609.
- el Ghouzzi, V., M. Le Merrer, F. Perrin-Schmitt, E. Lajeunie, P. Benit, D. Renier, P. Bourgeois, A. L. Bolcato-Bellemin, A. Munnich and J. Bonaventure (1997). "Mutations of the TWIST gene in the Saethre-Chotzen syndrome." *Nat Genet* 15(1): 42-46.
- Ellman, M. B., H. S. An, P. Muddasani and H. J. Im (2008). "Biological impact of the fibroblast growth factor family on articular cartilage and intervertebral disc homeostasis." *Gene* 420(1): 82-89.
- Erices, A., P. Conget and J. J. Minguell (2000). "Mesenchymal progenitor cells in human umbilical cord blood." *Br J Haematol* 109(1): 235-242.
- Fahy, N., M. Alini and M. J. Stoddart (2018). "Mechanical stimulation of mesenchymal stem cells: Implications for cartilage tissue engineering." *J Orthop Res* 36(1): 52-63.
- Fallon, J. F., A. López, M. A. Ros, M. P. Savage, B. B. Olwin and B. K. Simandl (1994). "FGF-2: apical ectodermal ridge growth signal for chick limb development." *Science* 264(5155): 104-107.
- Fan, W., J. Li, Y. Wang, J. Pan, S. Li, L. Zhu, C. Guo and Z. Yan (2016). "CD105 promotes chondrogenesis of synovium-derived mesenchymal stem cells through Smad2 signaling." *Biochem Biophys Res Commun* 474(2): 338-344.
- Farndale, R. W., D. J. Buttle and A. J. Barrett (1986). "Improved quantitation and discrimination of sulphated glycosaminoglycans by use of dimethylmethylene blue." *Biochim Biophys Acta* 883(2): 173-177.
- Farr, J. N., D. G. Fraser, H. Wang, K. Jaehn, M. B. Ogradnik, M. M. Weivoda, M. T. Drake, T. Tchkonja, N. K. LeBrasseur, J. L. Kirkland, L. F. Bonewald, R. J. Pignolo, D. G. Monroe and S. Khosla (2016). "Identification of Senescent Cells in the Bone Microenvironment." *J Bone Miner Res* 31(11): 1920-1929.
- Farrell, E., S. K. Both, K. I. Odörfer, W. Koevoet, N. Kops, F. J. O'Brien, R. J. Baatenburg de Jong, J. A. Verhaar, V. Cuijpers, J. Jansen, R. G. Erben and G. J. van Osch (2011). "In-vivo generation of bone via endochondral ossification by in-vitro chondrogenic priming of adult human and rat mesenchymal stem cells." *BMC Musculoskelet Disord* 12: 31.
- Fernandes, J. C., J. Martel-Pelletier and J. P. Pelletier (2002). "The role of cytokines in osteoarthritis pathophysiology." *Biorheology* 39(1-2):

237-246.

- Fielding, A. B., A. K. Willox, E. Okeke and S. J. Royle (2012). "Clathrin-mediated endocytosis is inhibited during mitosis." *Proc Natl Acad Sci U S A* 109(17): 6572-6577.
- Flannery, C. R., C. E. Hughes, B. L. Schumacher, D. Tudor, M. B. Aydelotte, K. E. Kuettner and B. Caterson (1999). "Articular cartilage superficial zone protein (SZP) is homologous to megakaryocyte stimulating factor precursor and is a multifunctional proteoglycan with potential growth-promoting, cytoprotective, and lubricating properties in cartilage metabolism." *Biochem Biophys Res Commun* 254(3): 535-541.
- Fontaine, F., J. Overman and M. François (2015). "Pharmacological manipulation of transcription factor protein-protein interactions: opportunities and obstacles." *Cell Regen* 4(1): 2.
- Forsyth, C. B., A. Cole, G. Murphy, J. L. Bienias, H. J. Im and R. F. Loeser, Jr. (2005). "Increased matrix metalloproteinase-13 production with aging by human articular chondrocytes in response to catabolic stimuli." *J Gerontol A Biol Sci Med Sci* 60(9): 1118-1124.
- Furumatsu, T., T. Ozaki and H. Asahara (2009). "Smad3 activates the Sox9-dependent transcription on chromatin." *Int J Biochem Cell Biol* 41(5): 1198-1204.
- Geissler, S., M. Textor, J. Kühnisch, D. Könnig, O. Klein, A. Ode, T. Pfitzner, J. Adjaye, G. Kasper and G. N. Duda (2012). "Functional comparison of chronological and in vitro aging: differential role of the cytoskeleton and mitochondria in mesenchymal stromal cells." *PLoS One* 7(12): e52700.
- Giannoni, P., S. Scaglione, A. Daga, C. Ilengo, M. Cilli and R. Quarto (2010). "Short-time survival and engraftment of bone marrow stromal cells in an ectopic model of bone regeneration." *Tissue Eng Part A* 16(2): 489-499.
- Giljohann, D. A., D. S. Seferos, P. C. Patel, J. E. Millstone, N. L. Rosi and C. A. Mirkin (2007). "Oligonucleotide loading determines cellular uptake of DNA-modified gold nanoparticles." *Nano Lett* 7(12): 3818-3821.
- Gnani, D., S. Crippa, L. Della Volpe, V. Rossella, A. Conti, E. Lettera, S. Rivis, M. Ometti, G. Frascini, M. E. Bernardo and R. Di Micco (2019). "An early-senescence state in aged mesenchymal stromal cells contributes to hematopoietic stem and progenitor cell

- clonogenic impairment through the activation of a pro-inflammatory program." *Aging Cell* 18(3): e12933.
- Godwin, J. W., A. R. Pinto and N. A. Rosenthal (2013). "Macrophages are required for adult salamander limb regeneration." *Proc Natl Acad Sci U S A* 110(23): 9415-9420.
- Golab, K., A. Krzystyniak, P. Langa, M. Piłkuła, S. Kunovac, P. Borek, P. Trzonkowski, J. M. Millis, J. Fung and P. Witkowski (2020). "Effect of serum on SmartFlare™ RNA Probes uptake and detection in cultured human cells." *Biomed J Sci Tech Res* 28(4): 21788-21793.
- Goldring, M. B. and S. R. Goldring (2007). "Osteoarthritis." *J Cell Physiol* 213(3): 626-634.
- Goldring, M. B. and M. Otero (2011). "Inflammation in osteoarthritis." *Curr Opin Rheumatol* 23(5): 471-478.
- Goldring, M. B., M. Otero, D. A. Plumb, C. Dragomir, M. Favero, K. El Hachem, K. Hashimoto, H. I. Roach, E. Olivotto, R. M. Borzì and K. B. Marcu (2011). "Roles of inflammatory and anabolic cytokines in cartilage metabolism: signals and multiple effectors converge upon MMP-13 regulation in osteoarthritis." *Eur Cell Mater* 21: 202-220.
- Goldring, M. B., K. Tsuchimochi and K. Ijiri (2006). "The control of chondrogenesis." *J Cell Biochem* 97(1): 33-44.
- Gonzalez, O. R., I. G. Gomez, A. L. Recalde and B. H. Landing (1991). "Postnatal development of the cystic lung lesion of Down syndrome: suggestion that the cause is reduced formation of peripheral air spaces." *Pediatr Pathol* 11(4): 623-633.
- Goodnough, L. H., A. T. Chang, C. Treloar, J. Yang, P. C. Scacheri and R. P. Atit (2012). "Twist1 mediates repression of chondrogenesis by beta-catenin to promote cranial bone progenitor specification." *Development* 139(23): 4428-4438.
- Greene, M. A. and R. F. Loeser (2015). "Aging-related inflammation in osteoarthritis." *Osteoarthritis Cartilage* 23(11): 1966-1971.
- Grezzella, C., E. Fernandez-Rebollo, J. Franzen, M. S. Ventura Ferreira, F. Beier and W. Wagner (2018). "Effects of senolytic drugs on human mesenchymal stromal cells." *Stem Cell Res Ther* 9(1): 108.
- Gu, S., T. G. Boyer and M. C. Naski (2012). "Basic helix-loop-helix transcription factor Twist1 inhibits transactivator function of master chondrogenic regulator Sox9." *J Biol Chem* 287(25): 21082-21092.
- Gu, Z., X. Cao, J. Jiang, L. Li, Z. Da, H. Liu and C. Cheng (2012). "Upregulation of p16INK4A promotes cellular senescence of bone

- marrow-derived mesenchymal stem cells from systemic lupus erythematosus patients.” *Cell Signal* 24(12): 2307-2314.
- Guo, Q., Y. Liu, R. Sun, F. Yang, P. Qiao, R. Zhang, L. Song, L. E and H. Liu (2020). “Mechanical stimulation induced osteogenic differentiation of BMSCs through TWIST/E2A/p21 axis.” *Biosci Rep* 40(5).
- Guzzo, R. M., V. Andreeva, D. B. Spicer and M. H. Drissi (2011). “Persistent expression of Twist1 in chondrocytes causes growth plate abnormalities and dwarfism in mice.” *Int J Dev Biol* 55(6): 641-647.
- Halvorsen, Y. C., W. O. Wilkison and J. M. Gimble (2000). “Adipose-derived stromal cells--their utility and potential in bone formation.” *Int J Obes Relat Metab Disord* 24 Suppl 4: S41-44.
- Hardingham, T. and M. Bayliss (1990). “Proteoglycans of articular cartilage: changes in aging and in joint disease.” *Semin Arthritis Rheum* 20(3 Suppl 1): 12-33.
- Harper, J. W., G. R. Adami, N. Wei, K. Keyomarsi and S. J. Elledge (1993). “The p21 Cdk-interacting protein Cip1 is a potent inhibitor of G1 cyclin-dependent kinases.” *Cell* 75(4): 805-816.
- Harris, Q., J. Seto, K. O’Brien, P. S. Lee, C. Kondo, B. J. Heard, D. A. Hart and R. J. Krawetz (2013). “Monocyte chemotactic protein-1 inhibits chondrogenesis of synovial mesenchymal progenitor cells: an in vitro study.” *Stem Cells* 31(10): 2253-2265.
- Hartmann, C. and C. J. Tabin (2000). “Dual roles of Wnt signaling during chondrogenesis in the chicken limb.” *Development* 127(14): 3141-3159.
- Haseeb, A., R. Kc, M. Angelozzi, C. de Charleroy, D. Rux, R. J. Tower, L. Yao, R. Pellegrino da Silva, M. Pacifici, L. Qin and V. Lefebvre (2021). “SOX9 keeps growth plates and articular cartilage healthy by inhibiting chondrocyte dedifferentiation/osteoblastic redifferentiation.” *Proc Natl Acad Sci U S A* 118(8).
- Hasei, J., T. Teramura, T. Takehara, Y. Onodera, T. Horii, M. Olmer, I. Hatada, K. Fukuda, T. Ozaki, M. K. Lotz and H. Asahara (2017). “TWIST1 induces MMP3 expression through up-regulating DNA hydroxymethylation and promotes catabolic responses in human chondrocytes.” *Sci Rep* 7: 42990.
- Hayflick, L. (1965). “The limited in vitro lifetime of human diploid cell strains.” *Exp Cell Res* 37: 614-636.
- Hayflick, L. and P. S. Moorhead (1961). “The serial cultivation of human

- diploid cell strains." *Exp Cell Res* 25: 585-621.
- Haynesworth, S. E., J. Goshima, V. M. Goldberg and A. I. Caplan (1992). "Characterization of cells with osteogenic potential from human marrow." *Bone* 13(1): 81-88.
- Hellingman, C. A., E. N. Davidson, W. Koevoet, E. L. Vitters, W. B. van den Berg, G. J. van Osch and P. M. van der Kraan (2011). "Smad signaling determines chondrogenic differentiation of bone-marrow-derived mesenchymal stem cells: inhibition of Smad1/5/8P prevents terminal differentiation and calcification." *Tissue Eng Part A* 17(7-8): 1157-1167.
- Hellingman, C. A., W. Koevoet, N. Kops, E. Farrell, H. Jahr, W. Liu, R. J. Baatenburg de Jong, D. A. Frenz and G. J. van Osch (2010). "Fibroblast growth factor receptors in in vitro and in vivo chondrogenesis: relating tissue engineering using adult mesenchymal stem cells to embryonic development." *Tissue Eng Part A* 16(2): 545-556.
- Henley, M. J. and A. N. Koehler (2021). "Advances in targeting 'undruggable' transcription factors with small molecules." *Nat Rev Drug Discov* 20(9): 669-688.
- Herlofsen, S. R., T. Høiby, D. Cacchiarelli, X. Zhang, T. S. Mikkelsen and J. E. Brinchmann (2014). "Brief report: importance of SOX8 for in vitro chondrogenic differentiation of human mesenchymal stromal cells." *Stem Cells* 32(6): 1629-1635.
- Hernandez-Segura, A., J. Nehme and M. Demaria (2018). "Hallmarks of Cellular Senescence." *Trends Cell Biol* 28(6): 436-453.
- Hernandez-Segura, A., R. Rubingh and M. Demaria (2019). "Identification of stable senescence-associated reference genes." *Aging Cell* 18(2): e12911.
- Heuertz, S., M. Le Merrer, B. Zabel, M. Wright, L. Legeai-Mallet, V. Cormier-Daire, L. Gibbs and J. Bonaventure (2006). "Novel FGFR3 mutations creating cysteine residues in the extracellular domain of the receptor cause achondroplasia or severe forms of hypochondroplasia." *Eur J Hum Genet* 14(12): 1240-1247.
- Hochane, M., V. Trichet, C. Pecqueur, P. Avril, L. Oliver, J. Denis, R. Brion, J. Amiaud, A. Pineau, P. Naveilhan, D. Heymann, F. M. Vallette and C. Olivier (2017). "Low-Dose Pesticide Mixture Induces Senescence in Normal Mesenchymal Stem Cells (MSC) and Promotes Tumorigenic Phenotype in Premalignant MSC." *Stem*

- Cells* 35(3): 800-811.
- Howard, T. D., W. A. Paznekas, E. D. Green, L. C. Chiang, N. Ma, R. I. Ortiz de Luna, C. Garcia Delgado, M. Gonzalez-Ramos, A. D. Kline and E. W. Jabs (1997). "Mutations in TWIST, a basic helix-loop-helix transcription factor, in Saethre-Chotzen syndrome." *Nat Genet* 15(1): 36-41.
- Huang, W., Z. Chen, X. Shang, D. Tian, D. Wang, K. Wu, D. Fan and L. Xia (2015). "Sox12, a direct target of FoxQ1, promotes hepatocellular carcinoma metastasis through up-regulating Twist1 and FGFBP1." *Hepatology* 61(6): 1920-1933.
- Hunter, D. J., L. March and M. Chew (2020). "Osteoarthritis in 2020 and beyond: a Lancet Commission." *Lancet* 396(10264): 1711-1712.
- Hunter, W. (1995). "Of the structure and disease of articulating cartilages. 1743." *Clin Orthop Relat Res*(317): 3-6.
- Ikegami, D., H. Akiyama, A. Suzuki, T. Nakamura, T. Nakano, H. Yoshikawa and N. Tsumaki (2011). "Sox9 sustains chondrocyte survival and hypertrophy in part through Pik3ca-Akt pathways." *Development* 138(8): 1507-1519.
- Im, G. I., N. H. Jung and S. K. Tae (2006). "Chondrogenic differentiation of mesenchymal stem cells isolated from patients in late adulthood: the optimal conditions of growth factors." *Tissue Eng* 12(3): 527-536.
- Imamura, M., F. Ezquerro, F. Marcon Alfieri, L. Vilas Boas, T. R. Tozetto-Mendoza, J. Chen, L. Ozcakar, L. Arendt-Nielsen and L. Rizzo Battistella (2015). "Serum levels of proinflammatory cytokines in painful knee osteoarthritis and sensitization." *Int J Inflamm* 2015: 329792.
- Inada, M., T. Yasui, S. Nomura, S. Miyake, K. Deguchi, M. Himeno, M. Sato, H. Yamagiwa, T. Kimura, N. Yasui, T. Ochi, N. Endo, Y. Kitamura, T. Kishimoto and T. Komori (1999). "Maturational disturbance of chondrocytes in Cbfa1-deficient mice." *Dev Dyn* 214(4): 279-290.
- Isenmann, S., A. Arthur, A. C. Zannettino, J. L. Turner, S. Shi, C. A. Glackin and S. Gronthos (2009). "TWIST family of basic helix-loop-helix transcription factors mediate human mesenchymal stem cell growth and commitment." *Stem Cells* 27(10): 2457-2468.
- Jablonski, C. L., C. Leonard, P. Salo and R. J. Krawetz (2019). "CCL2 But Not CCR2 Is Required for Spontaneous Articular Cartilage Regeneration Post-Injury." *J Orthop Res* 37(12): 2561-2574.

- James, E. L., R. D. Michalek, G. N. Pitiyage, A. M. de Castro, K. S. Vignola, J. Jones, R. P. Mohney, E. D. Karoly, S. S. Prime and E. K. Parkinson (2015). "Senescent human fibroblasts show increased glycolysis and redox homeostasis with extracellular metabolomes that overlap with those of irreparable DNA damage, aging, and disease." *J Proteome Res* 14(4): 1854-1871.
- Jeon, O. H., N. David, J. Campisi and J. H. Elisseeff (2018). "Senescent cells and osteoarthritis: a painful connection." *J Clin Invest* 128(4): 1229-1237.
- Jeon, O. H., C. Kim, R. M. Laberge, M. Demaria, S. Rathod, A. P. Vasserot, J. W. Chung, D. H. Kim, Y. Poon, N. David, D. J. Baker, J. M. van Deursen, J. Campisi and J. H. Elisseeff (2017). "Local clearance of senescent cells attenuates the development of post-traumatic osteoarthritis and creates a pro-regenerative environment." *Nat Med* 23(6): 775-781.
- Ji, Q., Y. Zheng, G. Zhang, Y. Hu, X. Fan, Y. Hou, L. Wen, L. Li, Y. Xu, Y. Wang and F. Tang (2019). "Single-cell RNA-seq analysis reveals the progression of human osteoarthritis." *Ann Rheum Dis* 78(1): 100-110.
- Jiang, T., W. Liu, X. Lv, H. Sun, L. Zhang, Y. Liu, W. J. Zhang, Y. Cao and G. Zhou (2010). "Potent in vitro chondrogenesis of CD105 enriched human adipose-derived stem cells." *Biomaterials* 31(13): 3564-3571.
- Johnstone, B., T. M. Hering, A. I. Caplan, V. M. Goldberg and J. U. Yoo (1998). "In vitro chondrogenesis of bone marrow-derived mesenchymal progenitor cells." *Exp Cell Res* 238(1): 265-272.
- Josephson, A. M., V. Bradaschia-Correa, S. Lee, K. Leclerc, K. S. Patel, E. Muinos Lopez, H. P. Litwa, S. S. Neibart, M. Kadiyala, M. Z. Wong, M. M. Mizrahi, N. L. Yim, A. J. Ramme, K. A. Egol and P. Leucht (2019). "Age-related inflammation triggers skeletal stem/progenitor cell dysfunction." *Proc Natl Acad Sci U S A* 116(14): 6995-7004.
- Jung, Y. K., G. W. Kim, H. R. Park, E. J. Lee, J. Y. Choi, F. Beier and S. W. Han (2013). "Role of interleukin-10 in endochondral bone formation in mice: anabolic effect via the bone morphogenetic protein/Smad pathway." *Arthritis Rheum* 65(12): 3153-3164.
- Jung, Y. S., Y. Qian and X. Chen (2010). "Examination of the expanding pathways for the regulation of p21 expression and activity." *Cell Signal* 22(7): 1003-1012.

- Kamachi, Y. and H. Kondoh (2013). "Sox proteins: regulators of cell fate specification and differentiation." *Development* 140(20): 4129-4144.
- Kandhaya-Pillai, R., F. Miro-Mur, J. Alijotas-Reig, T. Tchkonja, J. L. Kirkland and S. Schwartz (2017). "TNF α -senescence initiates a STAT-dependent positive feedback loop, leading to a sustained interferon signature, DNA damage, and cytokine secretion." *Aging (Albany NY)* 9(11): 2411-2435.
- Kang, J. S., T. Alliston, R. Delston and R. Derynck (2005). "Repression of Runx2 function by TGF- β through recruitment of class II histone deacetylases by Smad3." *Embo J* 24(14): 2543-2555.
- Kapoor, M., J. Martel-Pelletier, D. Lajeunesse, J. P. Pelletier and H. Fahmi (2011). "Role of proinflammatory cytokines in the pathophysiology of osteoarthritis." *Nat Rev Rheumatol* 7(1): 33-42.
- Kastrinaki, M.-C., I. Andreakou, P. Charbord and H. A. Papadaki (2008). "Isolation of human bone marrow mesenchymal stem cells using different membrane markers: comparison of colony/cloning efficiency, differentiation potential, and molecular profile." *Tissue Eng Part C Methods* 14(4): 333-339.
- Kato, K., P. Bhattaram, A. Penzo-Mendez, A. Gadi and V. Lefebvre (2015). "SOXC Transcription Factors Induce Cartilage Growth Plate Formation in Mouse Embryos by Promoting Noncanonical WNT Signaling." *J Bone Miner Res* 30(9): 1560-1571.
- Kengaku, M., J. Capdevila, C. Rodriguez-Esteban, J. De La Peña, R. L. Johnson, J. C. Izpisua Belmonte and C. J. Tabin (1998). "Distinct WNT pathways regulating AER formation and dorsoventral polarity in the chick limb bud." *Science* 280(5367): 1274-1277.
- Kim, M., C. Kim, Y. S. Choi, M. Kim, C. Park and Y. Suh (2012). "Age-related alterations in mesenchymal stem cells related to shift in differentiation from osteogenic to adipogenic potential: implication to age-associated bone diseases and defects." *Mech Ageing Dev* 133(5): 215-225.
- Kinnaird, T., E. Stabile, M. S. Burnett, C. W. Lee, S. Barr, S. Fuchs and S. E. Epstein (2004). "Marrow-derived stromal cells express genes encoding a broad spectrum of arteriogenic cytokines and promote in vitro and in vivo arteriogenesis through paracrine mechanisms." *Circ Res* 94(5): 678-685.
- Kirkland, J. L. and T. Tchkonja (2020). "Senolytic drugs: from discovery to translation." *J Intern Med* 288(5): 518-536.

- Knuth, C. A., C. H. Kiernan, V. Palomares Cabeza, J. Lehmann, J. Witte-Bouma, D. Ten Berge, P. A. Brama, E. B. Wolvius, E. M. Strabbing, M. J. Koudstaal, R. Narcisi and E. Farrell (2018). "Isolating Pediatric Mesenchymal Stem Cells with Enhanced Expansion and Differentiation Capabilities." *Tissue Eng Part C Methods* 24(6): 313-321.
- Komori, T., H. Yagi, S. Nomura, A. Yamaguchi, K. Sasaki, K. Deguchi, Y. Shimizu, R. T. Bronson, Y. H. Gao, M. Inada, M. Sato, R. Okamoto, Y. Kitamura, S. Yoshiki and T. Kishimoto (1997). "Targeted disruption of *Cbfa1* results in a complete lack of bone formation owing to maturational arrest of osteoblasts." *Cell* 89(5): 755-764.
- Kronig, M., M. Walter, V. Drendel, M. Werner, C. A. Jilg, A. S. Richter, R. Backofen, D. McGarry, M. Follo, W. Schultze-Seemann and R. Schule (2015). "Cell type specific gene expression analysis of prostate needle biopsies resolves tumor tissue heterogeneity." *Oncotarget* 6(2): 1302-1314.
- Kumari, R. and P. Jat (2021). "Mechanisms of Cellular Senescence: Cell Cycle Arrest and Senescence Associated Secretory Phenotype." *Front Cell Dev Biol* 9: 645593.
- Kwon, H., W. E. Brown, C. A. Lee, D. Wang, N. Paschos, J. C. Hu and K. A. Athanasiou (2019). "Surgical and tissue engineering strategies for articular cartilage and meniscus repair." *Nat Rev Rheumatol* 15(9): 550-570.
- Lahm, H., S. Doppler, M. Dressen, A. Werner, K. Adamczyk, D. Schrambke, T. Brade, K. L. Laugwitz, M. A. Deutsch, M. Schiemann, R. Lange, A. Moretti and M. Krane (2015). "Live fluorescent RNA-based detection of pluripotency gene expression in embryonic and induced pluripotent stem cells of different species." *Stem Cells* 33(2): 392-402.
- Leboy, P., G. Grasso-Knight, M. D'Angelo, S. W. Volk, J. V. Lian, H. Drissi, G. S. Stein and S. L. Adams (2001). "Smad-Runx interactions during chondrocyte maturation." *J Bone Joint Surg Am* 83-A Suppl 1(Pt 1): S15-22.
- Lee, B. Y., J. A. Han, J. S. Im, A. Morrone, K. Johung, E. C. Goodwin, W. J. Kleijer, D. DiMaio and E. S. Hwang (2006). "Senescence-associated beta-galactosidase is lysosomal beta-galactosidase." *Aging Cell* 5(2): 187-195.
- Lee, H. C., P. H. Yin, C. W. Chi and Y. H. Wei (2002). "Increase in mitochondrial mass in human fibroblasts under oxidative stress and

- during replicative cell senescence.” *J Biomed Sci* 9(6 Pt 1): 517-526.
- Lee, J. S. and G. I. Im (2011). “SOX trio decrease in the articular cartilage with the advancement of osteoarthritis.” *Connect Tissue Res* 52(6): 496-502.
- Lee, M. P. and K. E. Yutzey (2011). “Twist1 directly regulates genes that promote cell proliferation and migration in developing heart valves.” *PLoS One* 6(12): e29758.
- Lee, W. Y. and B. Wang (2017). “Cartilage repair by mesenchymal stem cells: Clinical trial update and perspectives.” *J Orthop Translat* 9: 76-88.
- Lefebvre, V. and P. Bhattaram (2016). “SOXC Genes and the Control of Skeletogenesis.” *Curr Osteoporos Rep* 14(1): 32-38.
- Lefebvre, V., P. Li and B. de Crombrughe (1998). “A new long form of Sox5 (L-Sox5), Sox6 and Sox9 are coexpressed in chondrogenesis and cooperatively activate the type II collagen gene.” *Embo J* 17(19): 5718-5733.
- Lehmann, J., R. Narcisi, N. Franceschini, D. Chatzivasileiou, C. G. Boer, W. Koevoet, D. Putavet, D. Drabek, R. van Haperen, P. L. J. de Keizer, G. van Osch and D. Ten Berge (2022). “WNT/beta-catenin signalling interrupts a senescence-induction cascade in human mesenchymal stem cells that restricts their expansion.” *Cell Mol Life Sci* 79(2): 82.
- Lennon, D. P. and A. I. Caplan (2006). “Isolation of human marrow-derived mesenchymal stem cells.” *Exp Hematol* 34(11): 1604-1605.
- Leroy, J. G., L. Nuytinck, J. Lambert, J. M. Naeyaert and G. R. Mortier (2007). “Acanthosis nigricans in a child with mild osteochondrodysplasia and K650Q mutation in the FGFR3 gene.” *Am J Med Genet A* 143A(24): 3144-3149.
- Li, B., U. Menzel, C. Loebel, H. Schmal, M. Alini and M. J. Stoddart (2016). “Monitoring live human mesenchymal stromal cell differentiation and subsequent selection using fluorescent RNA-based probes.” *Sci Rep* 6: 26014.
- Li, C., Y. Chai, L. Wang, B. Gao, H. Chen, P. Gao, F. Q. Zhou, X. Luo, J. L. Crane, B. Yu, X. Cao and M. Wan (2017). “Programmed cell senescence in skeleton during late puberty.” *Nat Commun* 8(1): 1312.
- Li, P., Y. Gan, Y. Xu, L. Song, L. Wang, B. Ouyang, C. Zhang and Q. Zhou (2017). “The inflammatory cytokine TNF- α promotes the premature senescence of rat nucleus pulposus cells via the PI3K/Akt signaling pathway.” *Sci Rep* 7: 42938.
- Li, Y., Q. Wu, Y. Wang, L. Li, H. Bu and J. Bao (2017). “Senescence of

- mesenchymal stem cells (Review).” *Int J Mol Med* 39(4): 775-782.
- Li, Y., X. Xu, L. Wang, G. Liu, Y. Li, X. Wu, Y. Jing, H. Li and G. Wang (2015). “Senescent mesenchymal stem cells promote colorectal cancer cells growth via galectin-3 expression.” *Cell Biosci* 5: 21.
- Li, Z., C. Liu, Z. Xie, P. Song, R. C. Zhao, L. Guo, Z. Liu and Y. Wu (2011). “Epigenetic dysregulation in mesenchymal stem cell aging and spontaneous differentiation.” *PLoS One* 6(6): e20526.
- Liu, C. F. and V. Lefebvre (2015). “The transcription factors SOX9 and SOX5/SOX6 cooperate genome-wide through super-enhancers to drive chondrogenesis.” *Nucleic Acids Res* 43(17): 8183-8203.
- Liu, C. F., W. E. Samsa, G. Zhou and V. Lefebvre (2017). “Transcriptional control of chondrocyte specification and differentiation.” *Semin Cell Dev Biol* 62: 34-49.
- Liu, J., Y. Ding, Z. Liu and X. Liang (2020). “Senescence in Mesenchymal Stem Cells: Functional Alterations, Molecular Mechanisms, and Rejuvenation Strategies.” *Front Cell Dev Biol* 8: 258.
- Loeser, R. F., J. A. Collins and B. O. Diekman (2016). “Ageing and the pathogenesis of osteoarthritis.” *Nat Rev Rheumatol* 12(7): 412-420.
- Lu, S., H. Wang, R. Ren, X. Shi, Y. Zhang and W. Ma (2018). “Reduced expression of Twist 1 is protective against insulin resistance of adipocytes and involves mitochondrial dysfunction.” *Sci Rep* 8(1): 12590.
- Lu, Z.-Y., W.-C. Chen, Y.-H. Li, L. Li, H. Zhang, Y. Pang, Z.-F. Xiao, H.-W. Xiao and Y. Xiao (2016). “TNF- α enhances vascular cell adhesion molecule-1 expression in human bone marrow mesenchymal stem cells via the NF- κ B, ERK and JNK signaling pathways.” *Mol Med Rep* 14(1): 643-648.
- Lunyak, V. V., A. Amaro-Ortiz and M. Gaur (2017). “Mesenchymal Stem Cells Secretory Responses: Senescence Messaging Secretome and Immunomodulation Perspective.” *Front Genet* 8: 220.
- Lv, F. J., R. S. Tuan, K. M. Cheung and V. Y. Leung (2014). “Concise review: the surface markers and identity of human mesenchymal stem cells.” *Stem Cells* 32(6): 1408-1419.
- Ma, B., E. B. Landman, R. L. Miclea, J. M. Wit, E. C. Robanus-Maandag, J. N. Post and M. Karperien (2013). “WNT signaling and cartilage: of mice and men.” *Calcif Tissue Int* 92(5): 399-411.
- Mackie, E. J., Y. A. Ahmed, L. Tatarczuch, K. S. Chen and M. Mirams (2008). “Endochondral ossification: how cartilage is converted into bone in

- the developing skeleton." *Int J Biochem Cell Biol* 40(1): 46-62.
- Maes, C., G. Carmeliet and E. Schipani (2012). "Hypoxia-driven pathways in bone development, regeneration and disease." *Nat Rev Rheumatol* 8(6): 358-366.
- Majumdar, M. K., V. Banks, D. P. Peluso and E. A. Morris (2000). "Isolation, characterization, and chondrogenic potential of human bone marrow-derived multipotential stromal cells." *J Cell Physiol* 185(1): 98-106.
- Makris, E. A., A. H. Gomoll, K. N. Malizos, J. C. Hu and K. A. Athanasiou (2015). "Repair and tissue engineering techniques for articular cartilage." *Nat Rev Rheumatol* 11(1): 21-34.
- Mankin, H. J. (1982). "The response of articular cartilage to mechanical injury." *J Bone Joint Surg Am* 64(3): 460-466.
- Markway, B. D., H. Cho, D. E. Anderson, P. Holden, V. Ravi, C. B. Little and B. Johnstone (2016). "Reoxygenation enhances tumour necrosis factor alpha-induced degradation of the extracellular matrix produced by chondrogenic cells." *Eur Cell Mater* 31: 425-439.
- Markway, B. D., G. K. Tan, G. Brooke, J. E. Hudson, J. J. Cooper-White and M. R. Doran (2010). "Enhanced chondrogenic differentiation of human bone marrow-derived mesenchymal stem cells in low oxygen environment micropellet cultures." *Cell Transplant* 19(1): 29-42.
- Maroudas, A., P. Bullough, S. A. Swanson and M. A. Freeman (1968). "The permeability of articular cartilage." *J Bone Joint Surg Br* 50(1): 166-177.
- Martin, J. A. and J. A. Buckwalter (2003). "The role of chondrocyte senescence in the pathogenesis of osteoarthritis and in limiting cartilage repair." *J Bone Joint Surg Am* 85-A Suppl 2: 106-110.
- Matsuo, N., H. Shiraha, T. Fujikawa, N. Takaoka, N. Ueda, S. Tanaka, S. Nishina, Y. Nakanishi, M. Uemura, A. Takaki, S. Nakamura, Y. Kobayashi, K. Nouse, T. Yagi and K. Yamamoto (2009). "Twist expression promotes migration and invasion in hepatocellular carcinoma." *BMC Cancer* 9: 240.
- McClellan, S., J. Slamecka, P. Howze, L. Thompson, M. Finan, R. Rocconi and L. Owen (2015). "mRNA detection in living cells: A next generation cancer stem cell identification technique." *Methods* 82: 47-54.
- McQueeney, K., R. Soufer and C. N. Dealy (2002). "Beta-catenin-dependent

- Wnt signaling in apical ectodermal ridge induction and FGF8 expression in normal and limbless mutant chick limbs." *Dev Growth Differ* 44(4): 315-325.
- Merrill, A. E., A. Sarukhanov, P. Krejci, B. Itoni, N. Camacho, K. D. Estrada, K. M. Lyons, H. Deixler, H. Robinson, D. Chitayat, C. J. Curry, R. S. Lachman, W. R. Wilcox and D. Krakow (2012). "Bent bone dysplasia-FGFR2 type, a distinct skeletal disorder, has deficient canonical FGF signaling." *Am J Hum Genet* 90(3): 550-557.
- Milanese, C., C. R. Bombardieri, S. Sepe, S. Barnhoorn, C. Payán-Goméz, D. Caruso, M. Audano, S. Pedretti, W. P. Vermeij, R. M. C. Brandt, A. Gyenis, M. M. Wamelink, A. S. de Wit, R. C. Janssens, R. Leen, A. B. P. van Kuilenburg, N. Mitro, J. H. J. Hoeijmakers and P. G. Mastroberardino (2019). "DNA damage and transcription stress cause ATP-mediated redesign of metabolism and potentiation of anti-oxidant buffering." *Nat Commun* 10(1): 4887.
- Miller, J. R. (2002). "The Wnts." *Genome Biol* 3(1): REVIEWS3001.
- Min, H., D. M. Danilenko, S. A. Scully, B. Bolon, B. D. Ring, J. E. Tarpley, M. DeRose and W. S. Simonet (1998). "Fgf-10 is required for both limb and lung development and exhibits striking functional similarity to *Drosophila* branchless." *Genes Dev* 12(20): 3156-3161.
- Miotla Zarebska, J., A. Chanalaris, C. Driscoll, A. Burleigh, R. E. Miller, A. M. Malfait, B. Stott and T. L. Vincent (2017). "CCL2 and CCR2 regulate pain-related behaviour and early gene expression in post-traumatic murine osteoarthritis but contribute little to chondropathy." *Osteoarthritis Cartilage* 25(3): 406-412.
- Murphy, G. and M. H. Lee (2005). "What are the roles of metalloproteinases in cartilage and bone damage?" *Ann Rheum Dis* 64 Suppl 4(Suppl 4): iv44-47.
- Myllyharju, J. and K. I. Kivirikko (2004). "Collagens, modifying enzymes and their mutations in humans, flies and worms." *Trends Genet* 20(1): 33-43.
- Narcisi, R., O. H. Arikian, J. Lehmann, D. Ten Berge and G. J. van Osch (2016). "Differential Effects of Small Molecule WNT Agonists on the Multilineage Differentiation Capacity of Human Mesenchymal Stem Cells." *Tissue Eng Part A* 22(21-22): 1264-1273.
- Narcisi, R., M. A. Cleary, P. A. Brama, M. J. Hoogduijn, N. Tüysüz, D. ten Berge and G. J. van Osch (2015). "Long-term expansion, enhanced chondrogenic potential, and suppression of endochondral

- ossification of adult human MSCs via WNT signaling modulation.” *Stem Cell Reports* 4(3): 459-472.
- Narcisi, R., L. Signorile, J. A. Verhaar, P. Giannoni and G. J. van Osch (2012). “TGF β inhibition during expansion phase increases the chondrogenic re-differentiation capacity of human articular chondrocytes.” *Osteoarthritis Cartilage* 20(10): 1152-1160.
- Naski, M. C., Q. Wang, J. Xu and D. M. Ornitz (1996). “Graded activation of fibroblast growth factor receptor 3 by mutations causing achondroplasia and thanatophoric dysplasia.” *Nat Genet* 13(2): 233-237.
- Nelson, G., O. Kucheryavenko, J. Wordsworth and T. von Zglinicki (2018). “The senescent bystander effect is caused by ROS-activated NF- κ B signalling.” *Mech Ageing Dev* 170: 30-36.
- Niswander, L., C. Tickle, A. Vogel, I. Booth and G. R. Martin (1993). “FGF-4 replaces the apical ectodermal ridge and directs outgrowth and patterning of the limb.” *Cell* 75(3): 579-587.
- O’Brian, C. A. and F. Chu (2005). “Post-translational disulfide modifications in cell signaling--role of inter-protein, intra-protein, S-glutathionyl, and S-cysteaminy disulfide modifications in signal transmission.” *Free Radic Res* 39(5): 471-480.
- Ohba, S., X. He, H. Hojo and A. P. McMahon (2015). “Distinct Transcriptional Programs Underlie Sox9 Regulation of the Mammalian Chondrocyte.” *Cell Rep* 12(2): 229-243.
- Ohuchi, H., T. Nakagawa, A. Yamamoto, A. Araga, T. Ohata, Y. Ishimaru, H. Yoshioka, T. Kuwana, T. Nohno, M. Yamasaki, N. Itoh and S. Noji (1997). “The mesenchymal factor, FGF10, initiates and maintains the outgrowth of the chick limb bud through interaction with FGF8, an apical ectodermal factor.” *Development* 124(11): 2235-2244.
- Ornitz, D. M. and N. Itoh (2015). “The Fibroblast Growth Factor signaling pathway.” *Wiley Interdiscip Rev Dev Biol* 4(3): 215-266.
- Ornitz, D. M. and P. J. Marie (2002). “FGF signaling pathways in endochondral and intramembranous bone development and human genetic disease.” *Genes Dev* 16(12): 1446-1465.
- Orr-Urtreger, A., D. Givol, A. Yayon, Y. Yarden and P. Lonai (1991). “Developmental expression of two murine fibroblast growth factor receptors, flg and bek.” *Development* 113(4): 1419-1434.
- Pacifici, M., E. Koyama, Y. Shibukawa, C. Wu, Y. Tamamura, M. Enomoto-Iwamoto and M. Iwamoto (2006). “Cellular and molecular

- mechanisms of synovial joint and articular cartilage formation.” *Ann NY Acad Sci* 1068: 74-86.
- Pan, D., M. Fujimoto, A. Lopes and Y. X. Wang (2009). “Twist-1 is a PPARdelta-inducible, negative-feedback regulator of PGC-1alpha in brown fat metabolism.” *Cell* 137(1): 73-86.
- Passos-Bueno, M. R., W. R. Wilcox, E. W. Jabs, A. L. Sertié, L. G. Alonso and H. Kitoh (1999). “Clinical spectrum of fibroblast growth factor receptor mutations.” *Hum Mutat* 14(2): 115-125.
- Pattappa, G., H. K. Heywood, J. D. de Bruijn and D. A. Lee (2011). “The metabolism of human mesenchymal stem cells during proliferation and differentiation.” *J Cell Physiol* 226(10): 2562-2570.
- Payne, K. A., D. M. Didiano and C. R. Chu (2010). “Donor sex and age influence the chondrogenic potential of human femoral bone marrow stem cells.” *Osteoarthritis Cartilage* 18(5): 705-713.
- Pelletier, J. P., P. J. Roughley, J. A. DiBattista, R. McCollum and J. Martel-Pelletier (1991). “Are cytokines involved in osteoarthritic pathophysiology?” *Semin Arthritis Rheum* 20(6 Suppl 2): 12-25.
- Peters, K. G., S. Werner, G. Chen and L. T. Williams (1992). “Two FGF receptor genes are differentially expressed in epithelial and mesenchymal tissues during limb formation and organogenesis in the mouse.” *Development* 114(1): 233-243.
- Pettersson, A. T., J. Laurencikiene, N. Mejhert, E. Näslund, A. Bouloumié, I. Dahlman, P. Arner and M. Rydén (2010). “A possible inflammatory role of twist1 in human white adipocytes.” *Diabetes* 59(3): 564-571.
- Pfaffl, M. W., A. Tichopad, C. Prgomet and T. P. Neuvians (2004). “Determination of stable housekeeping genes, differentially regulated target genes and sample integrity: BestKeeper--Excel-based tool using pair-wise correlations.” *Biotechnol Lett* 26(6): 509-515.
- Pham, D., J. W. Vincentz, A. B. Firulli and M. H. Kaplan (2012). “Twist1 regulates Ifng expression in Th1 cells by interfering with Runx3 function.” *J Immunol* 189(2): 832-840.
- Philipot, D., D. Guérit, D. Platano, P. Chuchana, E. Olivotto, F. Espinoza, A. Dorandeu, Y. M. Pers, J. Piette, R. M. Borzi, C. Jorgensen, D. Noel and J. M. Brondello (2014). “p16INK4a and its regulator miR-24 link senescence and chondrocyte terminal differentiation-associated matrix remodeling in osteoarthritis.” *Arthritis Res Ther* 16(1): R58.
- Pittenger, M. F., A. M. Mackay, S. C. Beck, R. K. Jaiswal, R. Douglas, J.

- D. Mosca, M. A. Moorman, D. W. Simonetti, S. Craig and D. R. Marshak (1999). "Multilineage potential of adult human mesenchymal stem cells." *Science* 284(5411): 143-147.
- Pollock, P. M., M. G. Gartside, L. C. Dejeza, M. A. Powell, M. A. Mallon, H. Davies, M. Mohammadi, P. A. Futreal, M. R. Stratton, J. M. Trent and P. J. Goodfellow (2007). "Frequent activating FGFR2 mutations in endometrial carcinomas parallel germline mutations associated with craniosynostosis and skeletal dysplasia syndromes." *Oncogene* 26(50): 7158-7162.
- Porée, B., M. Kypriotou, C. Chadjichristos, G. Beauchef, E. Renard, F. Legendre, M. Melin, S. Gueret, D. J. Hartmann, F. Malléin-Gerin, J. P. Pujol, K. Boumediene and P. Galéra (2008). "Interleukin-6 (IL-6) and/or soluble IL-6 receptor down-regulation of human type II collagen gene expression in articular chondrocytes requires a decrease of Sp1.Sp3 ratio and of the binding activity of both factors to the COL2A1 promoter." *J Biol Chem* 283(8): 4850-4865.
- Prabhu, S., A. Ignatova, S. T. Park and X. H. Sun (1997). "Regulation of the expression of cyclin-dependent kinase inhibitor p21 by E2A and Id proteins." *Mol Cell Biol* 17(10): 5888-5896.
- Price, J. S., J. G. Waters, C. Darrah, C. Pennington, D. R. Edwards, S. T. Donnell and I. M. Clark (2002). "The role of chondrocyte senescence in osteoarthritis." *Aging Cell* 1(1): 57-65.
- Prigodich, A. E., D. S. Seferos, M. D. Massich, D. A. Giljohann, B. C. Lane and C. A. Mirkin (2009). "Nano-flares for mRNA regulation and detection." *ACS Nano* 3(8): 2147-2152.
- Prockop, D. J. (1997). "Marrow stromal cells as stem cells for nonhematopoietic tissues." *Science* 276(5309): 71-74.
- Reinhold, M. I., R. M. Kapadia, Z. Liao and M. C. Naski (2006). "The Wnt-inducible transcription factor Twist1 inhibits chondrogenesis." *J Biol Chem* 281(3): 1381-1388.
- Ren, G., L. Zhang, X. Zhao, G. Xu, Y. Zhang, A. I. Roberts, R. C. Zhao and Y. Shi (2008). "Mesenchymal stem cell-mediated immunosuppression occurs via concerted action of chemokines and nitric oxide." *Cell Stem Cell* 2(2): 141-150.
- Rhinn, M., B. Ritschka and W. M. Keyes (2019). "Cellular senescence in development, regeneration and disease." *Development* 146(20).
- Rhodes, R. K. and E. J. Miller (1978). "Physicochemical characterization and molecular organization of the collagen A and B chains."

- Biochemistry* 17(17): 3442-3448.
- Rim, Y. A., Y. Nam and J. H. Ju (2020). "The Role of Chondrocyte Hypertrophy and Senescence in Osteoarthritis Initiation and Progression." *Int J Mol Sci* 21(7).
- Ritschka, B., M. Storer, A. Mas, F. Heinzmann, M. C. Ortells, J. P. Morton, O. J. Sansom, L. Zender and W. M. Keyes (2017). "The senescence-associated secretory phenotype induces cellular plasticity and tissue regeneration." *Genes Dev* 31(2): 172-183.
- Rodriguez, R., R. Rubio, M. Masip, P. Catalina, A. Nieto, T. de la Cueva, M. Arriero, N. San Martin, E. de la Cueva, D. Balomenos, P. Menendez and J. García-Castro (2009). "Loss of p53 induces tumorigenesis in p21-deficient mesenchymal stem cells." *Neoplasia* 11(4): 397-407.
- Romanov, Y. A., V. A. Svintsitskaya and V. N. Smirnov (2003). "Searching for alternative sources of postnatal human mesenchymal stem cells: candidate MSC-like cells from umbilical cord." *Stem Cells* 21(1): 105-110.
- Rountree, R. B., M. Schoor, H. Chen, M. E. Marks, V. Harley, Y. Mishina and D. M. Kingsley (2004). "BMP receptor signaling is required for postnatal maintenance of articular cartilage." *PLoS Biol* 2(11): e355.
- Ryu, J. H., S. Yang, Y. Shin, J. Rhee, C. H. Chun and J. S. Chun (2011). "Interleukin-6 plays an essential role in hypoxia-inducible factor 2 α -induced experimental osteoarthritic cartilage destruction in mice." *Arthritis Rheum* 63(9): 2732-2743.
- Sacchetti, B., A. Funari, S. Michienzi, S. Di Cesare, S. Piersanti, I. Saggio, E. Tagliafico, S. Ferrari, P. G. Robey, M. Riminucci and P. Bianco (2007). "Self-renewing osteoprogenitors in bone marrow sinusoids can organize a hematopoietic microenvironment." *Cell* 131(2): 324-336.
- Sahni, M., D. C. Ambrosetti, A. Mansukhani, R. Gertner, D. Levy and C. Basilico (1999). "FGF signaling inhibits chondrocyte proliferation and regulates bone development through the STAT-1 pathway." *Genes Dev* 13(11): 1361-1366.
- Sakaguchi, Y., I. Sekiya, K. Yagishita and T. Muneta (2005). "Comparison of human stem cells derived from various mesenchymal tissues: superiority of synovium as a cell source." *Arthritis Rheum* 52(8): 2521-2529.
- Salminen, A., A. Kauppinen and K. Kaarniranta (2012). "Emerging role of NF- κ B signaling in the induction of senescence-associated

- secretory phenotype (SASP)." *Cell Signal* 24(4): 835-845.
- Schellenberg, A., T. Stiehl, P. Horn, S. Jousen, N. Pallua, A. D. Ho and W. Wagner (2012). "Population dynamics of mesenchymal stromal cells during culture expansion." *Cytotherapy* 14(4): 401-411.
- Schepers, G. E., M. Bullejos, B. M. Hosking and P. Koopman (2000). "Cloning and characterisation of the Sry-related transcription factor gene Sox8." *Nucleic Acids Res* 28(6): 1473-1480.
- Seferos, D. S., D. A. Giljohann, H. D. Hill, A. E. Prigodich and C. A. Mirkin (2007). "Nano-flares: probes for transfection and mRNA detection in living cells." *J Am Chem Soc* 129(50): 15477-15479.
- Seftor, E. A., R. E. B. Seftor, D. Weldon, G. T. Kirsammer, N. V. Margaryan, A. Gilgur and M. J. C. Hendrix (2014). "Melanoma tumor cell heterogeneity: a molecular approach to study subpopulations expressing the embryonic morphogen nodal." *Semin Oncol* 41(2): 259-266.
- Sekine, K., H. Ohuchi, M. Fujiwara, M. Yamasaki, T. Yoshizawa, T. Sato, N. Yagishita, D. Matsui, Y. Koga, N. Itoh and S. Kato (1999). "Fgf10 is essential for limb and lung formation." *Nat Genet* 21(1): 138-141.
- Semenov, M. V., R. Habas, B. T. Macdonald and X. He (2007). "SnapShot: Noncanonical Wnt Signaling Pathways." *Cell* 131(7): 1378.
- Seo, S. K., J. H. Kim, H. N. Choi, T. B. Choe, S. I. Hong, J. Y. Yi, S. G. Hwang, H. G. Lee, Y. H. Lee and I. C. Park (2014). "Knockdown of TWIST1 enhances arsenic trioxide- and ionizing radiation-induced cell death in lung cancer cells by promoting mitochondrial dysfunction." *Biochem Biophys Res Commun* 449(4): 490-495.
- Severino, V., N. Alessio, A. Farina, A. Sandomenico, M. Cipollaro, G. Peluso, U. Galderisi and A. Chambery (2013). "Insulin-like growth factor binding proteins 4 and 7 released by senescent cells promote premature senescence in mesenchymal stem cells." *Cell Death Dis* 4(11): e911.
- Shapiro, F., S. Koide and M. J. Glimcher (1993). "Cell origin and differentiation in the repair of full-thickness defects of articular cartilage." *J Bone Joint Surg Am* 75(4): 532-553.
- Shibata, K. R., T. Aoyama, Y. Shima, K. Fukiage, S. Otsuka, M. Furu, Y. Kohno, K. Ito, S. Fujibayashi, M. Neo, T. Nakayama, T. Nakamura and J. Toguchida (2007). "Expression of the p16INK4A gene is associated closely with senescence of human mesenchymal stem cells and is potentially silenced by DNA methylation during in vitro

- expansion.” *Stem Cells* 25(9): 2371-2382.
- Shioda, M., T. Muneta, K. Tsuji, M. Mizuno, K. Komori, H. Koga and I. Sekiya (2017). “TNF α promotes proliferation of human synovial MSCs while maintaining chondrogenic potential.” *PLoS One* 12(5): e0177771.
- Shwartz, Y., S. Viukov, S. Krief and E. Zelzer (2016). “Joint Development Involves a Continuous Influx of Gdf5-Positive Cells.” *Cell Rep* 15(12): 2577-2587.
- Sivasubramanian, K., A. Harichandan, S. Schumann, M. Sobiesiak, C. Lengerke, A. Maurer, H. Kalbacher and H. J. Bühring (2013). “Prospective isolation of mesenchymal stem cells from human bone marrow using novel antibodies directed against Sushi domain containing 2.” *Stem Cells Dev* 22(13): 1944-1954.
- Sivasubramanian, K., D. C. Ilas, A. Harichandan, P. K. Bos, D. L. Santos, P. de Zwart, W. Koevoet, H. Owston, H. J. Bühring, E. Jones and G. van Osch (2018). “Bone Marrow-Harvesting Technique Influences Functional Heterogeneity of Mesenchymal Stem/Stromal Cells and Cartilage Regeneration.” *Am J Sports Med* 46(14): 3521-3531.
- Sivasubramanian, K., W. Koevoet, A. A. Hakimiyan, M. Sande, E. Farrell, M. J. Hoogduijn, J. A. N. Verhaar, S. Chubinskaya, H. J. Bühring and G. van Osch (2019). “Cell-surface markers identify tissue resident multipotential stem/stromal cell subsets in synovial intimal and sub-intimal compartments with distinct chondrogenic properties.” *Osteoarthritis Cartilage* 27(12): 1831-1840.
- Skene, P. J., J. G. Henikoff and S. Henikoff (2018). “Targeted in situ genome-wide profiling with high efficiency for low cell numbers.” *Nat Protoc* 13(5): 1006-1019.
- Skene, P. J. and S. Henikoff (2017). “An efficient targeted nuclease strategy for high-resolution mapping of DNA binding sites.” *Elife* 6.
- Smits, P., P. Li, J. Mandel, Z. Zhang, J. M. Deng, R. R. Behringer, B. de Crombrughe and V. Lefebvre (2001). “The transcription factors L-Sox5 and Sox6 are essential for cartilage formation.” *Dev Cell* 1(2): 277-290.
- Sock, E., K. Schmidt, I. Hermanns-Borgmeyer, M. R. Bösl and M. Wegner (2001). “Idiopathic weight reduction in mice deficient in the high-mobility-group transcription factor Sox8.” *Mol Cell Biol* 21(20): 6951-6959.
- Stenderup, K., J. Justesen, C. Clausen and M. Kassem (2003). “Aging is

- associated with decreased maximal life span and accelerated senescence of bone marrow stromal cells.” *Bone* 33(6): 919-926.
- Stockwell, R. A. (1978). “Chondrocytes.” *J Clin Pathol Suppl (R Coll Pathol)* 12: 7-13.
- Stolzing, A., E. Jones, D. McGonagle and A. Scutt (2008). “Age-related changes in human bone marrow-derived mesenchymal stem cells: consequences for cell therapies.” *Mech Ageing Dev* 129(3): 163-173.
- Storer, M., A. Mas, A. Robert-Moreno, M. Pecoraro, M. C. Ortells, V. Di Giacomo, R. Yosef, N. Pilpel, V. Krizhanovsky, J. Sharpe and W. M. Keyes (2013). “Senescence is a developmental mechanism that contributes to embryonic growth and patterning.” *Cell* 155(5): 1119-1130.
- Strawich, E. and M. E. Nimni (1971). “Properties of a collagen molecule containing three identical components extracted from bovine articular cartilage.” *Biochemistry* 10(21): 3905-3911.
- Su, B. G. and M. J. Henley (2021). “Drugging Fuzzy Complexes in Transcription.” *Front Mol Biosci* 8: 795743.
- Sutton, S., A. Clutterbuck, P. Harris, T. Gent, S. Freeman, N. Foster, R. Barrett-Jolley and A. Mobasher (2009). “The contribution of the synovium, synovial derived inflammatory cytokines and neuropeptides to the pathogenesis of osteoarthritis.” *Vet J* 179(1): 10-24.
- Suvakov, S., H. Cubro, W. M. White, Y. S. Butler Tobah, T. L. Weissgerber, K. L. Jordan, X. Y. Zhu, J. R. Woollard, F. T. Chebib, N. M. Milic, J. P. Grande, M. Xu, T. Tchkonja, J. L. Kirkland, L. O. Lerman and V. D. Garovic (2019). “Targeting senescence improves angiogenic potential of adipose-derived mesenchymal stem cells in patients with preeclampsia.” *Biol Sex Differ* 10(1): 49.
- Sward, P., R. Frobell, M. Englund, H. Roos and A. Struglics (2012). “Cartilage and bone markers and inflammatory cytokines are increased in synovial fluid in the acute phase of knee injury (hemarthrosis)--a cross-sectional analysis.” *Osteoarthritis Cartilage* 20(11): 1302-1308.
- ten Berge, D., S. A. Brugmann, J. A. Helms and R. Nusse (2008). “Wnt and FGF signals interact to coordinate growth with cell fate specification during limb development.” *Development* 135(19): 3247-3257.
- Thielen, N. G. M., P. M. van der Kraan and A. P. M. van Caam (2019). “TGFβ/BMP Signaling Pathway in Cartilage Homeostasis.” *Cells*

8(9).

- Tian, Y., Y. Xu, Q. Fu, M. Chang, Y. Wang, X. Shang, C. Wan, J. V. Marymont and Y. Dong (2015). "Notch inhibits chondrogenic differentiation of mesenchymal progenitor cells by targeting Twist1." *Mol Cell Endocrinol* 403: 30-38.
- Tsai, C. C., Y. J. Chen, T. L. Yew, L. L. Chen, J. Y. Wang, C. H. Chiu and S. C. Hung (2011). "Hypoxia inhibits senescence and maintains mesenchymal stem cell properties through down-regulation of E2A-p21 by HIF-TWIST." *Blood* 117(2): 459-469.
- Tsai, F. J., C. H. Tsai, J. G. Chang and J. Y. Wu (1999). "Mutations in the fibroblast growth factor receptor 3 (FGFR3) cause achondroplasia, hypochondroplasia, and thanatophoric dysplasia: Taiwanese data." *Am J Med Genet* 86(3): 300-301.
- Tsuchida, A. I., M. Beekhuizen, M. Rutgers, G. J. van Osch, J. E. Bekkers, A. G. Bot, B. Geurts, W. J. Dhert, D. B. Saris and L. B. Creemers (2012). "Interleukin-6 is elevated in synovial fluid of patients with focal cartilage defects and stimulates cartilage matrix production in an in vitro regeneration model." *Arthritis Res Ther* 14(6): R262.
- Tsuchida, A. I., M. Beekhuizen, M. C. t Hart, T. R. Radstake, W. J. Dhert, D. B. Saris, G. J. van Osch and L. B. Creemers (2014). "Cytokine profiles in the joint depend on pathology, but are different between synovial fluid, cartilage tissue and cultured chondrocytes." *Arthritis Res Ther* 16(5): 441.
- Tsutsumi, S., A. Shimazu, K. Miyazaki, H. Pan, C. Koike, E. Yoshida, K. Takagishi and Y. Kato (2001). "Retention of multilineage differentiation potential of mesenchymal cells during proliferation in response to FGF." *Biochem Biophys Res Commun* 288(2): 413-419.
- Tuli, R., S. Tuli, S. Nandi, X. Huang, P. A. Manner, W. J. Hozack, K. G. Danielson, D. J. Hall and R. S. Tuan (2003). "Transforming growth factor-beta-mediated chondrogenesis of human mesenchymal progenitor cells involves N-cadherin and mitogen-activated protein kinase and Wnt signaling cross-talk." *J Biol Chem* 278(42): 41227-41236.
- Uccelli, A., L. Moretta and V. Pistoia (2008). "Mesenchymal stem cells in health and disease." *Nat Rev Immunol* 8(9): 726-736.
- van Buul, G. M., E. Villafuertes, P. K. Bos, J. H. Waarsing, N. Kops, R. Narcisi, H. Weinans, J. A. Verhaar, M. R. Bernsen and G. J. van Osch (2012). "Mesenchymal stem cells secrete factors that inhibit

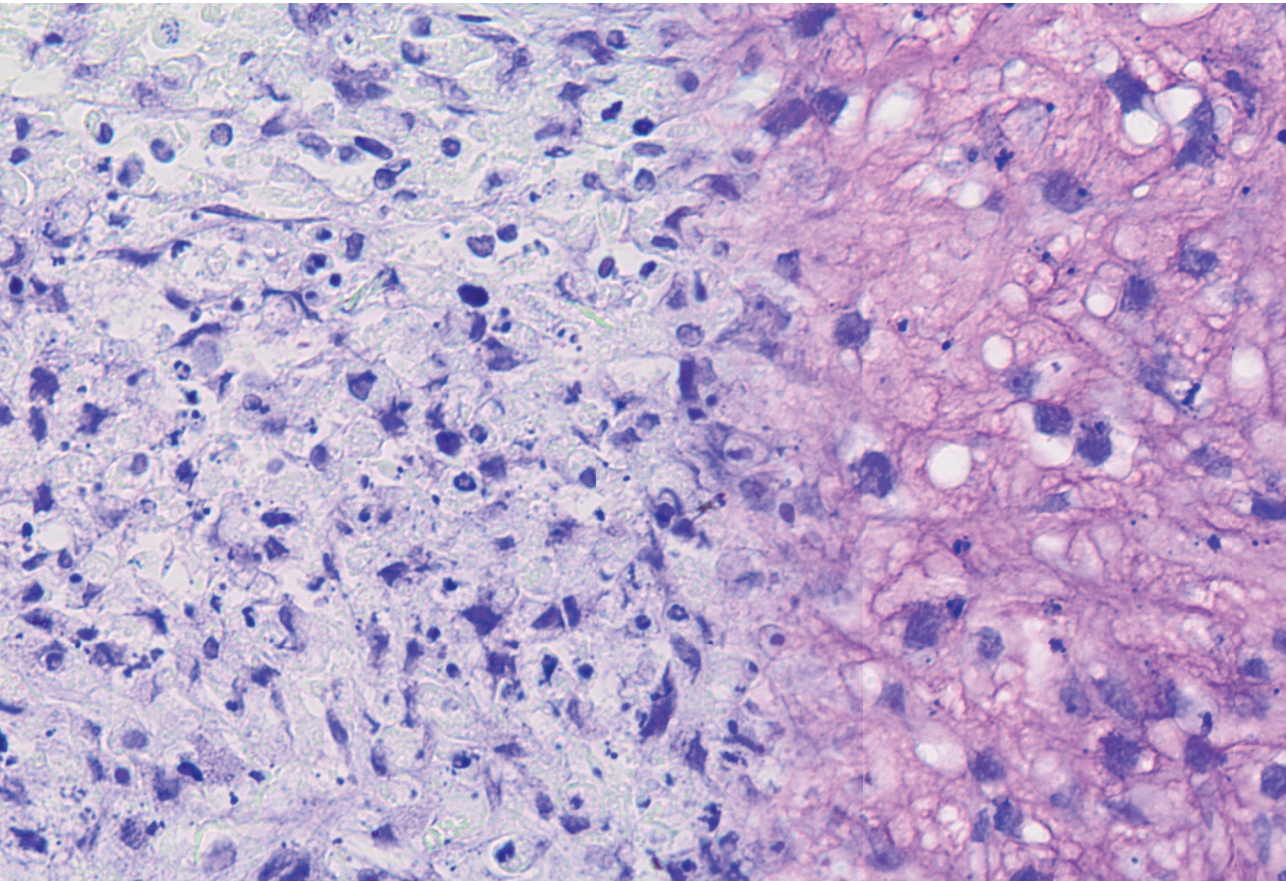
- inflammatory processes in short-term osteoarthritic synovium and cartilage explant culture.” *Osteoarthritis Cartilage* 20(10): 1186-1196.
- Verbruggen, G., M. Cornelissen, K. F. Almqvist, L. Wang, D. Elewaut, C. Broddelez, L. de Ridder and E. M. Veys (2000). “Influence of aging on the synthesis and morphology of the aggrecans synthesized by differentiated human articular chondrocytes.” *Osteoarthritis Cartilage* 8(3): 170-179.
- Vogel, A., C. Rodriguez and J. C. Izpisúa-Belmonte (1996). “Involvement of FGF-8 in initiation, outgrowth and patterning of the vertebrate limb.” *Development* 122(6): 1737-1750.
- von der Mark, K., T. Kirsch, A. Nerlich, A. Kuss, G. Weseloh, K. Glückert and H. Stöss (1992). “Type X collagen synthesis in human osteoarthritic cartilage. Indication of chondrocyte hypertrophy.” *Arthritis Rheum* 35(7): 806-811.
- Voskamp, C., L. A. Anderson, W. J. Koevoet, S. Barnhoorn, P. G. Mastroberardino, G. J. van Osch and R. Narcisi (2021). “TWIST1 controls cellular senescence and energy metabolism in mesenchymal stem cells.” *Eur Cell Mater* 42: 401-414.
- Voskamp, C., J. van de Peppel, S. Gasparini, P. Giannoni, J. van Leeuwen, G. van Osch and R. Narcisi (2020). “Sorting living mesenchymal stem cells using a TWIST1 RNA-based probe depends on incubation time and uptake capacity.” *Cytotechnology* 72(1): 37-45.
- Wagner, W., P. Horn, M. Castoldi, A. Diehlmann, S. Bork, R. Saffrich, V. Benes, J. Blake, S. Pfister, V. Eckstein and A. D. Ho (2008). “Replicative senescence of mesenchymal stem cells: a continuous and organized process.” *PLoS One* 3(5): e2213.
- Wakitani, S., M. Nawata, K. Tensho, T. Okabe, H. Machida and H. Ohgushi (2007). “Repair of articular cartilage defects in the patello-femoral joint with autologous bone marrow mesenchymal cell transplantation: three case reports involving nine defects in five knees.” *J Tissue Eng Regen Med* 1(1): 74-79.
- Wang, H., Y. Sun, W. Wu, X. Wei, Z. Lan and J. Xie (2013). “A novel missense mutation of FGFR3 in a Chinese female and her fetus with Hypochondroplasia by next-generation sequencing.” *Clin Chim Acta* 423: 62-65.
- Wang, N., J. Yin, N. You, S. Yang, D. Guo, Y. Zhao, Y. Ru, X. Liu, H. Cheng, Q. Ren, T. Cheng and X. Ma (2021). “TWIST1 preserves hematopoietic stem cell function via the CACNA1B/Ca²⁺/

- mitochondria axis." *Blood* 137(21): 2907-2919.
- Wang, W., D. Rigueur and K. M. Lyons (2014). "TGF β signaling in cartilage development and maintenance." *Birth Defects Res C Embryo Today* 102(1): 37-51.
- Wang, X., P. A. Manner, A. Horner, L. Shum, R. S. Tuan and G. H. Nuckolls (2004). "Regulation of MMP-13 expression by RUNX2 and FGF2 in osteoarthritic cartilage." *Osteoarthritis Cartilage* 12(12): 963-973.
- Wang, X. X., G. Q. Yin, Z. H. Zhang, Z. H. Rong, Z. Y. Wang, D. D. Du, Y. D. Wang, R. X. Gao and G. Z. Xian (2020). "TWIST1 transcriptionally regulates glycolytic genes to promote the Warburg metabolism in pancreatic cancer." *Exp Cell Res* 386(1): 111713.
- Wang, Y., Y. Lin, C. Cheng, P. Chen, P. Zhang, H. Wu, K. Li, Y. Deng, J. Qian, X. Zhang and B. Yu (2020). "NF- κ B/TWIST1 Mediates Migration and Phagocytosis of Macrophages in the Mice Model of Implant-Associated *Staphylococcus aureus* Osteomyelitis." *Front Microbiol* 11: 1301.
- Wang, Y., L. Wei, L. Zeng, D. He and X. Wei (2013). "Nutrition and degeneration of articular cartilage." *Knee Surg Sports Traumatol Arthrosc* 21(8): 1751-1762.
- Wehling, N., G. D. Palmer, C. Pilapil, F. Liu, J. W. Wells, P. E. Müller, C. H. Evans and R. M. Porter (2009). "Interleukin-1beta and tumor necrosis factor alpha inhibit chondrogenesis by human mesenchymal stem cells through NF-kappaB-dependent pathways." *Arthritis Rheum* 60(3): 801-812.
- Weiss, A. and L. Attisano (2013). "The TGFbeta superfamily signaling pathway." *Wiley Interdiscip Rev Dev Biol* 2(1): 47-63.
- White, K. E., J. M. Cabral, S. I. Davis, T. Fishburn, W. E. Evans, S. Ichikawa, J. Fields, X. Yu, N. J. Shaw, N. J. McLellan, C. McKeown, D. Fitzpatrick, K. Yu, D. M. Ornitz and M. J. Econs (2005). "Mutations that cause osteoglophonic dysplasia define novel roles for FGFR1 in bone elongation." *Am J Hum Genet* 76(2): 361-367.
- Wiedemann, B., J. Weisner and D. Rauh (2018). "Chemical modulation of transcription factors." *Medchemcomm* 9(8): 1249-1272.
- Wiley, C. D., M. C. Velarde, P. Lecot, S. Liu, E. A. Sarnoski, A. Freund, K. Shirakawa, H. W. Lim, S. S. Davis, A. Ramanathan, A. A. Gerencser, E. Verdin and J. Campisi (2016). "Mitochondrial Dysfunction Induces Senescence with a Distinct Secretory Phenotype." *Cell Metab* 23(2): 303-314.

- Wilkie, A. O., S. J. Patey, S. H. Kan, A. M. van den Ouweland and B. C. Hamel (2002). "FGFs, their receptors, and human limb malformations: clinical and molecular correlations." *Am J Med Genet* 112(3): 266-278.
- Xu, L., E. Shunmei, S. Lin, Y. Hou, W. Lin, W. He, H. Wang and G. Li (2019). "Sox11-modified mesenchymal stem cells accelerate cartilage defect repair in SD rats." *Cell Tissue Res* 376(2): 247-255.
- Xu, M., E. W. Bradley, M. M. Weivoda, S. M. Hwang, T. Pirtskhalava, T. Decklever, G. L. Curran, M. Ogradnik, D. Jurk, K. O. Johnson, V. Lowe, T. Tchkonja, J. J. Westendorf and J. L. Kirkland (2017). "Transplanted Senescent Cells Induce an Osteoarthritis-Like Condition in Mice." *J Gerontol A Biol Sci Med Sci* 72(6): 780-785.
- Xu, X., M. Weinstein, C. Li, M. Naski, R. I. Cohen, D. M. Ornitz, P. Leder and C. Deng (1998). "Fibroblast growth factor receptor 2 (FGFR2)-mediated reciprocal regulation loop between FGF8 and FGF10 is essential for limb induction." *Development* 125(4): 753-765.
- Yang, J., J. Anholts, U. Kolbe, J. A. Stegehuis-Kamp, F. H. J. Claas and M. Eikmans (2018). "Calcium-Binding Proteins S100A8 and S100A9: Investigation of Their Immune Regulatory Effect in Myeloid Cells." *Int J Mol Sci* 19(7).
- Yang, M. H., M. Z. Wu, S. H. Chiou, P. M. Chen, S. Y. Chang, C. J. Liu, S. C. Teng and K. J. Wu (2008). "Direct regulation of TWIST by HIF-1 α promotes metastasis." *Nat Cell Biol* 10(3): 295-305.
- Yang, Y., L. Topol, H. Lee and J. Wu (2003). "Wnt5a and Wnt5b exhibit distinct activities in coordinating chondrocyte proliferation and differentiation." *Development* 130(5): 1003-1015.
- Yang, Z., H. Li, Z. Yuan, L. Fu, S. Jiang, C. Gao, F. Wang, K. Zha, G. Tian, Z. Sun, B. Huang, F. Wei, F. Cao, X. Sui, J. Peng, S. Lu, W. Guo, S. Liu and Q. Guo (2020). "Endogenous cell recruitment strategy for articular cartilage regeneration." *Acta Biomater* 114: 31-52.
- Yew, T. L., F. Y. Chiu, C. C. Tsai, H. L. Chen, W. P. Lee, Y. J. Chen, M. C. Chang and S. C. Hung (2011). "Knockdown of p21(Cip1/Waf1) enhances proliferation, the expression of stemness markers, and osteogenic potential in human mesenchymal stem cells." *Aging Cell* 10(2): 349-361.
- Yoshida, C. A., H. Yamamoto, T. Fujita, T. Furuichi, K. Ito, K. Inoue, K. Yamana, A. Zanma, K. Takada, Y. Ito and T. Komori (2004). "Runx2 and Runx3 are essential for chondrocyte maturation, and Runx2 regulates limb growth through induction of Indian hedgehog." *Genes*

- Dev* 18(8): 952-963.
- Yousfi, M., F. Lasmoles and P. J. Marie (2002). "TWIST inactivation reduces CBFA1/RUNX2 expression and DNA binding to the osteocalcin promoter in osteoblasts." *Biochem Biophys Res Commun* 297(3): 641-644.
- Yun, M. H., H. Davaapil and J. P. Brookes (2015). "Recurrent turnover of senescent cells during regeneration of a complex structure." *Elife* 4.
- Zhang, Q., Q. Ji, X. Wang, L. Kang, Y. Fu, Y. Yin, Z. Li, Y. Liu, X. Xu and Y. Wang (2015). "SOX9 is a regulator of ADAMTSs-induced cartilage degeneration at the early stage of human osteoarthritis." *Osteoarthritis Cartilage* 23(12): 2259-2268.
- Zhang, X., N. Ziran, J. J. Goater, E. M. Schwarz, J. E. Puzas, R. N. Rosier, M. Zuscik, H. Drissi and R. J. O'Keefe (2004). "Primary murine limb bud mesenchymal cells in long-term culture complete chondrocyte differentiation: TGF-beta delays hypertrophy and PGE2 inhibits terminal differentiation." *Bone* 34(5): 809-817.
- Zhu, Y., J. L. Armstrong, T. Tchkonina and J. L. Kirkland (2014). "Cellular senescence and the senescent secretory phenotype in age-related chronic diseases." *Curr Opin Clin Nutr Metab Care* 17(4): 324-328.
- Zuk, P. A., M. Zhu, H. Mizuno, J. Huang, J. W. Futrell, A. J. Katz, P. Benhaim, H. P. Lorenz and M. H. Hedrick (2001). "Multilineage cells from human adipose tissue: implications for cell-based therapies." *Tissue Eng* 7(2): 211-228.

A



Appendices

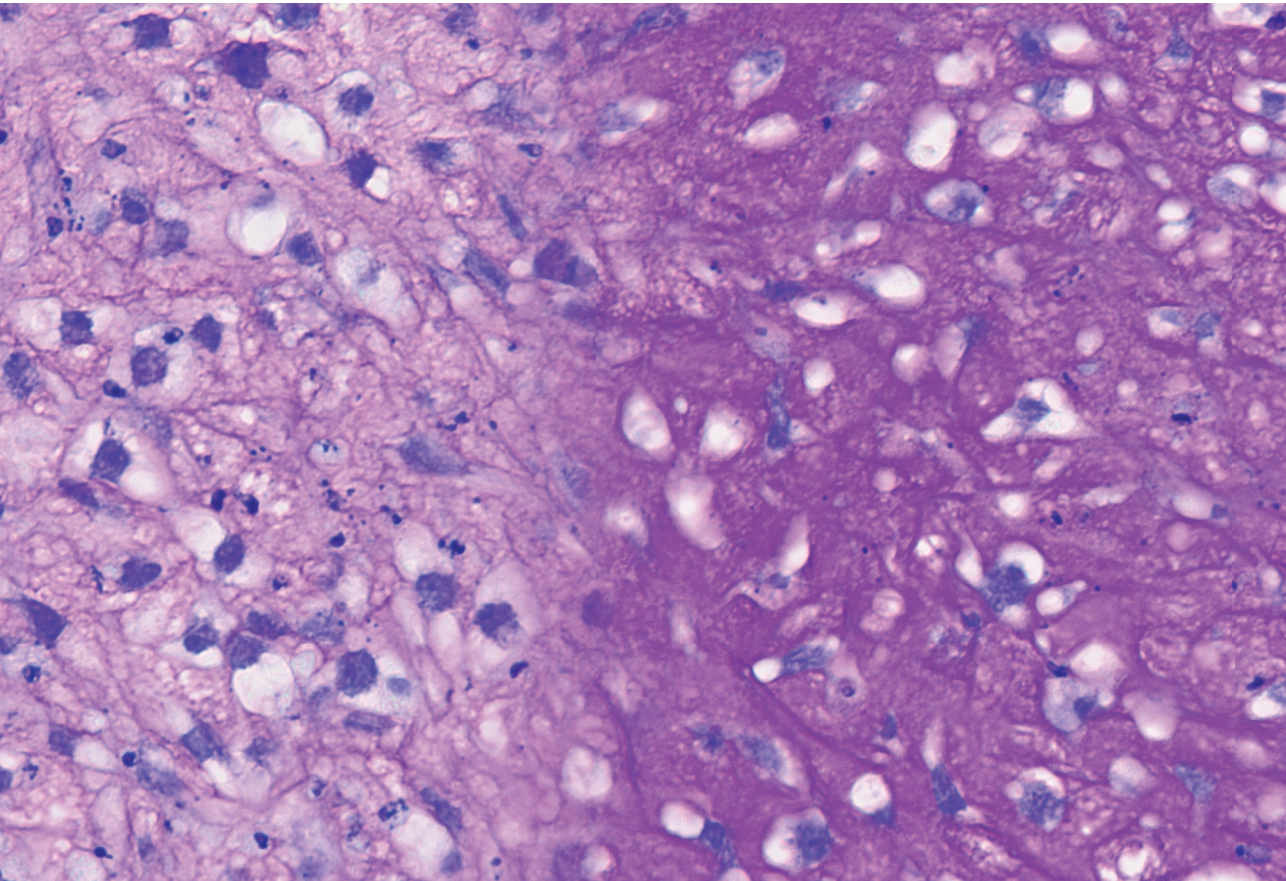
Nederlandse samenvatting

List of publications

Acknowledgements

PhD portfolio

Curriculum Vitae



Nederlandse samenvatting

Gewrichtskraakbeen is een weefsel dat zich bevindt aan de botuiteinden in gewrichten en zorgt voor een soepele beweging. Wanneer het kraakbeen beschadigd is door bijvoorbeeld (sport)letsel, kan het zich moeilijk herstellen. Afhankelijk van de kraakbeenschade en de aard van de klachten, kan kraakbeenletsel met verschillende chirurgische technieken behandeld worden. Het nadeel van deze behandelingen is dat ze er in beperkte mate in slagen het kraakbeenoppervlak te regenereren. Celtherapieën zouden een uitkomst kunnen bieden. Volwassen stamcellen zijn veelbelovend voor celtherapieën om kraakbeendefecten te herstellen, omdat deze cellen kunnen differentiëren naar kraakbeencellen (chondrocyten). Een nadeel van deze zogenoemde mesenchymale stamcellen is dat het een heterogene groep cellen betreft met een beperkt delings- en differentiatievermogen. Dit proefschrift beschrijft meerdere onderzoeken die gericht zijn op het verbeteren van het differentiatievermogen van mesenchymale stamcellen naar chondrocyten. Om dit te onderzoeken hebben we mesenchymale stamcellen van verschillende donoren gekweekt en vervolgens gedifferentieerd naar chondrocyten.

Wanneer cellen verouderen, kunnen ze onherstelbare beschadigingen oplopen. Deze verouderde cellen ondergaan een proces waarbij de cellen niet meer delen, maar nog wel metabool actief zijn. Om te onderzoeken wat het effect hiervan is op het differentiatievermogen hebben we in **hoofdstuk 2** celveroudering geïnduceerd. Op basis van weefselkleuringen, genexpressie en kwantificatie van geproduceerd kraakbeenmatrix concludeerden we dat verouderde mesenchymale stamcellen een verminderd vermogen hadden om te differentiëren naar chondrocyten. Verouderde cellen kunnen ook omliggende weefsels en cellen beschadigen, omdat ze ontstekingsfactoren uitscheiden. Daarom hebben we onderzocht hoe deze factoren, geproduceerd door verouderde cellen, omliggende niet-verouderde cellen beïnvloeden. De uitgescheiden factoren hadden geen effect op de genexpressie van kraakbeenweefselafbrekende -en producerende markers. De resultaten van dit onderzoek lieten zien dat verouderde mesenchymale stamcellen nadelig kunnen zijn voor celtherapieën om kraakbeendefecten te herstellen, voornamelijk door het verlies van het differentiatievermogen. Uit eerdere laboratoriumexperimenten is gebleken dat het eiwit TWIST1 invloed heeft op de veroudering van cellen. Daarom hebben we in **hoofdstuk 3**

de genexpressie van *TWIST1* gemanipuleerd in mesenchymale stamcellen. Wanneer de genexpressie van *TWIST1* was geremd, werd er een verhoogd percentage verouderde mesenchymale stamcellen gevonden die niet meer konden delen. Deze verouderde cellen hadden een lage productie van specifieke ontstekingsiwitten, IL6 en IL8. Uit eerdere laboratoriumonderzoeken is gebleken dat de productie van ontstekingsiwitten kan worden beïnvloed door het metabolisme van de cel. Om beter te begrijpen hoe *TWIST1* de productie van deze ontstekingsiwitten reguleert, hebben we daarom gekeken naar het metabolisme van de cellen. We concludeerden dat cellen met een geremde *TWIST1* genexpressie een andere metabole status hadden vergeleken met controlecellen. De resultaten van dit onderzoek tonen aan dat *TWIST1* een belangrijke rol speelt in het verouderen van mesenchymale stamcellen, mogelijk via het reguleren van het metabolisme en het produceren van ontstekingsiwitten.

In **hoofdstuk 4** hebben we getest of we mesenchymale stamcellen met een hoge *TWIST1* genexpressie konden selecteren. Hiervoor hebben we de cellen behandeld met een probe die *TWIST1* RNA kan detecteren. We vonden een grote variatie in probe-opname tussen de cellen, waarna we een protocol ontwikkelden om het verschil in probe-opname te corrigeren. Vervolgens hebben we cellen met een hoge en lage *TWIST1* genexpressie geselecteerd. Tot slot hebben we bevestigd dat cellen met een hoge *TWIST1* genexpressie een hoger delingsvermogen hadden dan cellen met een lage *TWIST1* genexpressie. De resultaten van dit onderzoek tonen aan dat *TWIST1* een potentiële marker is om een subpopulatie mesenchymale stamcellen te selecteren met een hoog delingsvermogen.

In **hoofdstuk 5** onderzochten we hoe we met een andere kweekmethode het delings- en differentiatievermogen van mesenchymale stamcellen zouden kunnen verbeteren. Uit eerdere laboratoriumexperimenten is gebleken dat het ontstekingsiwit TNFalfa de genexpressie van *TWIST1* kan verhogen. Aan de andere kant is uit andere onderzoeken gebleken dat TNFalfa tijdens de differentiatiefase de differentiatie naar chondrocyten vermindert. De resultaten in hoofdstuk 5 tonen aan dat TNFalfa tijdens de delingsfase het remmende effect van TNFalfa tijdens de differentiatiefase kan verminderen.

Concluderend hebben we in dit proefschrift verschillende aspecten tijdens de delingsfase gevonden die het differentiatievermogen van mesenchymale

stamcellen kunnen beïnvloeden. De kennis van dit proefschrift kan worden toegepast om mesenchymale stamceltherapieën voor kraakbeendefecten verder te verbeteren.

List of publications

Voskamp C, Anderson LA, Koevoet WJ, Barnhoorn S, Mastroberardino PG, van Osch GJ, Narcisi R. TWIST1 controls cellular senescence and energy metabolism in mesenchymal stem cells. *Eur Cell Mater.* 2021 Nov 25;42:401-414. doi: 10.22203/eCM.v042a25.

Voskamp C, Koevoet WJLM, Somoza RA, Caplan AI, Lefebvre V, van Osch GJVM, Narcisi R. Enhanced Chondrogenic Capacity of Mesenchymal Stem Cells After TNF α Pre-treatment. *Front Bioeng Biotechnol.* 2020 Jun 30;8:658. doi:10.3389/fbioe.2020.00658.

Voskamp C, van de Peppel J, Gasparini S, Giannoni P, van Leeuwen JPTM, van Osch GJVM, Narcisi R. Sorting living mesenchymal stem cells using a TWIST1 RNA-based probe depends on incubation time and uptake capacity. *Cytotechnology.* 2020 Feb;72(1):37-45. doi:10.1007/s10616-019-00355-w.

Sabatella M, Theil AF, Ribeiro-Silva C, Slyskova J, Thijssen K, **Voskamp C**, Lans H, Vermeulen W. Repair protein persistence at DNA lesions characterizes XPF defect with Cockayne syndrome features. *Nucleic Acids Res.* 2018 Oct 12;46(18):9563-9577. doi:10.1093/nar/gky774.

Acknowledgements

Lieve vrienden, familie en collega's, mijn promotietraject zit er nu bijna op! Ik kijk terug op een mooie periode die ik niet snel zal vergeten. Tijdens mijn promotietraject heb ik veel fantastische mensen ontmoet waarmee ik veel onvergetelijke ervaringen heb opgedaan. Bedankt iedereen die mij heeft geholpen bij het tot stand komen van dit proefschrift. Ik wil graag een aantal personen in het bijzonder bedanken.

First of all, I would like to thank my promotor and co-promotor. Beste **Prof. dr. Gerjo van Osch**, jouw gedrevenheid en enthousiasme voor het wetenschappelijk onderzoek werken aanstekelijk. Dankzij jou is mijn enthousiasme voor het kraakbeenweefsel begonnen. Gerjo, bedankt dat je mij altijd hebt gesteund en er alles aan hebt gedaan om mij verder te laten groeien in mijn wetenschappelijke carrière. Dear **dr. Roberto Narcisi**, I enjoyed working together during my PhD journey. Thank you for your scientific guidance and mentoring. You always kept me motivated with your calm, positive and encouraging words. Roberto, your input and support were of enormous value for this thesis. Gerjo en Roberto, ik hoop dat onze paden elkaar in toekomst nog vaak mogen kruisen.

I would also like to thank all the members of my doctoral committee **dr. Derk ten Berge**, **Prof. dr. Rebekka Schneider** and **Prof. dr. Martin Stoddart** for taking the time to read my thesis and your feedback. I would also like to thank **Prof. dr. Hans van Leeuwen** and **dr. Marjolein Caron** for completing my committee.

En dan mijn paranimfen: **Mauricio** en **Vera**. Bedankt dat ik altijd bij jullie terecht kon tijdens mijn PhD-traject. Mauricio, jouw aanwezigheid brengt een positieve energie. Ik heb enorm veel lol met jou gehad, zowel binnen als buiten het lab. Ik heb veel van jou geleerd op zowel wetenschappelijk als persoonlijk vlak. Vera, ik ken jou al meer dan 12 jaar en ik bewonder jouw creativiteit en organisatorisch vermogen. Ondanks dat jij niet in de wetenschappelijk wereld zit, bood je altijd een luisterend oor en wist jij altijd alles te relativeren met je humor. Mauricio en Vera, ik ben ontzettend dankbaar voor onze vriendschappen.

Alle staffleden en assistenten van de orthopedieafdeling, hartelijk dank voor het verzamelen van het beenmergmateriaal.

Dear **Sander Barnhoorn, dr. Pier Mastroberardino, dr. Simona Gasparini, dr. Paolo Giannoni, dr. Jeroen van de Peppel, Prof. dr. Hans van Leeuwen, Prof. dr. Arnold Caplan, dr. Rodrigo Somoza, Prof. dr. Véronique Lefebvre** thank you for the scientific contributions to the chapters in this thesis.

Natuurlijk wil ik ook alle collega's van het Connective Tissue Repair lab bedanken, dit proefschrift was niet tot stand gekomen zonder jullie hulp. Het was fijn om met jullie te werken.

Wendy, ik vond het ontzettend fijn om met jou samen te werken. Het was altijd gezellig om te kletsen en om te sparren over het onderzoek. Jouw bijdrage is van essentieel belang geweest voor het tot stand komen van dit proefschrift. Er is geen hoofdstuk in dit proefschrift waar jij niet aan hebt bijgedragen. Ik wil je daarom ontzettend bedanken voor al je inzet en hulp. **Nicole** en **Janneke** bedankt voor al jullie hulp in het lab en **Sandra**, bedankt voor het regelen van alle administratieve zaken. Ik kon altijd bij jullie terecht voor advies, waar ik jullie voor wil bedanken, en voor gezellige gesprekken tijdens de lunch of koffie.

Panithi, Shorouk, Callie, and Sohrab, it was nice working together, I have learned a lot from all of you. **Kavitha, Yvonne** and **Eric**, I am grateful for all your advice and feedback that you gave me during my PhD.

Virginia and **Enrique** my Spanish roomies, sometimes I still hear the Spanish swear words in my back. Virginia, it was fun sharing our office together, but during our adventurous 6-hour drive along the countryside of Ireland I really got to know you better. Thank you for all your help and advice during my endeavors. Enrique, thank you for all the times you have helped me when I was struggling in the laboratory. **Tim**, jij bracht wat Nederlandse nuchterheid in ons kantoor. Bedankt voor de Nederlandse steun in onze strijd tegen de Spaanse enclave 😊. Jouw klinische kijk op de wetenschap heeft mij veel geleerd. **Yannick**, thank you for adding a lot of laughs during our time in the lab. It was always fun to have you around and thank you for the organization of all the Friday afternoon “borrels”.

Niamh, thank you for the trips and tricks you gave me to develop as a scientist. It was really nice to have you around in the lab. Thanks for your Irish hospitality and showing us around in Ireland. **Andrea**, thank you for all the advice and feedback that you gave me during my PhD. You are truly an inspiring scientist and I hope our paths may cross again in the future. **Lizette**, toen ik begon was jij bijna klaar met je PhD. Toch kon ik in het begin altijd bij jou terecht voor advies. Ik vind het leuk dat we nu weer collega's zijn en kijk er erg naar uit om nu weer samen te werken.

My students, **Boudewijn, Laura, Sascha** and **Fjodor**, thank you for all your enthusiasm and hard work. I wish you all the best of luck in your future career.

Ook wil ik graag mijn vrienden bedanken. **Esther, Inge, Melissa, Michelle** en **Vera**, ik heb de afgelopen jaren alles met jullie kunnen delen. Jullie wisten altijd precies hoe jullie mij moesten steunen met een berichtje of een kaartje op het juiste moment. Ik ben ontzettend dankbaar om jullie als vriendinnen te hebben. **Quirine**, jij hebt de afgelopen jaren enorm veel met mij meegedeeld. Bedankt dat ik alle momenten van stress en frustratie met jou kon delen. **Anh, Kaylia, Marco, Arnaud** and **Angela**, you were my help and guidance in Philadelphia. I am really grateful that we have met and my time in the US would definitely have been less fun without you guys. Thank you for all the amazing moments, I will never forget our time in Atlantic City. Thank you for always being there to chat about anything and for all the times that you have motivated me to finish my thesis. I am grateful for our friendship.

Ook wil ik graag mijn familie bedanken. **Papa, mama** en **Sven**, bedankt dat jullie mij altijd gesteund hebben en er voor mij waren als ik dat nodig had. Lieve papa en mama, bedankt dat jullie mij altijd hebben gestimuleerd om te doen wat ik leuk vind en om mijn hart te volgen. Jullie interesse, steun en liefde betekent heel veel voor mij. Pap en mam, bedankt voor alles!

Lieve **Mark**, bedankt voor je onvoorwaardelijke steun en liefde. Het was de afgelopen tijd niet altijd makkelijk toen jij in Nederland bleef en ik naar Philadelphia ging. Gelukkig zijn we nu weer samen in Nederland. Ik vind het heel fijn om na een drukke werkdag weer bij jou thuis te komen. Samen met jou is alles leuker en ik kijk uit naar onze toekomst samen. Lieve Mark, één ding weet ik zeker, met jou kan ik alles aan. Ik hou van jou!

PhD portfolio

Personal details		
Name	Chantal Voskamp-Visser	
Department	Orthopaedics	
PhD Period	January 2017- June 2020	
Promotor	Prof. dr. Gerjo J.V.M. van Osch	
Co-promotor	Dr. Roberto Narcisi	

Courses and workshops	Year	Workload (ETCS)
Flow Cytometry Course – BD	2017	0.3
Basic Introduction Course on SPSS – Erasmus MC	2017	1.0
Cell-Based Therapies and Tissue Engineering – Case Western Reserve University	2017	1.0
PhD Day – Erasmus MC	2017	0.3
Research Integrity course – Erasmus MC	2017	0.3
The Monocytes: origins, destinations, functions and diagnostic targets – Erasmus MC	2017	0.2
Connecting Academia, Medicine, Entrepreneurs, Life Science & Education – Chameleon	2018	0.2
PhD Day – Erasmus MC	2018	0.3
Basic Course on ‘R’ – Erasmus MC	2019	2.0

Inter(national) conferences	Year	Workload (ETCS)
22 nd annual Molecular Medicine Day, Rotterdam – Elevator pitch and Poster Presentation	2018	0.5
Annual NVMB meeting, Lunteren – Podium Presentation	2018	1.0
eCM XVIII Cartilage and Disc, Davos – Poster Presentation (eCM poster prize)	2018	1.0
27 th annual NBTE meeting, Lunteren – Podium Presentation	2018	1.0

Inter(national) conferences	Year	Workload (ETCS)
NOV jaarcongres 2019, 's Hertogenbosch – Podium Presentation (Prof. dr. Rik Huiskes presentation prize)	2019	1.0
Gordon Research Seminar on Cartilage Biology and Pathology, Galveston – Podium Presentation	2019	1.0
Gordon Research Conference on Cartilage Biology and Pathology, Galveston – Poster Presentation	2019	1.0
SCORE/Systems Biomedicine ACE DAY, Rotterdam – ACE Force presentation	2019	0.5
Teaching and student supervision	Year	Workload (ETCS)
Supervision Master research project (Laura Anderson), Erasmus University Rotterdam	2018-2019	5.0
Supervision Higher education traineeship (Sascha Schmidt)	2018-2019	3.0
Showcase, minor stem cells, Erasmus University Rotterdam	2019	0.2
Supervision Master thesis project (Fjodor Bekedam), Erasmus University Rotterdam/Wageningen University and Research	2019-2020	5.0
Supervision Master literature review project (Lizzy Munnik), Erasmus University Rotterdam	2019-2020	0.5
Department meetings and presentations	Year	Workload (ETCS)
Research meetings depts of Orthopaedics and Oral Maxillofacial Surgery, weekly	2017-2020	2.0
Meetings depts of Orthopaedics and Internal Medicine, weekly	2017-2020	2.0

Department meetings and presentations	Year	Workload (ETCS)
Orthopaedics Science Day, annually	2017-2020	0.5
Journal Club, monthly	2017-2020	1.0
Department meetings and presentations	Year	Workload (ETCS)
Organization Lab day Orthopaedics, ENT, Oral Maxillofacial Surgery	2018	0.5
Organization Orthopaedics Science Day	2019	0.5
Visiting PhD student at Hong Kong University Prof. D. Chan laboratory, 4 weeks	2019	5.0
		Total ECTS: 37.8

Curriculum vitae

Chantal Voskamp-Visser was born on February 18th 1993 in Zwijndrecht, The Netherlands. In 2011 she obtained her athenium diploma at Develstein College in Zwijndrecht and started her Biomedical Science Bachelor degree program at the University of Utrecht. During her Bachelor degree program, she became interested in the fields of stems cells and genetics. In 2014, she obtained her Bachelor degree and started the Research Master Molecular Medicine at the Erasmus MC in Rotterdam. During her first year of the Research Master, Chantal studied the dynamics and regulation of the ERCC1-XPF complex in DNA damage response at the department of Molecular Genetics under the supervision of Prof. dr. W. Vermeulen and Dr. H. Lans. In the second year of her Research Master, she conducted research at the department of Reproduction and Development under supervision of Prof. dr. J. Gribnau and dr. H. Mira-Bontenbal. In 2016, she successfully defended her master thesis entitled: 'Activators of X chromosome activation'. During her Research Master, Chantal was active as board member of the Student Union for Research Masters of the Erasmus MC (SURE).



In 2017 she started her PhD research at the department of Orthopaedics and Sports Medicine at Erasmus MC in Rotterdam under the supervision of Prof. dr. G.J.V.M. van Osch and dr. R. Narcisi, the findings of which make up this thesis. During her time as PhD candidate she won the Rik Huiskes presentation award at the Dutch Orthopaedic Society (NOV) meeting in 2019 and best poster presentation award at the 18th eCM meeting in Davos. She also conducted research at the University of Hong Kong under the supervision of Prof. dr. D. Chan and Ms A. Ng for one month to learn the in situ hybridization technique to understand the dynamics of chondrogenic differentiation using adult stem cells.

From February 2021 till June 2022, she worked in the laboratory of Prof. dr. V. Lefebvre as a postdoctoral fellow at the Department of Orthopaedic Surgery at The Children's Hospital of Philadelphia. During her postdoctoral research she used different mouse models to determine cooperative functions of key transcription factors in growth plate chondrocytes.

Chantal is currently working at the University of Utrecht at the Faculty of Veterinary Medicine in the laboratory of Prof. dr. M.A. Tryfonidou where she focusses on an RNA-based therapy for intervertebral disc regeneration.

On April 9th 2022 Chantal got married to Mark Visser-Voskamp.

